

AFRL-SN-RS-TR-2006-44
In-House Final Report
February 2006



MODULE EVALUATION

APPROVED FOR PUBLIC RELEASE; DISTRIBUTION UNLIMITED.

AIR FORCE RESEARCH LABORATORY
SENSORS DIRECTORATE
ROME RESEARCH SITE
ROME, NEW YORK

Although this report references limited and classified documents (*), listed on pages 4, 14, 41 & 90, no limited information or classified information has been extracted.

STINFO FINAL REPORT

This report has been reviewed by the Air Force Research Laboratory, Information Directorate, Public Affairs Office (IFOIPA) and is releasable to the National Technical Information Service (NTIS). At NTIS it will be releasable to the general public, including foreign nations.

AFRL-SN-RS-TR-2006-44 has been reviewed and is approved for publication

APPROVED: /s/

MICHAEL T. SHEEHAN
Chief, Surveillance Radar Technology Branch
Sensors Directorate

FOR THE DIRECTOR: /s/

RICHARD G. SHAUGHNESSY
Chief, Rome Operations Office
Sensors Directorate

REPORT DOCUMENTATION PAGE

Form Approved
OMB No. 074-0188

Public reporting burden for this collection of information is estimated to average 1 hour per response, including the time for reviewing instructions, searching existing data sources, gathering and maintaining the data needed, and completing and reviewing this collection of information. Send comments regarding this burden estimate or any other aspect of this collection of information, including suggestions for reducing this burden to Washington Headquarters Services, Directorate for Information Operations and Reports, 1215 Jefferson Davis Highway, Suite 1204, Arlington, VA 22202-4302, and to the Office of Management and Budget, Paperwork Reduction Project (0704-0188), Washington, DC 20503

1. AGENCY USE ONLY (Leave blank)		2. REPORT DATE FEBRUARY 2006	3. REPORT TYPE AND DATES COVERED In-House Jun 80 – Sep 90	
4. TITLE AND SUBTITLE MODULE EVALUATION			5. FUNDING NUMBERS C - N/A PE - 62702F PR - 4506 TA - 12 WU - 68	
6. AUTHOR(S) Michael O. Little				
7. PERFORMING ORGANIZATION NAME(S) AND ADDRESS(ES) Air Force Research Laboratory/SNRD 26 Electronic Parkway Rome New York 13441-4514			8. PERFORMING ORGANIZATION REPORT NUMBER N/A	
9. SPONSORING / MONITORING AGENCY NAME(S) AND ADDRESS(ES) Air Force Research Laboratory/SNRD 26 Electronic Parkway Rome New York 13441-4514			10. SPONSORING / MONITORING AGENCY REPORT NUMBER AFRL-SN-RS-TR-2006-44	
11. SUPPLEMENTARY NOTES AFRL Project Engineer: Michael O. Little/SNRD/(315) 330-7964 Michael.Little@rl.af.mil				
12a. DISTRIBUTION / AVAILABILITY STATEMENT APPROVED FOR PUBLIC RELEASE; DISTRIBUTION UNLIMITED.			12b. DISTRIBUTION CODE	
13. ABSTRACT (Maximum 200 Words) This report describes the research performed to develop and demonstrate various testing methodologies for the evaluation and characterization of Transmit/Receive (T/R) modules for phased array radars. Discussed are techniques for characterizing T/R modules in transmit and receive modes under ideal and emulated operation environments. Further, techniques for life testing these modules are discussed. Data from the evaluation of typical T/R modules is provided to show the capabilities of these techniques and the characteristics of T/R modules developed during the early and mid 1980's. Data provided shows the performance in terms of gain and phase for both transmit and receive, as well as the receive noise figure. Further, data showing how modules degrade as a function of time and temperature is provided.				
14. SUBJECT TERMS Radar, life testing, phased array radar, T/R modules, automated testing.			15. NUMBER OF PAGES 146	
			16. PRICE CODE	
17. SECURITY CLASSIFICATION OF REPORT UNCLASSIFIED	18. SECURITY CLASSIFICATION OF THIS PAGE UNCLASSIFIED	19. SECURITY CLASSIFICATION OF ABSTRACT UNCLASSIFIED	20. LIMITATION OF ABSTRACT UL	

TABLE OF CONTENTS

1.0	INTRODUCTION	1
2.0	TEST SYSTEM DESCRIPTION	3
2.1	PULSED POWER TEST SYSTEM (MEL-2).....	3
2.1.1	<i>PHASE DISCRIMINATOR CIRCUIT</i>	9
2.1.2.1	TEMPERATURE AND ATMOSPHERIC PRESSURE.....	13
2.1.2.2	LOAD VSWR.....	15
2.1.2.3	BIAS VOLTAGES.....	17
2.1.2.4	MICROWAVE EXCITATION.....	18
2.1.2.5	DUT STATE CONTROL.....	22
2.2	LONG TERM PERFORMANCE TEST SYSTEM (MELTS).....	24
2.2.1	<i>DATA ACQUISITION AND CONTROL</i>	31
2.2.2	<i>ENVIRONMENTAL CONDITIONS</i>	33
2.3	PULSED PHASE MEASUREMENT SYSTEM.....	37
3.0	EXPERIMENTS/RESULTS	41
3.1	EARLY L & S BAND MODULES (CHARACTERIZATION).....	41
3.1.1	<i>TEST RESULTS</i>	42
3.2	C BAND MODULES.....	61
3.2.1	<i>MODULE DESCRIPTION</i>	61
3.2.2	<i>LIFE TEST CONDITIONS</i>	63
3.3	S-BAND MODULES.....	84
3.3.1	<i>MODULE DESCRIPTION</i>	84
3.3.2	<i>TEMPERATURE TEST</i>	84
4.0	CONCLUSIONS	89
	BIBLIOGRAPHY	90
	GLOSSARY	91

LIST OF FIGURES

FIGURE 2.1.1 - BLOCK DIAGRAM OF MEL	5
FIGURE 2.1.2 - EARLY PICTURE OF MEL.....	5
FIGURE 2.1.3 – BLOCK DIAGRAM OF MEL-2.....	6
FIGURE 2.1.4 – PICTURE OF MEL-2.....	9
FIGURE 2.1.5 - BLOCK DIAGRAM OF PHASE DISCRIMINATOR.....	11
FIGURE 2.1.6 - PICTURE OF A PHASE DISCRIMINATOR.....	12
FIGURE 2.1.7 – VOLTAGE OUTPUTS VERSE POWER INPUTS.....	12
FIGURE 2.1.8 – MEASURED PHASE ERROR RESULTING FROM ROUND OFF ERRORS	13
FIGURE 2.1.9 – PICTURE OF THERMAL PLATE	14
FIGURE 2.1.10 – SPACE CHAMBER WITH THERMAL TEST FIXTURE	15
FIGURE 2.1.11 – DYNAMIC LOAD CIRCUIT	16
FIGURE 2.1.12 – DYNAMIC LOAD WITH STEPPER MOTOR CONTROLLED PHASE SHIFTER....	17
FIGURE 2.1.13 – DC BIAS BOARD FOR S & C BAND DUTS	18
FIGURE 2.1.14 – WIDEBAND WAVEFORM GENERATOR	21
FIGURE 2.1.15 – PULSE CONDITIONER WAVEFORM.....	22
FIGURE 2.1.16 – PULSE CONDITIONER & LFM WAVEFORM GENERATOR	22
FIGURE 2.1.17 – C BAND MODULE CONTROLLER	23
FIGURE 2.1.18 – L BAND MODULE CONTROLLER	24
FIGURE 2.2.1 – LONG TERM PERFORMANCE TEST SYSTEM VERSION 1	25
FIGURE 2.2.2 - LONG TERM PERFORMANCE TEST SYSTEM VERSION 1	26
FIGURE 2.2.3 – BLOCK DIAGRAM OF LONG TERM PERFORMANCE TEST SYSTEM VERSION 2	27
FIGURE 2.2.4 - LIFE TEST SYSTEM TIMING DIAGRAM	30
FIGURE 2.2.5 - LIFE TEST SYSTEM CONTROLLER	32
FIGURE 2.2.6 – TYPICAL LIFE TEST SYSTEM DISPLAY	32
FIGURE 2.2.7 – DATA LOGGER	33
FIGURE 2.2.8 – LIFE TEST VERSION 1 DUT TEST CHAMBER.....	34
FIGURE 2.2.9 – DUT LIFE TEST FIXTURE MOUNTED ON COPPER BLOCK	35
FIGURE 2.2.10 - LIFE TEST VERSION 2 DUT TEST CHAMBER.....	36
FIGURE 2.3.1 – PULSED PHASE MEASUREMENT SYSTEM.....	38
FIGURE 2.3.2 – PULSED PHASE MEASUREMENT SYSTEM DIAGRAM.....	39
FIGURE 2.3.3 – PULSE MEASUREMENT SYSTEM RISE TIME DATA.....	40
FIGURE 3.1.1 – EARLY L & S BAND MODULES.....	41
FIGURE 3.1.2 – EARLY S BAND MODULE UNDER TEST	42
FIGURE 3.1.3 (A) – GAIN VERSUS GATE VOLTAGE	43
FIGURE 3.1.4 (A) – GAIN VERSUS GATE VOLTAGE (0 DEGREE C)	44
FIGURE 3.1.5 (A) – GAIN VERSUS TEMPERATURE.....	45
FIGURE 3.1.5 (B) – NOISE FIGURE VERSUS TEMPERATURE.....	45
FIGURE 3.1.6 (A) – GAIN VERSUS SOURCE MISMATCH	46
FIGURE 3.1.6 (B) – NOISE FIGURE VERSUS SOURCE MISMATCH	46
FIGURE 3.1.7 – SOURCE MISMATCH BLOCK DIAGRAM.....	47
FIGURE 3.1.8 – S09 GAIN, PHASE & PHASE LINEARITY DATA	48
FIGURE 3.1.9 – S10 GAIN, PHASE & PHASE LINEARITY DATA	49
FIGURE 3.1.10 – S11 GAIN, PHASE & PHASE LINEARITY DATA	50
FIGURE 3.1.11 – S12 GAIN, PHASE & PHASE LINEARITY	51
FIGURE 3.1.12 – T01 GAIN, PHASE & PHASE LINEARITY	52
FIGURE 3.1.13 – T02 – GAIN, PHASE & PHASE LINEARITY	53
FIGURE 3.1.14 – GAIN, PHASE & PHASE LINEARITY DATA.....	54
FIGURE 3.1.15 – T04 GAIN, PHASE & PHASE LINEARITY DATA	55
FIGURE 3.1.16 – T01 PHASE SHIFTER SETTING SENSITIVITY DATA	56

FIGURE 3.1.17 – TO2 PHASE SHIFTER SETTING SENSITIVITY DATA	57
FIGURE 3.1.18 - T01 PULSE WIDTH SENSITIVITY DATA.....	58
FIGURE 3.1.19 – LOW POWER S BAND MODULE TO MODULE TRACKING DATA.....	59
FIGURE 3.1.20 – HIGH POWER S BAND MODULE TO MODULE TRACKING DATA.....	60
FIGURE 3.2.1 – C BAND T/R MODULE (EXPLODED VIEW).....	61
FIGURE 3.2.2 – C BAND T/R MODULE SCHEMATIC DIAGRAM.....	62
FIGURE 3.2.3 - C BAND T/R MODULE SPECTRUM OUTPUT WITHOUT RF INPUT (UPPER) AND WITH RF INPUT (LOWER).....	64
FIGURE 3.2.4 – C BAND T/R MODULES IN LIFE TEST CHAMBER (LEFT SIDE).....	67
FIGURE 3.2.5 – C BAND T/R MODULE PHASE I RF TRANSMIT COMPOSITE DATA.....	73
FIGURE 3.2.6 - C BAND T/R MODULE PHASE I RF RECEIVE COMPOSITE DATA.....	74
FIGURE 3.2.7 - C BAND T/R MODULE PHASE I DC TRANSMIT COMPOSITE DATA.....	75
FIGURE 3.2.8 - C BAND T/R MODULE PHASE I DC RECEIVE COMPOSITE DATA	76
FIGURE 3.2.9 – C BAND COMPOSITE LIFE TEST.....	77
FIGURE 3.2.10 – ROOM TEMPERATURE 14 & 15 MARCH 1989.....	78
FIGURE 3.2.11 – ROOM TEMPERATURE 18 & 19 MAY 1989.....	79
FIGURE 3.2.12 - C-BAND T/R MODULE PHASE III RF TRANSMIT COMPOSITE DATA	80
FIGURE 3.2.13 - C-BAND T/R MODULE PHASE III RF RECEIVER COMPOSITE DATA.....	81
FIGURE 3.2.14 - C-BAND T/R MODULE PHASE III DC TRANSMIT COMPOSITE DATA	82
FIGURE 3.2.15 - C-BAND T/R MODULE PHASE III DC RECEIVER COMPOSITE DATA	83
FIGURE 3.3.1 – S-BAND T/R MODULE	84
FIGURE 3.3.2 – “BEER COOLER” BATH TEMPERATURE TEST	85
FIGURE 3.3.3 – S-BAND MODULE TRANSMIT GAIN & PHASE VS TEMPERATURE	86
FIGURE 3.3.4 – S-BAND MODULE SMALL SIGNAL CW GAIN & NOISE FIGURE VS TEMPERATURE.....	87
FIGURE 3.3.5 – S-BAND MODULE RECEIVE “FREEZE-OUT” MMIC CHIP AND CONTROLLER TEMPERATURES VS GAIN.....	87
FIGURE 3.3.6 – S-BAND MODULE TRANSMIT GAIN MODULE TO MODULE TRACKING VS TEMPERATURE.....	88

List of Tables

TABLE 2.1.1 - SURVEYED TESTING TECHNIQUES	4
TABLE 2.1.2 – MEL-2 SPECIFICATION (PAGE 1 OF 2)	7
TABLE 2.1.2 – MEL-2 SPECIFICATION (PAGE 2 OF 2)	8
TABLE 2.1.3 – WIDEBAND WAVEFORM GENERATOR CAPABILITIES	20
TABLE 2.2.1 – LONG TERM PERFORMANCE TEST SYSTEM VERSION 2 SPECIFICATIONS (PAGE 1 OF 2).....	28
TABLE 2.2.1 – LONG TERM PERFORMANCE TEST SYSTEM VERSION 2 SPECIFICATIONS (PAGE 2 OF 2).....	29
TABLE 3.2.1 – TYPICAL BIAS VOLTAGES	63

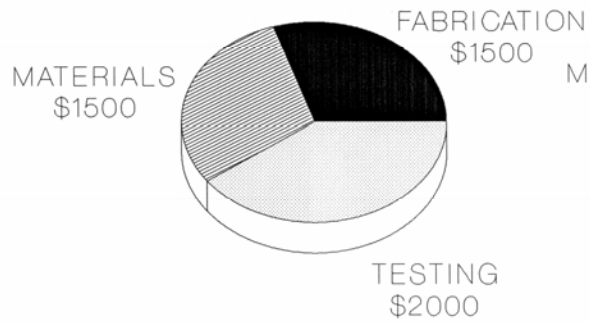
1.0 INTRODUCTION

Since the late 1970's, the Sensor's Directorate of the Air Force Research Laboratory (a.k.a. Rome Laboratory (RL) from 1991-1997 and Rome Air Development Center (RADC) from 1950 to 1990), and other agencies have been developing Monolithic Microwave Integrated Circuit (MMIC) technology for use within Transmit/Receive (T/R) modules for phased array radars. The impetus for using MMIC technology in T/R modules is to reduce the cost, size and weight and to increase the performance and reliability over what can be achieved utilizing other technologies. By judiciously formulating a testing methodology that utilizes the right type of testing at a critical location within the fabrication process, a major cost savings with an increase in performance and reliability can be achieved. Table 1.1 illustrates a documented example where such a methodology had an impact on the cost of a T/R module. The module is from the Module Validation (MODVAL) contract with Raytheon in which over 250 T/R modules at X band were fabricated. Note the percentage of testing cost and the impact of adding on-wafer pulsed RF testing would have had to the total per module cost. By putting more test up front (and screening out bad power amplifiers), the amount of rework was significantly decreased and the overall cost per good module was almost cut in half.

To provide for a continual and progressive development of the more cost effective testing methods for T/R modules, RL initiated an in-house program in 1980 entitled "Module Evaluation". Its purpose was two fold, (1) to develop and demonstrate novel testing techniques for T/R modules, and (2) to determine the performance capabilities of specific T/R modules and their sub-components. Over the eleven year life of the effort, various testing techniques were developed and evaluated. The demonstration vehicles for validating those techniques were T/R modules, deliverables from research and development contracts.

MODVAL MODULE COST (QTY OF 250 MODULES)

ACTUAL COST



PROJECTED COST WITH ON-WAFER TEST

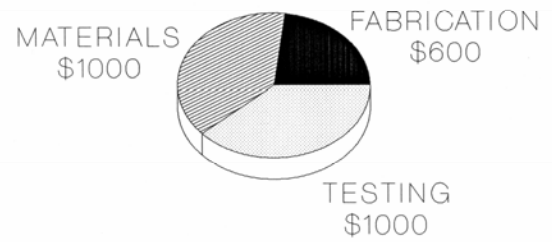


FIGURE 1.1.1 - MODVAL T/R MODULE COST BREAK-OUT

2.0 TEST SYSTEM DESCRIPTION

The test system developed is actually a number of test systems tied together and collocated within the same facility. These systems include the following:

- Pulsed Power Test System (MEL-2)
- Long Term Performance Test System (MELTS)
- Pulsed Phase Measurement System

Each of these systems meets a need that was not previously addressed by industry. All are computer controlled using a Motorola 68000 computer with Basic as the operating system. The specific instrument controllers are Hewlett Packard 9000 Series 200 and 300 computers utilizing HPBasic/WS operating systems versions 4.0 and 5.0 respectively.

2.1 PULSED POWER TEST SYSTEM (MEL-2)

Experience from the Pave Paws radar development showed that testing under actual radar operating conditions was needed to insure that T/R modules actually perform as designed when placed within an operational system. When Pave Paws was first turned on, a significant portion of the hybrid T/R modules burned out. The modules had been tested as good using CW small signal measurement equipment. However, when first operated in the actual system, the modules tended to burn up due to the complex impedance caused by their operation under pulsed conditions. Pulse testing had not performed on these modules because there was no commercial Automatic Test Equipment (ATE) capable of subjecting a Device Under Test (DUT) to a pulsed power waveform to measure their performance. The solution included a survey of the possible testing techniques and the development and demonstration of the most promising technique. A list of the surveyed techniques with their most prevalent assets and drawbacks is presented in Table 2.1.1. The technique chosen as the most promising involved the phase discriminator.

The first pulsed power ATE system developed became commonly known as MEL (short for Module Evaluation Lab). It was split into two subsystems; the Automatic Pulsed Measurement System (APMS) and the Noise Figure Measurement System (NFMS). A block diagram of this early test system is presented in Figure 2.1.1. This system was not fully automated and had limitations in operating frequency. It was highly reconfigurable by manually changing the microwave plumbing and could be set up to do a variety of experiments. Its full capabilities were outlined in RADC-TR-83-21 "Monolithic Amplifier Evaluation" by Edward J. Jones, RADC/OCTP. A picture of this early system is shown in Figure 2.1.2.

The latest version of MEL is MEL-2, the second generation module evaluation system. It is also split into two subsystems, APMS and NFMS. MEL-2 is fully automated and incorporates all of the advances identified during the development of MEL. A block

diagram of MEL-2 is depicted in Figure 2.1.3 and a list of its specification is presented in Table 2.1.2. The system is constructed with the capability to operate from 1 to 12 GHz in both transmit and receive. Detailed information is presented in RADC-TR-89-225 “Module Evaluation Lab (MEL-2 Report)” by Atlantic Research Corporation. A picture of MEL-2 is shown in Figure 2.1.4.

	Modified ANA	Four Port	Six Port	Digital Detection
Cost	Total \$180K W/o ANA \$20K	\$95K	\$130K	\$180K
Frequency Range	45 MHz to 110 GHz	1 GHz to 18 GHz	1 GHz to 110 GHz	500 MHz to 18 GHz
Pulse Width	>200 usec	>1 usec	Power Meter >500 msec Diode > 1 usec	> 1 usec
Speed	1 sec	50 msec	Power Meter 4 sec Diode 0.5 sec	100 msec
Intra-pulse Measurement	NO	Yes	Yes, but not with Power Meter sensors	Yes
Amplitude Accuracy	± 0.1 dB	< 1 dB peak w/o correction < 0.5 dB corrected	Power Meter < 0.03 dB Diode < 0.3 dB	± 0.06 dB RMS
Amplitude Repeatability	< 0.04 dB	< 0.5 dB	< 0.003 dB	
Phase Accuracy	± 0.15 deg	< 7 deg peak w/o correction 0.67 deg RMS 1.0 deg peak corrected	Limited sensor & Calc	± 0.3 deg RMS
Phase Repeatability	< 0.1 deg	< 0.4 deg	Dependent on Amplitude Repeatability	
Notes	No Warranty Own Service	Temp Control Required 20 dB Dynamic Range	Temp Control Required 60 dB Dynamic Range	Not Yet Built

* Table Compiled in 1987

TABLE 2.1.1 - SURVEYED TESTING TECHNIQUES

* RADC-TR-89-225 is Distribution limited to DOD and Their Contractors - Export Control

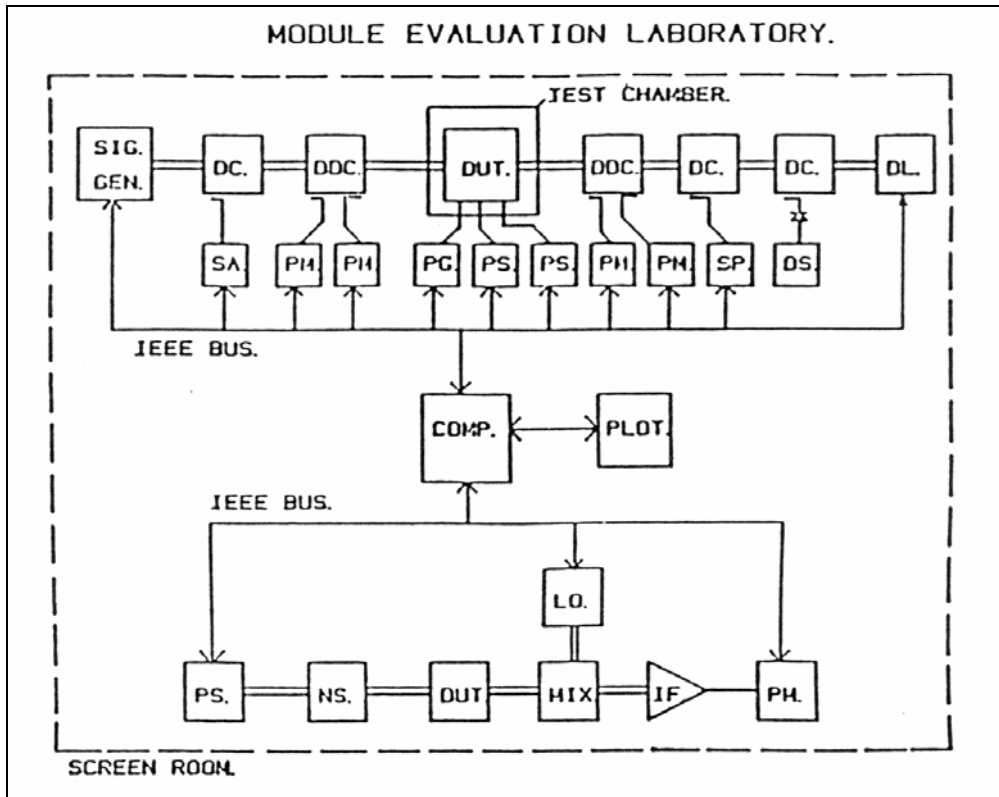


FIGURE 2.1.1 - BLOCK DIAGRAM OF MEL

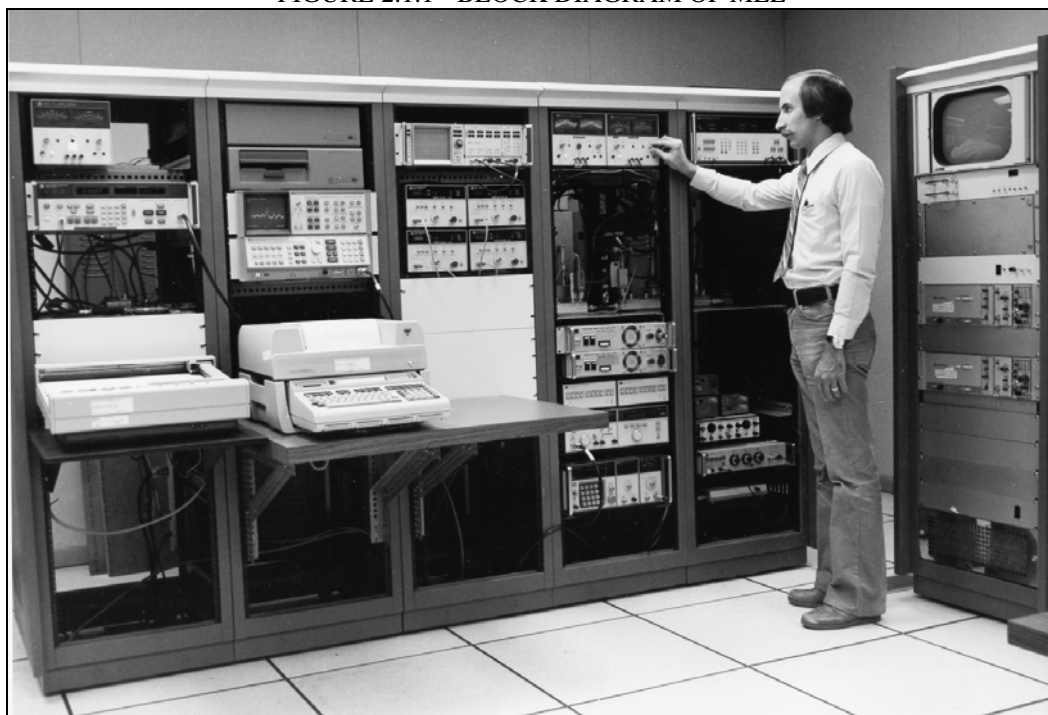


FIGURE 2.1.2 - EARLY PICTURE OF MEL

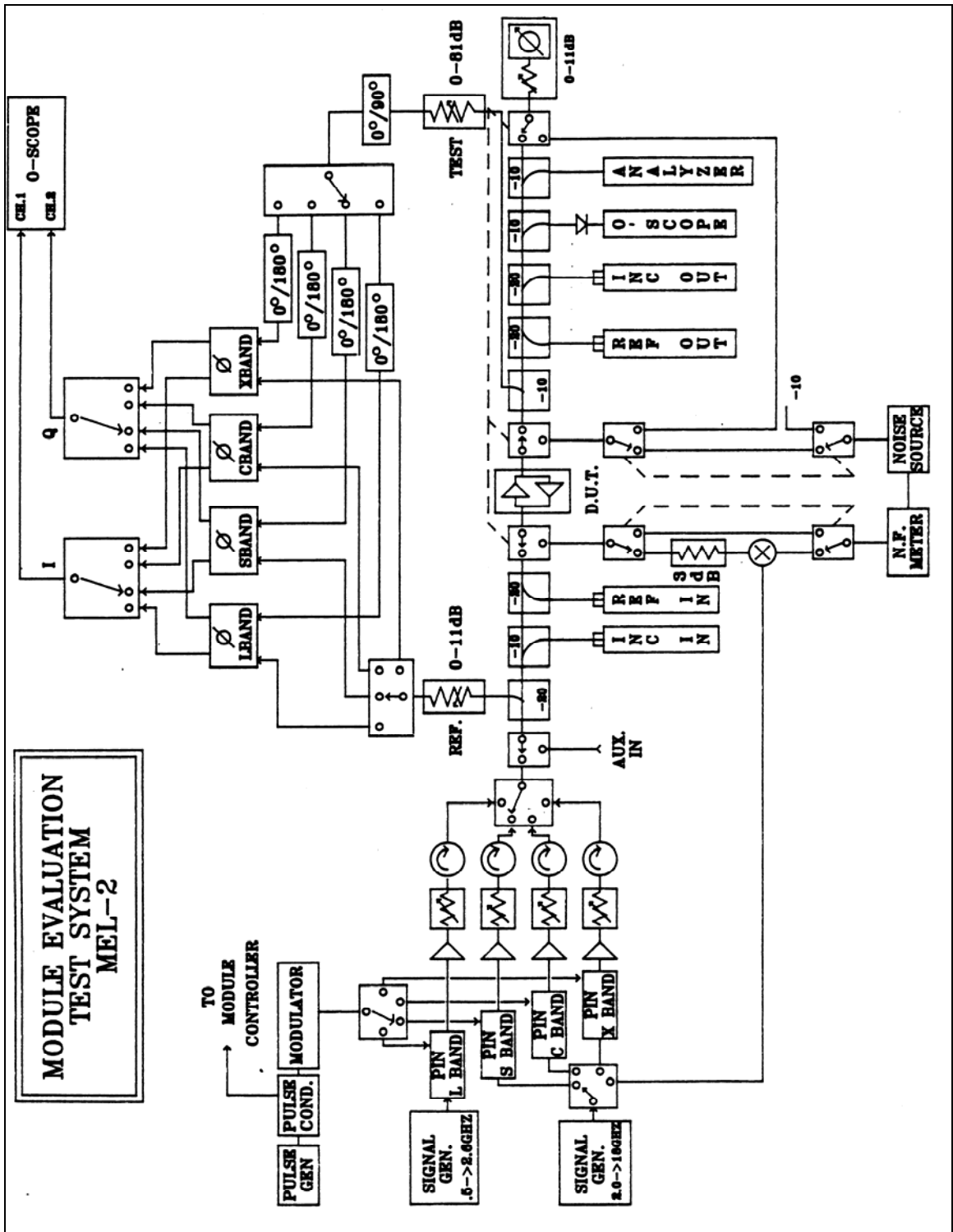


FIGURE 2.1.3 - BLOCK DIAGRAM OF MEL-2

MEL-2 System Specifications

Electrical Characteristics

Operating Mode

1. Remote - Computer controlled for measurement sequence
2. Local - Used primarily for troubleshooting or specialized test

Interface - IEEE 488/HPIB
Nominal Measurement Time - 10 sec./data pt.
DC Bias Control 0 - 60 V
 0 - 12 A

Primary Power

Voltage	120 Vac \pm 10%
Number of Breakers	Four at 20 A Each
Frequency	50/60 Hz
System Power	4800 W (maximum)
System Controller and Peripherals	1000 W (maximum)

Service Conditions

Operation	Continuous
Temperature	0° - +55° C

Physical Characteristics

Dimensions

Height - 71"
Width - 112"
Depth - 33"

Approximate weight - 1800 lbs. (Controller not included)

Environmental

Temperature	
No Load	-30° to 30° C
5 Watt Load	-20° to 30° C

Low Temperature Cycle Time from Ambient - 30 minutes

Source	Thermoelectric Modules
Cooling	Forced Air
Accuracy	\pm 1° C

TABLE 2.1.2 - MEL-2 SPECIFICATION (page 1 of 2)

Noise Figure Measurement

Frequency Range

Fundamental* 10 to 1500 MHz

* Extended Range is accomplished by mixing techniques, see H.P. 8970A Noise Figure Operating and Service Manual.

Nominal Operating Input Power + 10dBm

Dynamic Range 30 dB
Resolution 0.01 dB

R.F. Transmit/Receive

Frequency Range

1.0 to 12.0 GHz (Four Bands)

Maximum Drive Power

[Average Power at 1dB Compression Point]

L-Band - 20 dBm
S-Band - 18 dBm
C-Band - 17 dBm
X-Band - 10 dBm

Dynamic Range (All Bands)

From nominal setting -20dBm ±6 dB

Modulation

Pulse Width 1 us (minimum)
Duty Cycle 50% (maximum)

Pulse Repetition Frequency 1 kHz - 10 MHz

Dynamic Load

VSWR (Nominal)
Load/Source 1.2:1 to 3.0:1
Phase 0° to 360° in 90° steps

Accuracy (Rms - Midband Dynamic Range)

Phase 1.0 deg
Amplitude <0.5 dB

Repeatability (Rms - Midband Dynamic Range)

Phase 0.5 deg
Amplitude 0.2 dB

TABLE 2.1.2 - MEL-2 SPECIFICATION (page 2 of 2)

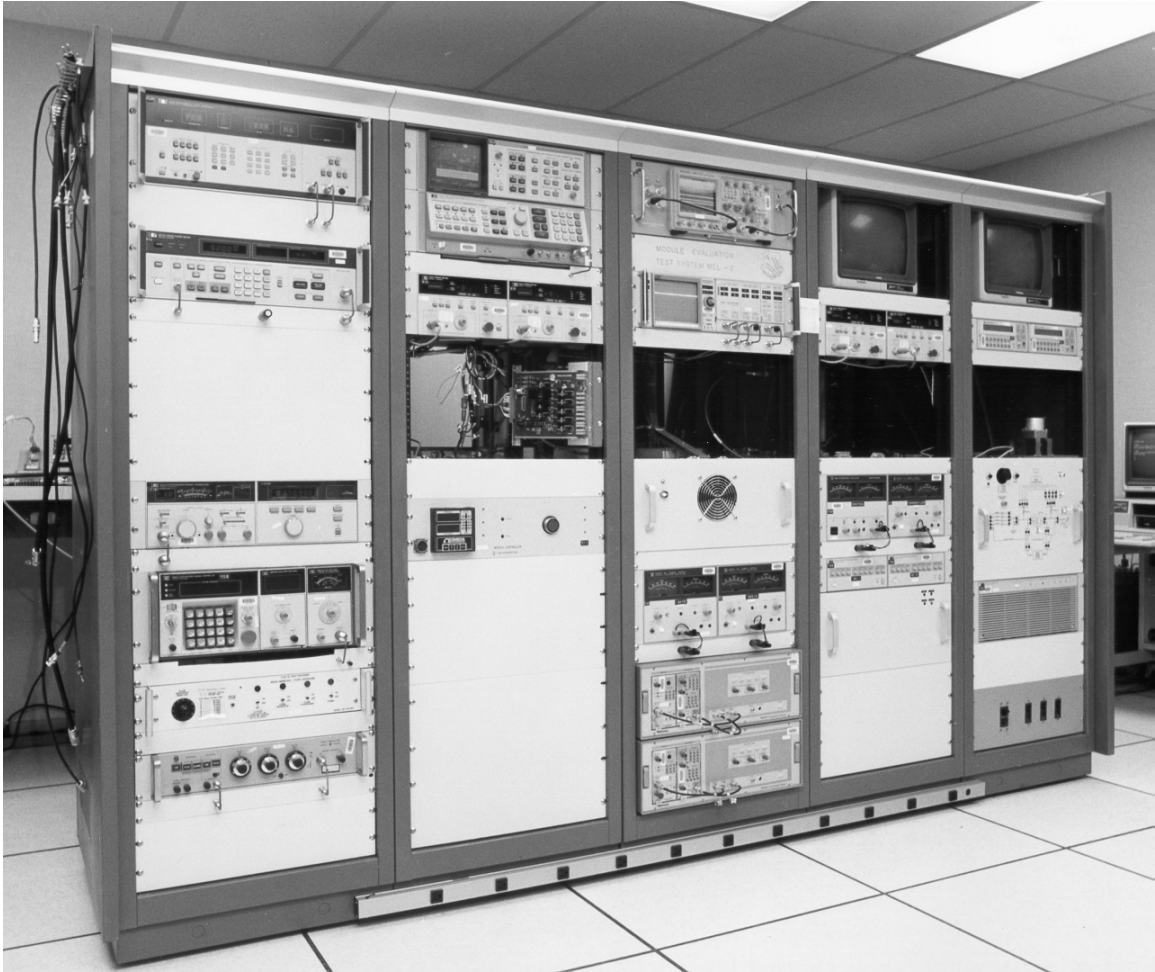


FIGURE 2.1.4 – PICTURE OF MEL-2

2.1.1 PHASE DISCRIMINATOR CIRCUIT

The heart of both MEL and MEL-2 is the use of the phase discriminator to measure the complex (amplitude and phase) transfer function of the DUT. This device takes a reference and test signal (signal sampled prior to and after the DUT respectively) as input and provides an I (in-phase) and Q (quadrature) signal as output. The I and Q voltage signals are then digitized and the computer calculates the DUT's transfer function. The specific phase discriminators used in MEL-2 are made by Anaren (models 2A0755, 2A0756, 2A0757, 2A0758) and operate over an octave bandwidth; L Band 1-2 GHz, S Band 2-4 GHz, C Band 4-8 GHz and X Band 8-12.4 GHz.

The phase discriminator is a direct conversion device that converts the microwave signal directly to base band video using quadrature couplers and diode detectors. The four voltages that are the output of the diode detectors are combined in a video amplifier section to form the I and Q signals. A block diagram of this setup is shown in Figure 2.1.5. A picture of a Phase Discriminator is shown in Figure 2.1.6. With a given test and reference signal with amplitudes A and B respectively and with a phase difference of θ , the following voltages would be the output of an ideal set of diode detectors:

$$V_1 = (A^2+B^2) + 2AB \cos\theta$$

$$V_2 = (A^2+B^2) - 2AB \cos\theta$$

$$V_3 = (A^2+B^2) + 2AB \sin\theta$$

$$V_4 = (A^2+B^2) - 2AB \sin\theta$$

The video section then converts these four voltages to I and Q voltage signals by performing the following math functions.

$$I = V_1 - V_2 = 4AB \cos\theta$$

$$Q = V_3 - V_4 = 4AB \sin\theta$$

With these two equations, the amplitude and phase transfer function of the DUT can be calculated. With the added priori knowledge of the input power to the device, the output power can also be calculated. Unfortunately, there is no such thing as an ideal phase discriminator. The “real” version has errors and limitations. To correct for these errors, a technique developed by Atlantic Research Corporation is utilized. This technique utilizes measured and calculated coefficients in a matrix that is accessed during the measurement process. The formula to model these errors are as follows:

$$I/B^2 = L_1 + L_2 + L_3R \cos\theta + L_4R \sin\theta$$

$$Q/B^2 = H_1 + H_2 + H_3R \cos\theta + H_4R \sin\theta$$

Where:

- A = DUT output signal amplitude
- B = DUT input signal amplitude
- R = A/B
- θ = DUT input to output relative phase
- L = modeling coefficients for I channel
- H = modeling coefficients for Q channel

Details of this technique are described in two papers presented to the Automated RF Techniques Group at the Spring 86 and Spring 87 conferences. The papers were “Coherent (I/Q) Detector Performance Under Extended Drive Signal Conditions” and “Application of Phase Discriminator Error Model to Pulsed RF Measurement System Calibration” respectively.

Because of the use of non-linear devices (diodes) as the voltage detectors, various distortions occur during the measurements. Two sources of distortions are most common; 1) providing too much or too little power to the input of the phase discriminators (operating the diode in the non-linear range), and 2) providing an unbalanced set of inputs. In figure 2.1.7, these non-linear effects are illustrated. The potential resultant phase errors are illustrated in figure 2.1.8.

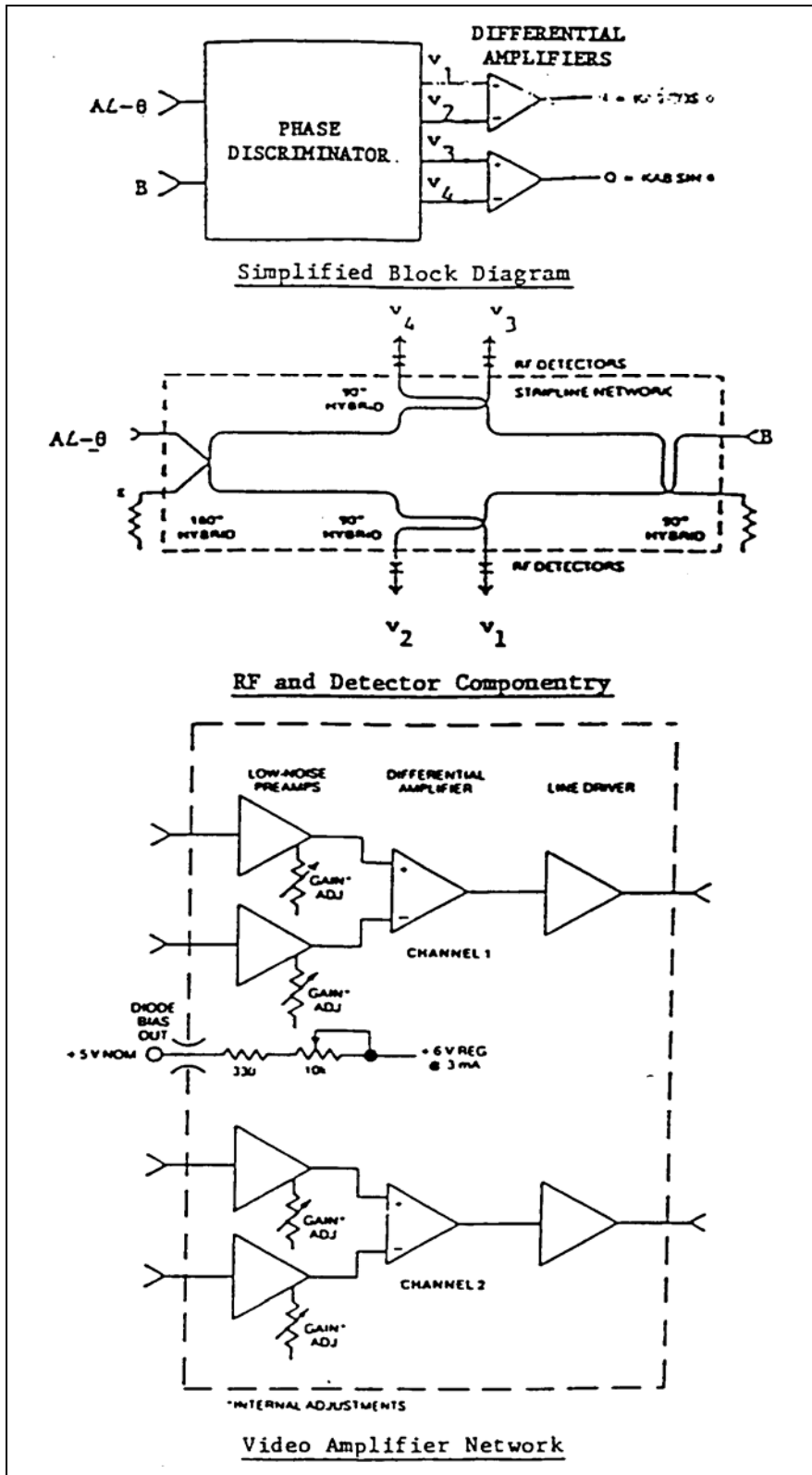


FIGURE 2.1.5 - BLOCK DIAGRAM OF PHASE DISCRIMINATOR

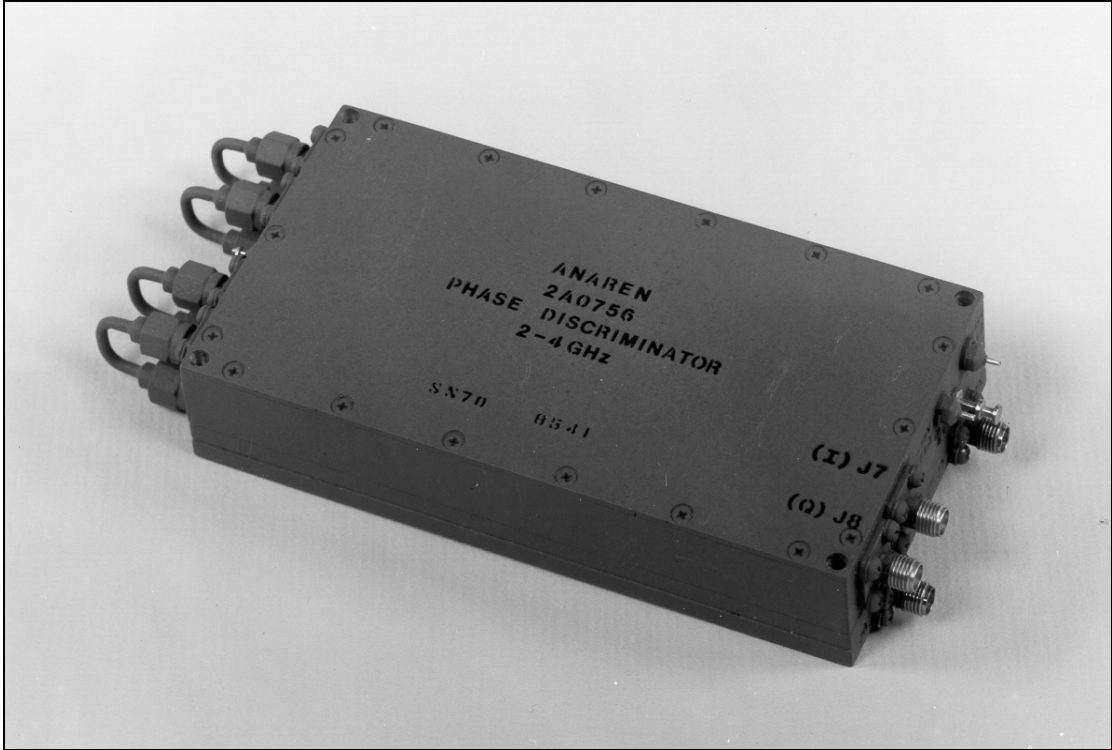


FIGURE 2.1.6 - PICTURE OF A PHASE DISCRIMINATOR

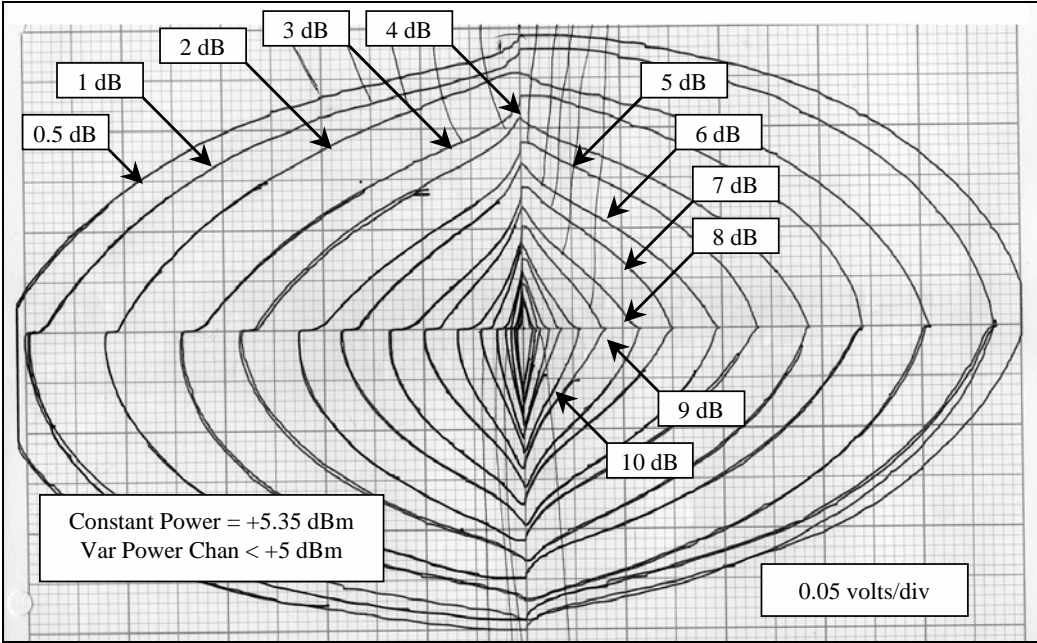


FIGURE 2.1.7 - VOLTAGE OUTPUTS VERSE POWER INPUTS

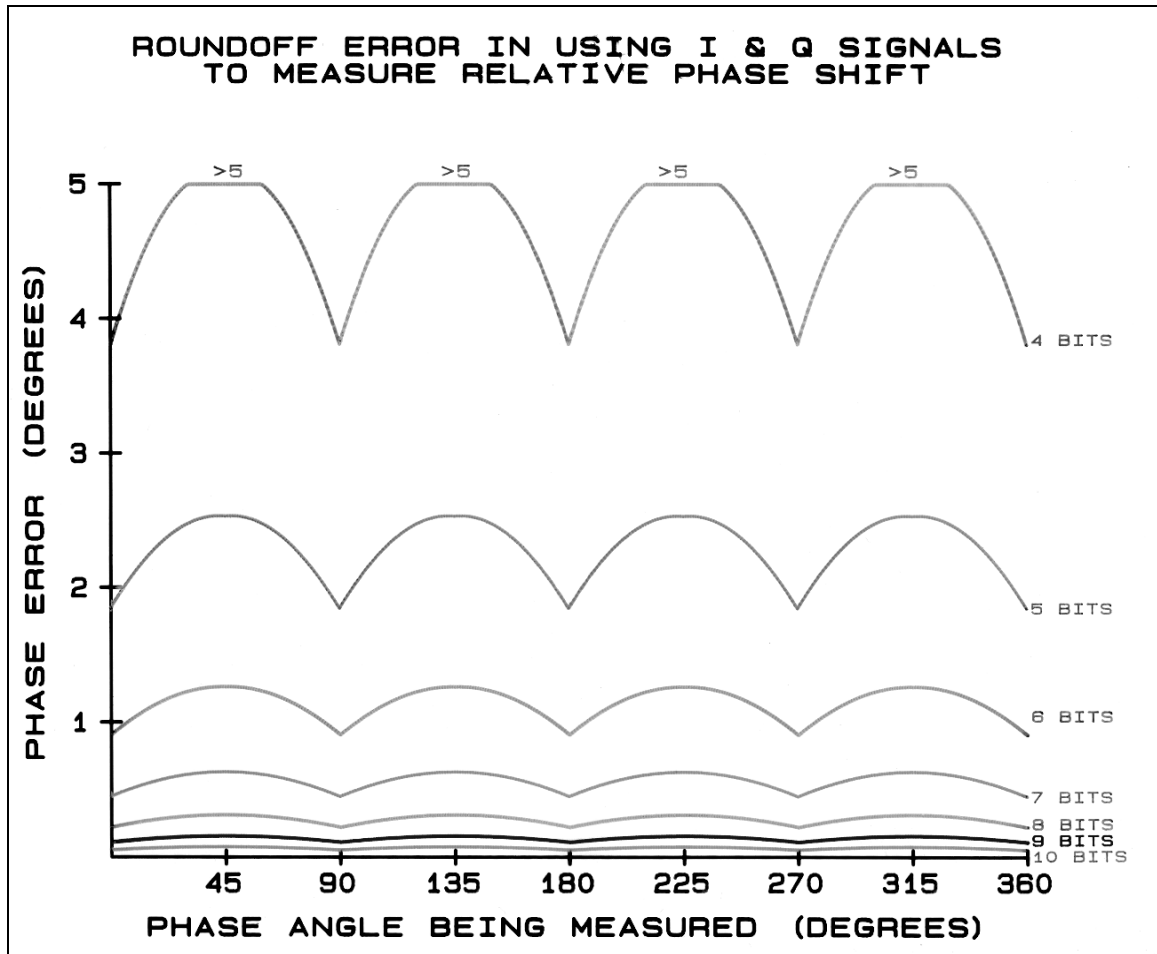


FIGURE 2.1.8 – MEASURED PHASE ERROR RESULTING FROM ROUND OFF ERRORS

2.1.2 RADAR SYSTEM EMULATION

One of the important points to remember is that the reason for testing in a pulsed mode is to determine how the DUTs will operate in a fielded system. What better way to determine that operation, than to operate the devices as they would be operated in such a system. To accomplish this operation, the system has been configured to provide the electrical and mechanical environment that the DUT is projected to see in a fielded system. The environments include various parameters in the dimensions of temperature, atmospheric pressure, load VSWR (Voltage Standing Wave Ratio), bias voltages, microwave excitation (waveform and drive level), and DUT state control. All of which, except the temperature and atmospheric pressure environments, are computer controlled.

2.1.2.1 TEMPERATURE AND ATMOSPHERIC PRESSURE

The temperature and atmospheric pressure environment is controlled manually using various methods. All methods involve the addition of a special apparatus that must be inserted into the basic MEL-2 configuration for the specific experiment. Available equipment includes a thermal plate, an oven, and a space chamber.

A picture of the Thermal Plate is shown in Figure 2.1.9. The plate will be replacing the nitrogen bath technique described in Section 3.3.4. A combination of liquid nitrogen and heating coils are embedded within the base plate to maintain the proper temperature. Also, the thick baseplate allows for holes to be drilled and tapped to mount DUTs.

Figure 2.1.8 shows a picture of the space chamber. The chamber has two access ports that can provide DC, RF, and gas/liquid interface points to experiments within. Also, shown in the picture is the first item that was tested. Four “dummy” MODVAL T/R modules were placed in an emulated space environment to test a new heat removal technique. That experiment is fully documented in RADC-TR-90-56 entitled “Transmit/Receive Module Thermal Dissipation Measurements”.

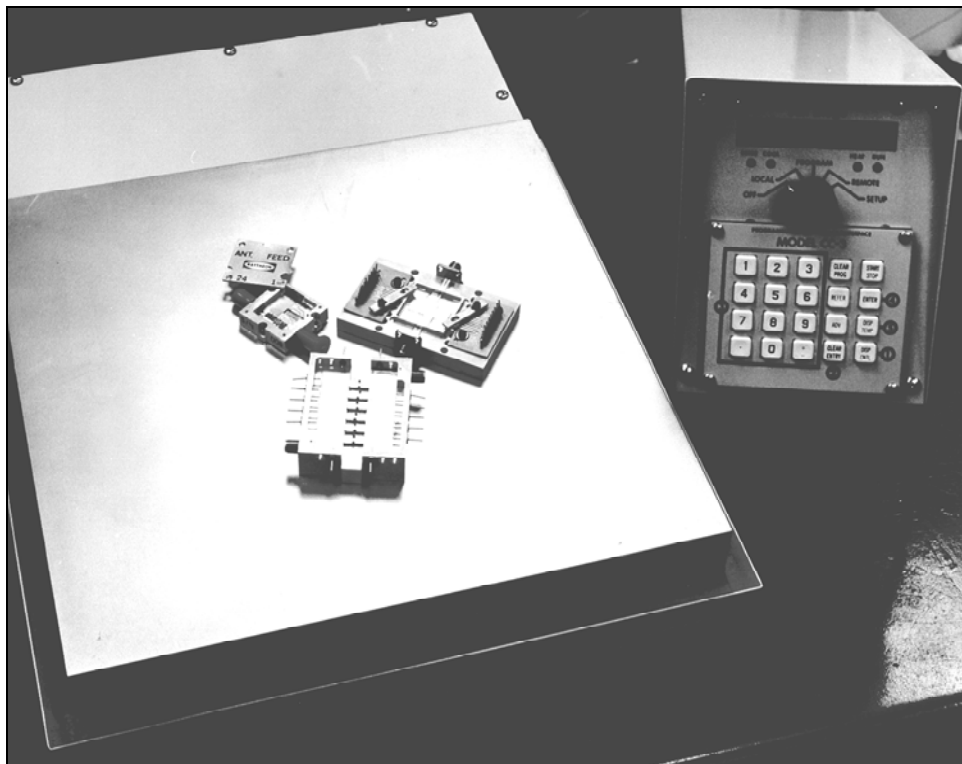


FIGURE 2.1.9 – PICTURE OF THERMAL PLATE

* RADC-TR-90-56 is Distribution limited to U.S. Government and Their Contractors - Export Controlled.



FIGURE 2.1.10 – SPACE CHAMBER WITH THERMAL TEST FIXTURE

2.1.2.2 LOAD VSWR

To provide a variable complex load on the antenna port of the DUT, a dynamic load was developed and implemented. This load provides VSWRs from 1.2:1 to 3.0:1 to emulate the load that a T/R module would experience in a phase array while it is electronically scanned off bore sight. The apparent VSWR that a DUT would see in an actual system is the signal coupled into its antenna element from an adjacent element that is electrically not one half wave length away in phase (due to phase shifter settings needed to scan the beam). This effect is called mutual coupling. In MEL-2 this VSWR is emulated by reflecting a proportionate amount of the DUT's signal back into itself. The device that performs this function is called a dynamic load and is made up of a programmable attenuator, a coaxial phase shifter and a short circuit. Figure 2.1.11 provides a pictorial representation of this circuit. Note that the programmable attenuator sets the diameter for the VSWR circle on the Smith chart and the coaxial phase shifter moves the complex impedance around that circle. A picture of the phase shifter with a stepper motor mounted on it is shown in Figure 3.1.12.

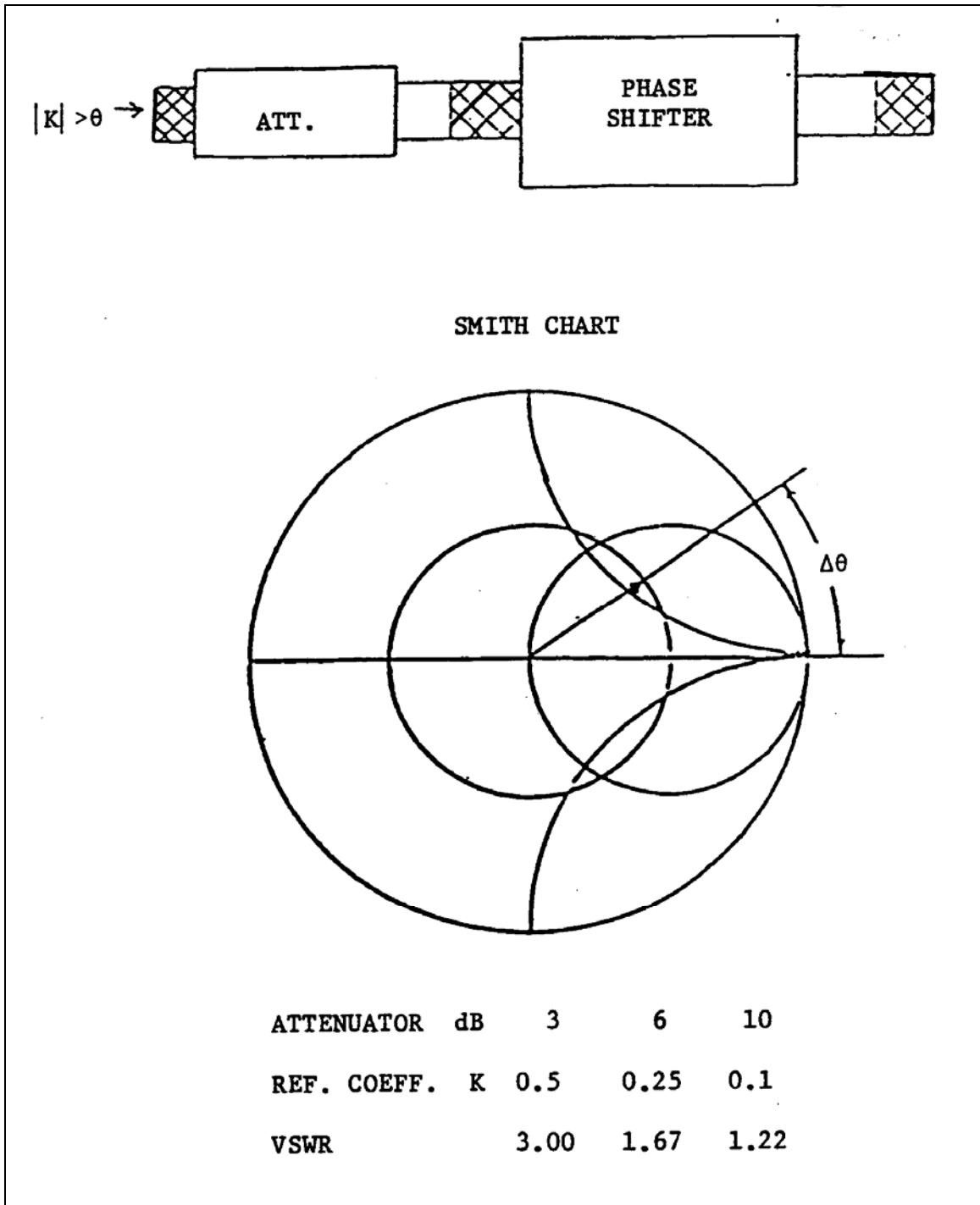


FIGURE 2.1.11 – DYNAMIC LOAD CIRCUIT

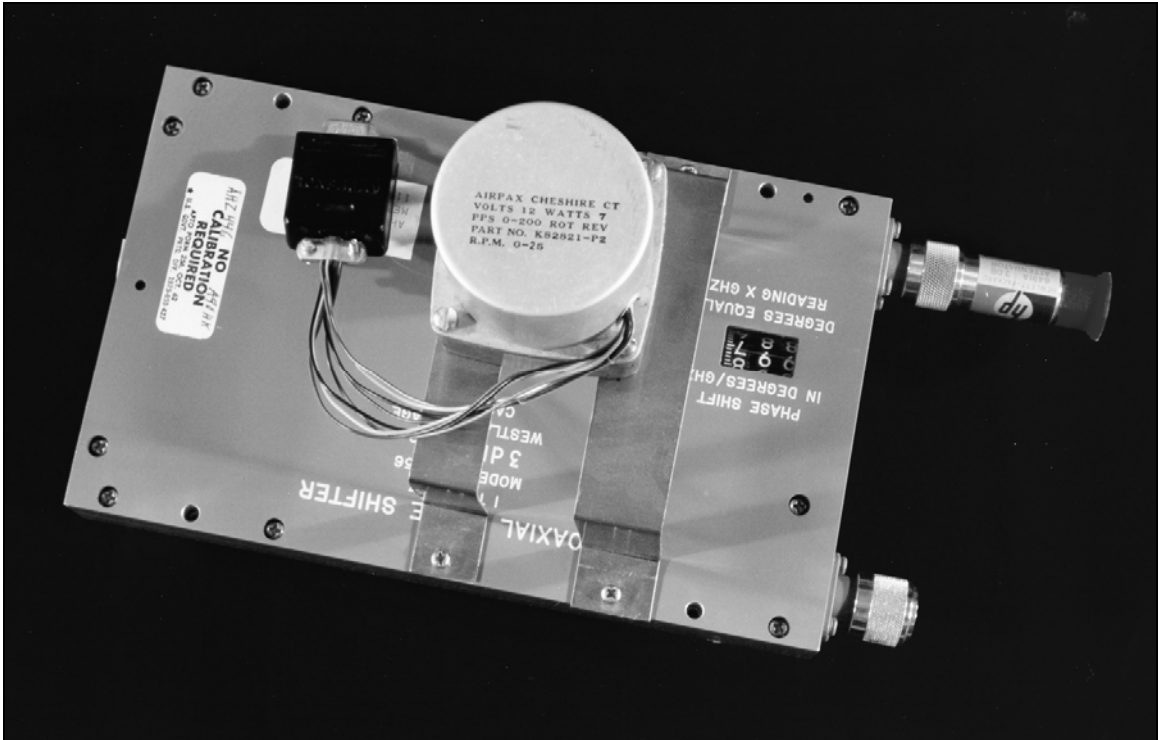


FIGURE 2.1.12 – DYNAMIC LOAD WITH STEPPER MOTOR CONTROLLED PHASE SHIFTER

2.1.2.3 BIAS VOLTAGES

The test system has individual control, via the computer, to adjust up to 4 different bias voltages. Generally these supplies will be used to provide a negative gate bias, a positive drain bias, a negative control circuit bias, and an additional miscellaneous voltage. Each power supply is controlled by the computer via the IEEE-488 bus, commonly known as HP-IB, as well as having a capability to be manually set. Each power supply provides 200 watts of DC with a maximum capability of up to 60 volts or 12 amps.

The current system configuration has the capability of testing a DUT under brown out conditions (reduced bias voltages) and under voltage stress conditions (increased voltages). In addition, provisions have been made to subdivide the four basic voltages to support special purpose regulation, current monitoring and bias switching (i.e., drain pulsing). An example of such a special regulator board is the one presented in Figure 2.1.13. This board provided up to 8 different regulated biases; four positive and four negative. It was specifically designed for use as a regulator board in life testing T/R modules at S Band and C Band, but was later adapted to test C Band power amplifiers as well.

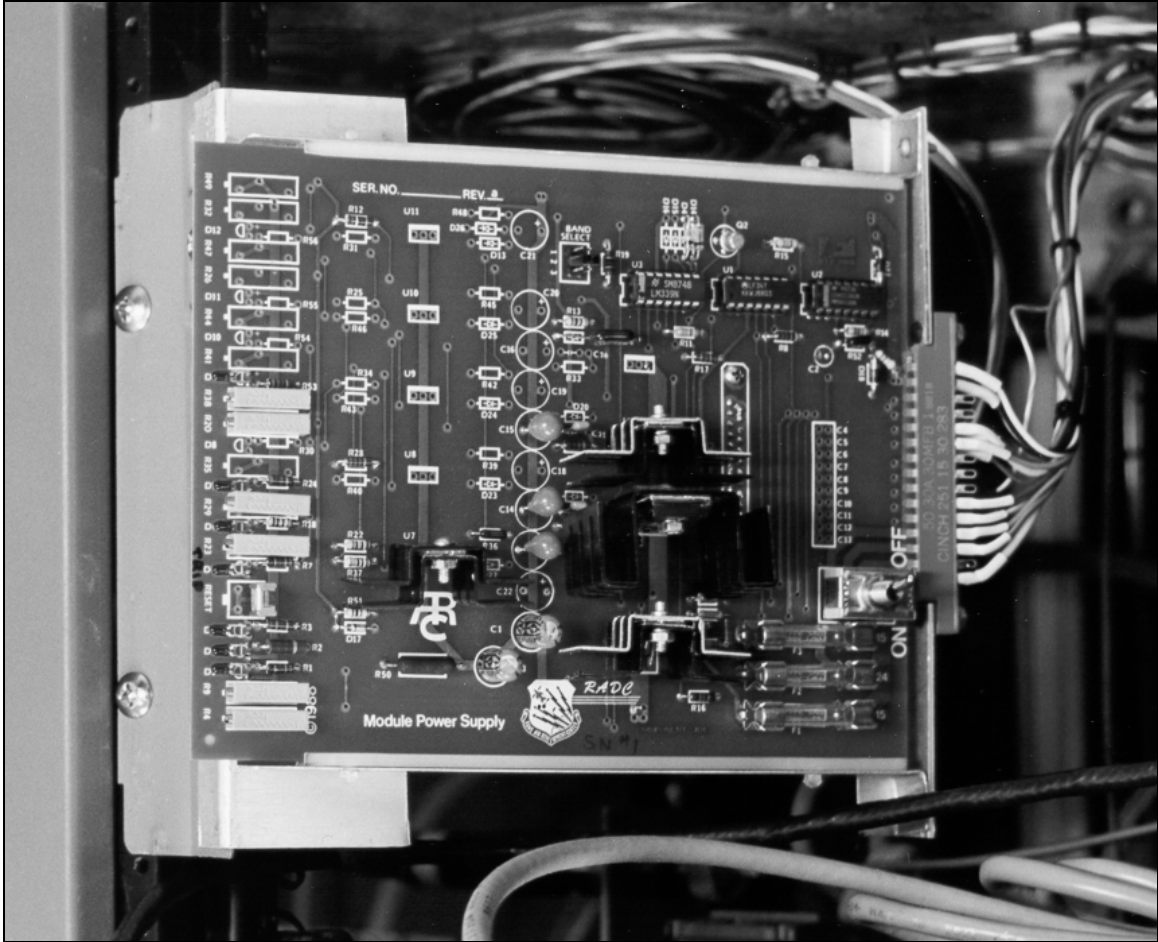


FIGURE 2.1.13 – DC BIAS BOARD FOR S & C BAND DUTS

2.1.2.4 MICROWAVE EXCITATION

The test system has the capability of providing discrete frequency and complex waveforms. In all cases, the drive power, pulse width and duty cycle can be varied. The waveform can be controlled using either manual controls or the computer commands. The most common waveform for characterization of a DUT is a discrete frequency pulsed waveform with a constant pulse width, duty cycle and power level at set frequency points across the measurement bandwidth.

To provide a LFM (Linear Frequency Modulation) waveform, there are two exciters available at S Band - one built by RCA in the late 1970's and another built in-house during the mid 1980's. The RCA exciter is described in the "Operation and Maintenance Manual for the Wideband Waveform Generator and Signal Processor" (not published). A highlight of its operational capabilities is presented in Table 2.1.3 and a picture of it being used in an experiment is shown in Figure 2.1.14. The LFM generator built in-house is described as an appendix in the "Module Evaluation Lab (MEL-2 Report)" previously mentioned. This in-house built LFM generator was collocated with a circuit called a pulse conditioner. The pulse conditioner was designed to take the test system

master clock pulse and provide two output pulses called drain enable and RF enable. The purpose of such conditioning is to provide a pulse within a pulse. It is occasionally desirable to have one of the pulses to encompass the other pulse by a given amount of time (i.e. 10 usec or so). An example is shown in Figure 2.1.15. The RF is then pulsed using the RF pulse enable to drive a PIN diode switch. Both of the generators utilize a VCO (Voltage Controlled Oscillator) driven by a saw tooth waveform to create the LFM. A picture of this box is shown in Figure 2.1.16.

For complex waveforms, there is an AWS (Arbitrary Waveform Synthesizer) available. The AWS allows the user to define the waveform via a mathematical description, which is then fed into memory by the computer controller. Then, through repetitive scanning of the memory, the waveform is generated via a D/A converter.

Characteristic	Description
Wideband Waveform Output	Linear FM up chirp
Pulsewidth	48 \pm 0.1 microseconds
Sweep Bandwidth (3 dB)	300 MHz, minimum
Center Frequency	3,300 MHz
Output Level	+10 dBm, minimum
Pulse-to-Pulse Phase Coherence	\leq 3 degrees RMS with respect to cw reference
Pulse Jitter	\leq 100 picoseconds RMS
Time Sidelobes	-37 dB peak for \pm 0.2 μ s window -32 dB peak for \pm 0.8 μ s window
Pulse Rate	7.8125 to 2,000 Hz in 256 steps or as designated in remote mode
Sweep Rate	6.25 MHz per microsecond
Pulse Pair Spacing	10 to 3,000 microseconds in 0.1 μ s steps
Impedance	50 ohms
VSWR	1.5:1, maximum
Spurious Output	60 dB, minimum
Correlation Reference Output	Linear FM up chirp
Pulsewidth	51.2 \pm 0.1 microseconds
Bandwidth	320 MHz, minimum
Center Frequency	3820 MHz
Output Level	+10 dBm, nominal
Impedance	50 ohms
VSWR	1.3:1, maximum

TABLE 2.1.3 – WIDEBAND WAVEFORM GENERATOR CAPABILITIES

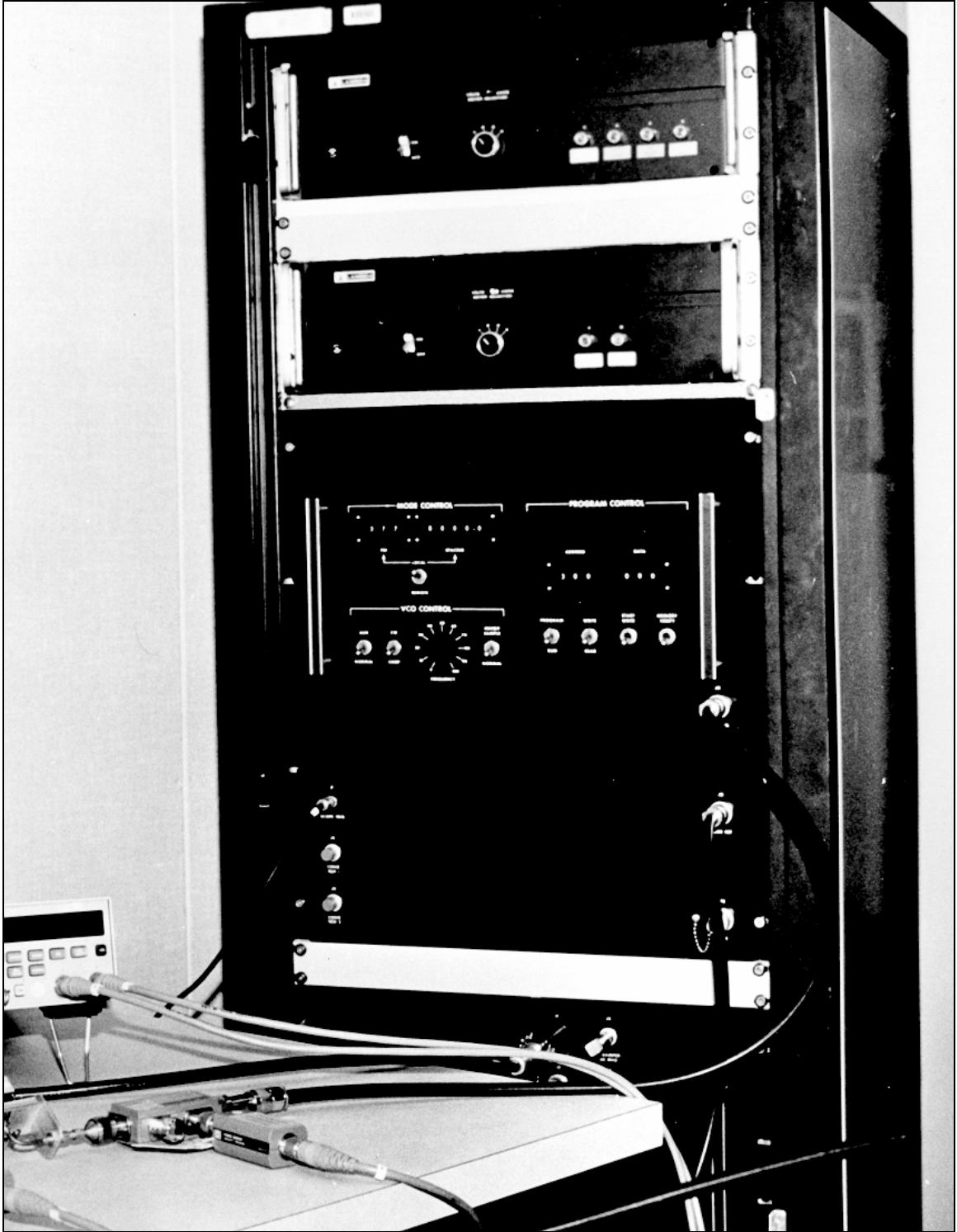


FIGURE 2.1.14 – WIDEBAND WAVEFORM GENERATOR

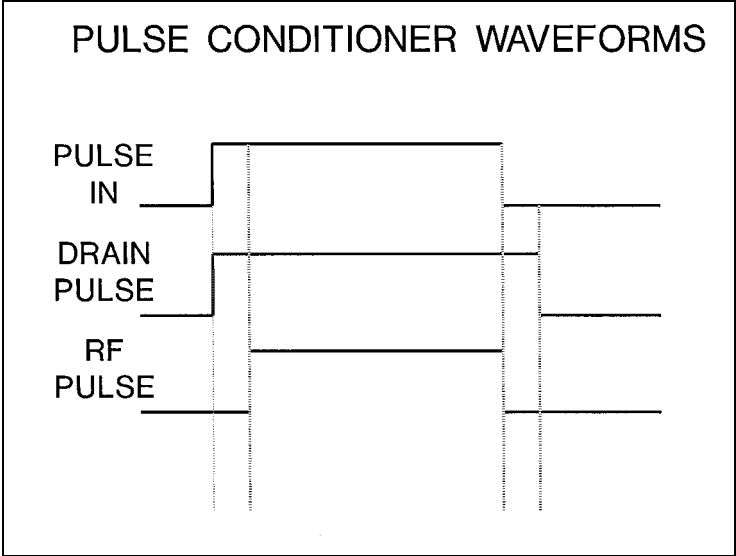


FIGURE 2.1.15 – PULSE CONDITIONER WAVEFORM



FIGURE 2.1.16 – PULSE CONDITIONER & LFM WAVEFORM GENERATOR

2.1.2.5 DUT STATE CONTROL

The DUTs that were tested tended to require very complex control schemes in order to be fully characterized. As such, specialized controllers need to be developed for each type of DUT. An example of such a controller is one developed in-house to control the GE C

Band module. This module has a CMOS beam steering controller built-in that accepts digital commands that are transmitted to the module using a frequency shift keying (FSK) modulation technique. To create FSK commands, a circuit was fabricated that continually dumped commands that had been previously stored on an EEPROM. A picture of this apparatus is shown in Figure 2.1.15.

Other controllers include the manual controller built to control simpler modules. A good example of this type of controller is shown in Figure 2.1.16. It was no more than a box with a voltage regulator, a drain switch for automatically toggling the drain bias, and toggle switches for changing the phase shifter settings.



FIGURE 2.1.17 – C BAND MODULE CONTROLLER

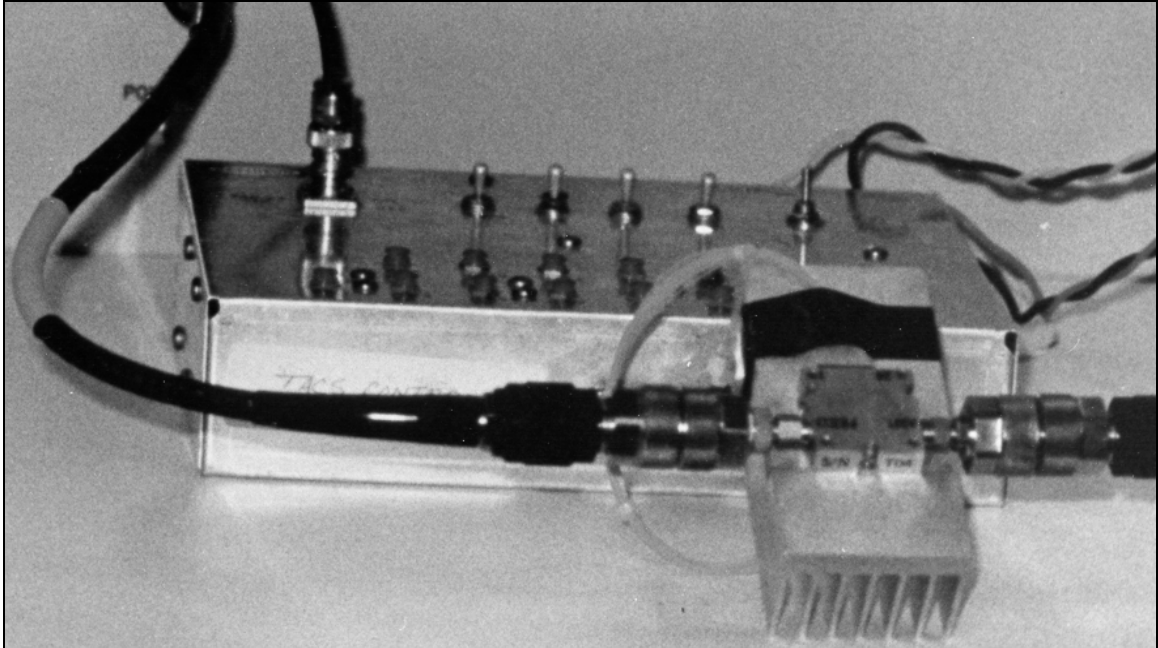


FIGURE 2.1.18 – L BAND MODULE CONTROLLER

2.2 LONG TERM PERFORMANCE TEST SYSTEM (MELTS)

This system is designed to operate a number of devices simultaneously for long periods of time under specified conditions. It is used to perform the second of three tests that a DUT undergoes when being subjected to life testing. The first and third tests involve the characterization of the DUT on the large signal pulsed test system (MEL-2).

The details of MELTS and how it operates is the subject of a unpublished RADC technical (see bibliography). The test system is designed to operate T/R modules and sub-components under both DC only and RF operating conditions within an emulated radar environment. Performance data of the devices under test are continuously monitored and recorded for later evaluation. The control of the test system is fully automated using a Hewlett Packard series 200 computer (HP 9836). A picture of the first version of the life test system is shown in Figure 2.2.1. A picture of version 2, with greater testing capabilities is shown in figure 2.2.2 with a corresponding block diagram presented in Figure 2.2.3.

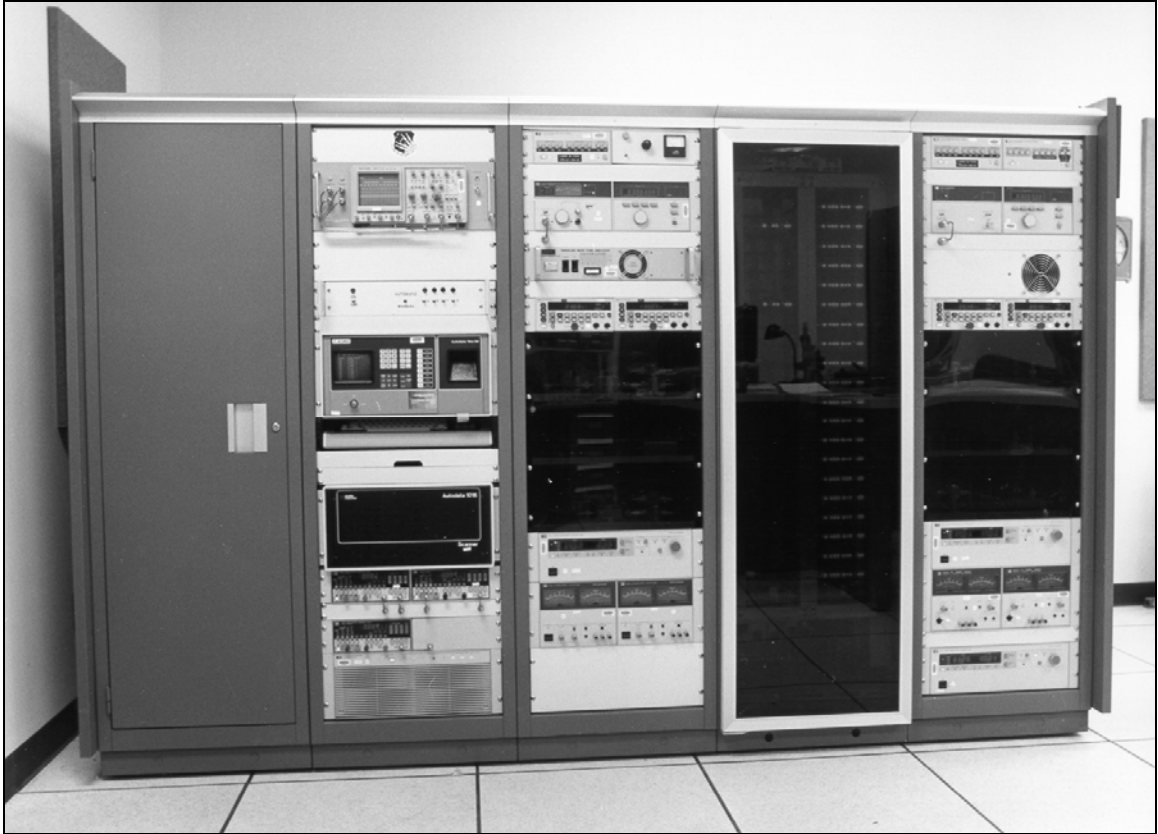


FIGURE 2.2.1 – LONG TERM PERFORMANCE TEST SYSTEM VERSION 1

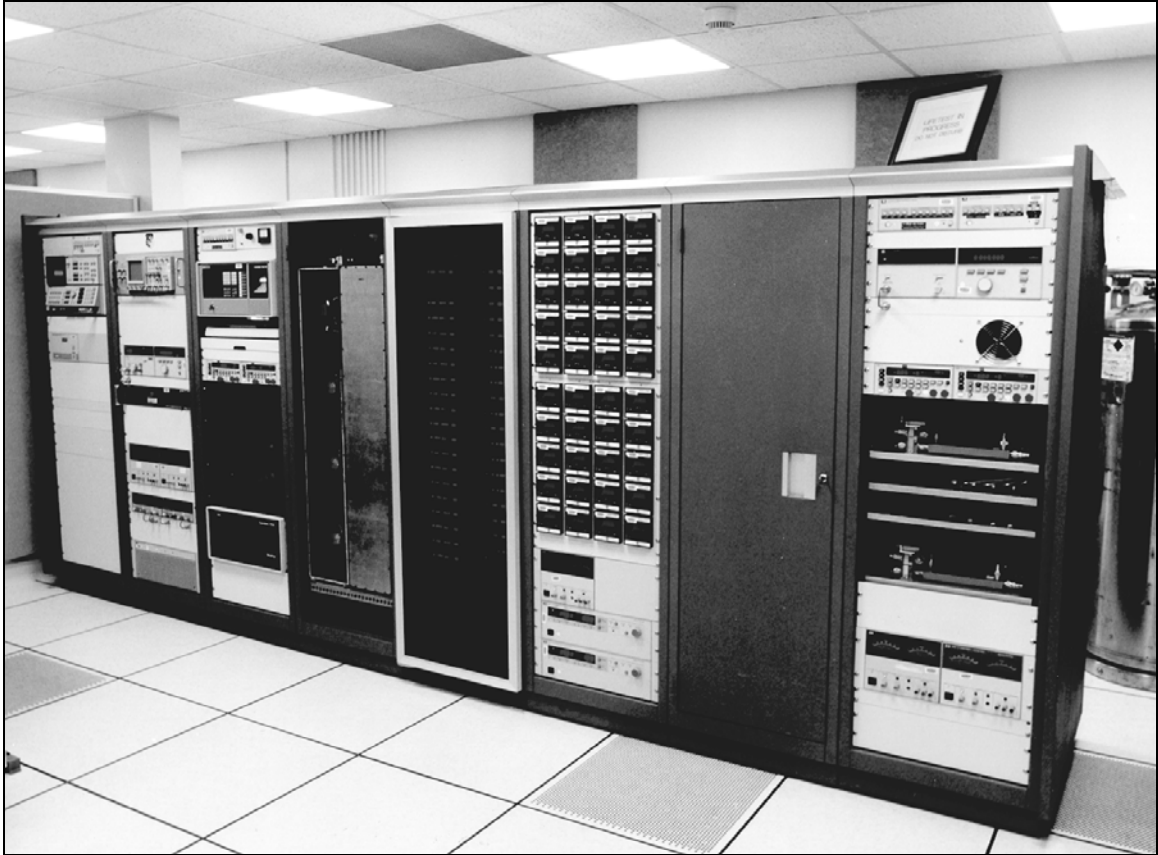


FIGURE 2.2.2 - LONG TERM PERFORMANCE TEST SYSTEM VERSION 1

Version 2 of MELTS, the last version to be used for testing devices, was configured to test up to 40 devices. A maximum of 20 of these could be tested under microwave operating conditions. Hardware limitations constrained the microwave testing to a maximum of ten wide band (S through X Band) and a maximum of ten C band devices. The first test conducted (using version 1 of the system) had 20 C Band modules (10 DC and 10 RF) and 20 S Band modules (10 DC and 10 RF). Table 2.2.1 shows the specific capabilities of version 2 of the system, which was being utilized as part of the DARPA MIMIC program to test the reliability of MMICs and T/R modules. This configuration was a compromise between the desire to constantly monitor the performance of each device and the expense involved in capital equipment. The DUTs were exercised in both transmit and receive modes, including operating the phase shifter bits during transmit mode. A diagram indicating the timing of this exercising is shown in Figure 2.2.4. Measurements were at regular intervals to determine how various operating parameters changed as a function of time (i.e., 4 months, 9 months, 1 year, etc.). The parameters monitored included the drain current, the gate current, the base plate temperature, and the microwave gain of the DUT.

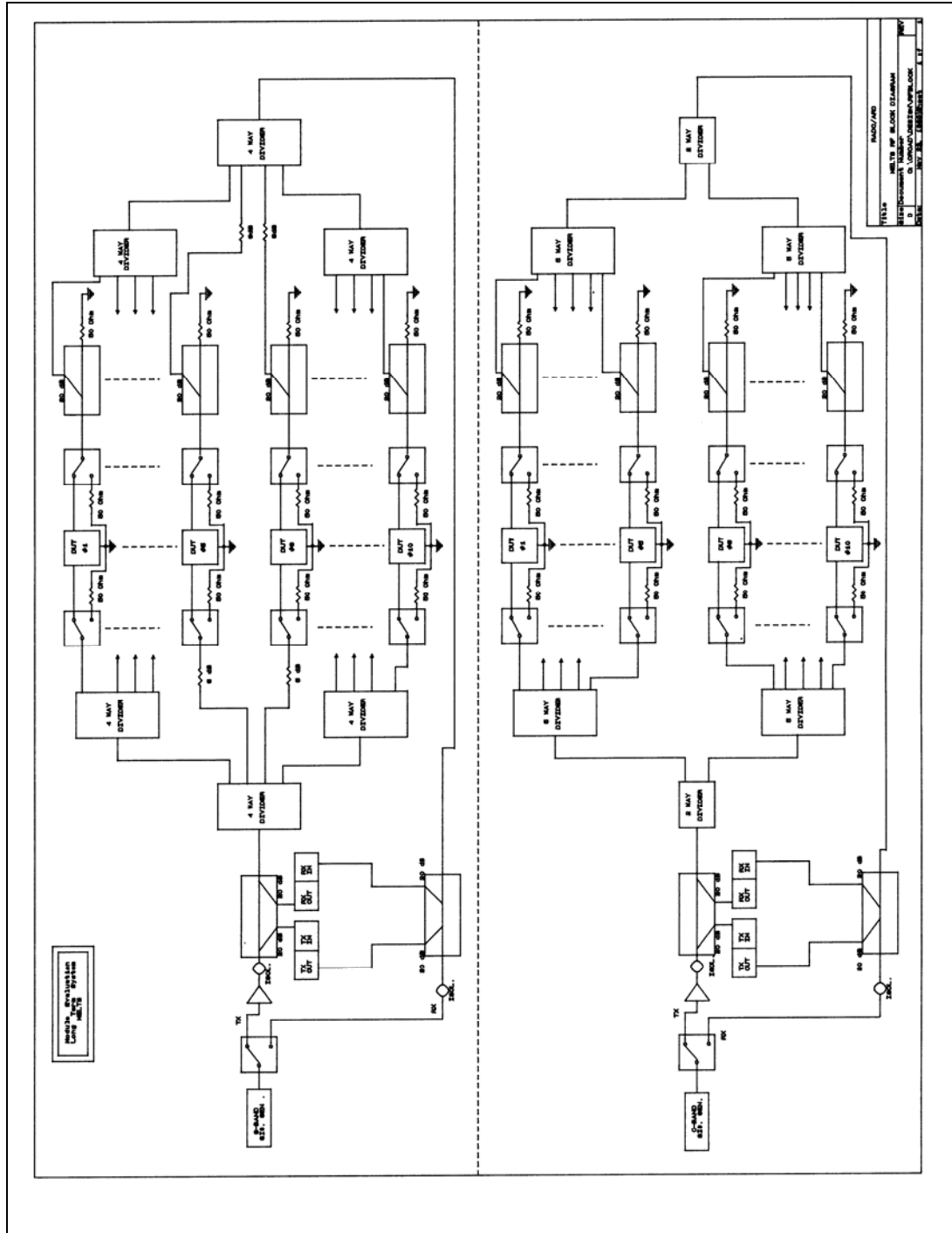


FIGURE 2.2.3 – BLOCK DIAGRAM OF LONG TERM PERFORMANCE TEST SYSTEM VERSION 2

1. <u>Electrical Characteristics</u>	
a. <u>Operating Mode</u>	
1. Remote	- Fully automated controlled operating sequence and data acquisition.
2. Local	- Used primarily for trouble shooting or system verification
b. <u>Interface</u>	
1. IEEE 488	
2. RS-232	
c. <u>Primary Power</u>	
Voltage	120 VAC ±10%
Frequency	50/60 Hz
System Power	6500 watts (maximum)
System Controller and Peripherals	800 watts (maximum)
Service Conditions:	
Operation	Continuous
Temperature	0° to +55° C
2. <u>Physical Characteristics</u>	
a. <u>Dimensions</u>	
Height	71"
Width	112"
Depth	33"

TABLE 2.2.1 – LONG TERM PERFORMANCE TEST SYSTEM VERSION 2 SPECIFICATIONS
(PAGE 1 OF 2)

b. Approximate weight 1900 lbs.
(controller not included)

c. Maximum Test Article Quantities

40 modules total

1. 20 S-band
 - 10 RF applied
 - 10 No RF applied
2. 20 C-band
 - 10 RF applied
 - 10 No RF applied

3. Operational Characteristics

a. Frequency Range

2.0 to 6.2 GHz

b. Average Drive Power

Tx mode 0 dBm

Rx mode -25 dBm

c. Drive Modulation

CW only

d. Power Meter Accuracy

<0.1 dB

Repeatability < Accuracy specification (see 438A manual,
Part# 0438-90015)

e. Autodata Accuracy

Voltage/Current $\pm 0.005\%$ of Reading

Temperature < 0.5° C

Repeatability $\pm 0.002\%$ of full scale

Scan time for 140 channels \rightarrow 11 seconds

TABLE 2.2.1 – LONG TERM PERFORMANCE TEST SYSTEM VERSION 2 SPECIFICATIONS
(PAGE 2 OF 2)

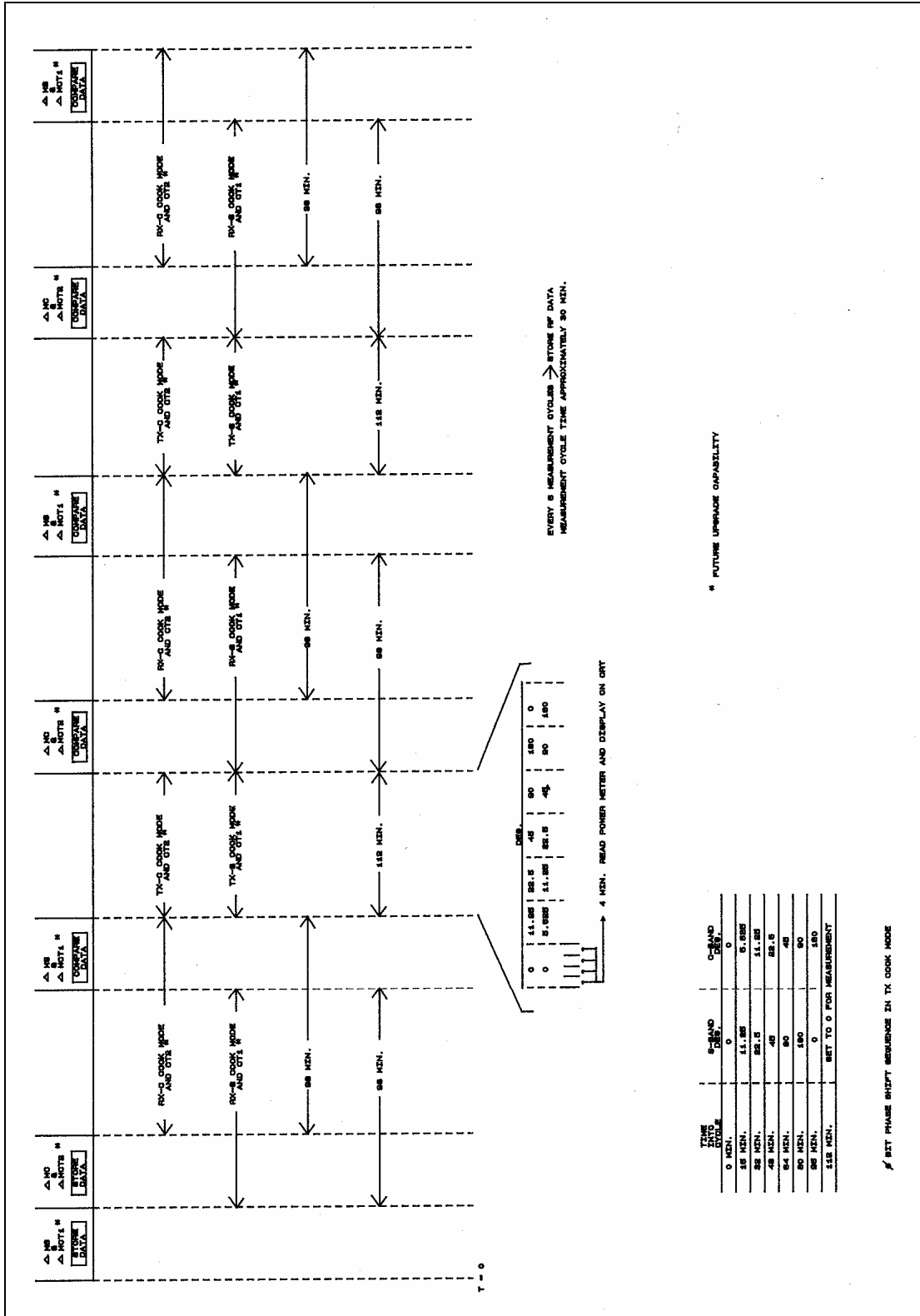


FIGURE 2.2. LIFE TEST SYSTEM TIMING DIAGRAM

2.2.1 DATA ACQUISITION AND CONTROL

The control of the test system is fully automated using a Hewlett Packard series 200 computer (HP 9836). The operating system used was HP Basic 4.0. A picture of the computer is shown in figure 2.2.5. A typical screen showing the status of the devices being tested is shown in figure 2.2.6. Performance data of the devices under test are continuously monitored and recorded for later evaluation. HP-IB interface boards in the 9836 were used to control and collect data from the various instruments within the system. A data logger, shown in figure 2.2.7, was used to collect temperature data. A multi-programmer was used to command the temperature controllers. The data that is acquired and recorded by this test system is the following:

- DUT gain in dB (microwave only case)
- Frequency of signal (microwave only case)
- DUT drain bias current
- DUT gate bias current
- DUT base plate temperature
- Date/Time of measurement
- DUT operating state

Each record of data is stored on hard disc and is then copied periodically to tape for analysis. Data, although acquired regularly (every four hours), is only recorded on disc every 24 hours, or when a test parameter has changed significantly.



FIGURE 2.2.5 - LIFE TEST SYSTEM CONTROLLER

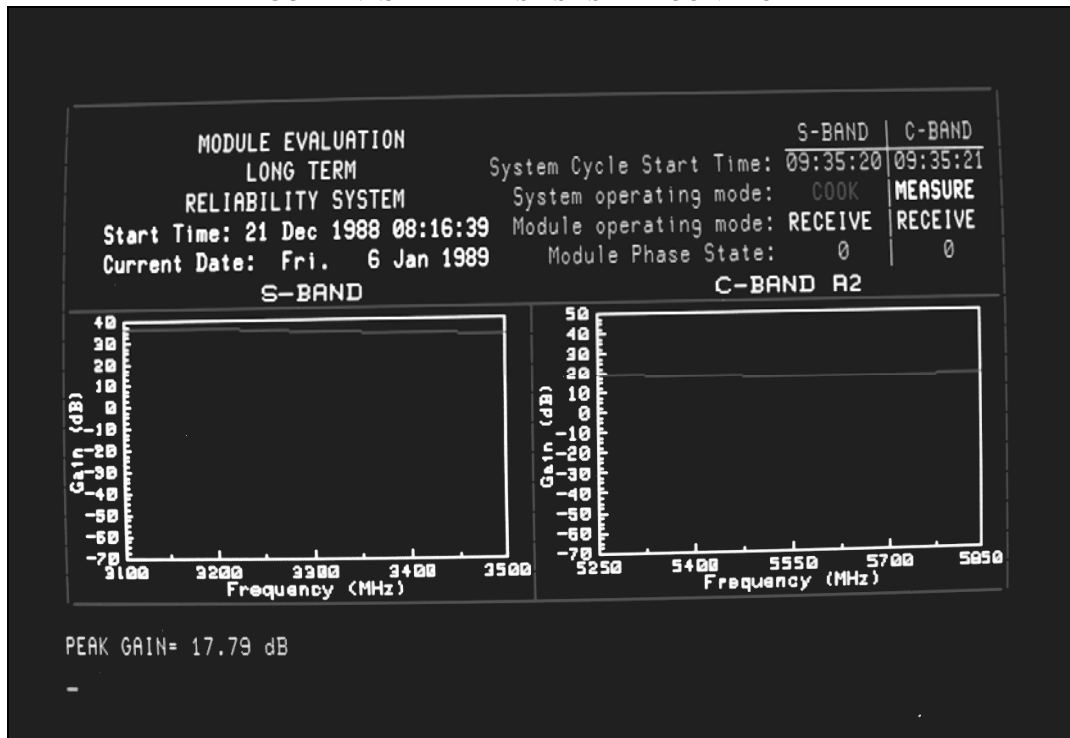


FIGURE 2.2.6 - TYPICAL LIFE TEST SYSTEM DISPLAY

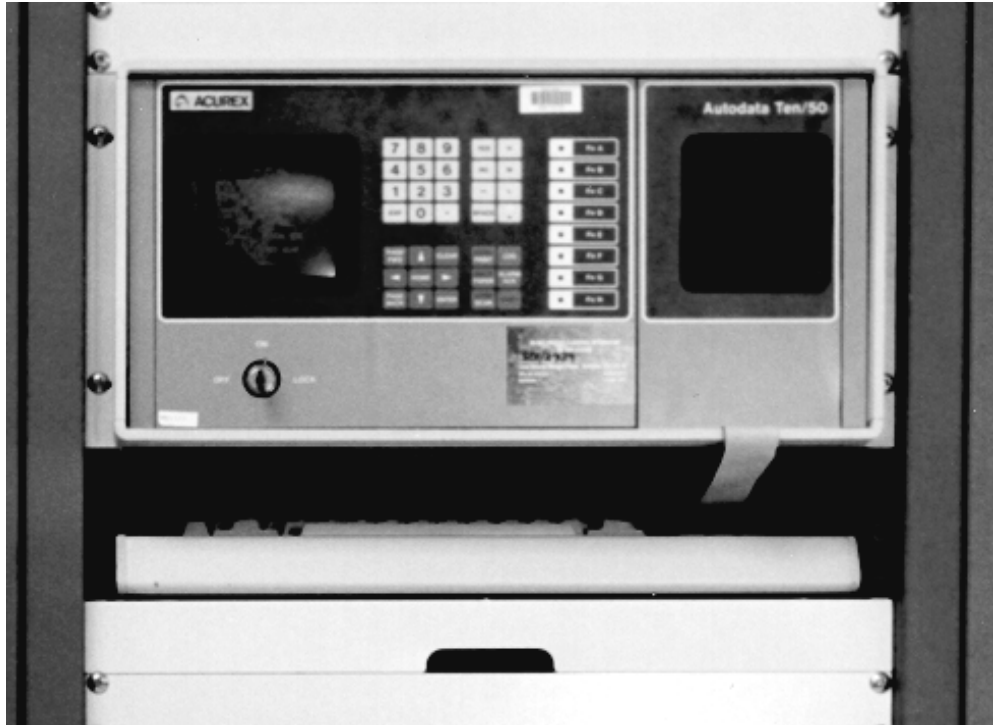


FIGURE 2.2.7 – DATA LOGGER

2.2.2 ENVIRONMENTAL CONDITIONS

The test system was configured to emulate a radar system. The various electrical and environmental conditions could be varied to correspond to conditions that would be experienced in an actual phased array radar system. For the purpose of most tests, which are generally reliability driven, a majority of the conditions were maintained in a constant and benign condition.

In the first version of the test system, the only environmental condition allowed to vary was the temperature. The module's base plate temperature was maintained by limiting the use of convection cooling and/or forced air ventilation. In addition, four resistors were incorporated within the thermal chamber (made from Styrofoam construction insulation) to allow for additional heat to be inserted. This heating technique provided a 25 degree Centigrade variation between the coolest and warmest periods (4 hour temperature cycling). The exact temperature level was dependent on the individual module's efficiency and output power level. Data on the module temperature variations are presented in Section 3.2. A picture of version one's test chamber is shown in Figure 2.2.8.



FIGURE 2.2.8 – LIFE TEST VERSION 1 DUT TEST CHAMBER

The second version of the test system only allowed the temperature to be the environmental condition to vary as well. However, this time the temperature was more precisely controlled and the DUT was subjected to a dry nitrogen atmosphere. The module's base plate temperature was maintained by heating the copper baseplate with an electric heating element as shown in figure 2.2.9. This heating element was controlled by a temperature controller that monitored the copper blocks temperature with a thermal couple. A picture of version two's test chamber is shown in Figure 2.2.10.

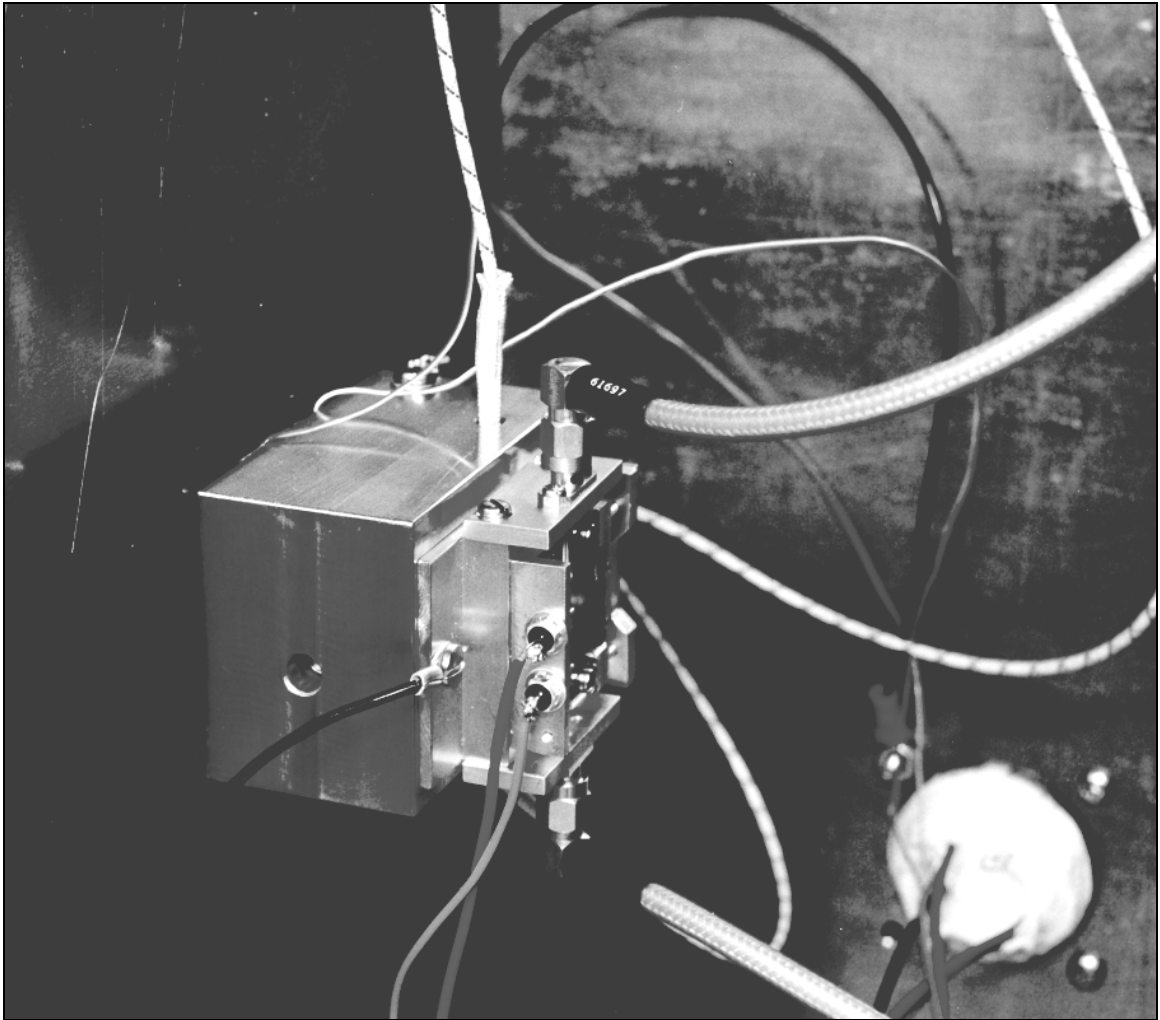


FIGURE 2.2.9 – DUT LIFE TEST FIXTURE MOUNTED ON COPPER BLOCK



Figure 2.2.10 - LIFE TEST VERSION 2 DUT TEST CHAMBER

2.3 PULSED PHASE MEASUREMENT SYSTEM

To provide a means of measuring intra pulse and inter pulse phase and amplitude stability, the pulsed phase measurement system was developed. This system attaches to MEL-2 in place of the digital sampling scope which takes an average across many pulses.

In this system, the I and Q signals are simultaneously processed through an A/D converter by using two transient digitizers (Tektronics 7912) with a 500 MHz bandwidth. A picture of this system is shown in Figure 2.3.1. This configuration is shown in Figure 2.3.2 and is described in detail in a paper entitled "Computer Controlled Pulse Power Measurement System" by M. Little and L. L. Stevens.

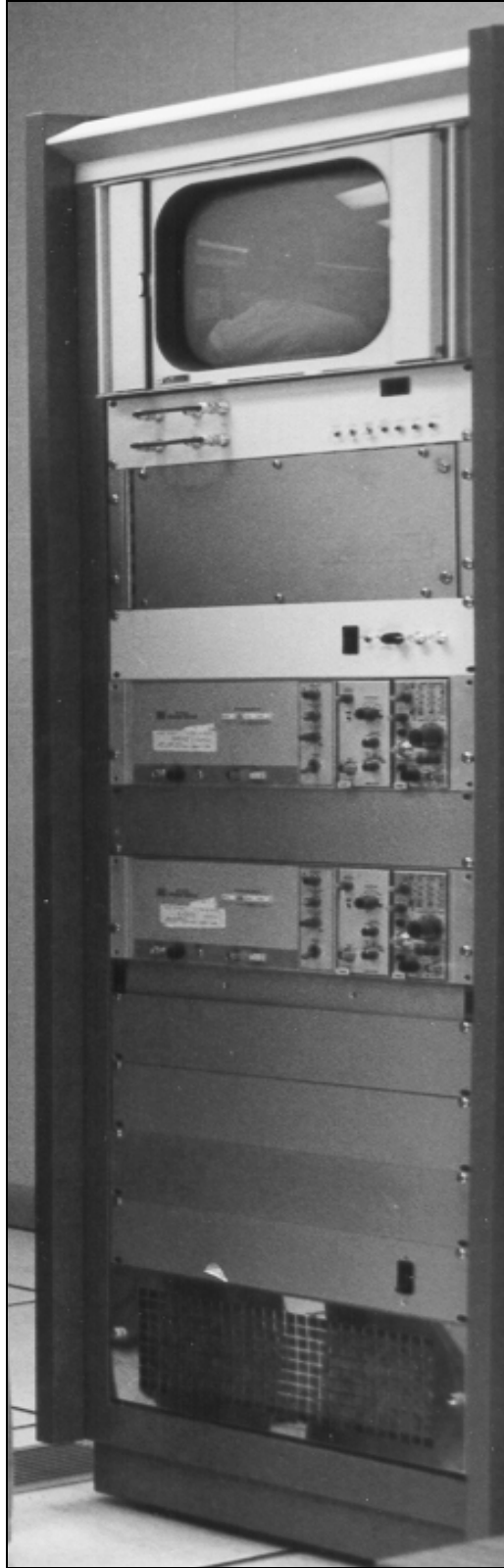


FIGURE 2.3.1 – PULSED PHASE MEASUREMENT SYSTEM

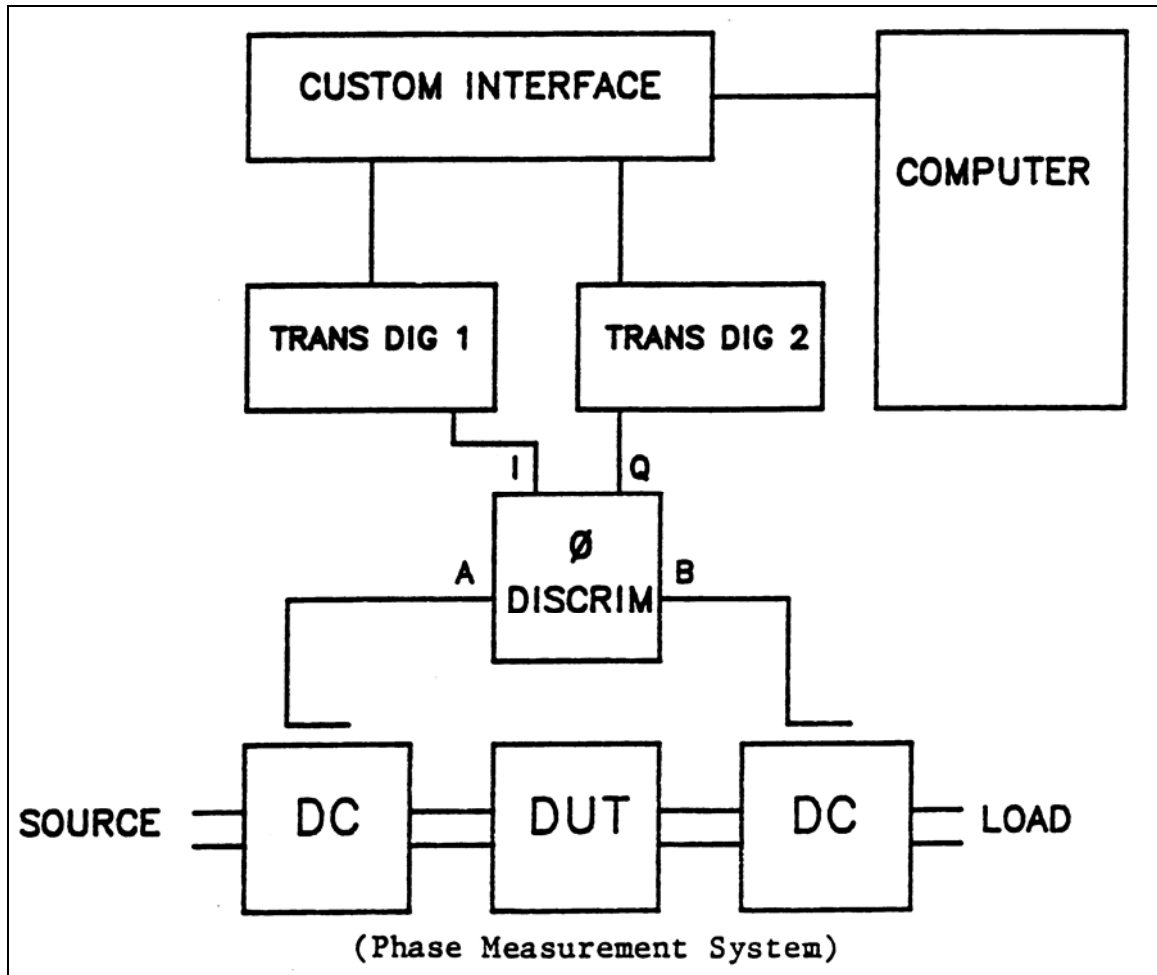


FIGURE 2.3.2 – PULSED PHASE MEASUREMENT SYSTEM DIAGRAM

The system uses one digitizer to capture the I signal and the second digitizer to capture the Q signal. The video I and Q signals are fed into the digitizer which acts as an array of sample and holds an A/D converter through the use of scan converters. A scan converter is a cathode ray tube with both a write gun and a read gun. The write gun scans a beam of electrons across an array of diodes; thus, discharging those diodes. The read gun then scans the diodes array charging those diodes which had been previously discharged. The charging of the diodes creates a current flow which identifies those diodes as having been written on.

Depending on the number of samples per pulse desired and the duty cycle of the waveform, the one-shot digitization can incorporate from a fraction of a pulse to multiple pulses. The number of samples is limited to 500. The actual measurement limitations are caused by the phase discriminator which has a rise time limit and by the capacitive coupling of the video amplifier. The discriminator rise time is on the order of 35 nsec (see figure 2.3.3); thus limiting the pulse width to greater than 100 nsec. The capacitive coupling limits the pulse width to less than 1 msec. The A/D converter uses 8 bits; thus not becoming the limiting factor in the accuracy of the measurement (limitations are caused by phase discriminator).

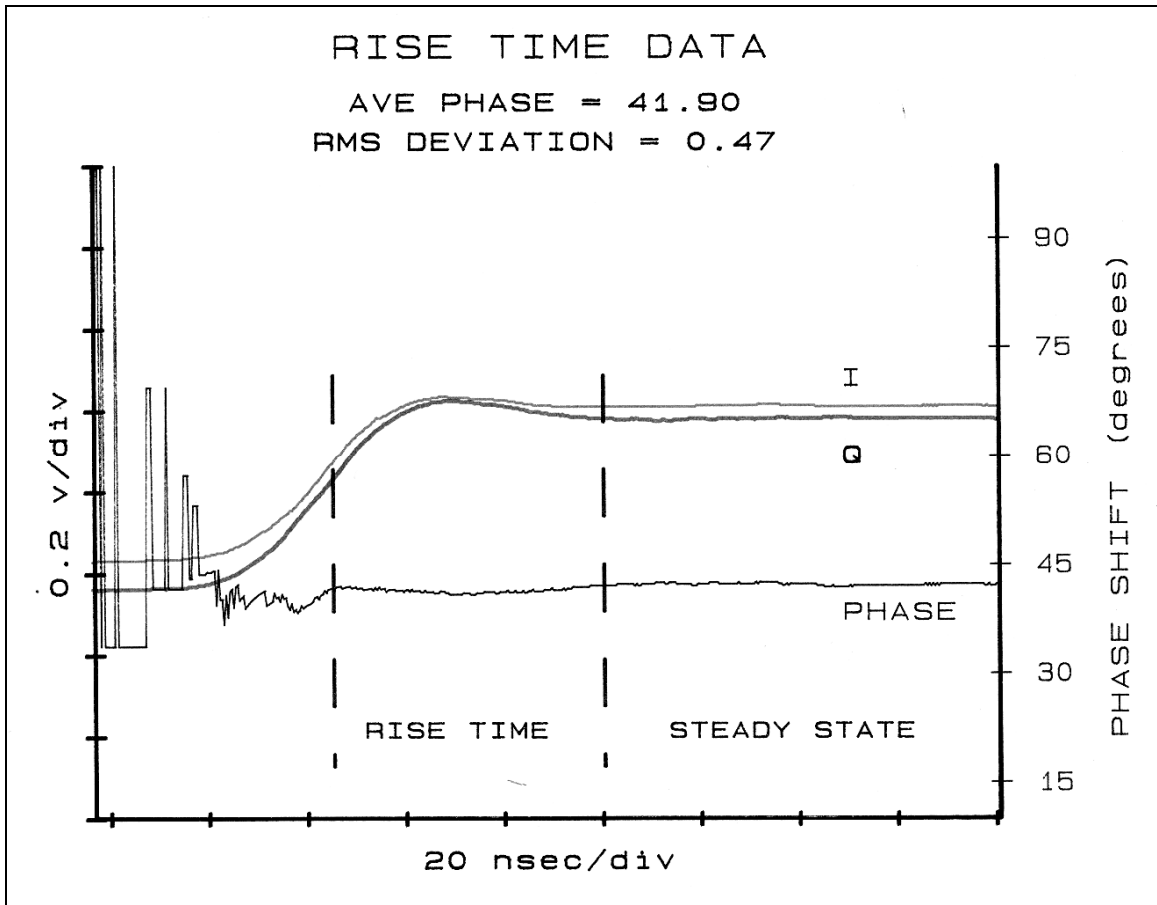


FIGURE 2.3.3 – PULSE MEASUREMENT SYSTEM RISE TIME DATA

3.0 EXPERIMENTS/RESULTS

As an aid to evaluating the testing techniques developed and to keep track of the characteristics and capabilities of the components and T/R modules being developed, various tests were performed. This section provides the major achievements and highlights the data acquired in conducting those tests.

3.1 EARLY L & S BAND MODULES (CHARACTERIZATION)

These modules were the deliverables from a set of efforts, started in 1978. A selection of these modules is shown in Figure 3.1.1. Some experiments were performed on these modules and on their individual circuits. The early work was done at L band using Silicon-on-Sapphire (SoS) technology. Later work was performed at both L and S bands using GaAs technology. SoS technology was abandoned due to its high loss and low gain in the active circuits. This was especially true with the power amplifier circuits.

- * The results of the SoS T/R module experiments have been reported previously in RADC-TR-84-34 and will not be discussed here.

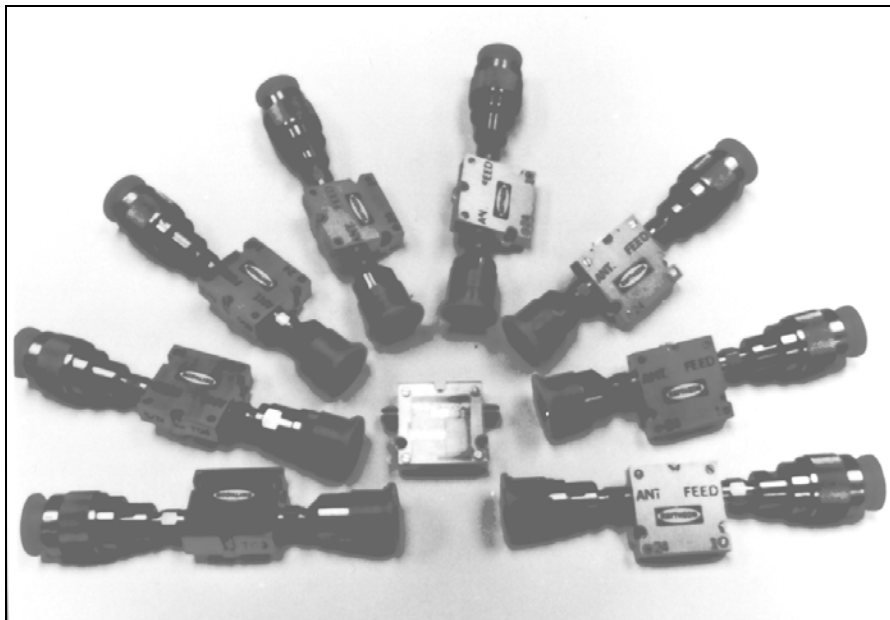


FIGURE 3.1.1 – EARLY L & S BAND MODULES

The test that will be covered by this report were conducted on S band GaAs T/R modules. Some of these modules had a added final power amplifier providing 10 Watts of output power. Some of the phase data taken shows the effects of an extra length of cable the test channel of the phase discriminator. This cable caused an increase in the measured phase length of the DUT. The data is, however, provided as a reference of the advances that have been achieved in both MMIC T/R modules and in measurement technology. These measurements were made on the earlier version of MEL. A picture of one of these modules is shown in Figure 3.1.2 during room temperature testing.

* RADC-TR-84-34 is Distribution CONTROLLED; DOD CONTROLLED

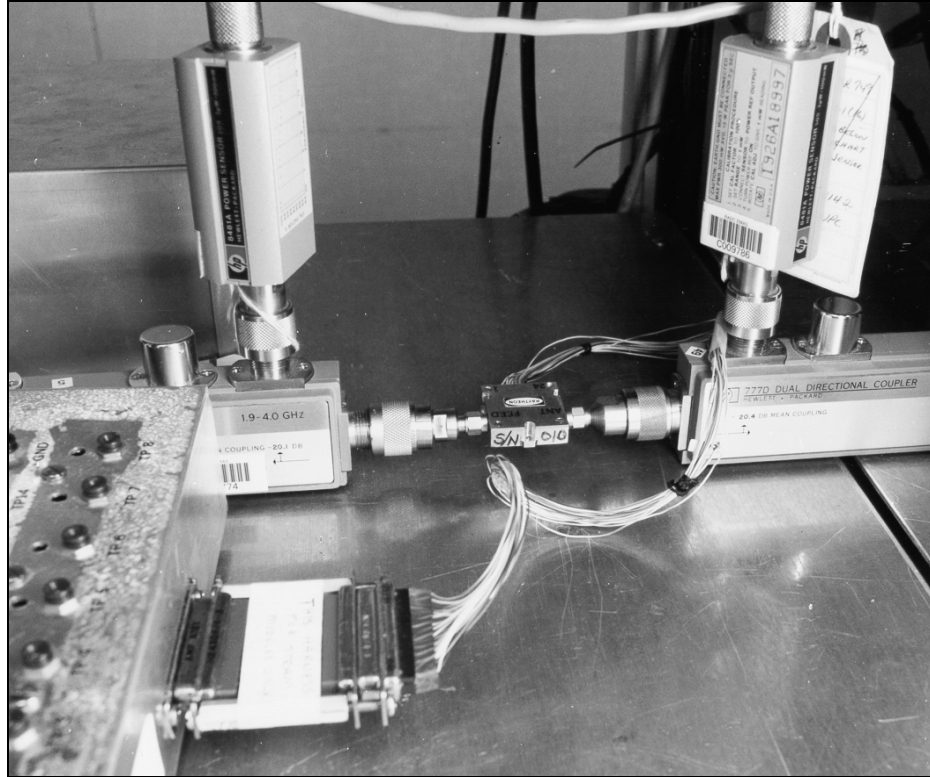


FIGURE 3.1.2 – EARLY S BAND MODULE UNDER TEST

3.1.1 TEST RESULTS

One of the more significant tests was the parametric test conducted on the receiver. The receiver parametric test involved independently varying the temperature, the gate bias and the source mismatch and observing the changes in noise figure and small signal gain. The first results shown were conducted at -20 degrees centigrade. Note that adjusting the gate bias had little effect on the noise figure and provided only small variations in the gain. In all cases not involving device failure or measurement error, the gain and noise figure curves retained their shape. The gain change was proportional to the magnitude of the negative voltage of the gate bias (see Figure 3.1.3). The same measurements conducted at zero degrees centigrade yielded a definite gate bias sensitivity (see Figure 3.1.4). Note that one measurement is significantly different than the other two. This was caused by a bad DC/Control connector. The subminiature connector was subject to many failures during the testing program. Test varying the temperature of a module indicated that gain changes inversely proportional and noise figure changes proportional with temperature change. The measurements were taken every 20 degrees centigrade from +40 to -20. The data is shown in Figure 3.1.5. The source mismatch test was performed using a directional coupler to isolate the noise source from the source mismatch. Figure 3.1.6 provides the data that resulted. A block diagram of this unique test setup is shown in Figure 3.1.7.

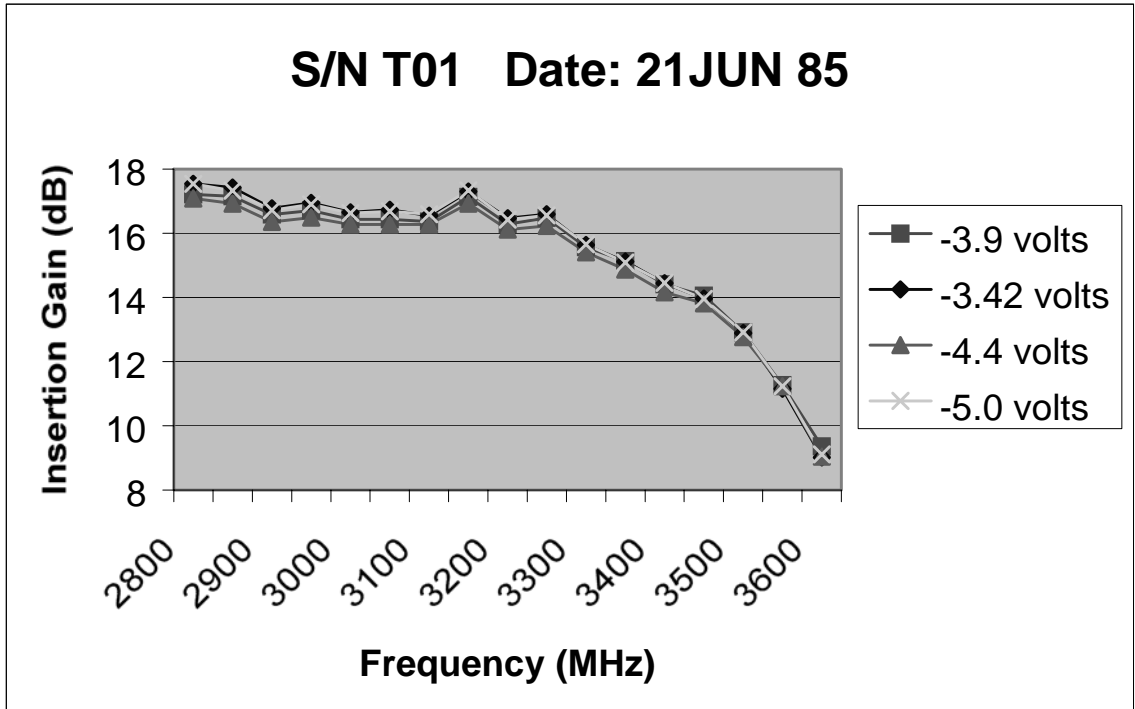


FIGURE 3.1.3 (A) – GAIN VERSUS GATE VOLTAGE

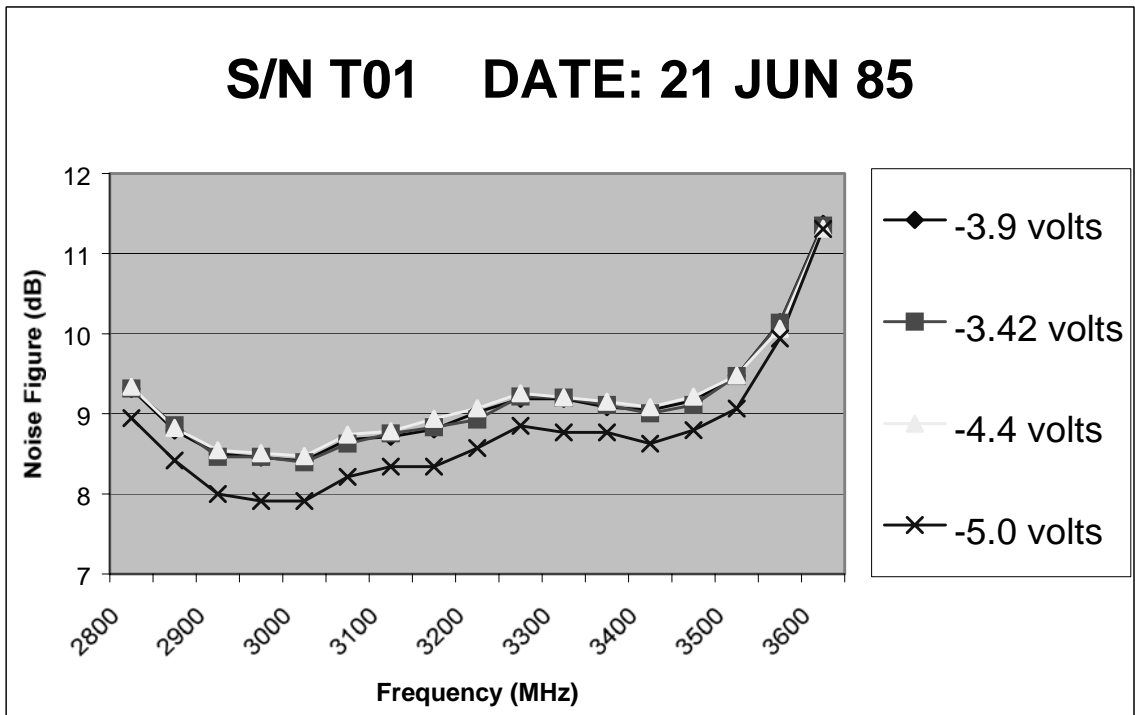


FIGURE 3.1.3 (B) – NOISE FIGURE VERSUS GATE VOLTAGE

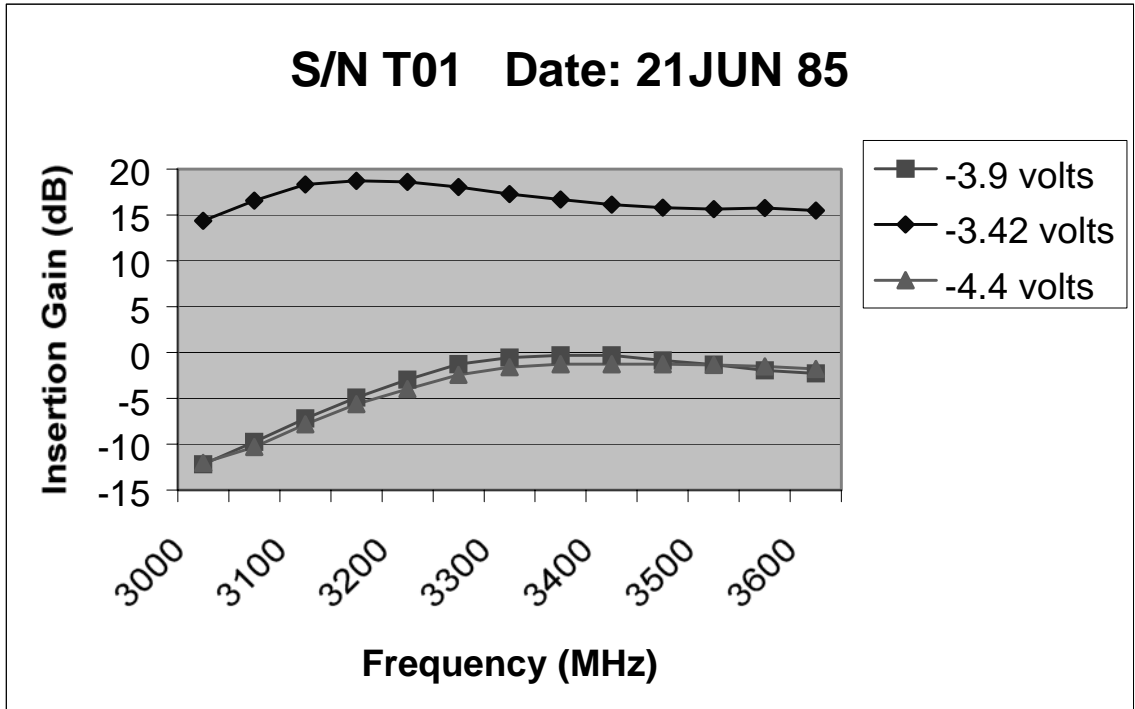


FIGURE 3.1.4 (A) – GAIN VERSUS GATE VOLTAGE (0 DEGREE C)

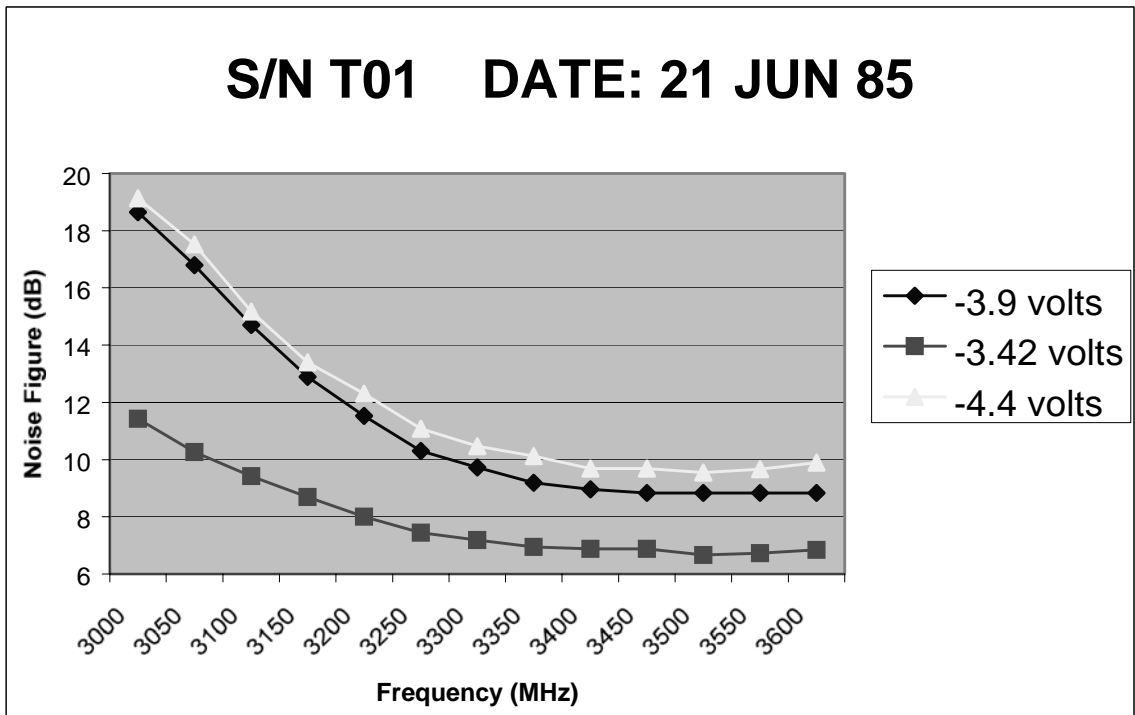


FIGURE 3.1.4 (B) – NOISE FIGURE VERSUS GATE VOLTAGE (0 DEGREE C)

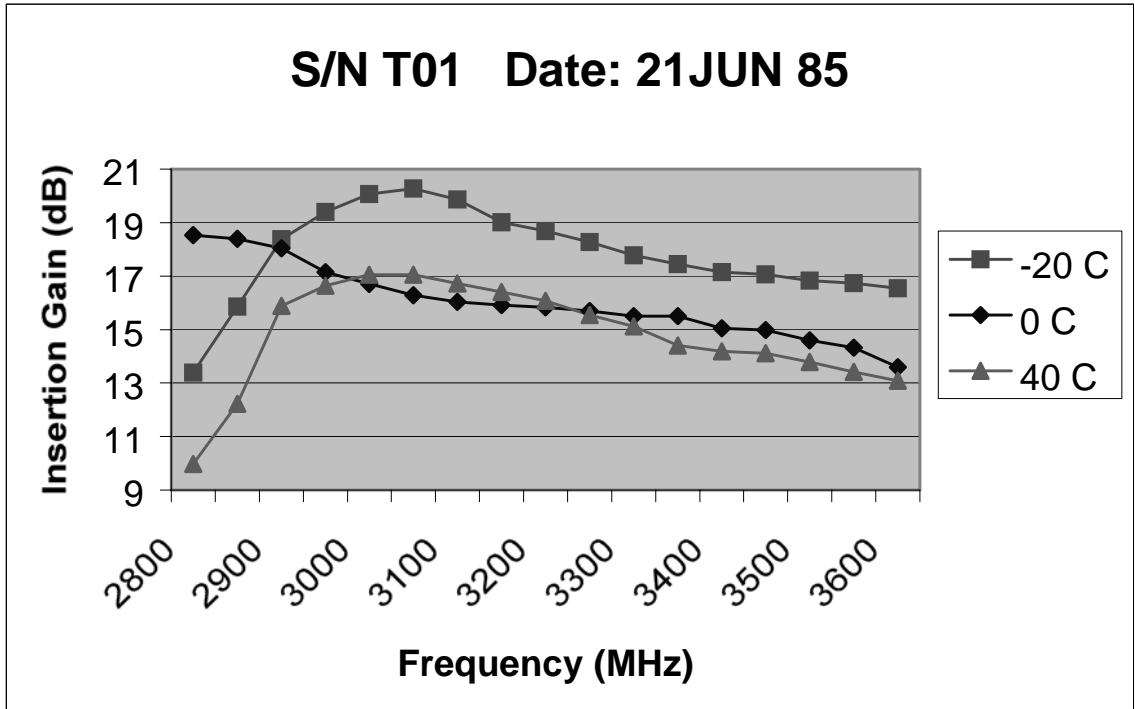


FIGURE 3.1.5 (A) – GAIN VERSUS TEMPERATURE

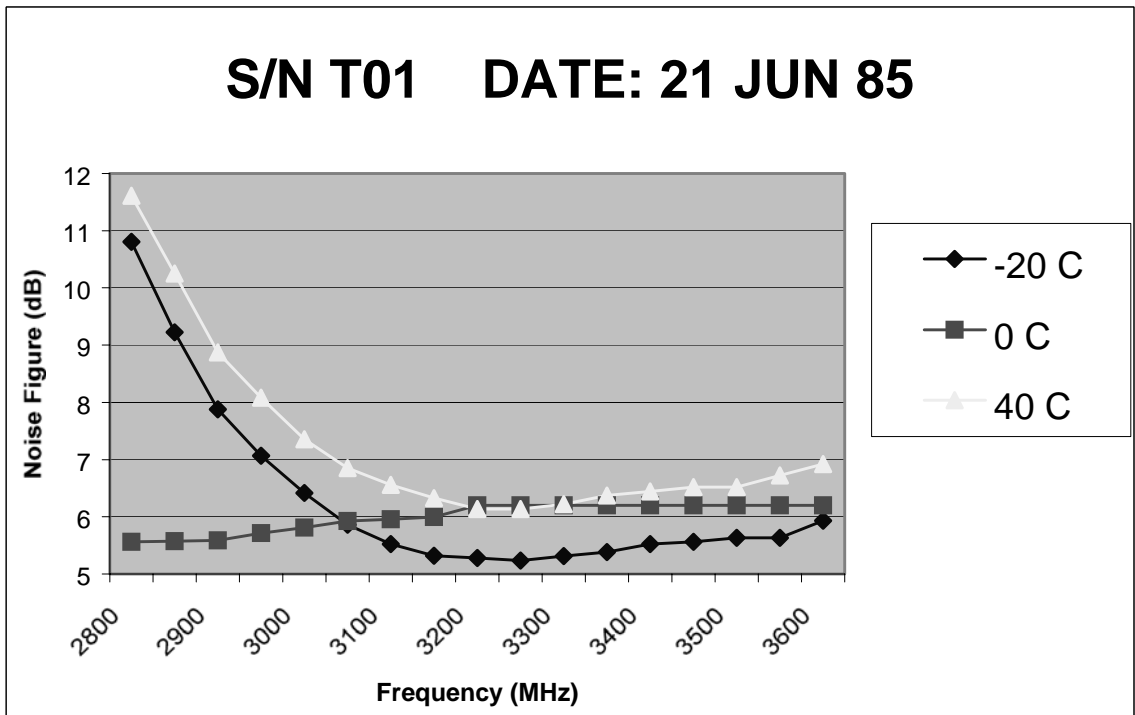


FIGURE 3.1.5 (B) – NOISE FIGURE VERSUS TEMPERATURE

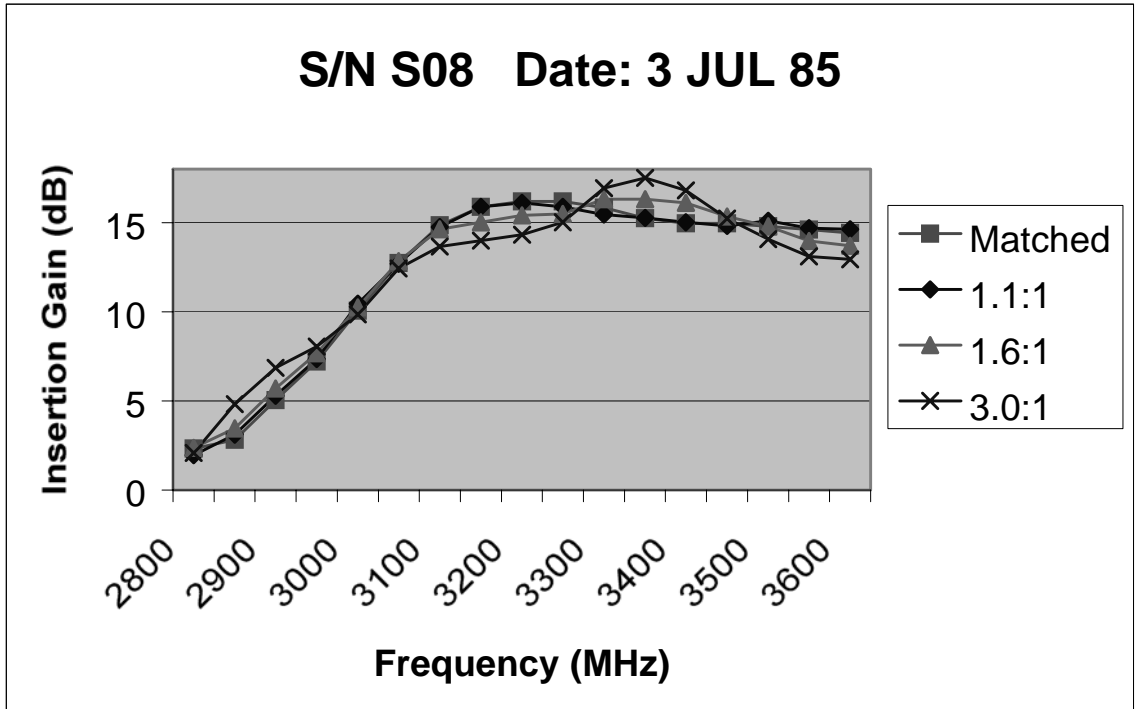


FIGURE 3.1.6 (A) – GAIN VERSUS SOURCE MISMATCH

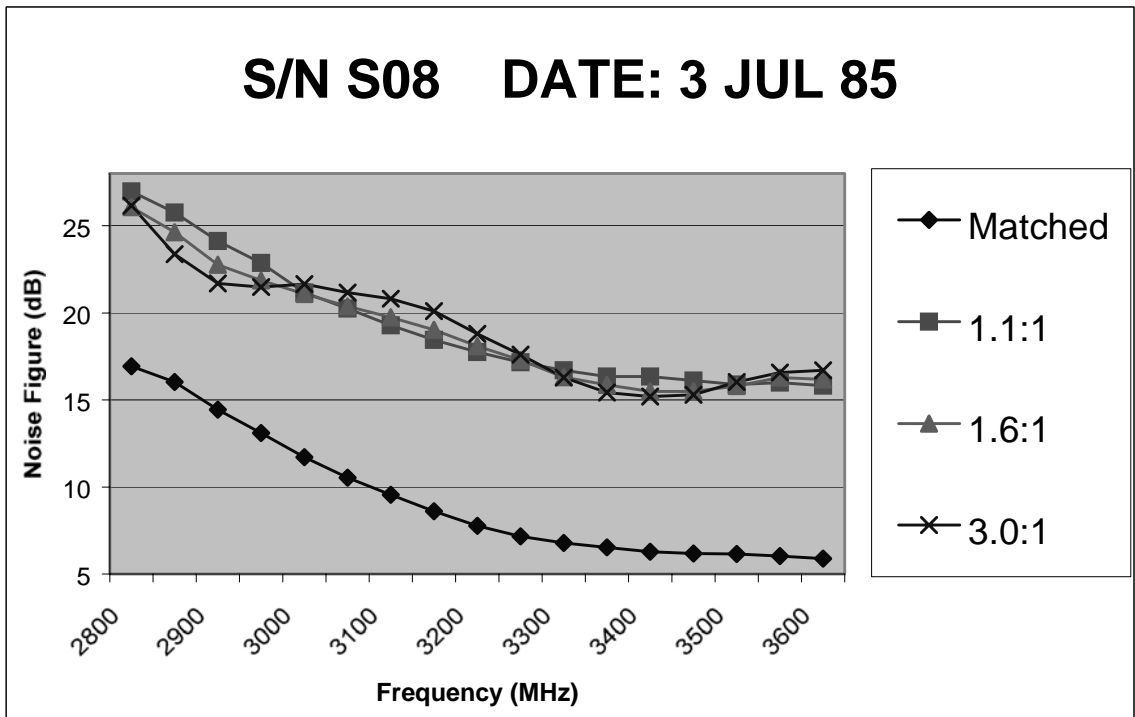


FIGURE 3.1.6 (B) – NOISE FIGURE VERSUS SOURCE MISMATCH

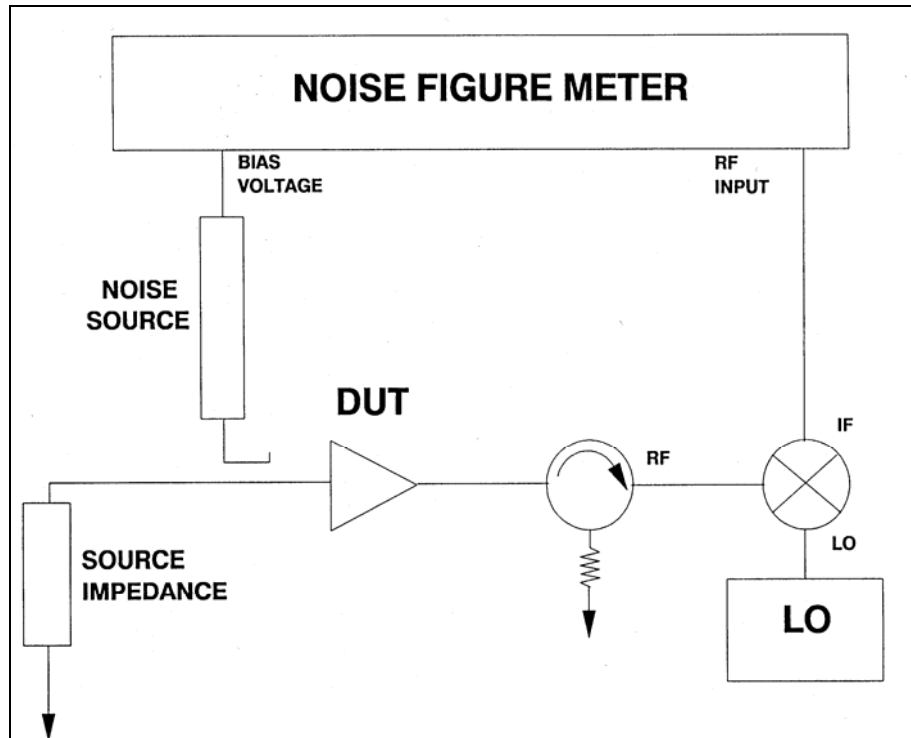


FIGURE 3.1.7 – SOURCE MISMATCH BLOCK DIAGRAM

Pulsed transmit tests were also conducted on both the lower and higher power modules. These tests were conducted at room temperature (20 degrees Centigrade) and within an oven/refrigerator at -20, 0 and 40 degrees Centigrade. Gain, phase and phase linearity data for modules serial numbers S09 through S12 and T01 through T04 are presented in Figures 3.1.8 through 3.1.15. Note that the phase data for these modules taken at non-room temperatures includes the extra electrical length mentioned earlier. This is due to the additional cabling needed to place the DUT in the temperature test chamber. All of these measurements were taken with nominal drive levels and bias voltages. To demonstrate the effect the phase shifter has on gain, data on modules T01 and T02 is provided comparing all phase bits off with all phase bits on (Figure 3.1.16 and 3.1.17). Figure 3.1.18 shows the effect changes in the pulse width will have on performance. Module to module tracking for the lower power modules is shown in Figure 3.1.19 and for the four higher power modules in Figure 3.1.20.

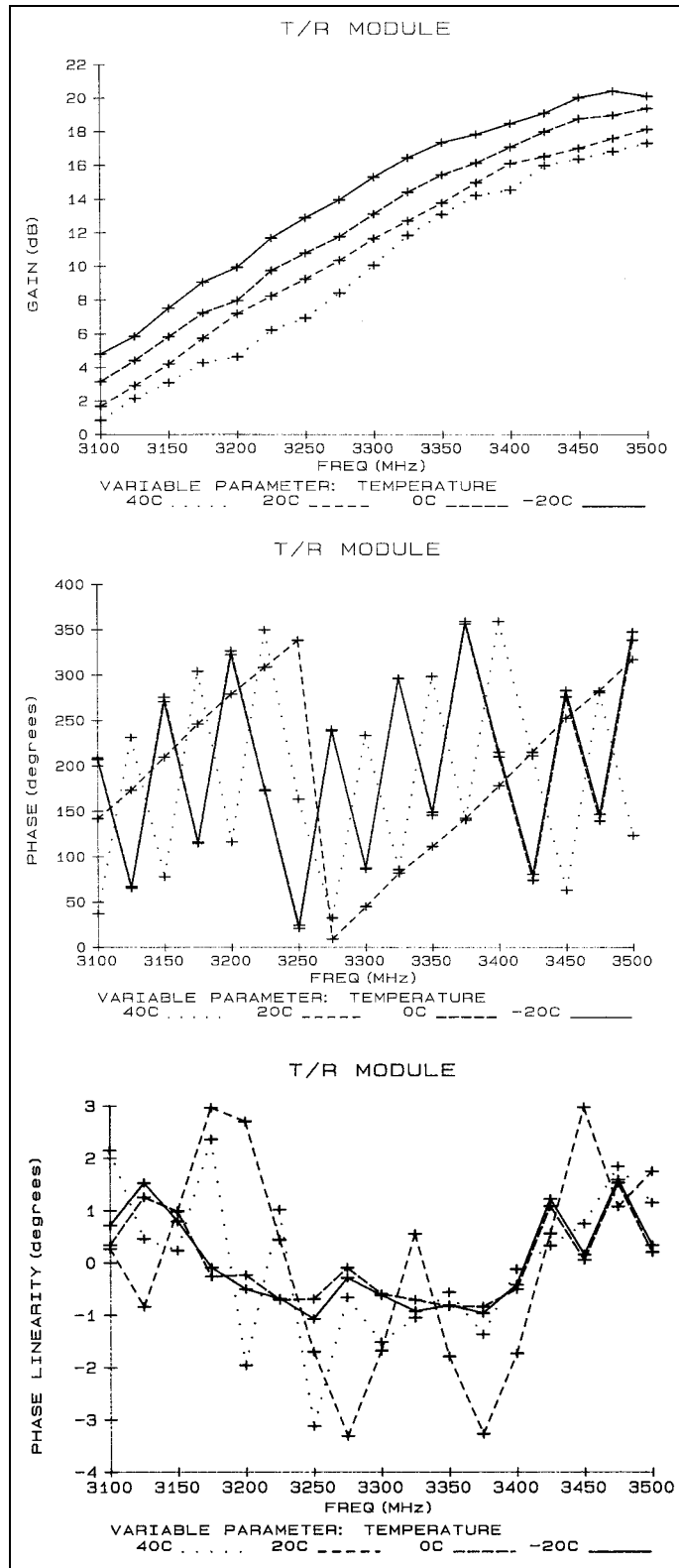


FIGURE 3.1.8 – S09 GAIN, PHASE & PHASE LINEARITY DATA

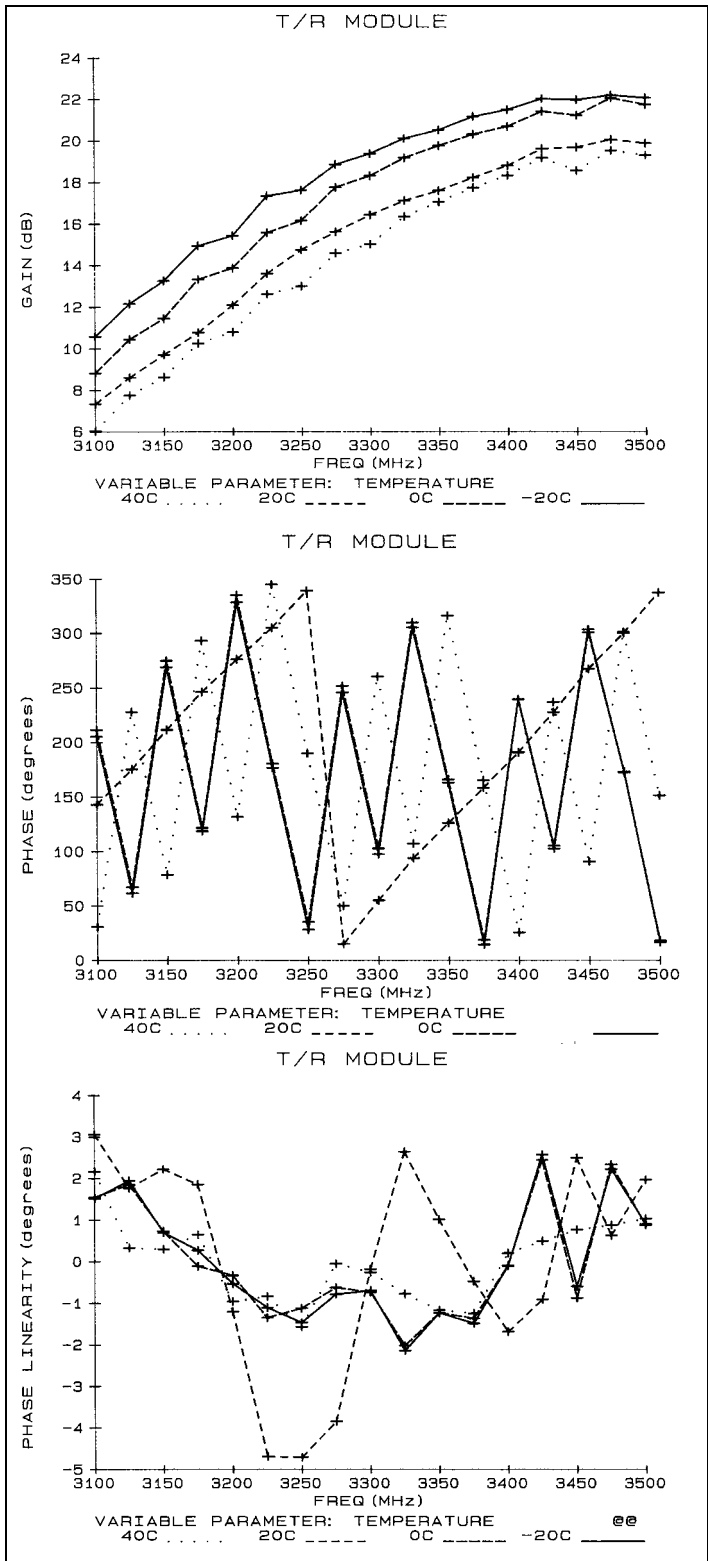


FIGURE 3.1.9 – S10 GAIN, PHASE & PHASE LINEARITY DATA

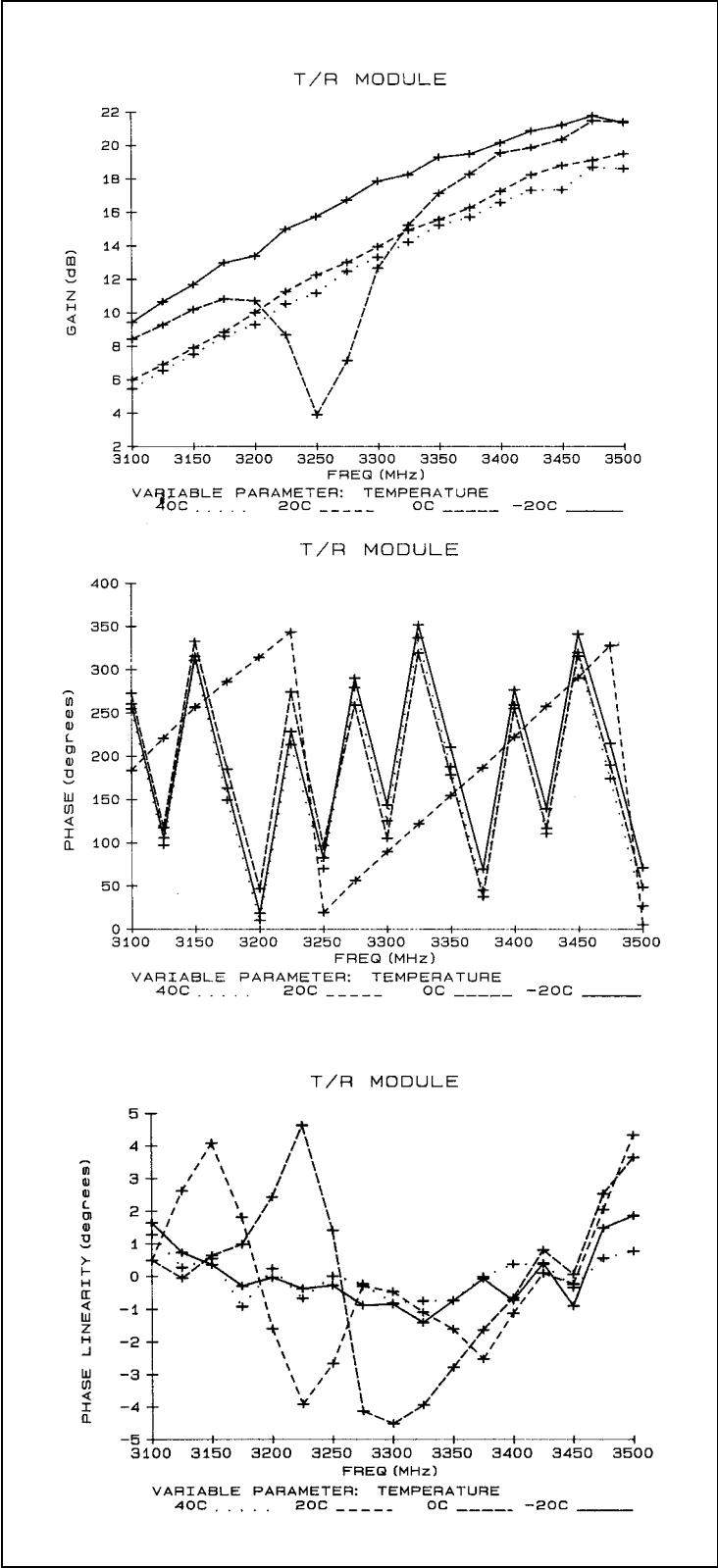


FIGURE 3.1.10 – S11 GAIN, PHASE & PHASE LINEARITY DATA

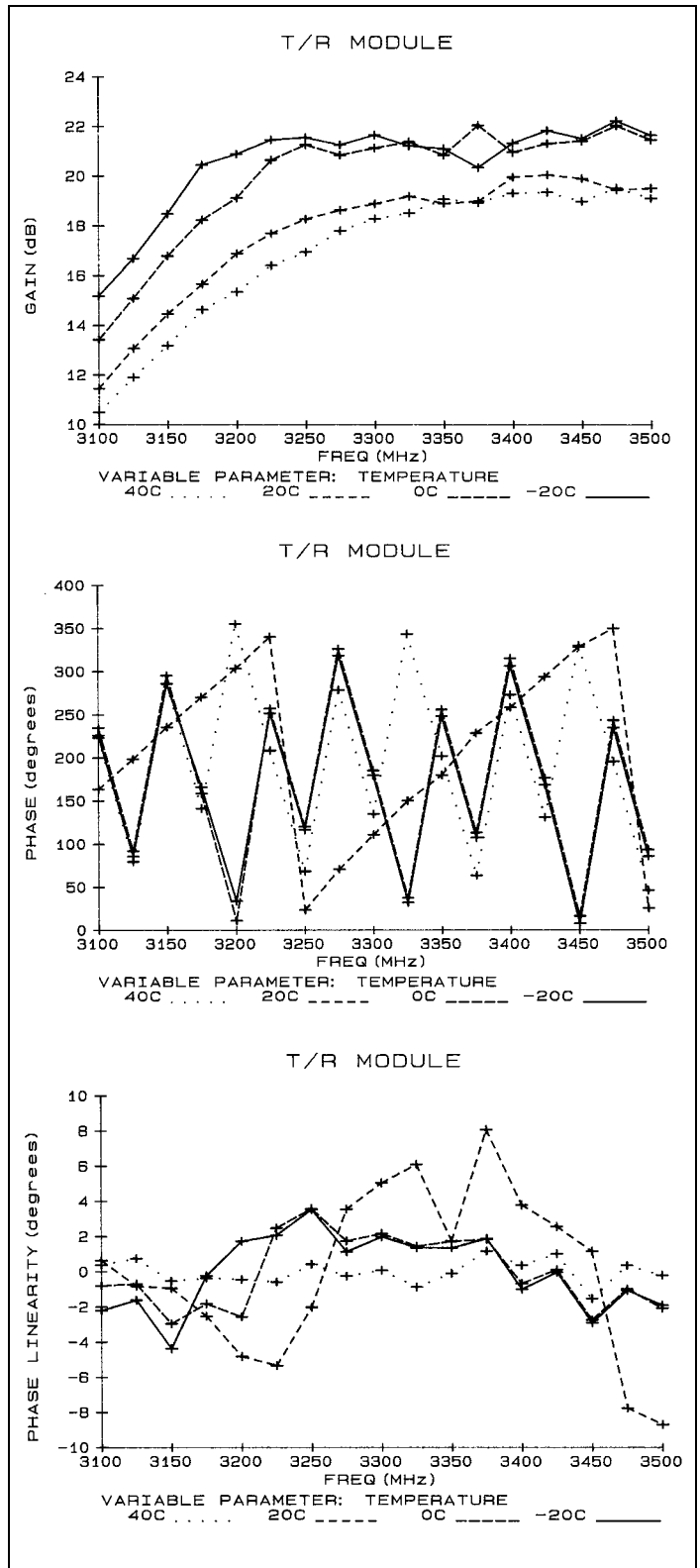


FIGURE 3.1.11 – S12 GAIN, PHASE & PHASE LINEARITY

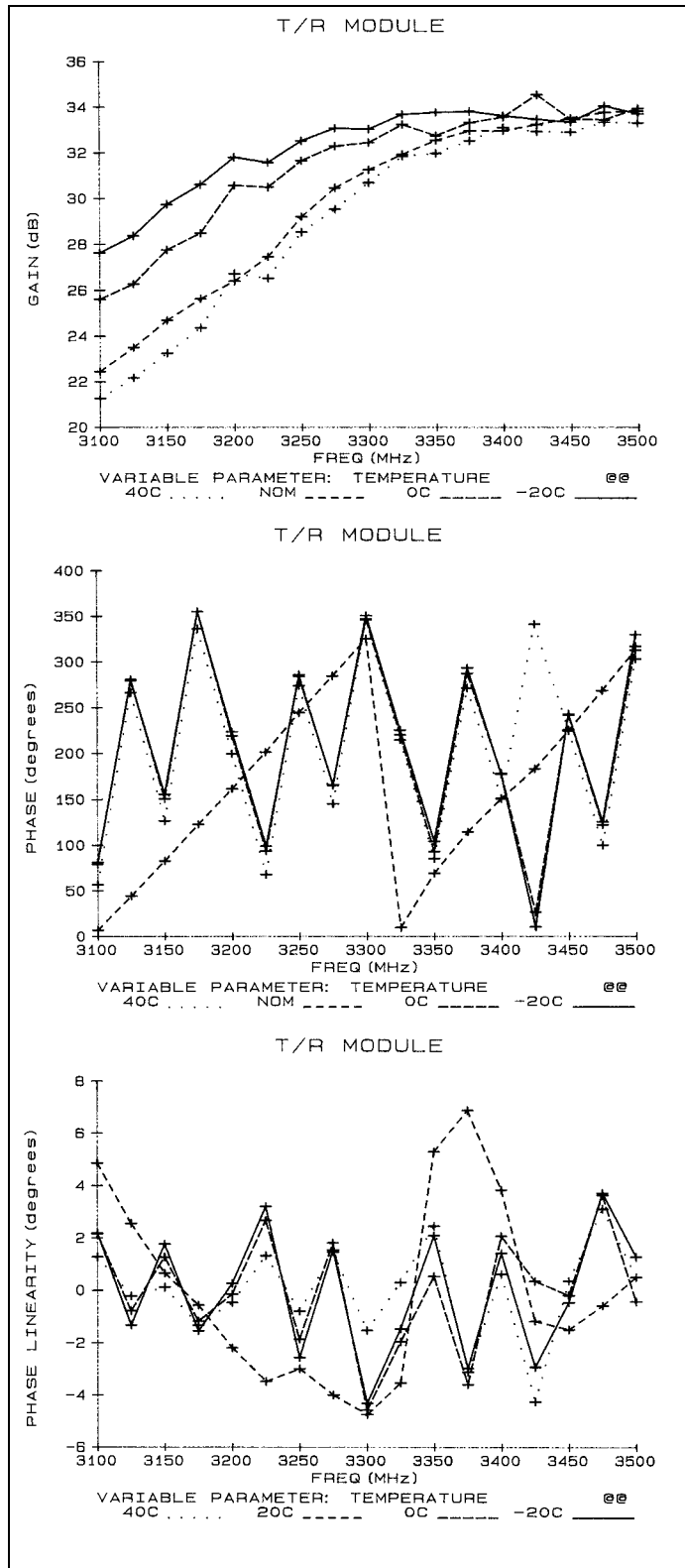


FIGURE 3.1.12 – T01 GAIN, PHASE & PHASE LINEARITY

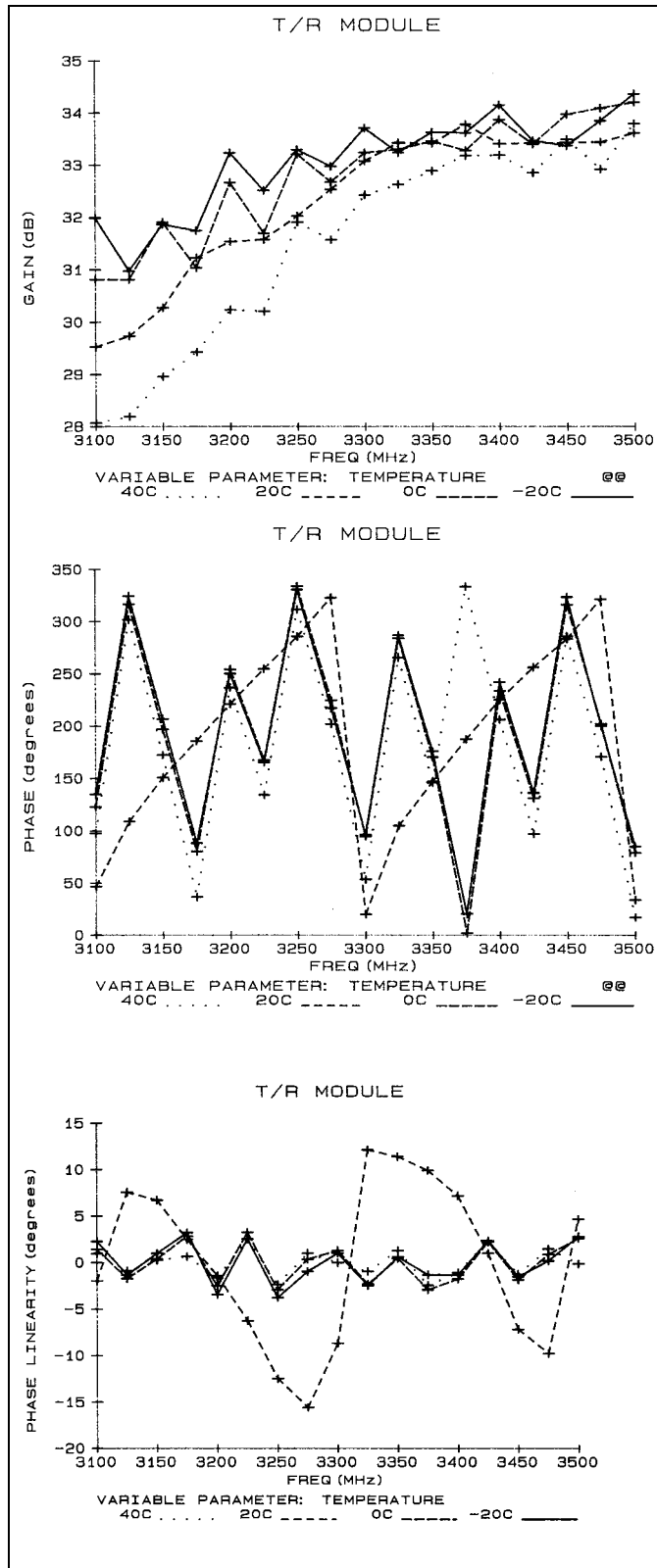


FIGURE 3.1.13 – T02 – GAIN, PHASE & PHASE LINEARITY

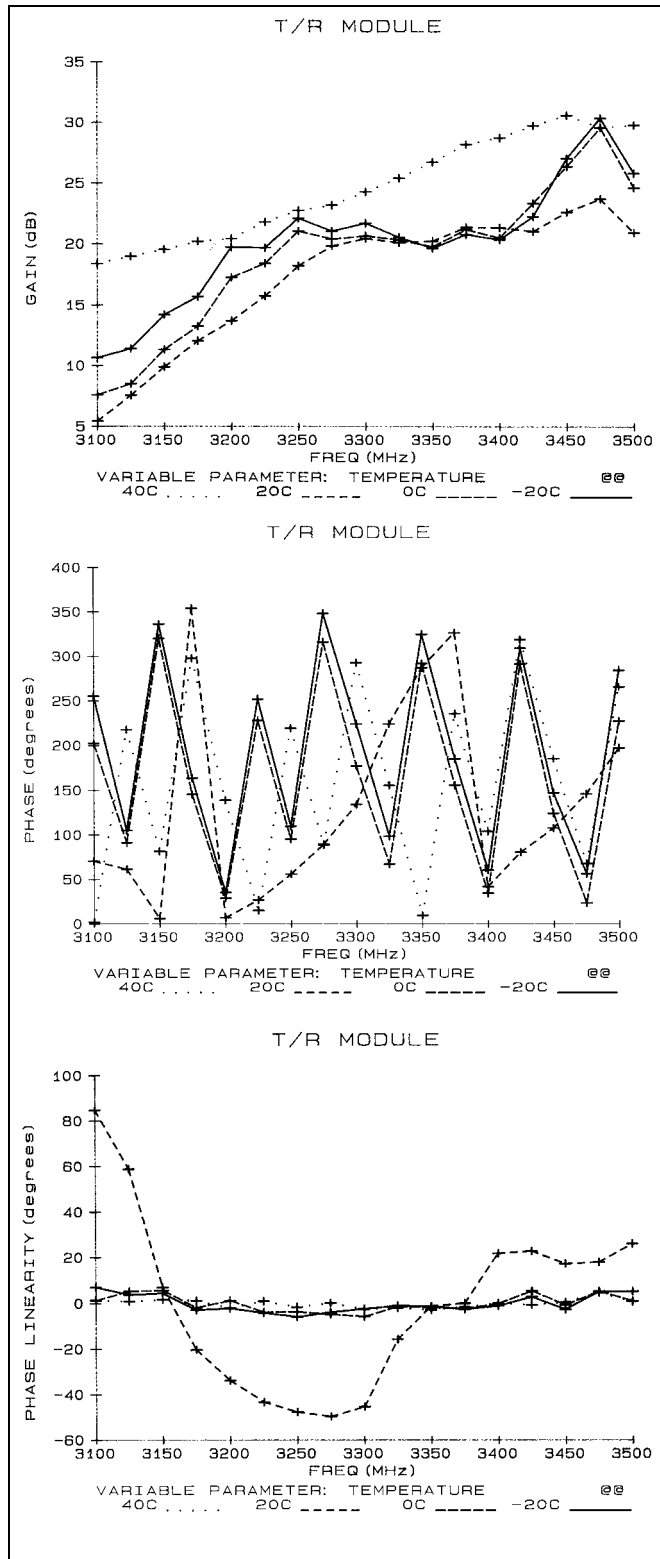


FIGURE 3.1.14 – GAIN, PHASE & PHASE LINEARITY DATA

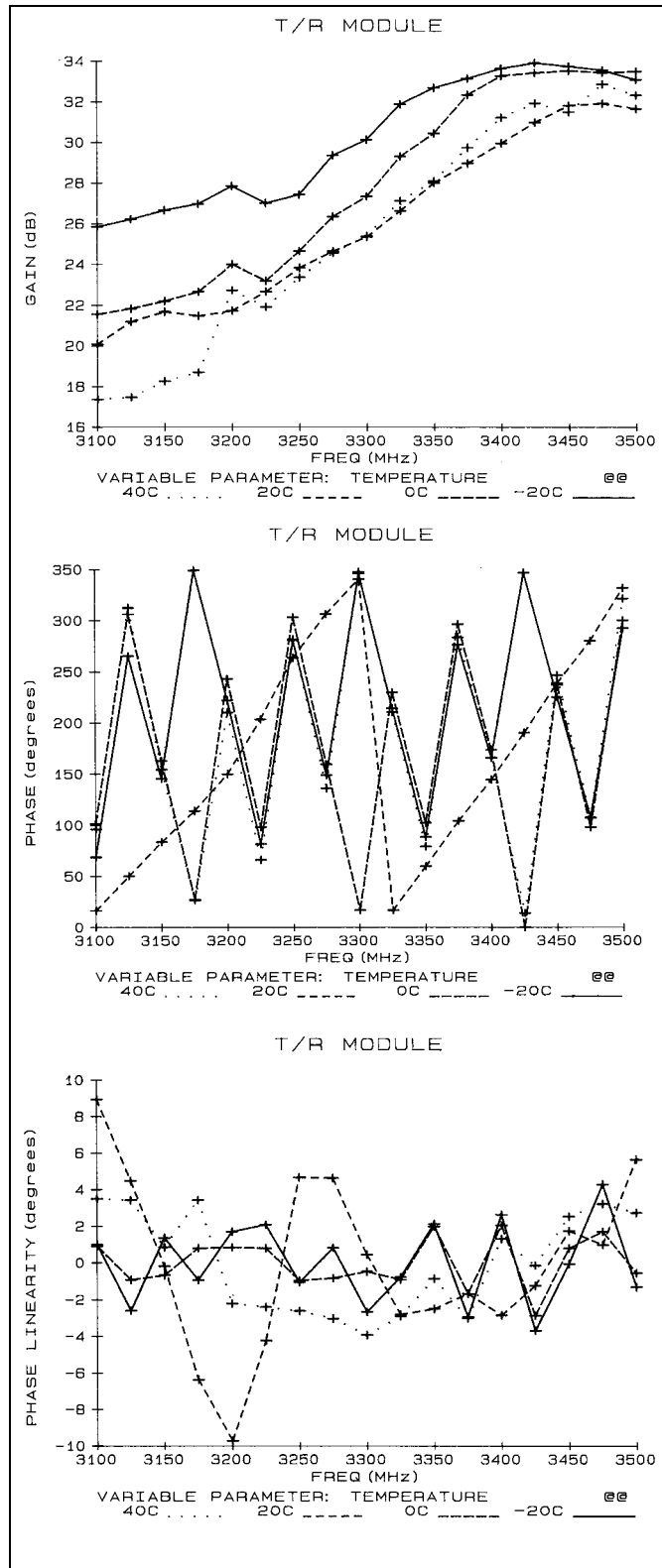


FIGURE 3.1.15 – T04 GAIN, PHASE & PHASE LINEARITY DATA

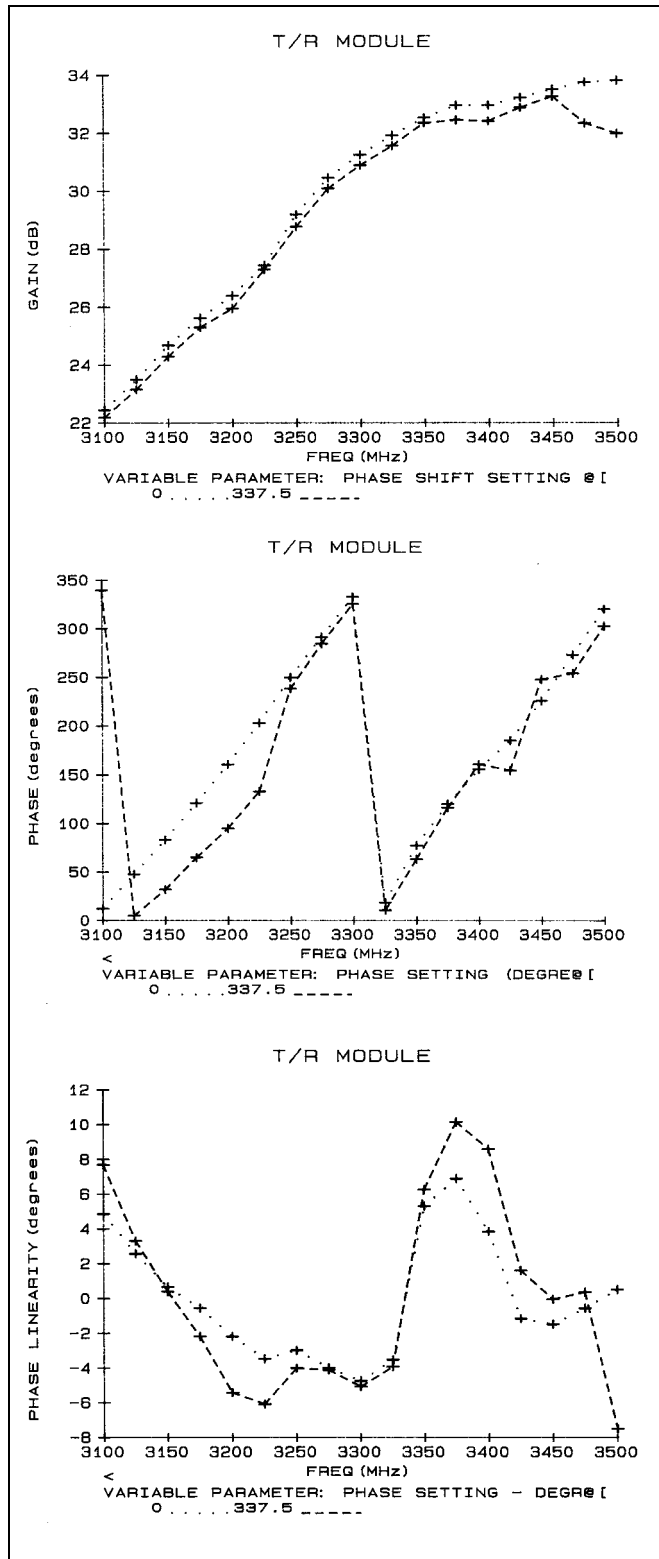


FIGURE 3.1.16 – T01 PHASE SHIFTER SETTING SENSITIVITY DATA

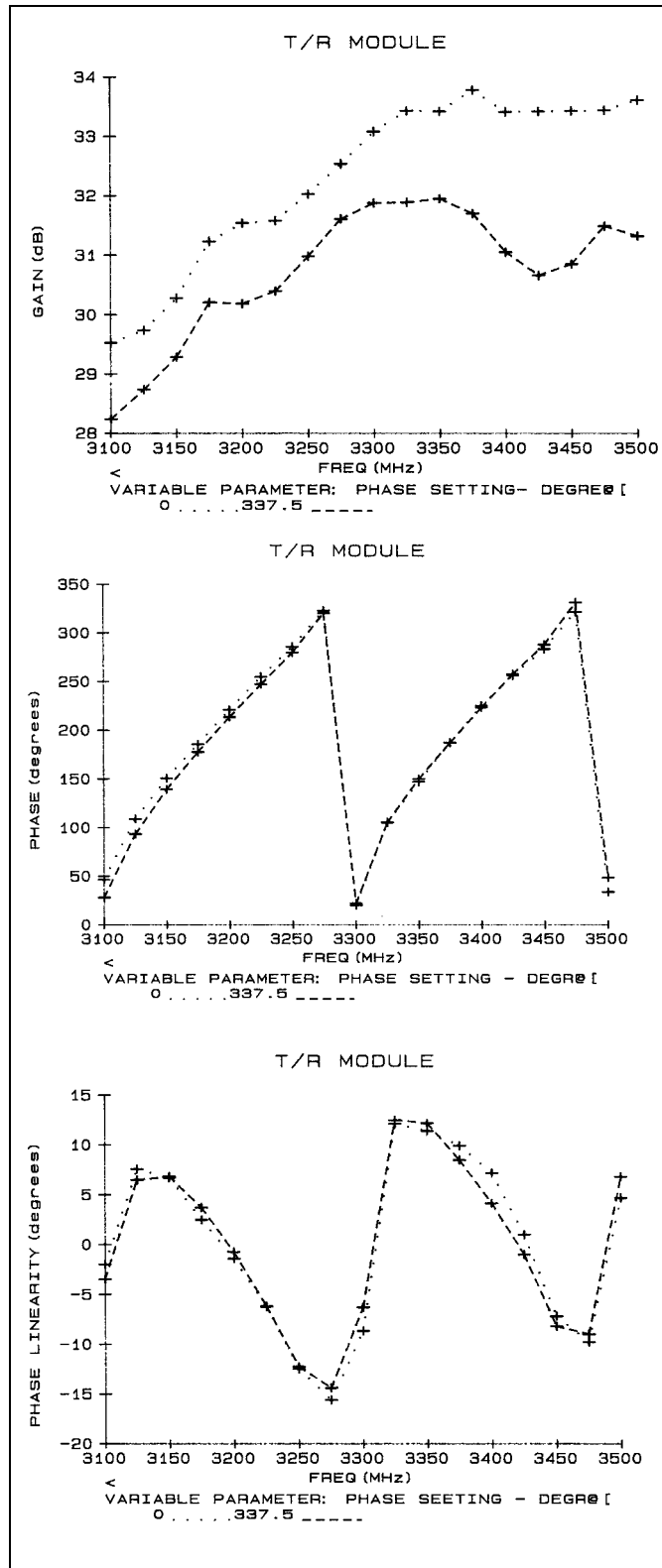


FIGURE 3.1.17 – TO2 PHASE SHIFTER SETTING SENSITIVITY DATA

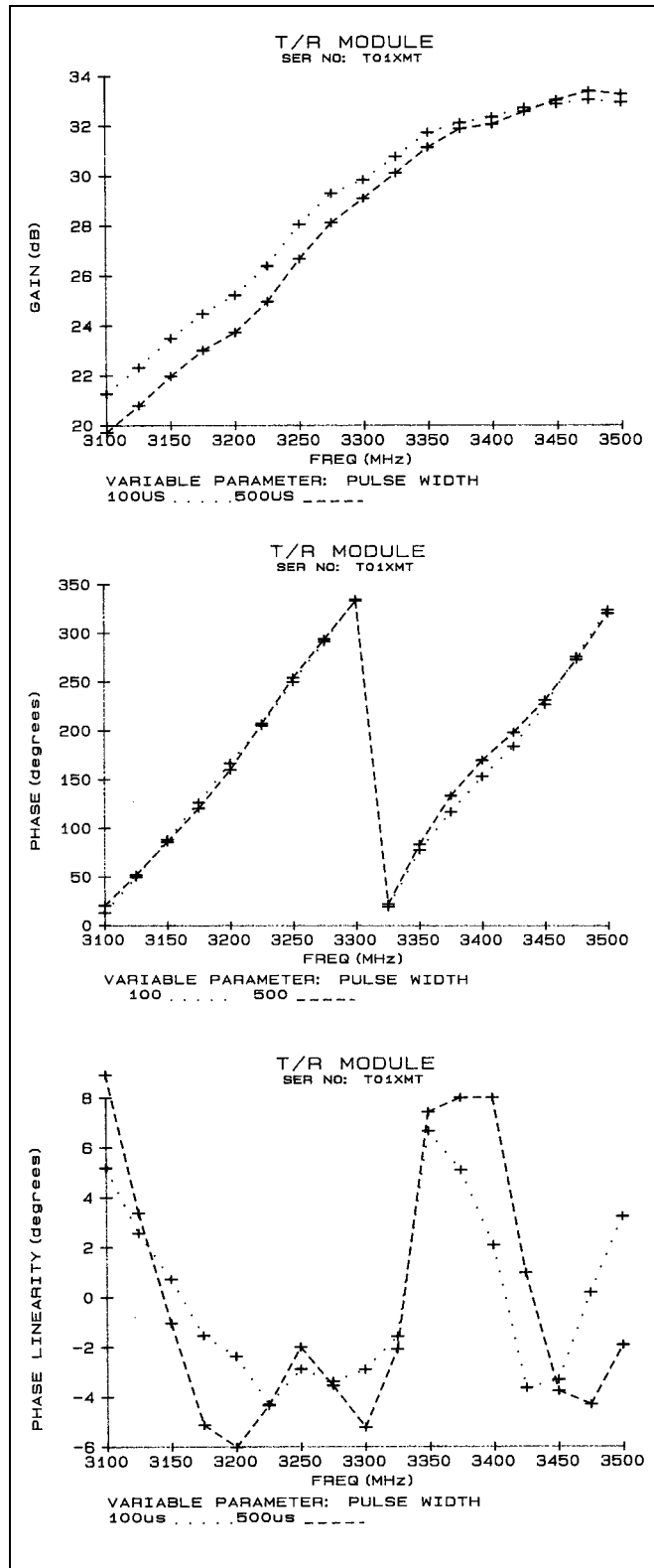


FIGURE 3.1.18T01 PULSE WIDTH SENSITIVITY DATA

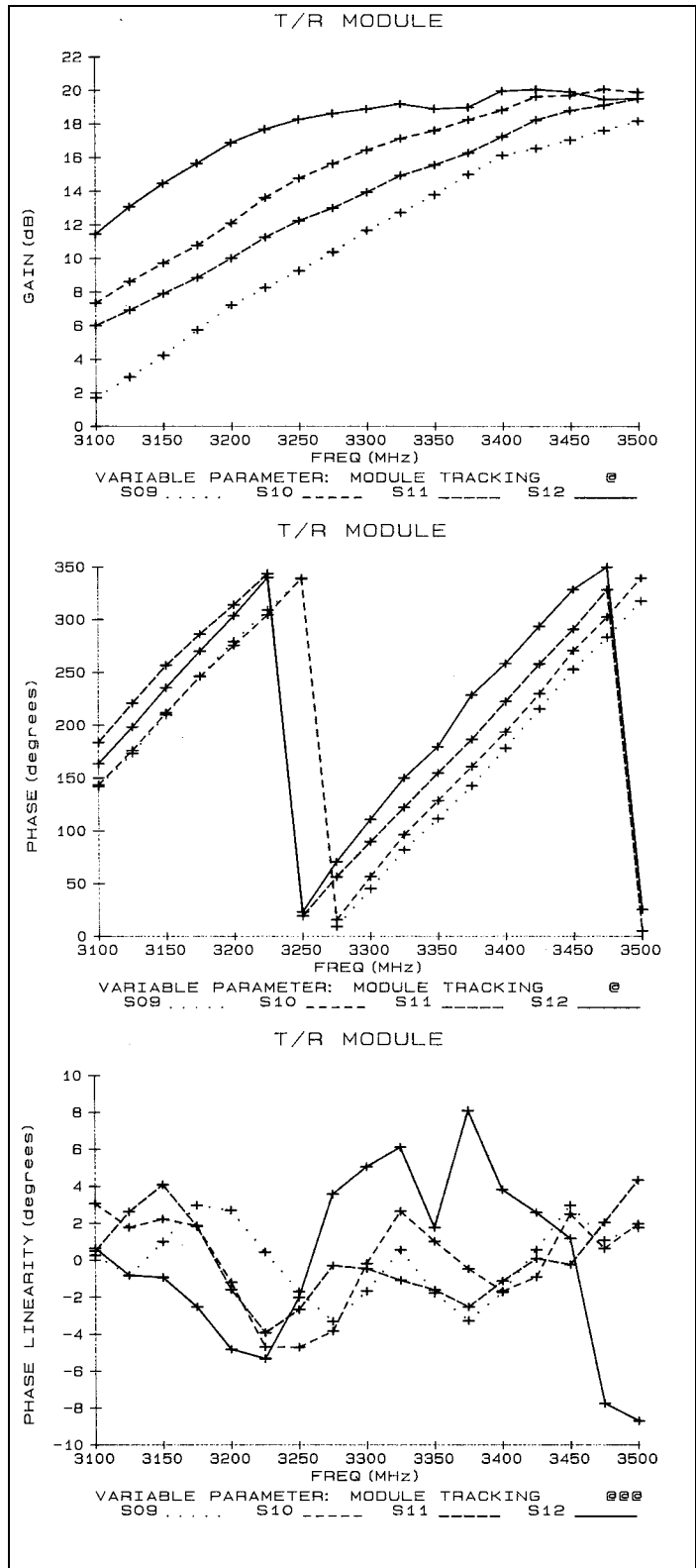


FIGURE 3.1.19 – LOW POWER S BAND MODULE TO MODULE TRACKING DATA

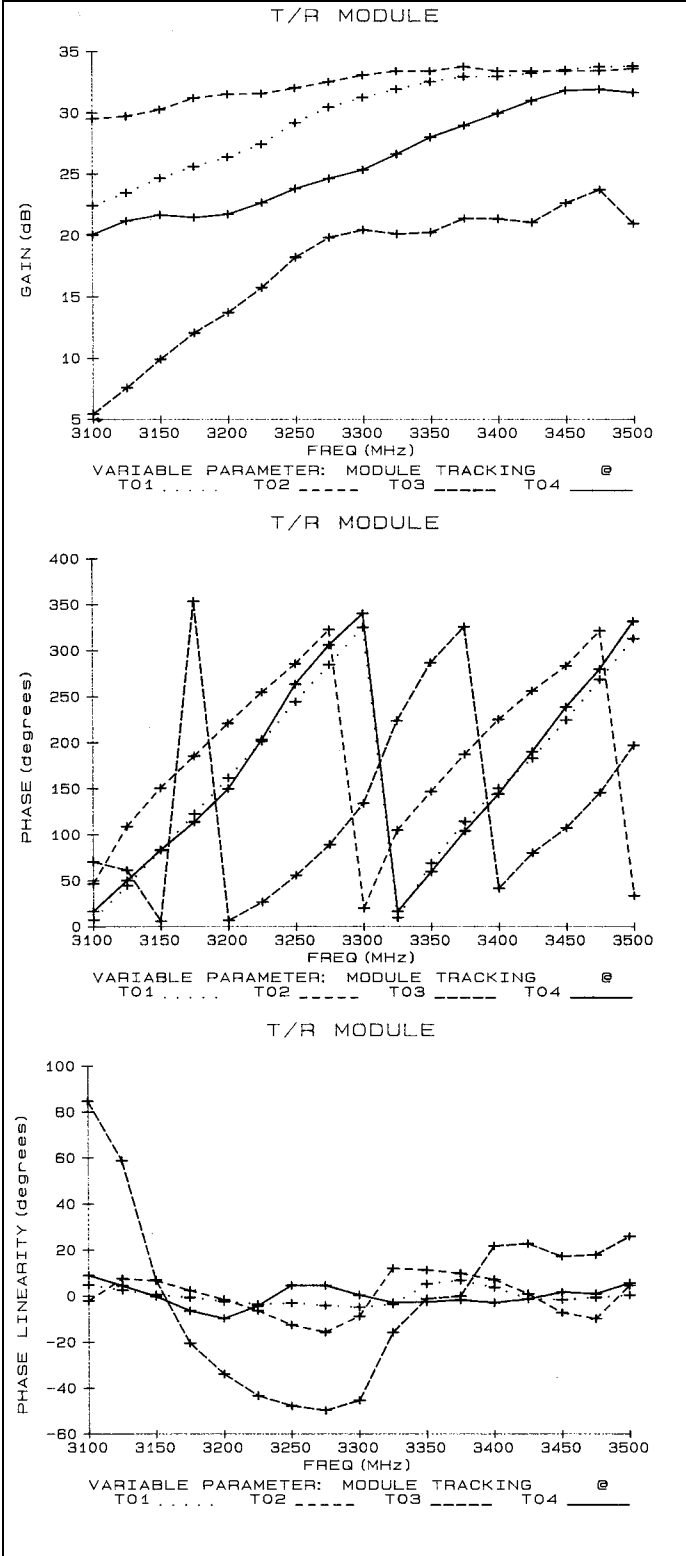


FIGURE 3.1.20 – HIGH POWER S BAND MODULE TO MODULE TRACKING DATA

3.2 C BAND MODULES

A group of C Band T/R modules that were developed under a contract with RADC were subjected to a variety of test, also. The most significant of these tests was a life test. In fact, these devices were the first subjected to life testing within the MELTS system. One hundred of these modules were manufactured, of which 20 were placed under life test at RADC and 29 were life tested by the contractor. Additional modules were expended in other performance and reliability tests and are reported on elsewhere.

3.2.1 MODULE DESCRIPTION

The microwave circuits of these modules are predominately of GaAs technology in the form of Monolithic Microwave Integrated Circuits (MMIC). The only variation was in the discrete power amplifier which is an IMFET (Internally Matched Field Effect Transistor). A picture of the module is shown in Figure 3.2.1. Notice that the right half of the 10.5 inch module is the microwave portion and the left half is the controller portion.

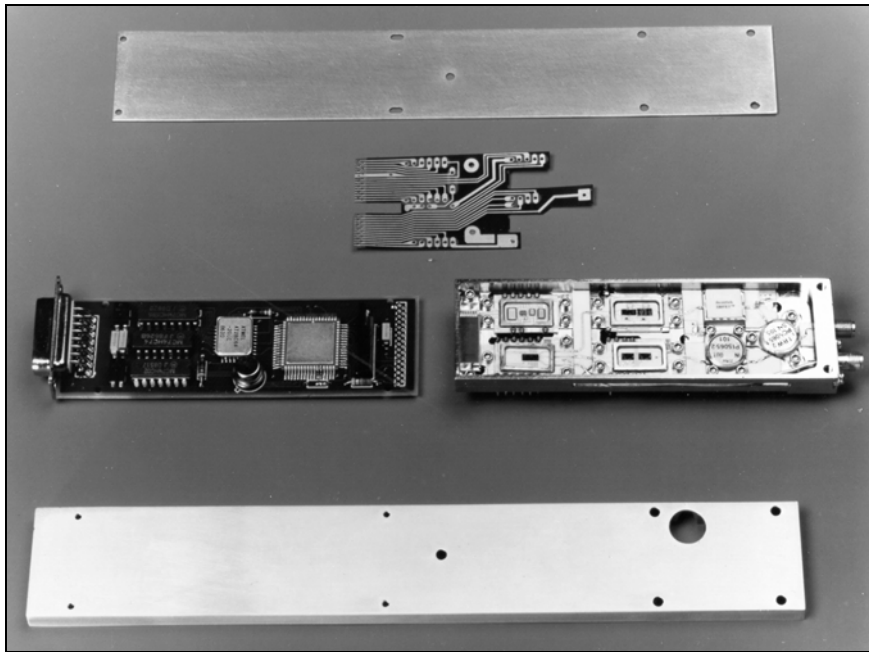


FIGURE 3.2.1 – C BAND T/R MODULE (EXPLODED VIEW)

The block diagram shown in Figure 3.2.2 shows the architecture of this module. Notice that the module consists of a two chip power amplifier driver, the IMFET power amplifier, a three chip LNA section that has gain control and a multi-bit phase shifter. The controller is a custom CMOS processor with some TTL “glue” logic and an EEPROM look-up table for performance correction factors. The power conditioning is limited to HEXFET switching of the drain bias. This module operates from 8 power supply voltages as noted in Table 3.2.1. Typical module performance parameters are presented in Table 3.2.2.

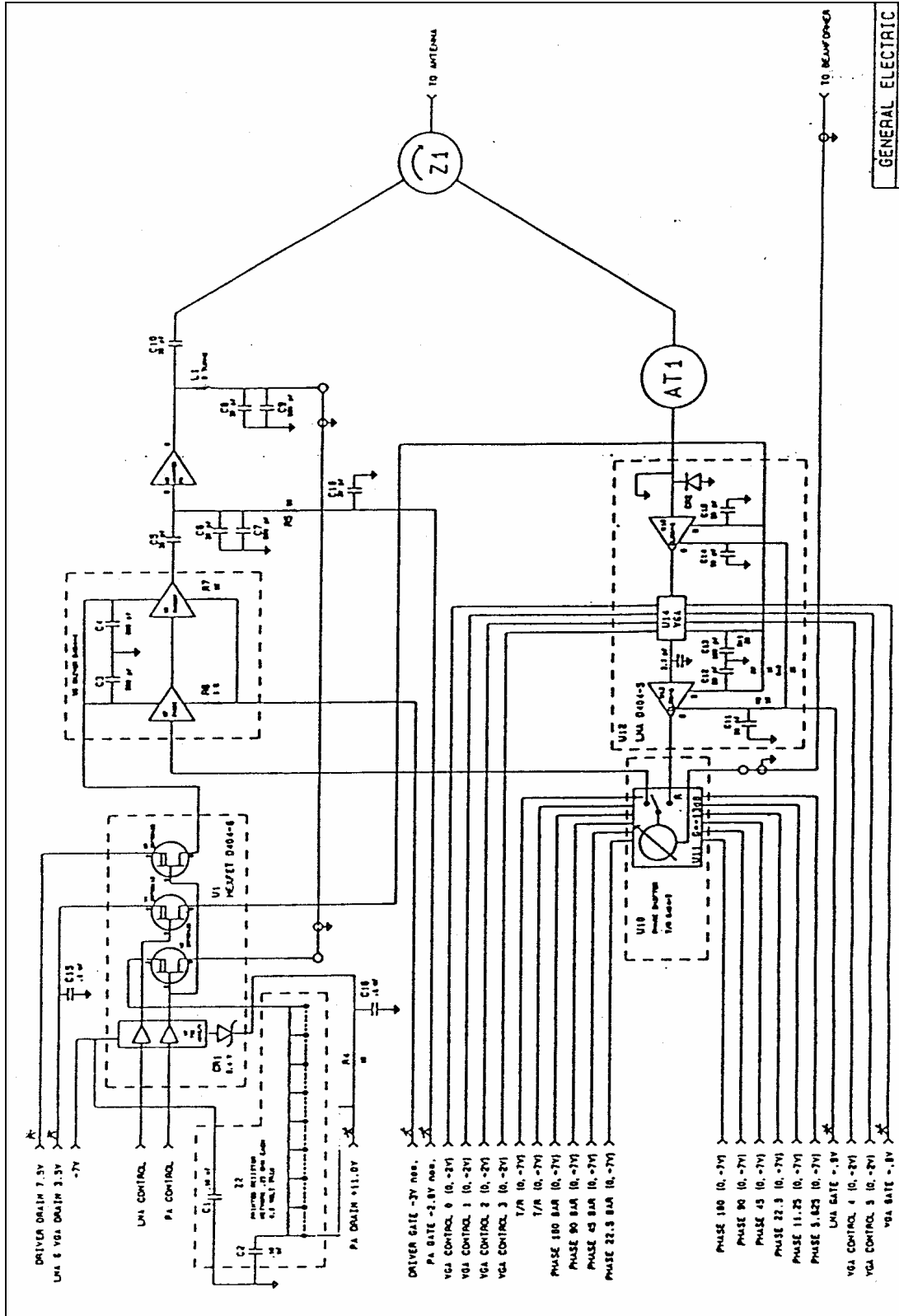


FIGURE 3.2.2 – C BAND T/R MODULE SCHEMATIC DIAGRAM

Power Amplifier Drain Voltage	+14.0 Volts
Driver Amplifier Drain Voltage	+ 9.0 Volts
Receiver Amplifier Drain Voltage	+ 5.0 Volts
Power Amplifier Gate Voltage	- 7.0 Volts
Driver Amplifier Gate Voltage	- 6.0 Volts
Low Noise Amplifier Gate Voltage	- 2.0 Volts
Logic Voltage	- 8.0 Volts
Controller Voltage (MSC)	- 7.5 Volts

TABLE 3.2.1 – TYPICAL BIAS VOLTAGES

TRANSMIT MODE	
POWER OUTPUT	2 WATTS AVE, 10 WATTS PEAK
GAIN	20 dB +/- 1 dB
FREQUENCY RANGE	5.25 TO 5.85 GHz
PHASE SHIFT BITS	6 BITS +/- 3 DEGREES RMS
RECEIVE MODE	
GAIN	25 dB +/- 1 dB
FREQUENCY RANGE	5.25 TO 5.85 GHz
PHASE SHIFT BITS	6 BITS +/- 3 DEGREES RMS

TABLE 3.2.2 - TYPICAL MODULE PERFORMANCE PARAMETERS

3.2.2 LIFE TEST CONDITIONS

This module placed some major mechanical constraints on the test conditions. These included a built-in heat-sink and degradation temperatures of various components. The components with the lowest performance degradation temperature were the circulator, the dielectric, and the epoxy mounting of the power amplifier driver. The circulator's performance will theoretically permanently degrade at about 100 degrees Centigrade and the dielectric and epoxy will each degrade at about 125 degrees Centigrade. Later tests proved that the circulator could actually handle a far greater temperature without any significant performance impact. During the life test, the epoxy mounting caused the driver to operate at a failure point when the channel temperature was above 125 degrees Centigrade. Further failures occurred because there was a lack of strain relief between the individual component packages; causing conductor failure during temperature cycling.

The only electrical constraints that were placed on the test by this module were in the area of bias voltages for both the drain and gates. The transmit chain had a tendency to operate in the unstable region at the settings supplied by the manufacturer (an example of this is shown in Figure 3.2.3). Note that the module oscillated even when no RF was applied. These DC settings were selected by the contractor to achieve the maximum RF output power as measured by a CW power meter with no effort to maintain a good spectrum response. During the pretest characterization, the bias voltages used to achieve the maximum stable output power were determined. Table 3.2.3 provides the manufacturer suggested bias settings and the bias settings that were used to achieve stable operation.

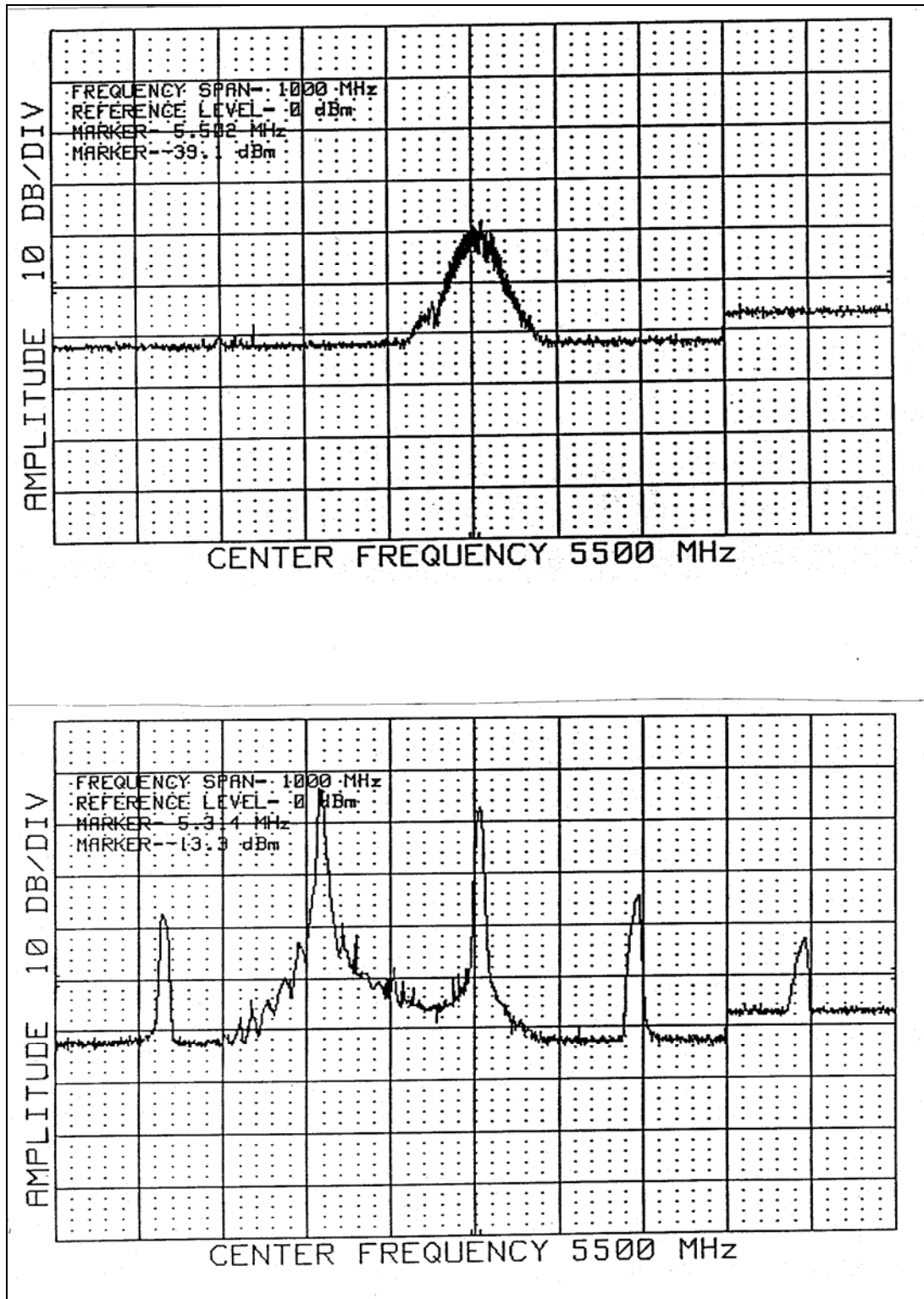


FIGURE 3.2.3 - C BAND T/R MODULE SPECTRUM OUTPUT WITHOUT RF INPUT (UPPER) AND WITH RF INPUT (LOWER)

Stable operation was deemed necessary for this test in order to eliminate as many unknown operating conditions as possible. Oscillations within the amplifier circuits could cause unique heating effects and initiate undesired failure mechanisms. The

drawback to reducing the bias to a stable operating point was that the channel temperatures would then be lower during the test; thus, increasing the time to failure. The channel temperature is a function of the base plate temperature and the DC power dissipated within the circuit. The actual channel temperatures were calculated based on data from IR measurements taken on discrete circuits and calculations made during finite element analysis.

LOCATION	SERIAL NO.	PA (Contractor)	PA (MELTS)	DRV (Contractor)	DRV (MELTS)
CA1	058	+11.0 VOLTS	+10.3 VOLTS	+ 7.5 VOLTS	+ 3.64 VOLTS
CB1	085	+11.0 VOLTS	+10.13 VOLTS	+ 7.5 VOLTS	+ 3.10 VOLTS
CC1	006	+11.0 VOLTS	+10.81 VOLTS	+ 7.5 VOLTS	+ 3.40 VOLTS
CD1	033	+11.0 VOLTS	+110.06 VOLTS	+ 7.5 VOLTS	+ 7.54 VOLTS
CE1	032	+11.0 VOLTS	+ 7.02 VOLTS	+ 7.5 VOLTS	+ 4.23 VOLTS
CA2	065	+11.0 VOLTS	+11.03 VOLTS	+ 7.5 VOLTS	+ 7.53 VOLTS
CB2	057	+11.0 VOLTS	+ 9.49 VOLTS	+ 7.5 VOLTS	+ 4.01 VOLTS
CC2	118	+11.0 VOLTS	+ 7.19 VOLTS	+ 7.5 VOLTS	+ 3.52 VOLTS
CD2	056	+11.0 VOLTS	+11.07 VOLTS	+ 8.0 VOLTS	+ 4.24 VOLTS
CE2	063	+11.0 VOLTS	+11.08 VOLTS	+ 7.5 VOLTS	+ 7.55 VOLTS
CA4	070	+11.0 VOLTS	+ 6.91 VOLTS	+ 8.0 VOLTS	+ 4.60 VOLTS
CB4	042	+11.0 VOLTS	+ 7.17 VOLTS	+ 7.5 VOLTS	+ 3.31 VOLTS
CC4	017	+11.0 VOLTS	+ 8.74 VOLTS	+ 7.5 VOLTS	+ 3.35 VOLTS
CD4	022	+11.0 VOLTS	+ 6.48 VOLTS	+ 7.5 VOLTS	+ 3.16 VOLTS
CE4	084	+11.0 VOLTS	+11.08 VOLTS	+ 8.5 VOLT S	+ 8.56 VOLTS
CA3	089	+11.0 VOLTS	+ 7.61 VOLTS	+ 7.5 VOLTS	+ 3.13 VOLTS
CB3	040	+11.0 VOLTS	+ 6.96 VOLTS	+ 8.5 VOLT S	+ 3.71 VOLTS
CC3	044	+11.0 VOLTS	+12.83 VOLTS	+ 7.5 VOLTS	+ 3.41 VOLTS
CD3	039	+11.0 VOLTS	+ 7.52 VOLTS	+ 7.0 VOLTS	+ 3.71 VOLTS
CE3	073	+11.0 VOLTS	+ 7.06 VOLTS	+ 7.5 VOLTS	+ 3.25 VOLTS

TABLE 3.2.3 - ACTUAL BIAS SETTINGS FOR C BAND T/R MODULES

This initial test was designed to validate the test system and to provide some early reliability data on components. The rationale used to select the parameters for this test included: (1) consideration of the module's specification and known operating capability, (2) minimizing the impact of test system reliability and performance, (3) predicted time required to achieve module failure, and (4) adequacy of data to be acquired for reliability and performance evaluation.

To limit the effect that pulsing the drain voltage has on the system power supplies, the 20 modules were pulsed at 20 percent duty in five groups of four modules. These groups were staggered so that the current draw on the main power supplies would be relatively constant. The pulse width of each group was 100 microseconds long. Test results from this initial life test run indicated that the power supplies had sufficient capacity to negate the need for such staggering during subsequent test.

To acquire a reasonable amount of data in a cost effective manner, while not significantly prolonging the test, a specific test sequence was employed. This test sequence provided that the modules be subjected to 112 minutes of a cook mode while operating in the transmit mode. At the end of the transmit cook mode, the modules are then individually exercised through a measurement mode that lasts for approximately 30 minutes. The sequence then culminates in a 98 minute receive cook mode. Each cycle is 240 minutes

long and there are 6 cycles per day. An illustration of this sequence was shown earlier in Figure 2.2.4. To limit the quantity of data to reasonable levels, it was determined that data would be stored only every 24 hours, unless a significant change occurred in the drain current or the module gain. An arbitrary limit was defined to determine if a module's performance had degraded to the point where it should be considered a dead module. When a module reached that defined death level, it was either tested till a catastrophic failure occurred, or removed from test for detailed analysis. The exact course of action was determined on an individual case based on that module's historical data. The drain current and module microwave gain were defined as the parameters to watch as indicators of performance change.

The base plate temperature that each module was operated at was determined as a function of the DC power input, the module's efficiency, its cooling efficiency, and the ambient temperature of the surrounding environment. Ideally, the modules would all be operating at the same base plate temperature. Such consistency would theoretically lead to the channels all operating at the same temperature. Because the bias voltages for the modules are all set at different levels, and the module efficiency does not track from module to module, each module has a different amount of DC power being dissipated; thus, a different base plate temperature. Table 3.2.4 provides the base plate temperatures that the modules were operating at when the testing began. Figure 3.2.4 shows how these modules were mounted in the test chamber, note the large wattage resistors that were used to raise the ambient temperature in the test chamber.



FIGURE 3.2.4 – C BAND T/R MODULES IN LIFE TEST CHAMBER (LEFT SIDE)

MODULE	TRANSMIT TEMP
CA1	54.8°C
CB1	65.3°C
CC1	70.5°C
CD1	75.2°C
CE1	68.5°C
CA2	72.1°C
CB2	60.4°C
CC2	65.2°C
CD2	75.0°C
CE2	72.0°C
CA4	59.6°C
CB4	58.5°C
CC4	54.5°C
CD4	50.7°C
CE4	64.7°C
CA3	49.6°C
CB3	54.3°C
CC3	56.1°C
CD3	47.1°C
CE3	50.3°C
ABIENIT AIR TEMPERATURE	45.0°C

TABLE 3.2.4 - C BAND BASE PLATE TEMPERATURES

During the course of the test, various events occurred. These events are of two types: (1) test system related, and (2) DUT related. The test system related events provided information on how the structure and operation of the test system needed improvement and/or change, as well as information on the test environment. The DUT related events provided information on how the modules fared in performance and reliability within the test system environment. Table 3.2.5 provides a log of these events. It is important to note the interaction between system level and module level events (i.e., a test system failure can cause a premature module failure, module failures can change the thermal environment and effect power supply loading, etc). Although complicating the test results, these events did not invalidate the results. The event log entries helped in determining what was happening. Further, test system failure that caused a module failure would be a valid emulation of a radar system failure that would cause modules in the array to fail. Analysis of such a failure could lead to modules with a lower susceptibility to radar system “glitches”.

DATE /TIME	EVENT
21 DEC 88/0816	SYSTEM TURN-ON
13 JAN 89/0830	SYSTEM DOWN FOR SOFTWARE MODIFICATION
13 JAN 89/1500	SYSTEM RESTARTED
13 JAN 89//2128	SYSTEM HUNGUP IN RCVR COOK
16 JAN 89/1031	SYSTEM RESTARTED
19 JAN 89	TAPPED ON RF SWITCHES 1A1813 & 1A88 AFTER FIRST MEASUREMENT FREQUENCY & GAIN INCREASED APROX. 8dB (STICKY SWITCHES ?)
19 JAN 89/1600	CHANGED XMTR POWER SENSOR FROM MEDIUM POWER TO LOW POWER
20 JAN 89/1500	MODULE CE2 IS OSCILATING IN RCVR MODE
23 JAN 89/1330	MODULE CC2 IS OSCILATING IN RCVR MODE; STICKY RF SWITCH IS CAUSE OF CC4 LOW RCVR GAIN
30 JAN 89/2235	SYSTEM HUNGUP WHEN PRINTER RAN OUT OF PAPER
31 JAN 89/0935	SYSTEM WAS RESTARTED
3 FEB 89/2055	SYSTEM HUNGUP IN RCVR COOK MODE; CAUSED BY POWER METER NOT ZEROING PROPERLY
6 FEB 89/1000	ZEROED POWER METER & RESTARTED SYSTEM
6 FEB 89/2336	SYSTEM HUNGUP IN RCVR COOK MODE; CAUSED BY POWER METER NOT ZEROING PROPERLY
7 FEB 89/1000	ZEROED POWER METER & RESTARTED SYSTEM
7 FEB 89/2300	SYSTEM HUNGUP IN RCVR COOK MODE; CAUSED BY POWER METER NOT ZEROING PROPERLY
8 FEB 89/1000	ZEROED POWER METER & RESTARTED SYSTEM; REPLACED POWER METER
8 FEB 89/1800	SYSTEM HUNGUP IN RCVR COOK MODE; CAUSED BY S BAND SYNTHESIZER EQUIPMENT FAILURE
9 FEB 89/1300	FAILED SYNTHESIZER REPLACED; SOFTWARE MODIFIED
10 FEB 89/1340	RESTARTED SYSTEM
10 FEB 89/1430	SYSTEM PAUSED FOR CODE MODIFICATION
10 FEB 89/1559	SYSTEM RESTARTED
13 FEB 89/1720	SYSTEM HUNGUP IN RCVR COOK MODE
14 FEB 89/0930	SYSTEM RESTARTED WITH CLEAR I/O
16 FEB 89/0358	SYSTEM HUNGUP IN RCVR COOK MODE; PRINTER OUT OF PAPER
16 FEB 89/1031	SYSTEM RESTARTED
17 FEB 89/0845	POWER SUPPLY BOARD CC3 CURRENT SENSE TRIPPED; RESET BOARD
17 FEB 89/1015	POWER SUPPLY BOARD CC3 CURRENT SENSE TRIPPED; NOT RESET
21 FEB 89/0950	POWER SUPPLY BOARD CC3 RESET
21 FEB 89/1135	POWER SUPPLY BOARD CC3 CURRENT SENSE TRIPPED; NOT RESET
4 MAR 89	SYSTEM HUNGUP; CAUSE PRINTER OUT OF PAPER
6 MAR 89/0923	SYSTEM RESTARTED
9 MAR 89	SYSTEM HUNGUP; CAUSE PRINTER OUT OF PAPER
10 MAR 89/0907	SYSTEM RESTARTED
13 MAR 89/0201	SYSTEM HUNGUP; CAUSE PRINTER OUT OF PAPER
13 MAR 89/0921	SYSTEM RESTARTED
15 MAR 89/1130	ROOM TEMPERATURE IS AT 82°C
27 MAR 89/1600	ROOM AIR CONDITIONER CONTINUES TO MALFUNCTION; ROOM TEMPERATURE IS AT 85°C
7 APR 89/0900	SWITCH DRIVER FAILED; ALL MEASUREMENTS BECAME COMPOSITES
11 APR 89/2200	SYSTEM HUNGUP; CAUSE PRINTER OUT OF PAPER
12 APR 89/1500	SYSTEM RESTARTED; SWITCH DRIVER FIXED
17 APR 89/1645	REMOVED MODULES CA1, CC3, CB4, CE4, CE2 FROM TEST
19 APR 89/1145	SYSTEM HALTED IN RCVR COOK MODE; SOFTWARE UPDATE INSTALLED
20 APR 89/1215	RESTARTED SYSTEM

21 APR 89/0400	SYSTEM HUNGUP IN RCVR COOK MODE; CAUSE WAS TAPE BACK UP
21 APR 89/0945	SYSTEM RESTARTED
28 APR 89/0100	SYSTEM HUNGUP; SOFTWARE ERROR, REPAIRED
28 APR 89/0955	SYSTEM RESTARTED
10 MAY 89/1226	SYSTEM HUNGUP IN RCVR COOK MODE; CAUSE SOFTWARE ERROR
10 MAY 89/1430	SYSTEM RESTARTED
11 MAY 89/0900	SYSTEM HALTED FOR SOFTWARE MODIFICATIONS
11 MAY 89/1000	SYSTEM RESTARTED
12 MAY 89/0331	SYSTEM HUNGUP IN RCVR COOK MODE; CAUSE IS TAPE BACKUP
12 MAY 89/0915	SYSTEM RESTARTED
16 MAY 89/1545	SYSTEM HUNGUP IN XMTR MESURE MODE; CAUSED BY MAINTANCE
16 MAY 89/1615	SYSTEM RESTARTED
19 MAY 89/0830	SYSTEM HUNGUP; CAUSED BY SOFTWARE ERROR
19 MAY 89/0932	SYSTEM RESTARTED
18 MAY 89/1930	AIR CONDITIONING FAILED
19 MAY 89/0930	ROOM TEMPERATURE AT 80°C
19 MAY 89/1510	ROOM TEMPERATURE AT 88°C
19 MAY 89/1532	SYSTEM SHUTDOWN DUE TO ROOM TEMPERATURE
6 JUN 89/0830	SYSTEM RESTARTED
6 JUN 89/1000	RESET SYSTEM CLOCK
12 JUN 89/1116	OPENED CHAMBER DOOR FOR THREE MINUTES FOR TOUR
20 JUN 89/1012	SYSEM HALTED TO INSTALL S BAND MODULES
22 JUN 89/1630	SYSTEM RESTARTED
23 JUN 89/1005	SYSTEM HUNGUP; CAUSED BY TAPE BACKUP
23 JUN 89/1015	SYSTEM RESTARTED
24 JUN 89/1750	SYSTEM HUNGUP; AC POWER LOW VOLTAGE CHANGED EQUIPMENT ADRESSES
26 JUN 89/1000	SYSTEM RESTARTED; ADRESSES RESET
28 JUN 89/1000	SYSTEM HALTED; ADDITIONAL S BAND MODULES INSTALLED
29 JUN 89/1540	SYSTEM RESTARTED
30 JUN 89/0919	SYSTEM HUNGUP; CAUSED BY TAPE BACKUP
30 JUN 89/0920	SYSTEM RESTARTED
14 JUL 89/1630	SYSTEM HALTED; PLANNED POWER OUTAGE
17 JUL 89/1326	SYSTEM RESTARTED
21 JUL 89/0350	SYSTEM HUNGUP; CAUSED BY TAPE BACKUP
21 JUL 89/0912	SYSTEM RESTARTED
24 JUL 89/1700	SYSTEM HUNGUP; CAUSED BY POWER METER FAILURE
26 JUL 89/1010	SYSTEM RESTARED
4 AUG 89/1310	SYSTEM HUNGUP; CAUSED BY TAPE BACKUP
4 AUG 89/1310	SYSTEM RESTARTED
13 AUG 89/0700	SYSTEM HALTED BY POWER OUTAGE
14 AUG 89/1000	SYSTEM RESTARTED
22 AUG 89/1600	SYSTEM HALTED; CAUSED BY PLANNED POWER OUTAGE
25 AUG 89/1145	SYSTEM RESTARTED
5 SEP 89/1630	SYSTEM HALTED; CAUSED BY PLANNED POWER OUTAGE
16 SEP 89/1430	SYSTEM RESTARTED
16 SEP 89/1733	SYSTEM HALTED; CAUSED BY UNANOUNCED POWER OUTAGE
17 SEP 89/1400	SYSTEM RESTARTED
1 NOV 89/0915	SYSTEM HALTED; CAUSED BY TEST TERMINATED

TABLE 3.2.5 - LIFE TEST LOG OF EVENTS

3.2.3 LIFE TEST RESULTS

A composite of data from all 20 C band modules, as measured on MEL-2 prior to MELTS testing, is presented in Figures 3.2.5 (RF module transmit gain, phase, gain linearity, phase linearity), 3.2.6 (RF module receive gain, phase, gain linearity, phase linearity), 3.2.7 (DC module transmit gain, phase, gain linearity, phase linearity), 3.2.8 (DC module receive gain, phase, gain linearity, phase linearity). The data is divided into two sets, the RF modules are those that were subjected to microwave excitation during the life test, and the DC modules are those that did not receive any excitation during life test (DC only). The microwave gain for the RF modules shows a wide spread between about 15 dB of gain to nearly 40 dB of gain, for a spread of about 25 dB. The DC modules exhibit a similar 25 dB spread starting from 5 dB of gain to a top end at just over 30 dB of gain. This data was measured after the transmit gate and drain bias voltages had been adjusted for stable operation. The phase data shows a wide spread of actual phase differences from module to module. Note that more of the DC modules than the RF modules match in phase across the band. This could be caused by numerous reasons including: (1) manufacturing tolerances, (2) connector tolerances, (3) load line differences due to the wide spread of bias settings, or (4) amplifier saturation. The most likely is a difference in load lines. The modules that are bunched together in gain are also the modules that are bunched together in phase. Note that the phase and gain linearity still at a reasonable level even with the inadequate module-to-module tracking. Individual plots for each module are presented in Appendix C.

In Figure 3.2.9, transmit and receive gain data taken during MELTS testing is presented in composite form. The figures shows the transmit and receive gain versus time at the center frequency of 5550 MHz, and the transmit and receive gain versus frequency at one point in time part way through the test. The date and time for each is noted. Note that data is presented only from the RF excited modules. The data that was recorded for the DC modules was corrupted during testing and could not be recovered. In the RF data presented, the gain is perturbed in steps, predominately in a downward direction. Each step is an indication of a major change in the module's performance. The upwards steps indicate that the module either became unstable, the problem somehow improved, or a test system failure occurred. The downward steps indicate that the module either became stable again, or experienced a partial or complete failure. Because the modules did not have a temperature controller to maintain a constant temperature, these modules were susceptible to the temperature variations of the room. Daily variations in the gain of these modules are due to the daily fluctuation in room temperature. Further, as noted in the module data, there is also a seasonal temperature effect that varies the daily average. Sample room temperature data is shown in Figures 3.2.10 & 3.2.11. Individual plots for each module are presented in Appendix C.

Five modules were removed from testing during the latter half of April 89 (see events chart - Table 3.2.6). Three of these modules had received microwave excitation and two were tested under DC only conditions. The remaining modules were removed from test at the beginning of November 89. Upon removal from life testing, each module was

retested on MEL-2 (referred to as phase three). A composite of the phase three module performance is presented in Figures 3.2.12, 3.2.13, 3.2.14 & 3.2.15. Note that each module has a different level of degradation. Individual plots for each module are presented in Appendix C.

The modules were then subjected to a post mortem to determine the cause for the significant changes in performance. The root cause was not failures on the part of the MMICs. The failures are attributed to the specific packaging technique employed.

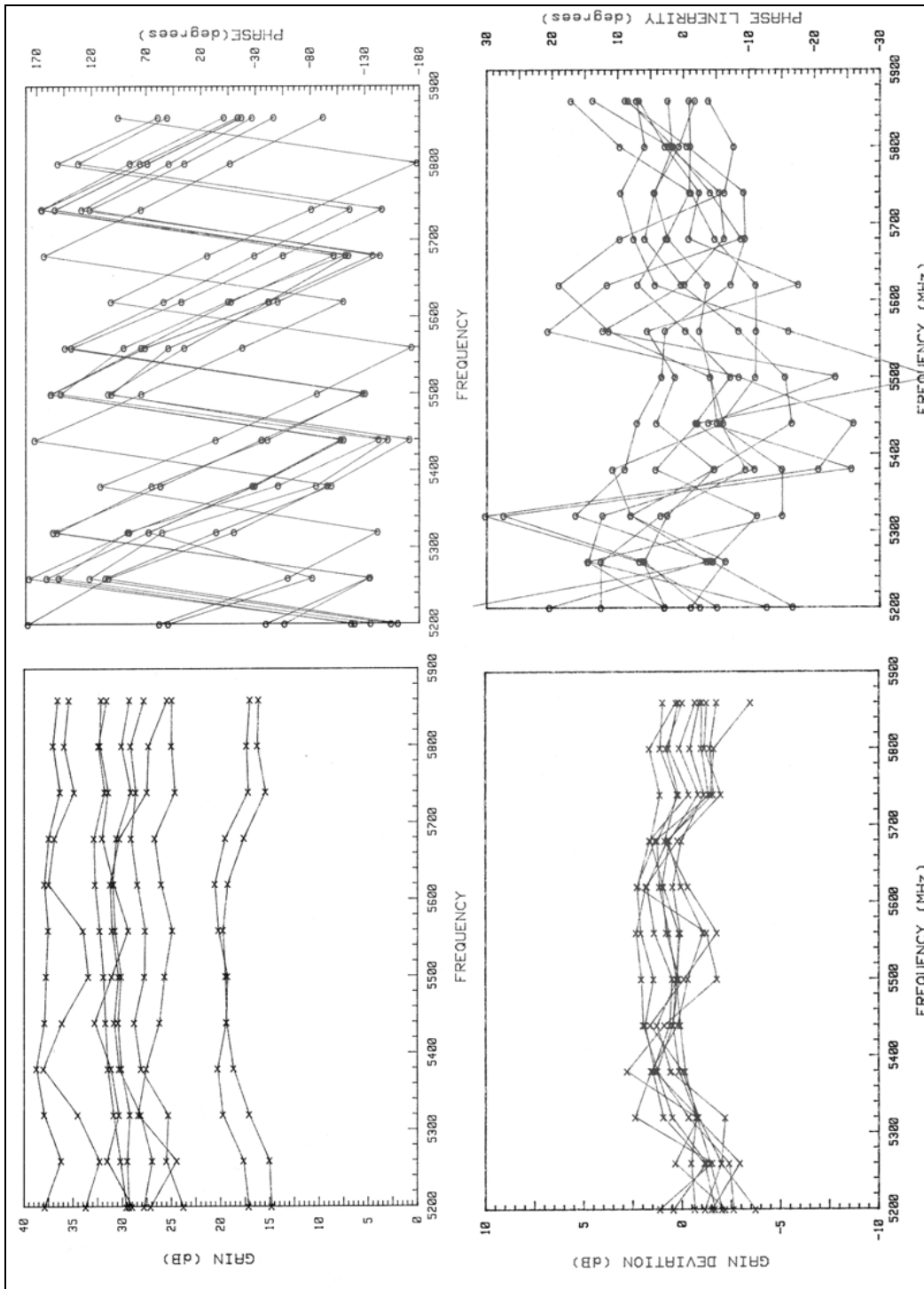


FIGURE 3.2.5 – C BAND T/R MODULE PHASE I RF TRANSMIT COMPOSITE DATA

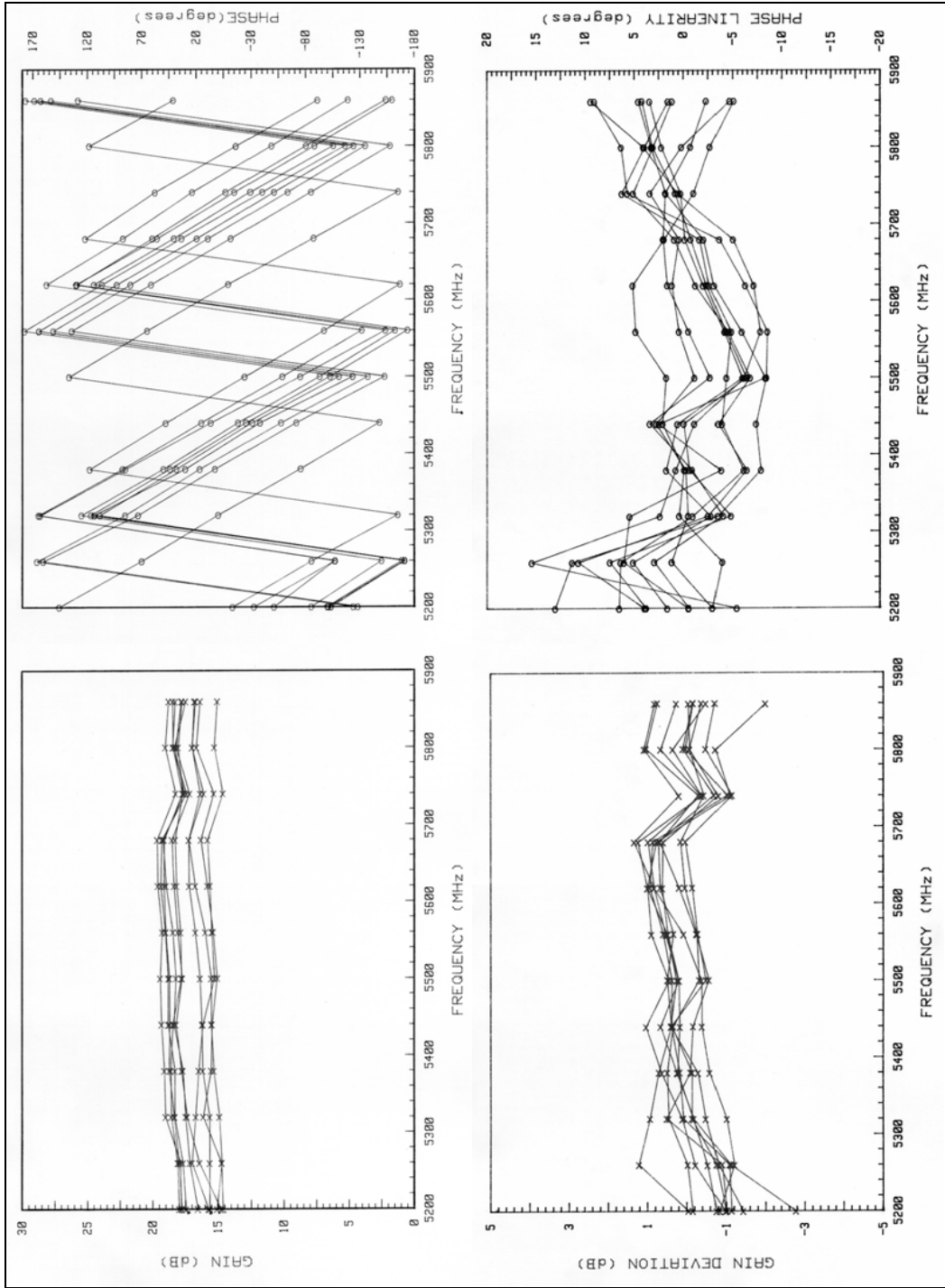


FIGURE 3.2.6 - C BAND T/R MODULE PHASE 1 RF RECEIVE COMPOSITE DATA

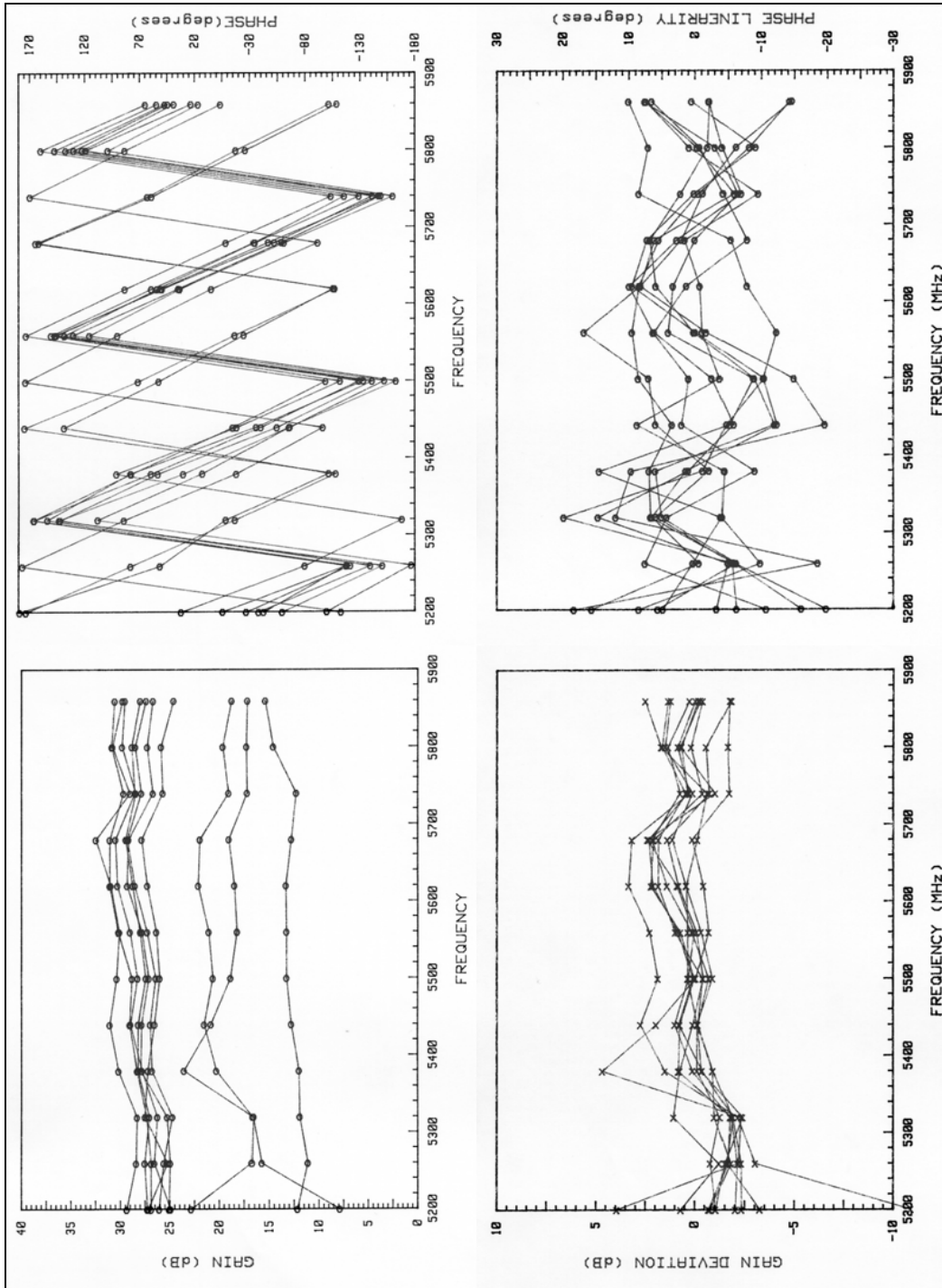


FIGURE 3.2.7 - C BAND T/R MODULE PHASE 1 DC TRANSMIT COMPOSITE DATA

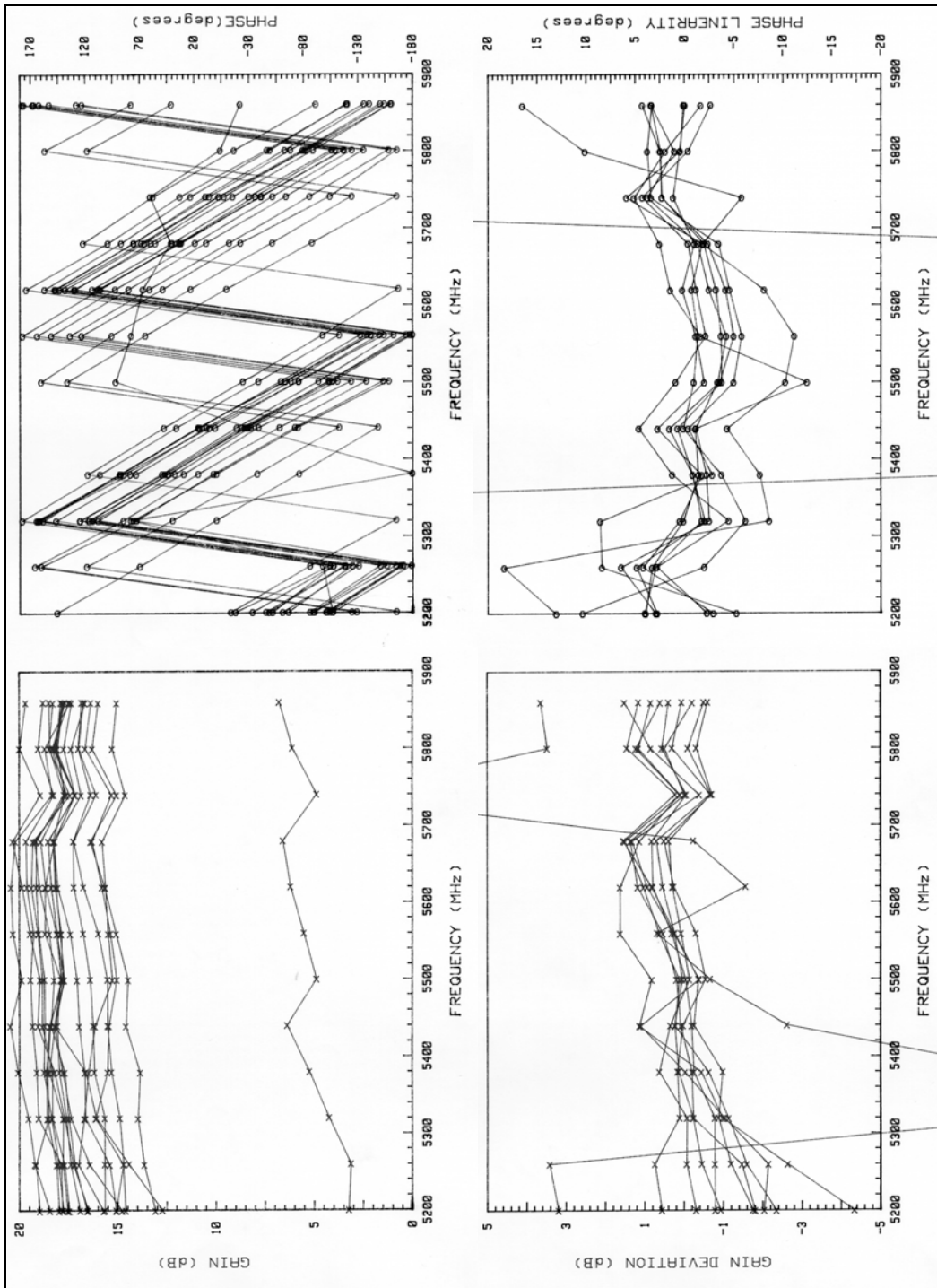


FIGURE 3.2.8 - C BAND T/R MODULE PHASE 1 DC RECEIVE COMPOSITE DATA

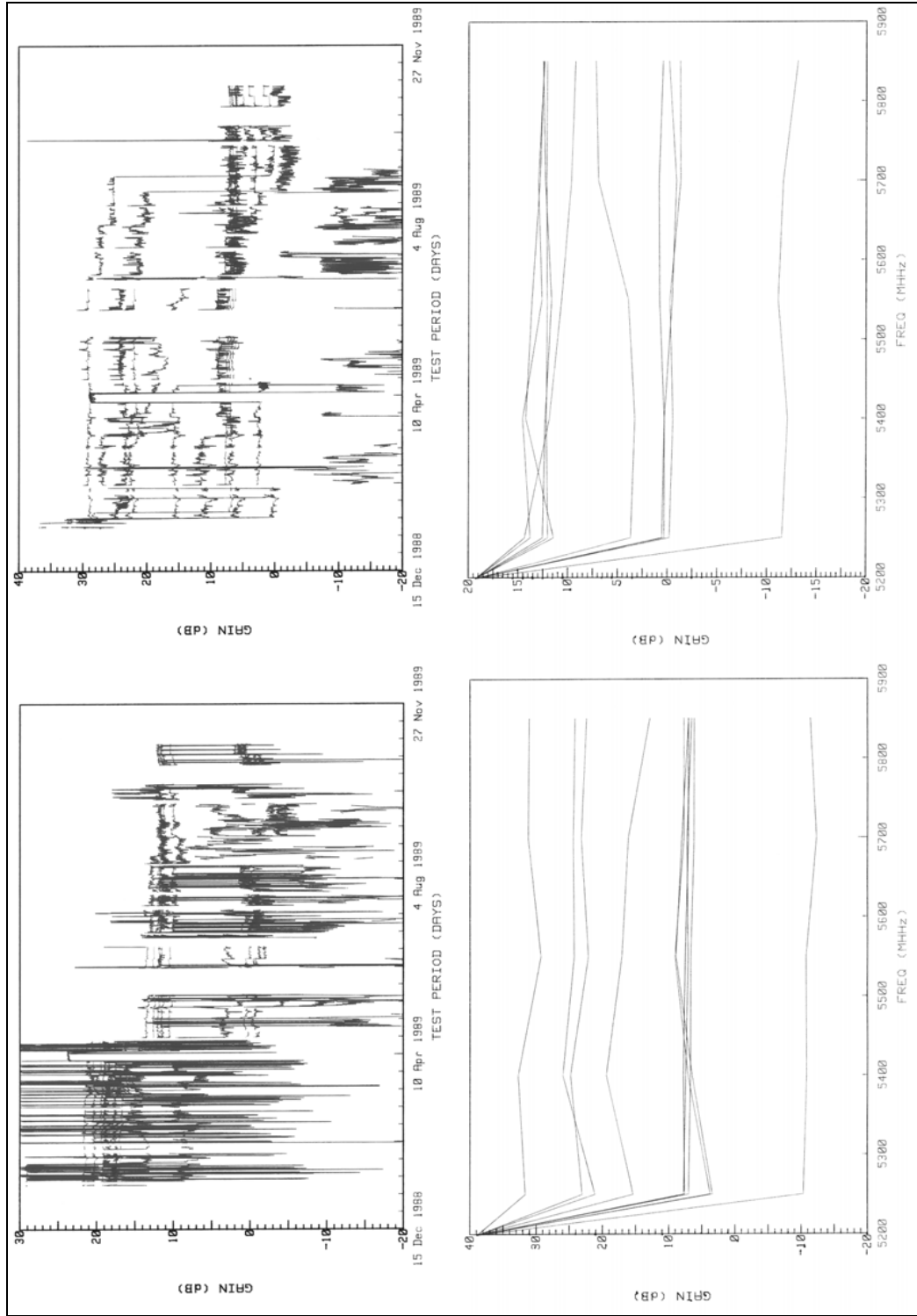


FIGURE 3.2.9 – C BAND COMPOSITE LIFE TEST

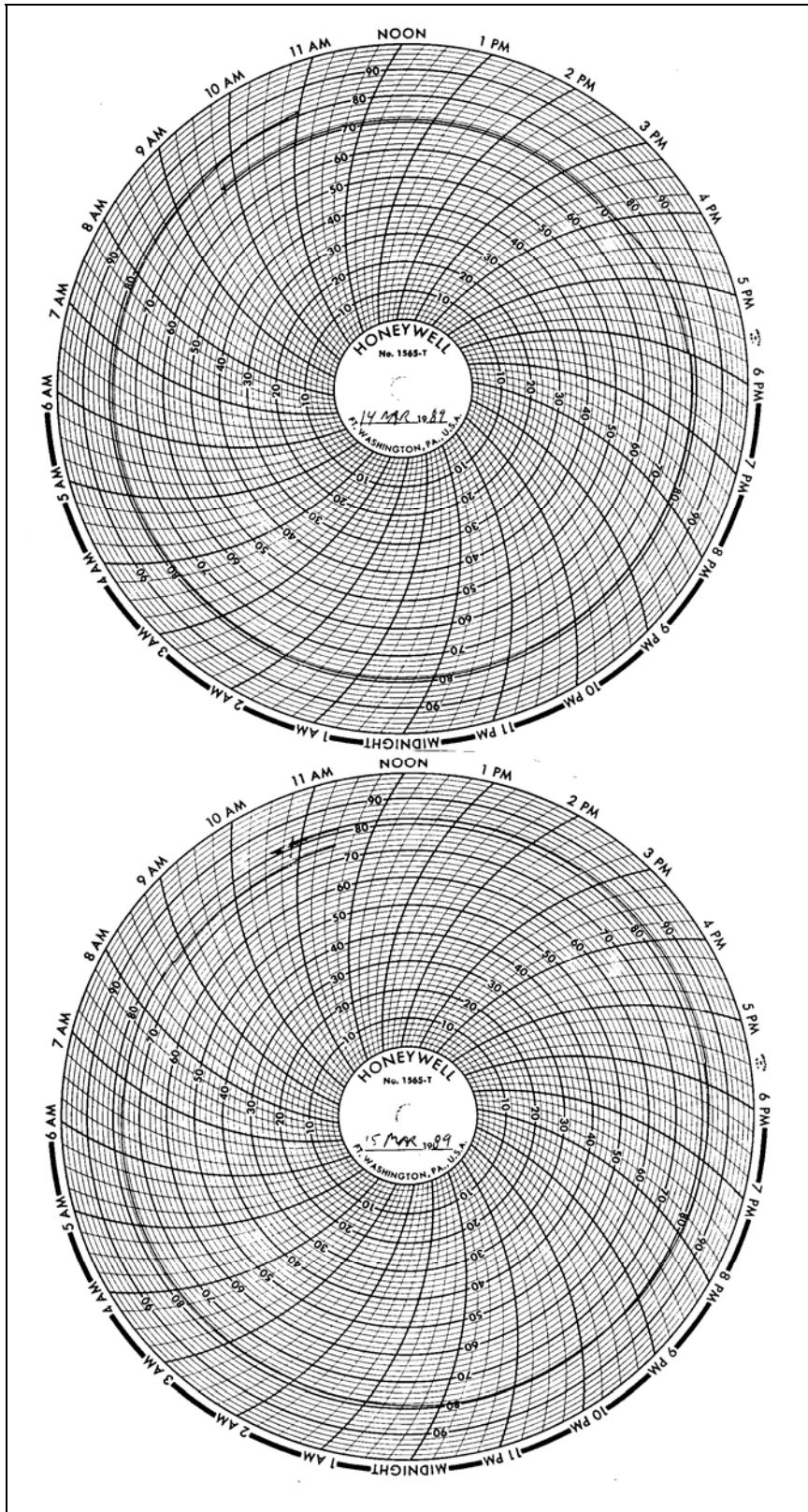


FIGURE 3.2.10 – ROOM TEMPERATURE 14 & 15 MARCH 1989

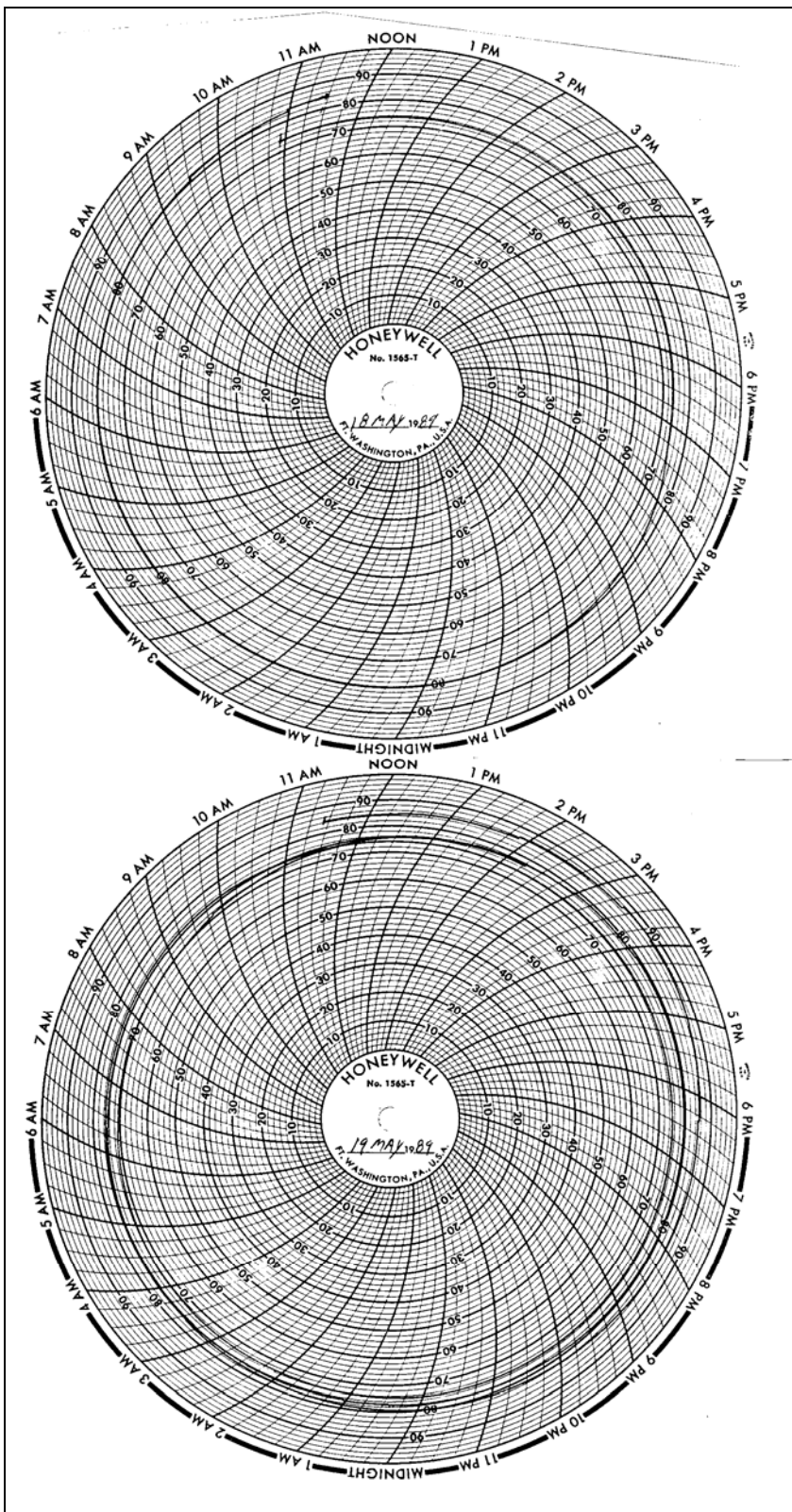


FIGURE 3.2.11 – ROOM TEMPERATURE 18 & 19 MAY 1989

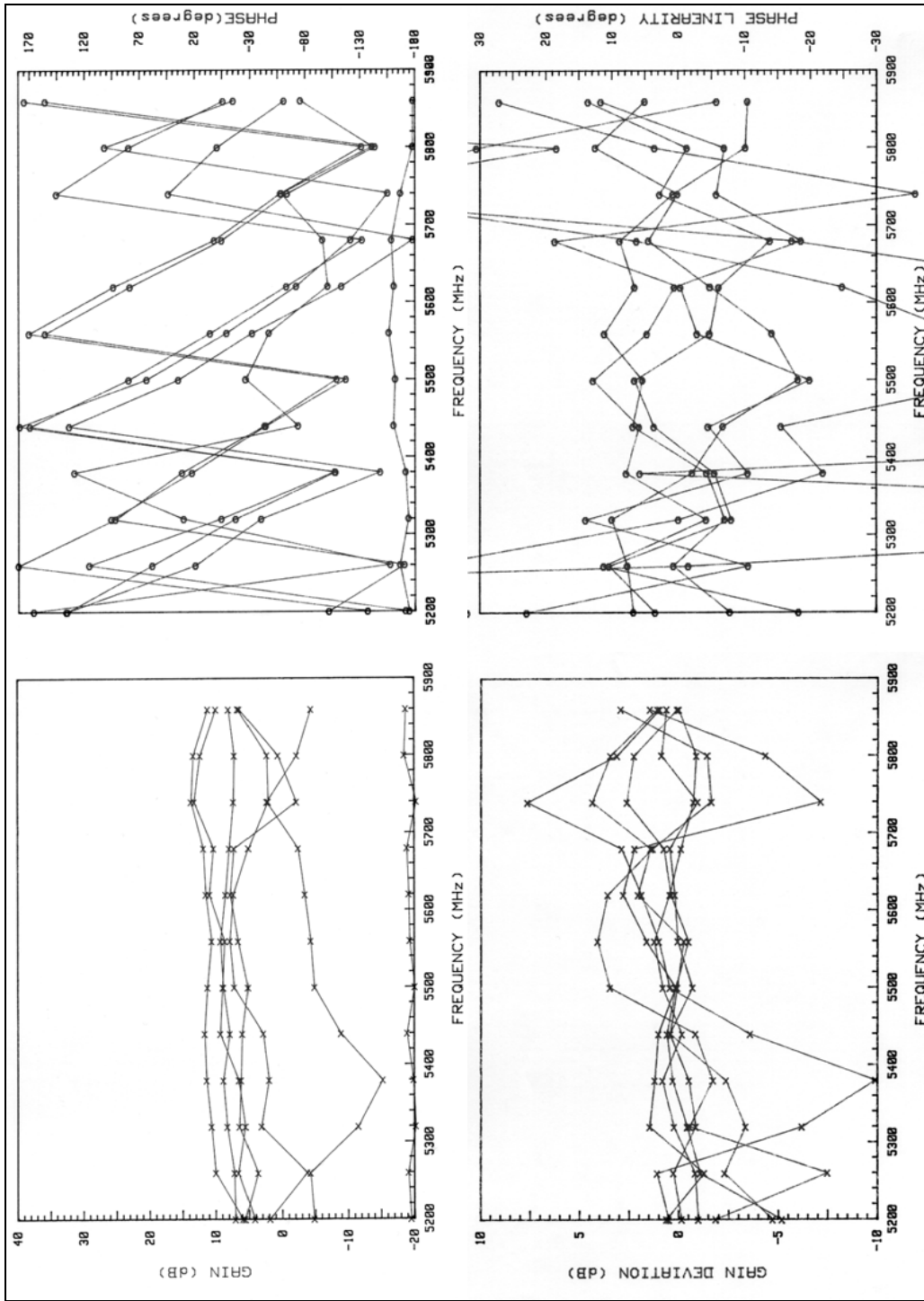


FIGURE 3.2.12 - C-BAND T/R MODULE PHASE III RF TRANSMIT COMPOSITE DATA

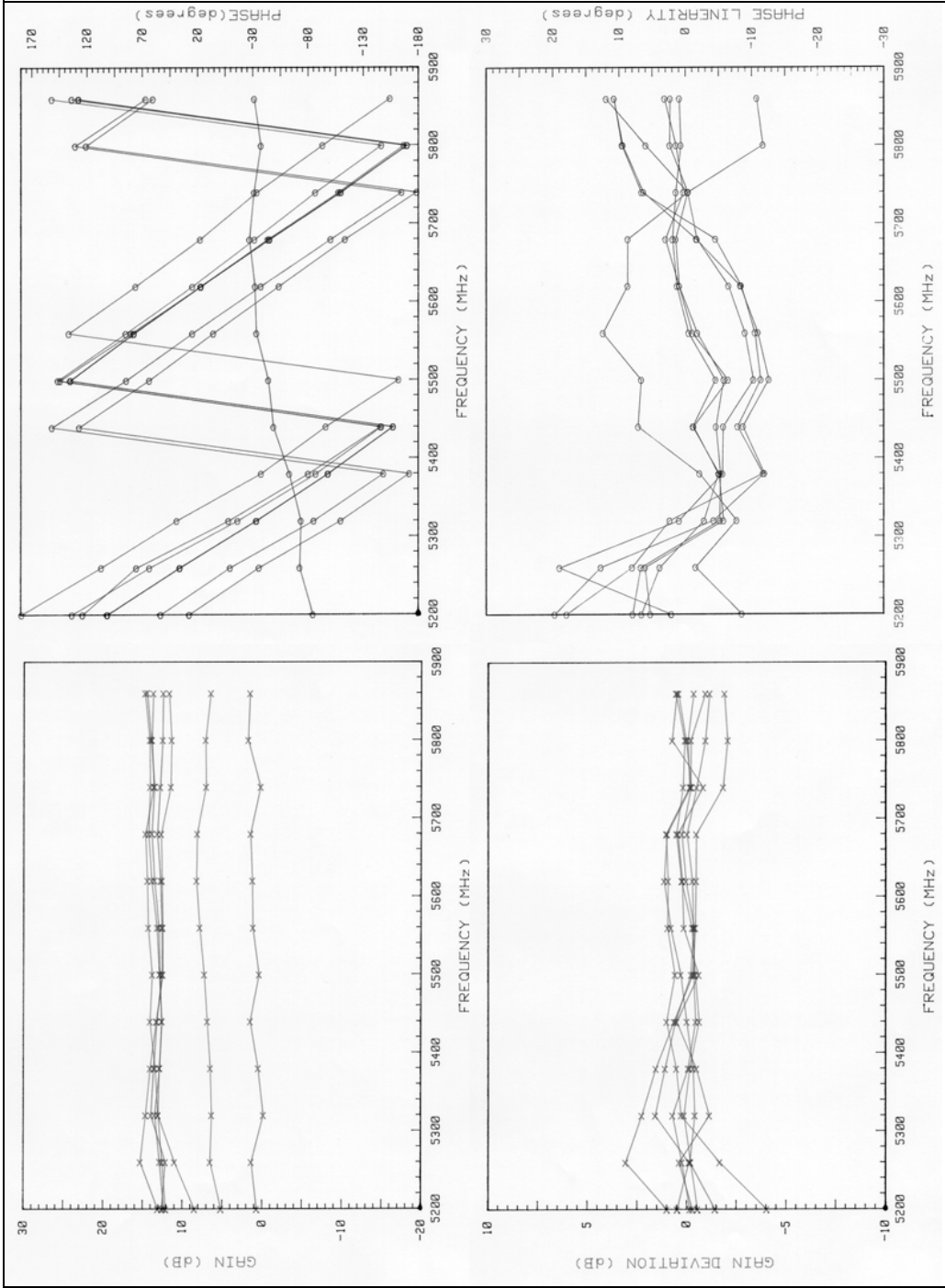


FIGURE 3.2.13 - C-BAND T/R MODULE PHASE III RF RECEIVER COMPOSITE DATA

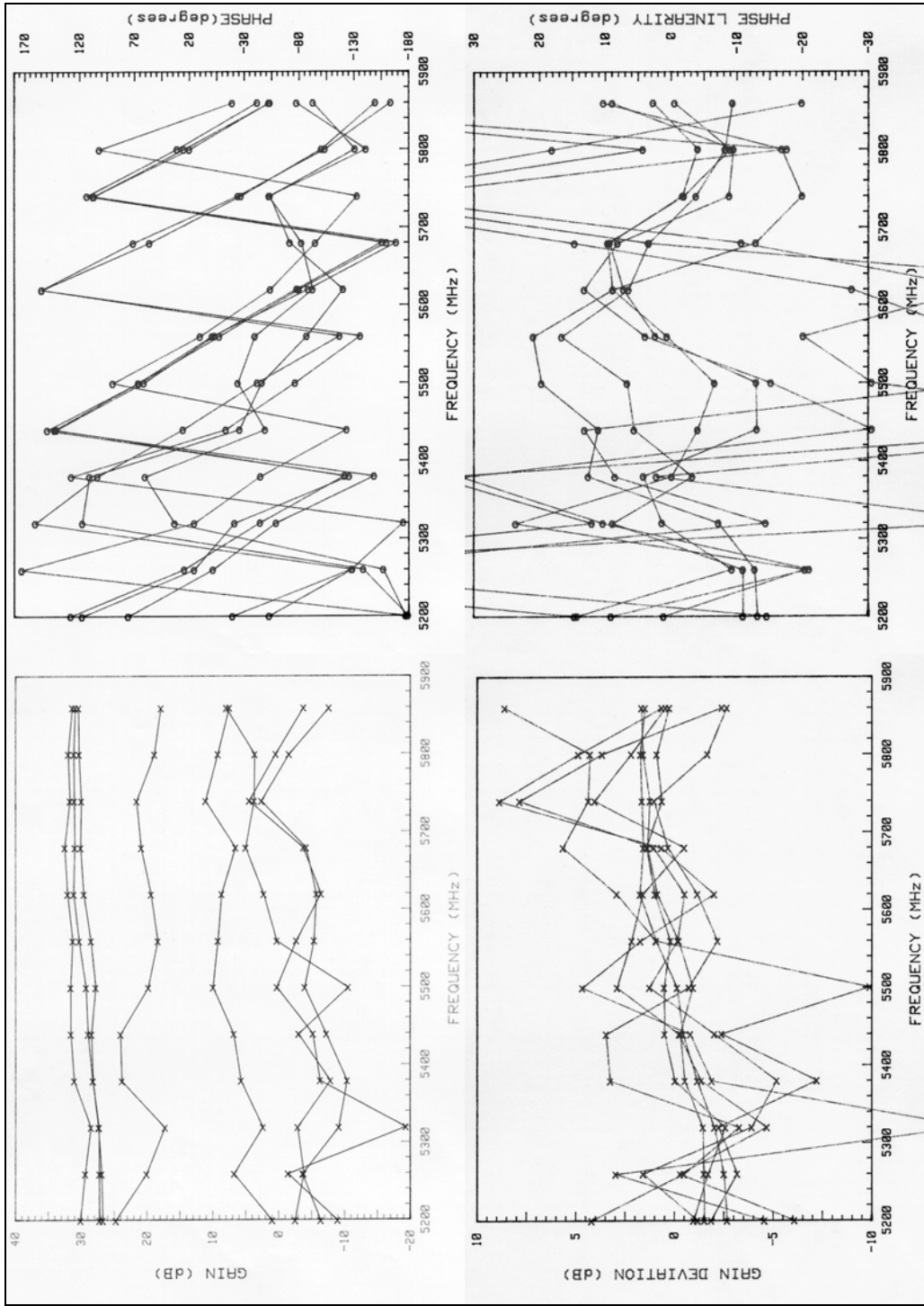


FIGURE 3.2.14 - C-BAND T/R MODULE PHASE III DC TRANSMIT COMPOSITE DATA

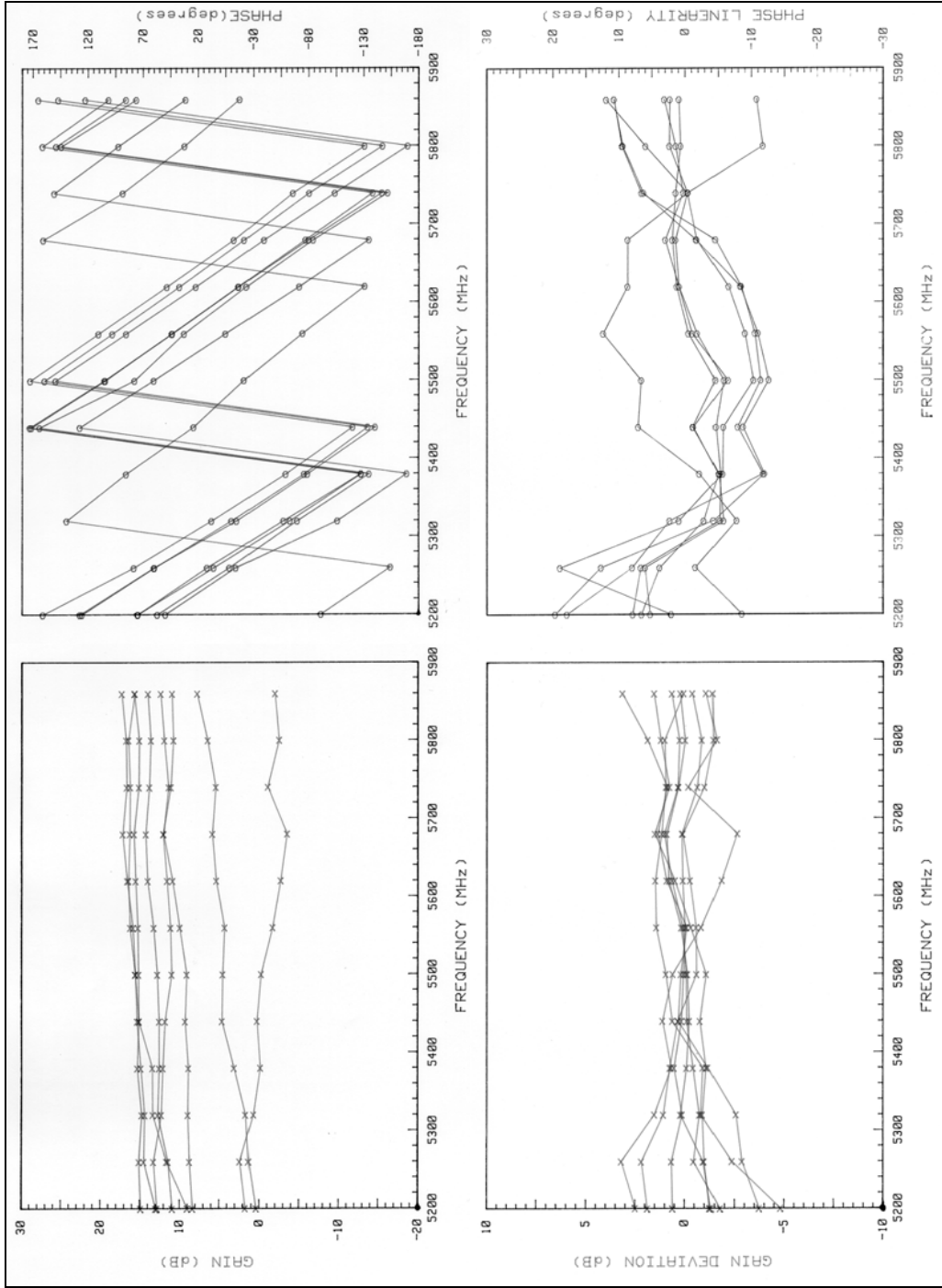


FIGURE 3.2.15 - C-BAND T/R MODULE PHASE III DC RECEIVER COMPOSITE DATA

3.3 S-BAND MODULES

These devices were subjected to a variety of test. The test discussed here are the temperature test that were conducted to determine their temperature related characteristics.

3.3.1 MODULE DESCRIPTION

The microwave circuits of these modules are of GaAs technology in the form of Monolithic Microwave Integrated Circuits (MMIC). This module was configured into two different packages. Both packages have identical electronics; thus, allowing data from one configuration to provide information on the reliability and performance of the other. The module configuration tested is shown in Figure 3.3.1 (with a close up of the microwave components). This package was the chosen for life testing due to its flat base plate surface's ability to mount onto the thermal heat sink. Notice that the module consists of a MMIC section, a circulator and a control section. This module operates from 3 power supply voltages.

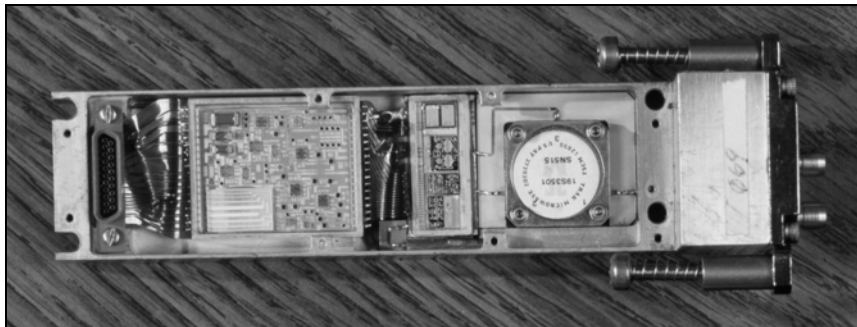


FIGURE 3.3.1 – S-BAND T/R MODULE

3.3.2 TEMPERATURE TEST

Tests were conducted on these modules across a large temperature differential to determine how temperature affects various operating characteristics. These tests included operation during temperature cycling from room temperature down to liquid nitrogen temperatures (-197 degrees Centigrade).

A liquid nitrogen bath, commonly referred to as the “beer cooler” bath, was constructed to enable the cooling of modules down to cryogenic temperatures. The devices were securely attached to a vertically oriented copper plate and suspended over the cold bath. By adjusting the height of the table supporting the bath, the extent to which the copper plate is immersed in the coolant is varied, hence controlling the temperature of the module. A picture of this setup is shown in Figure 3.3.2.



Figure 3.3.2 – “BEER COOLER” BATH TEMPERATURE TEST

Acquisition of the data required to characterize the module is accomplished by utilizing the MEL-2 test system to automatically measure pulsed RF and noise figure. Both small signal CW and pulse power transmit/receive testing enable the gain, noise figure, and phase data to be obtained during programmed temperature variation.

Temperature is measured using thermocouples judiciously attached to locations within the device itself. Thus, the performance of an operating module is continually monitored as a function of temperature, down to as low as that of liquid nitrogen, almost 200 degrees below zero Centigrade.

Figure 3.3.3 features the transmit performance of one of the S-Band modules as it is cooled. Note that the cooling initially improves the gain, albeit at a rate of 0.5 DB/10°C.

Gain peaks at about -70°C and declines upon further cooling. Although gain fluctuations are not evident, the frequency spectra (not shown) revealed oscillations.

Small signal CW measurements of the T/R module are portrayed in Figure 3.3.4, highlighting the classical inverse relation between gain and noise as temperature falls. On cooling, gain and noise figure improved -170°C, whereupon activity precipitously collapses and the module ceases operation. This shutdown is “forgiving”, activity resumes unaltered upon warming.

Tracking the individual temperatures of the MMIC chip and controller in pulse receive mode points to the controller as being responsible for this “freeze-out”. Close inspection (Figure 3.3.5) shows that while the MMIC chip is at liquid nitrogen temperature, it is the warming of the controller that turns the module on.

To validate that this phenomenon really exist, a total of 5 modules were tested. A plot of the module to module tracking of transmit gain is shown in Figure 3.3.6.

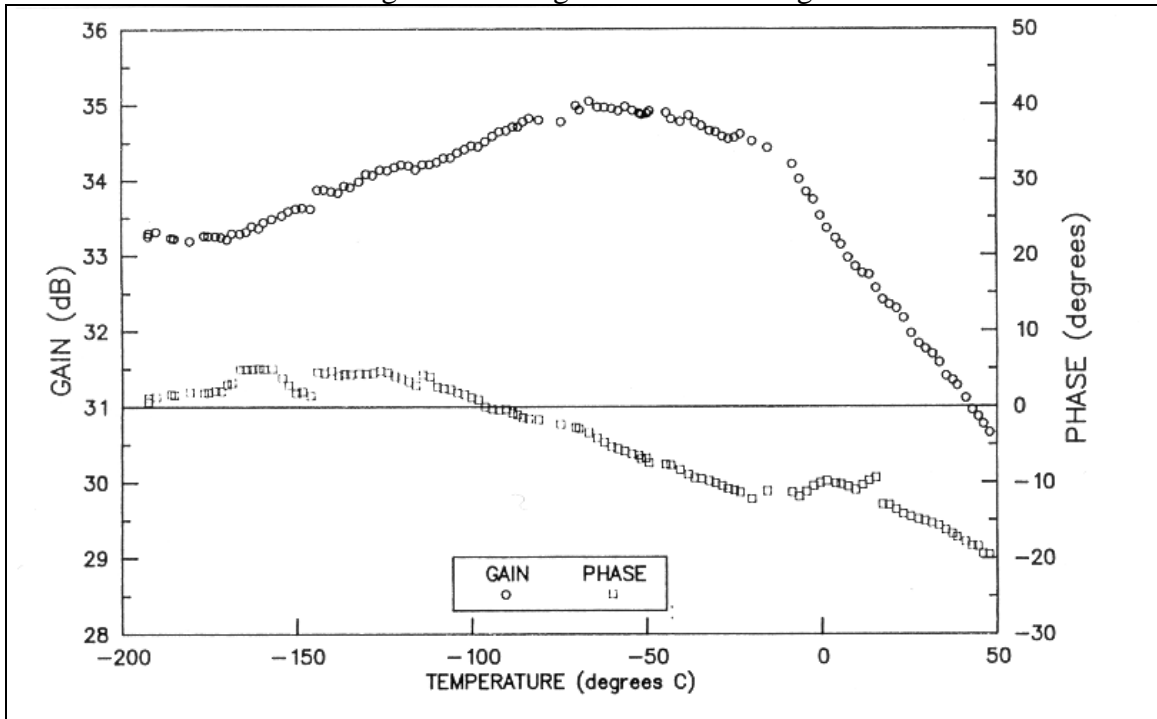


FIGURE 3.3.3 – S-BAND MODULE TRANSMIT GAIN & PHASE VS TEMPERATURE

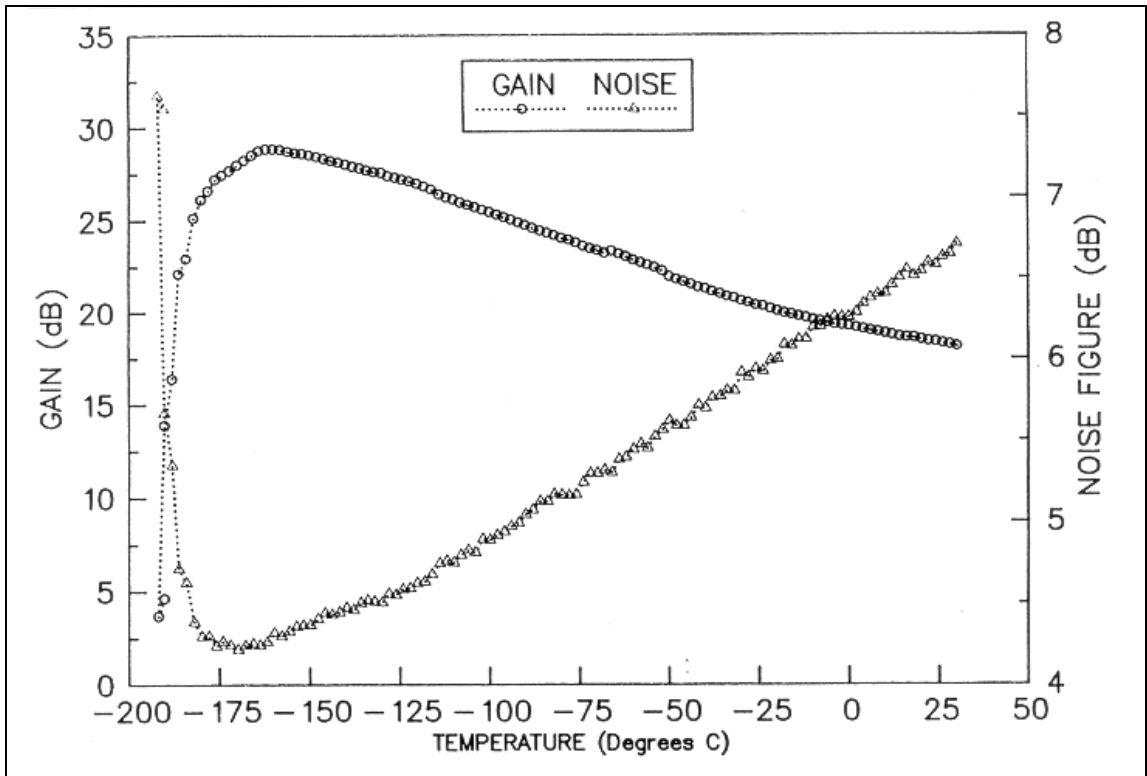


FIGURE 3.3.4 – S-BAND MODULE SMALL SIGNAL CW GAIN & NOISE FIGURE VS TEMPERATURE

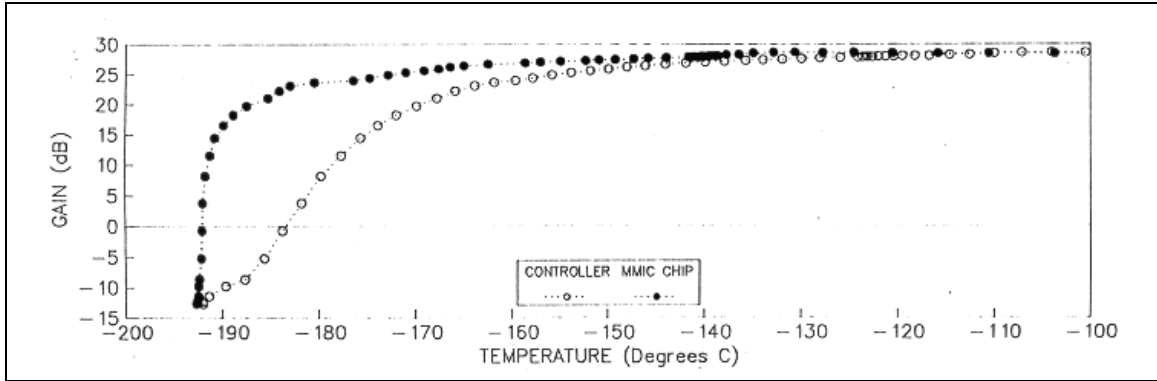


FIGURE 3.3.5 – S-BAND MODULE RECEIVE "FREEZE-OUT" MMIC CHIP AND CONTROLLER TEMPERATURES VS GAIN

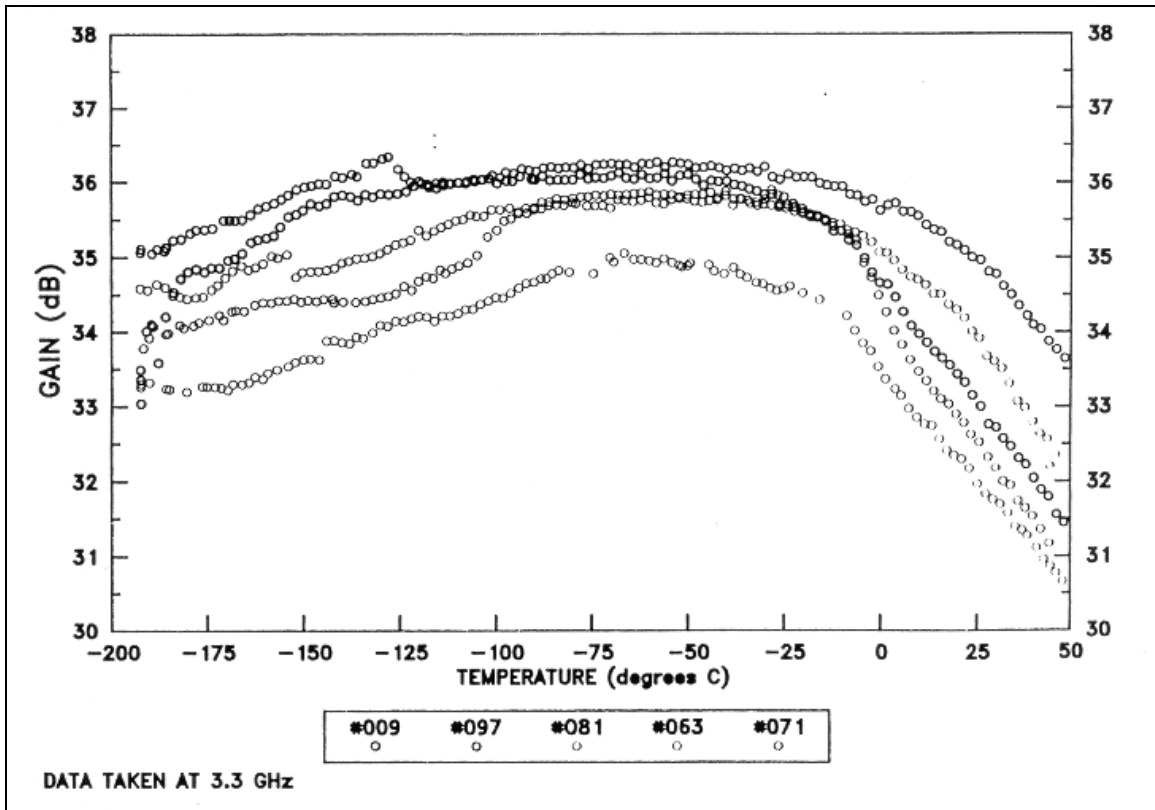


FIGURE 3.3.6 – S-BAND MODULE TRANSMIT GAIN MODULE TO MODULE TRACKING VS TEMPERATURE

4.0 CONCLUSIONS

The testing methodologies developed and demonstrated as part of this effort have made a significant impact on T/R module technology development. One of the more significant examples is the impact that this work had on convincing the Automated Network Analyzer manufacturers to develop a pulsed version of their product (Hewlett Packard and Wiltron). These products are now used widely by the various T/R module fabricators in their engineering development and on the manufacturing lines. The impact is on the cost and performance of the modules is consistent with the cost projections described back in introduction of this document. The savings was so significant that it has enabled the transition of this technology into the commercial arena. Specifically, T/R modules are a key component of the phased array antenna on the Iridium Satellite.

A significant byproduct of developing these testing methodologies is the testing that was conducted as part of their demonstration. Information of the characteristics of T/R modules and there performance under various operating conditions were evaluated and feed back to the various module developers for design and fabrication technique modifications. Examples of this are as follows:

1. The C band life test data showed that packaging can be a grater reliability issue than the devices are. Specifically, in fabricating a T/R module that must meet both the high performance and reliability requirements a trade-off must be made between how much packaging is used and the probability that a bad component will require some rework.
2. The early L-Band and S-Band modules showed that the interfacing, specifically the connectors can have a great impact on the performance and reliability of the module. Here the DC and Control connectors failed causing a significant change in performance. These failures were a function of the multiple connections that had to be made and the large temperature variations that the modules were subjected to.
3. At very low temperatures (i.e., -197 degrees Centigrade) GaAs devices continue to increase in performance, while silicon devices stop performing. Cryogenic performance yields insight into the underlying physics of module operation. The achieved results complement and extend previous research. This emphasis the need to keep in mine the various environments that the modules will be subjected to when designing and testing. Designing for performance at ambient temperatures and other conditions may not provide the best system performance. Further, the interaction of various technologies, with good individual performance needs to be evaluated as a complete system as well.

BIBLIOGRAPHY

- * 1. R. Macior, B. Sweatland; "Module Evaluation Lab (MEL-2 Report)"; RADC-TR-89-225 (Vol. 1 & 2); October 1989
2. "Coherent (I/Q) Detector Performance Under Extended Drive Signal Conditions"; 27th ARFTG Conference; June 1986
3. "Application of Phase Discriminator Error Model to Pulsed RF Measurement System Calibration"; 29th ARFTG Conference; June 1987
4. E. J. Jones; "The Requirements for a General Purpose Automatic Pulse Measuring System"; 22nd ARFTG Conference; December 1983
5. E. J. Jones; "T/R Module Evaluation Test System"; 20th ARFTG Conference; December 1982
6. M. O. Little, L. L. Stevens, T. A. McEwen, E. J. Jones; "Computer Controlled Pulse Phase Measurement System"; 24th ARFTG Conference; December 1984
- * 7. H. R. Irwin, H. F. Purdula, E. J. Collins; "Technical Feasibility Study Applicable to Automatic Pulse Measurement"; RADC-TR-85-222; December 1986
8. "Panel Discussion: Advantages, and Disadvantages of Six-Port Analyzers"; 13th ARFTG Conference; May 1979
9. "Hewlett Packard 8510A Network Analyzer Operating and Service Manual Volume 4"
10. "C. A. Hoer; "A Network Analyzer Incorporating Two Six-Port Reflectometers"; IEEE Trans. Microwave Theory Tech; Vol. MTT-25; pp. 1070-1074; December 1977
11. M. O. Little, E. J. Jones, D. J. Ducharme, T. A. McEwen; "Techniques for Pulsed Microwave Measurement"; 27th ARFTG Conference; June 1986
12. RCA Government Systems Division, Missile and Surface Radar; "Operation and Maintenance Manual, Wideband Waveform Generator and Signal Processor"; August 1978, Unpublished.
- * 13. C. R. Thomas, E. J. Jones, R. F. Brass; "MMIC Wideband Measurement Techniques"; RADC-TR-89-49; June 1989
14. E. J. Jones; "Monolithic Amplifier Evaluation"; RADC-TR-83-21; Jan 1983.
21. M. O. Little; "Panel Discussion: A Look to the Future - Large Volume Production of GaAs MMICs"; 30th ARFTG Conference; December 1987.
24. D. W. Griffin; "Evaluation of Amplitude and Phase Characteristics of Microwave Solid State Amplifier"; RADC-TR-76-241 (Part 1); August 1976.
25. Hewlett Packard Application Note 64-3; "Accurate and Automatic Noise Figure Measurements"; June 1980.
- * 26. J.W. Price, C. Mark; "Automatic Pulsed Measurement System"; RADC-TR-87-252; December 87.
- * 30. L. Baum, L. Santalesa; "Transmit/Receive Module Thermal Dissipation Measurements"; RADC-TR-90-56; May 90.

* RADC-TR-89-225 is Distribution limited to DOD AND THEIR CONTRACTORS - EXPORT CONTROL

* RADC-TR-85-222 is Distribution limited to DOD AND THEIR CONTRACTORS - EXPORT CONTROL

* RADC-TR-89-49 is Distribution limited to DOD AND THEIR CONTRACOTRS - EXPORT CONTROL

* RADC-TR-87-252 is Distribution limited to DOD ONLY: DOD CONTROLLED - EXPORT CONTROL

* RADC-TR-90-56 is Distribution limited to U.S. GOV'T. AND THEIR CONTRACTORS - EXPORT CONTROL

GLOSSARY

- ARFTG - Automatic Radio Frequency Techniques Group which is a professional organization, an affiliate of the IEEE's Microwave Theory and Techniques Society, that specializes in automated methods of measuring RF performance of various devices.
- DARPA - Defense Advanced Research Project Agency.
- EEPROM - Electrically Erasable Programmable Read Only Memory.
- FSK - Frequency Shift Keying modulation.
- GHz - Gigahertz.
- IEEE - Institute of Electrical and Electronic Engineers which is an international professional organization.
- IMFET - Internally Matched Field Effect Transistor
- KHz - kilohertz.
- LFM - Linear Frequency Modulation.
- MEL - Module Evaluation Laboratory, a name given to both the facility that all of the module testing has occurred during the last decade and the primary characterization system that operates in that lab.
- MELTS - Module Evaluation Life Test System which is the common name for the Long Term Performance Test System, a system designed to subject DUTs to a consistent set of operating environments over a long period of time while continuously monitoring and recording data on their performance.
- MHz - megahertz.
- MIMIC - Microwave and Millimeter wave Integrated Circuit program sponsored by DARPA to develop MMIC foundry technology. The program is phased; Phase 0 - concept exploration, Phase 1 - Foundry & Demonstration Vehicle development, Phase 2 - Foundry & Brassboard demonstration, Phase 3 - Supporting Technology development.
- MMIC - Monolithic Microwave Integrated Circuit, the technology of building microwave circuits on a single substrate (i.e. GaAs, Si, etc) using integrated circuit techniques.

MODVAL - MODule VALidation was a RADC contract with Raytheon and Texas Instruments to develop X Band modules for a Space Defense Initiative (SDI) mid course discriminating radar.

RF - Radio Frequency.

RL - Rome Laboratory (Formerly Rome Air Development Center (RADC)), is Air Force Material Command (AFMC) laboratory with the mission of C³I.

VCO - Voltage Controlled Oscillator.

APPENDIX A – C-BAND MODULE DATA

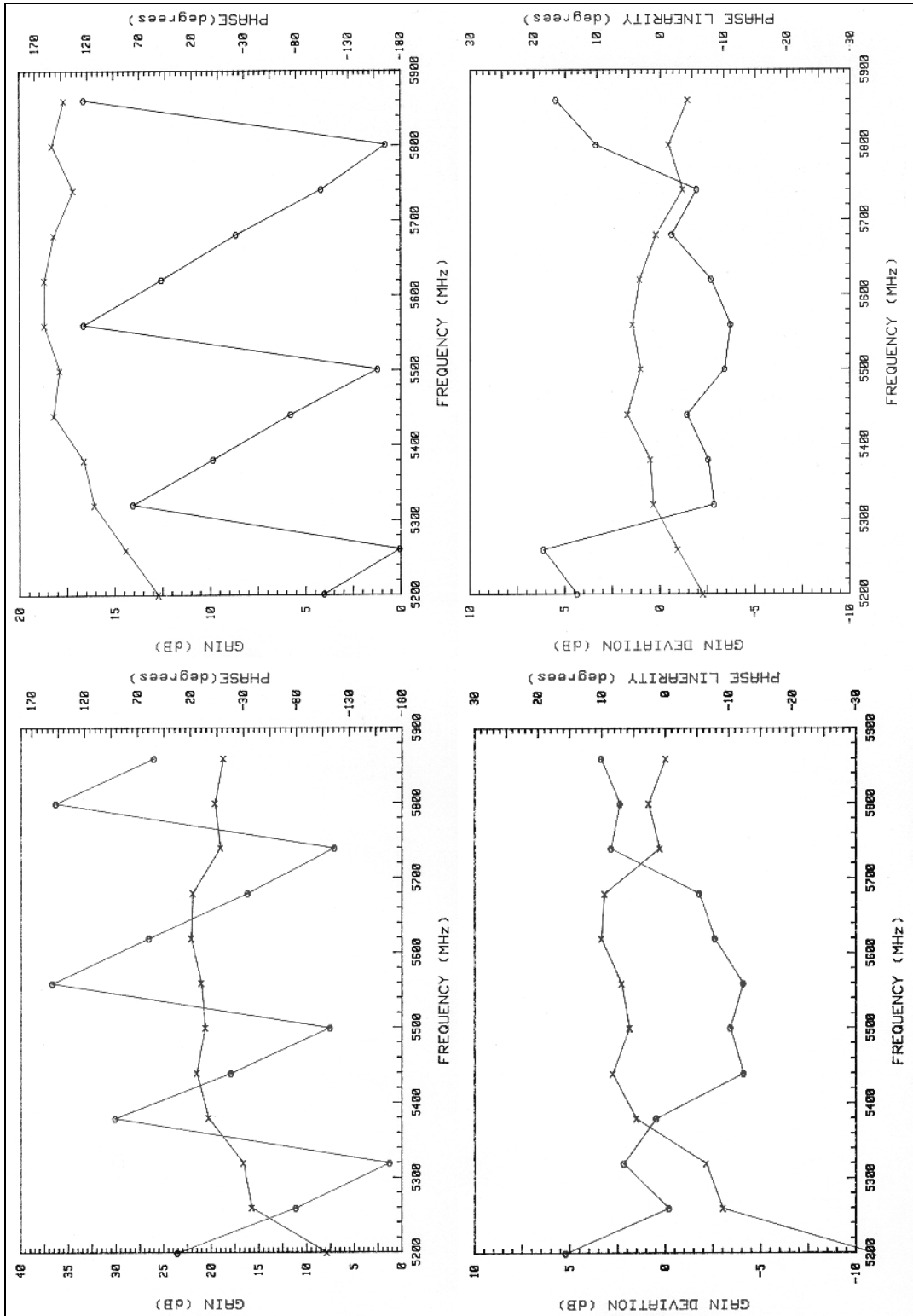


FIGURE A.2 - PHASE 1 TESTING C-BAND MODULE SN006 (LEFT) TRANSMIT & (RIGHT) RECEIVE

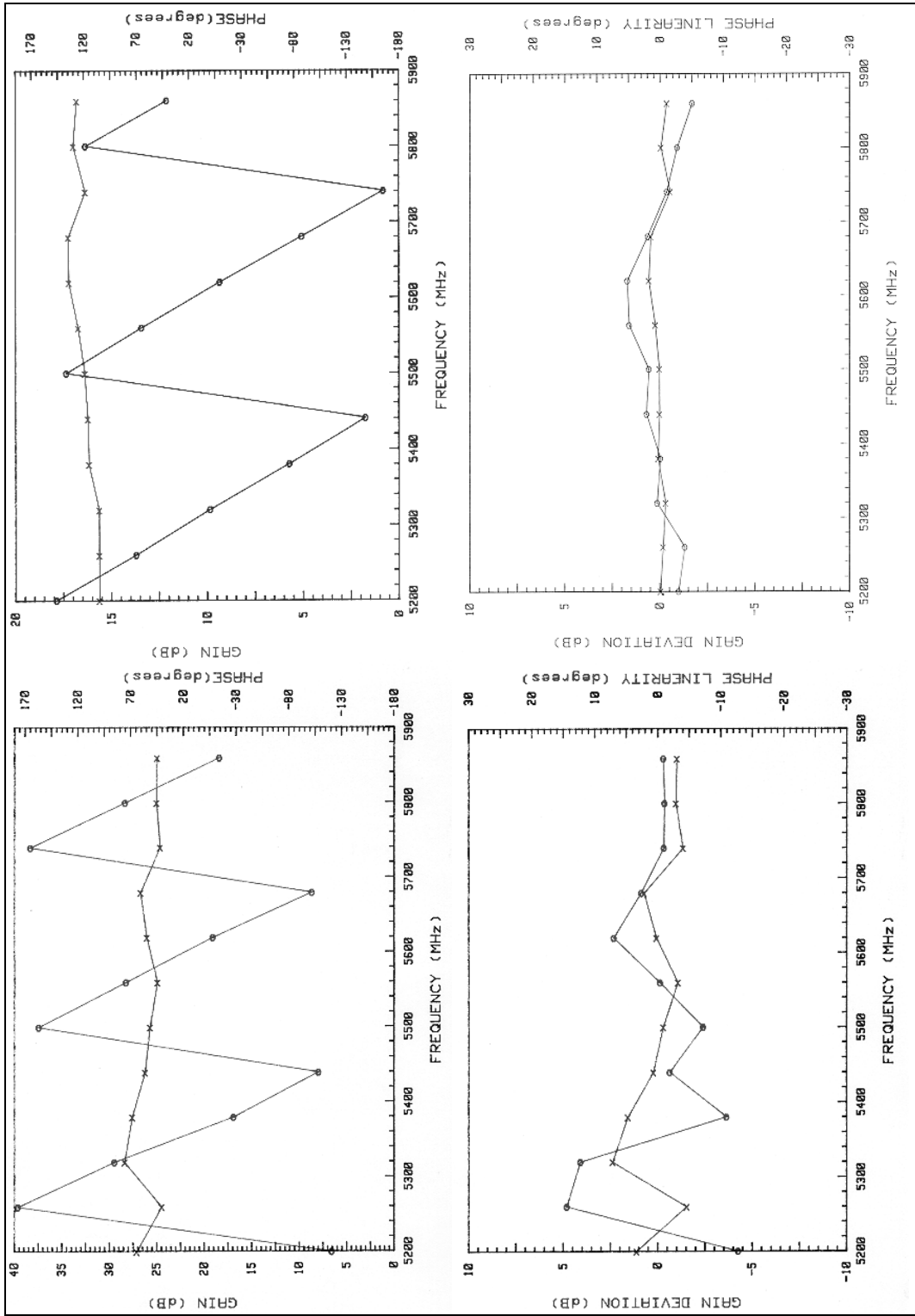


FIGURE A.3 - PHASE 1 TESTING C-BAND MODULE SN017 (LEFT) TRANSMIT & (RIGHT) RECEIVE

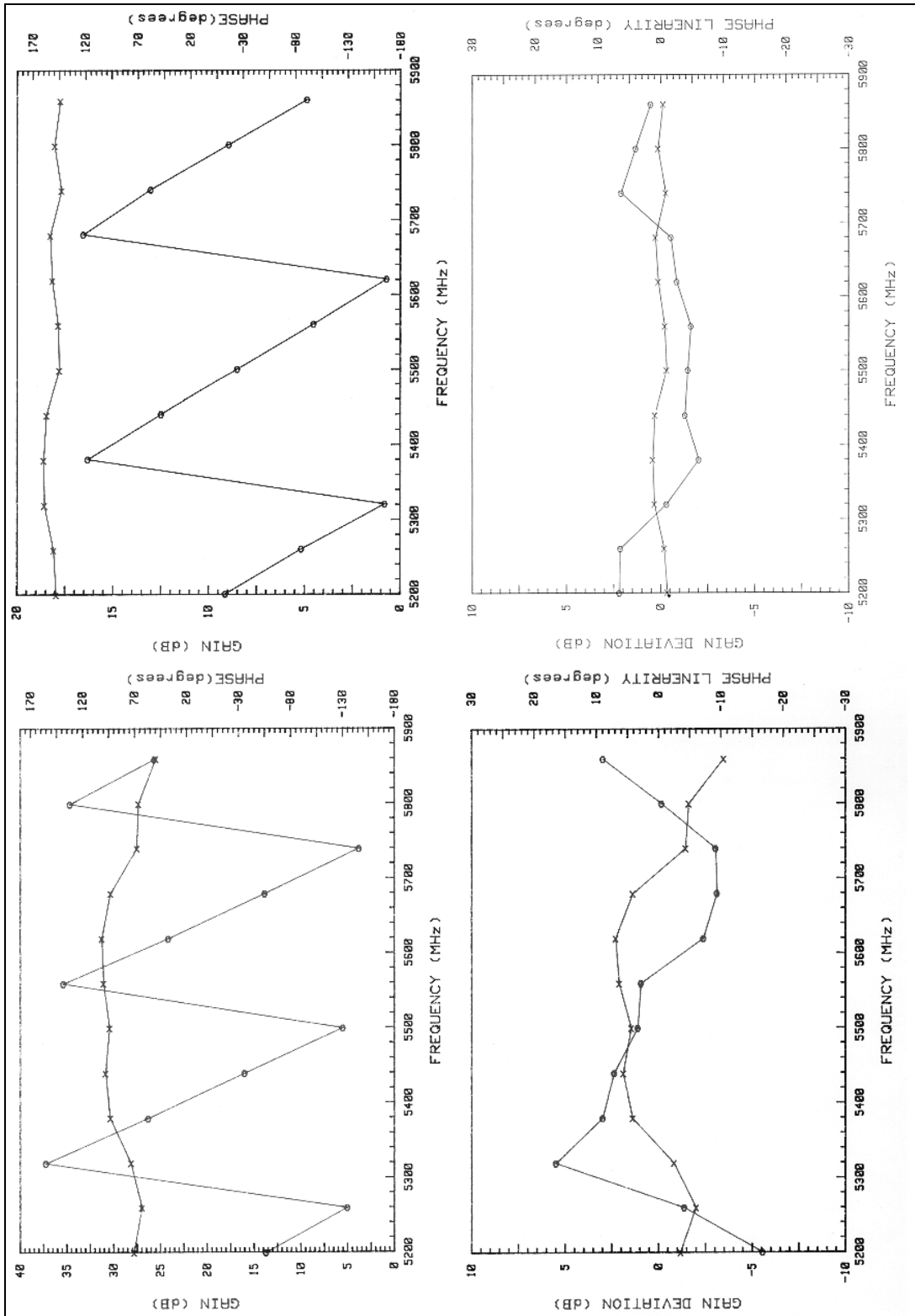


FIGURE A.4 - PHASE I TESTING C-BAND MODULE SN022 (LEFT) TRANSMIT & (RIGHT) RECEIVE

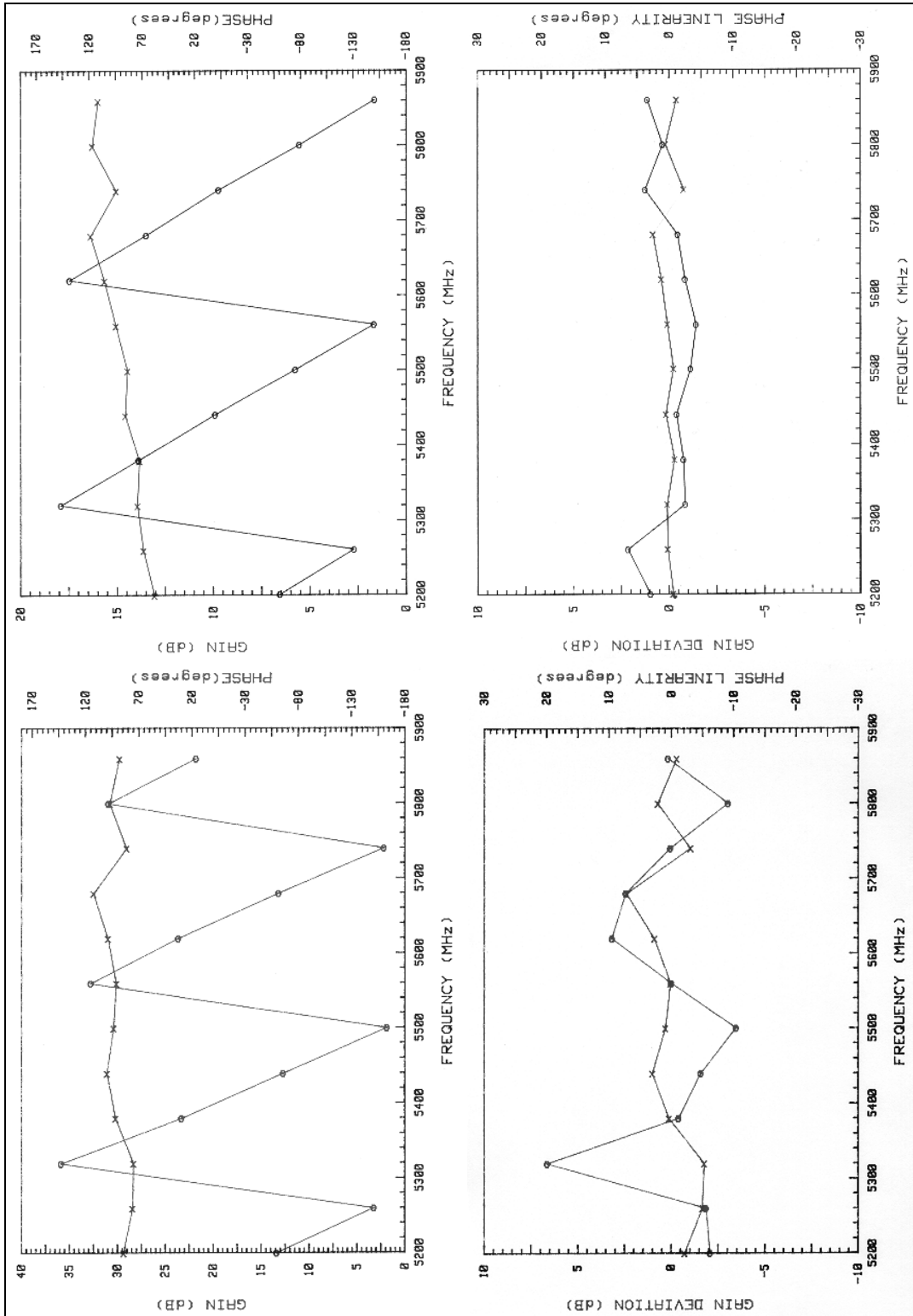


FIGURE A.5 - PHASE I TESTING C-BAND MODULE SN032 (LEFT) TRANSMIT & (RIGHT) RECEIVE

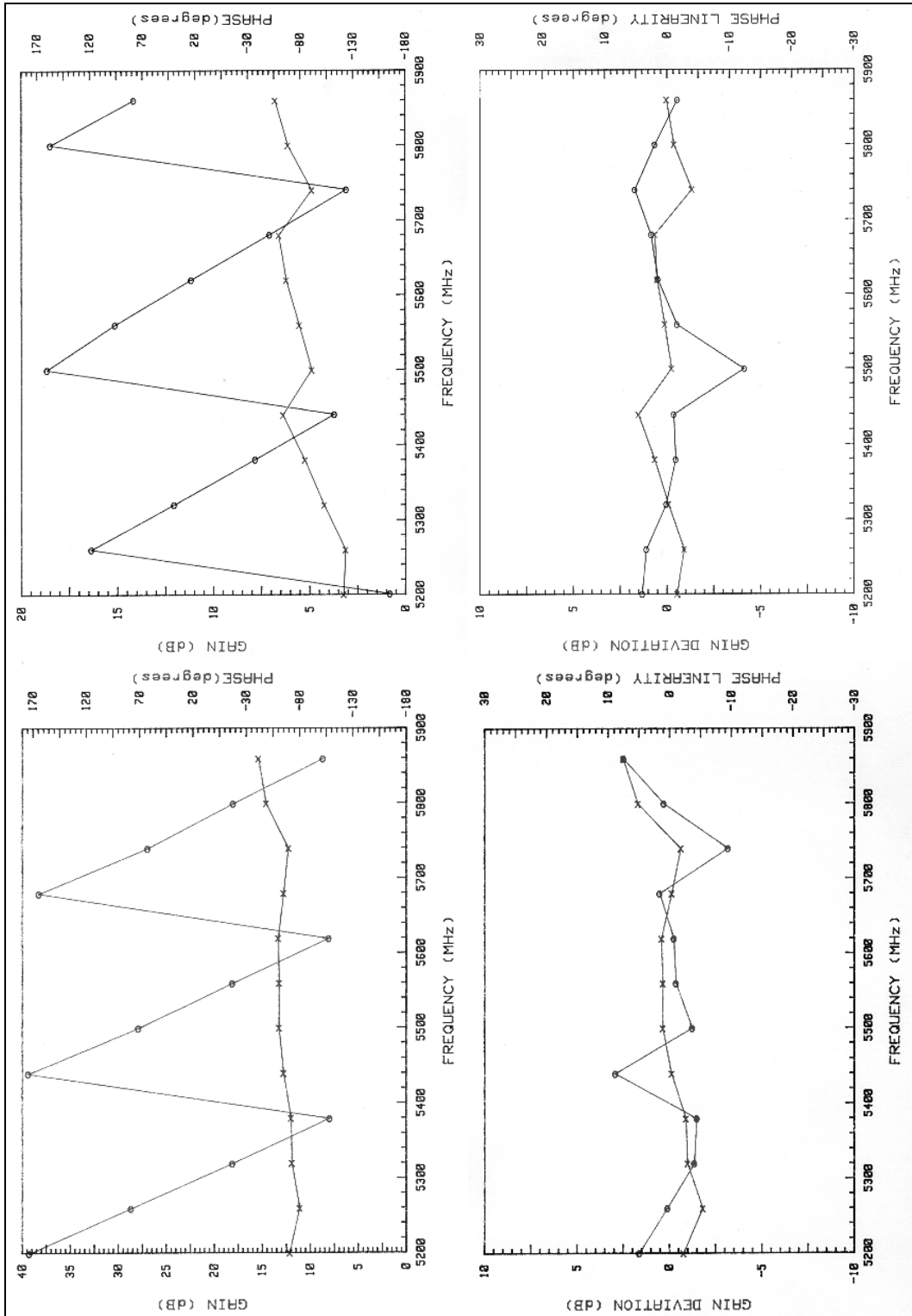


FIGURE A.6 - PHASE 1 TESTING C-BAND MODULE SN033 (LEFT) TRANSMIT & (RIGHT) RECEIVE

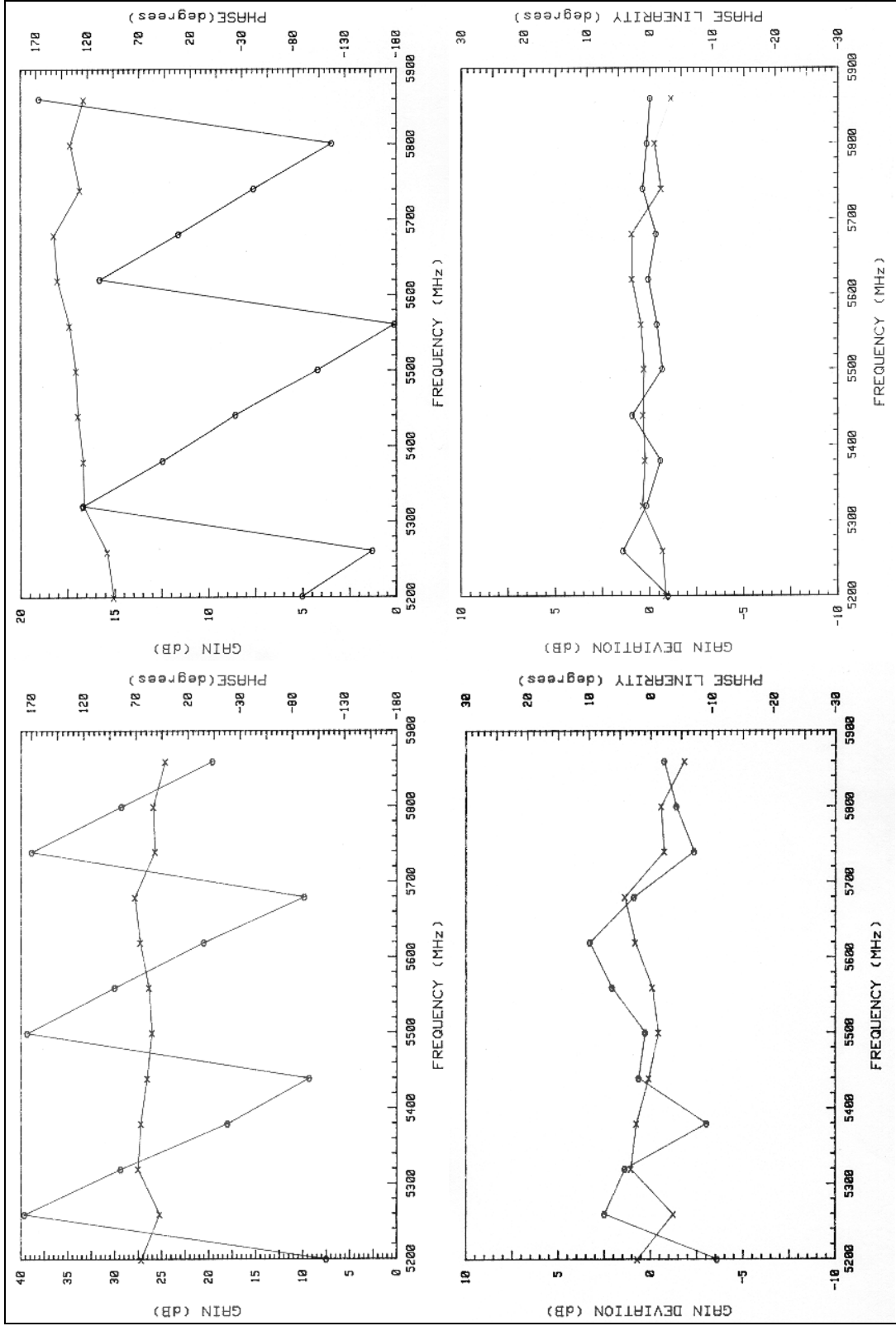


FIGURE A.7 - PHASE 1 TESTING C-BAND MODULE SN039 (LEFT) TRANSMIT & (RIGHT) RECEIVE

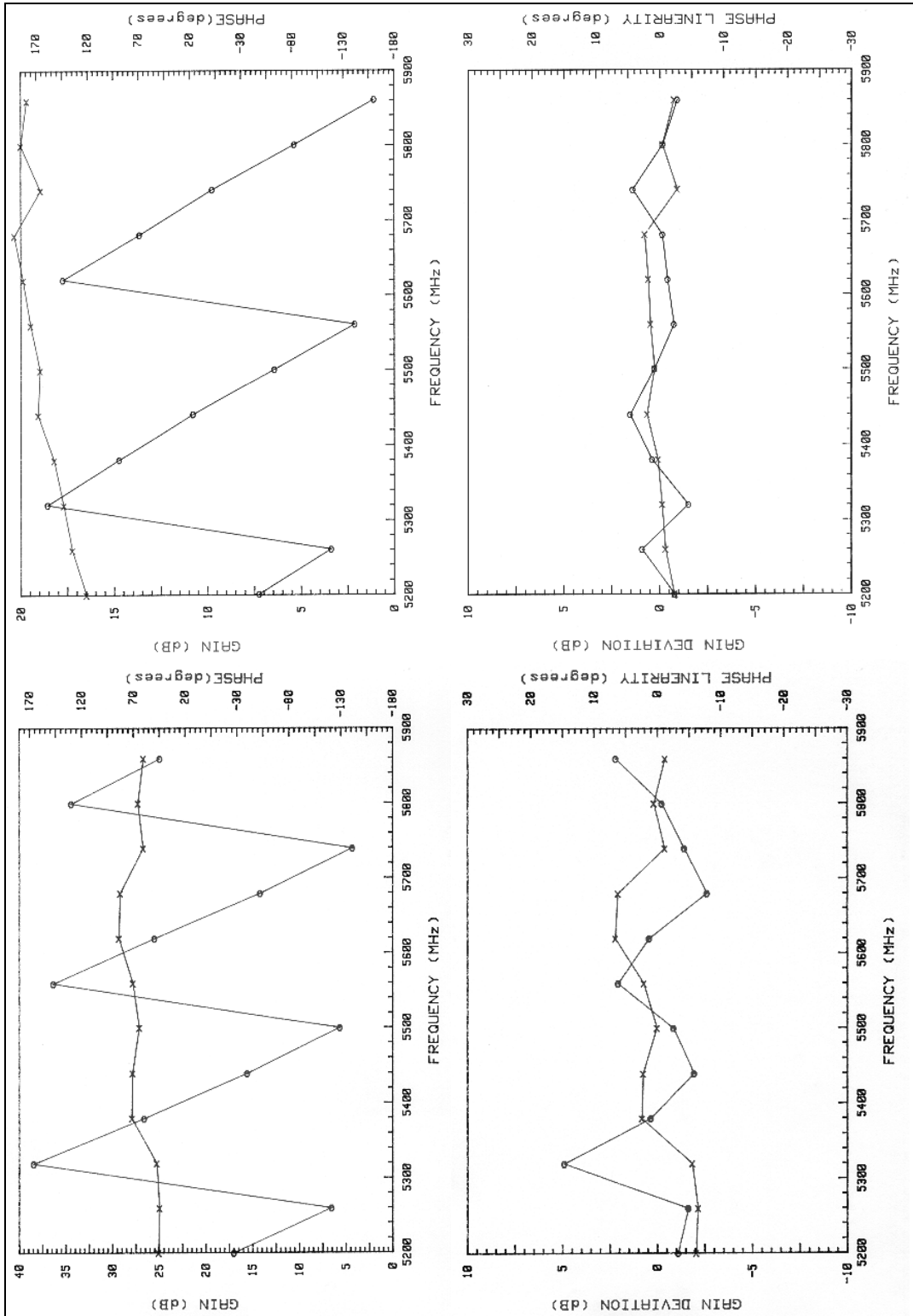


FIGURE A.8 - PHASE I TESTING C-BAND MODULE SN040 (LEFT) TRANSMIT & (RIGHT) RECEIVE

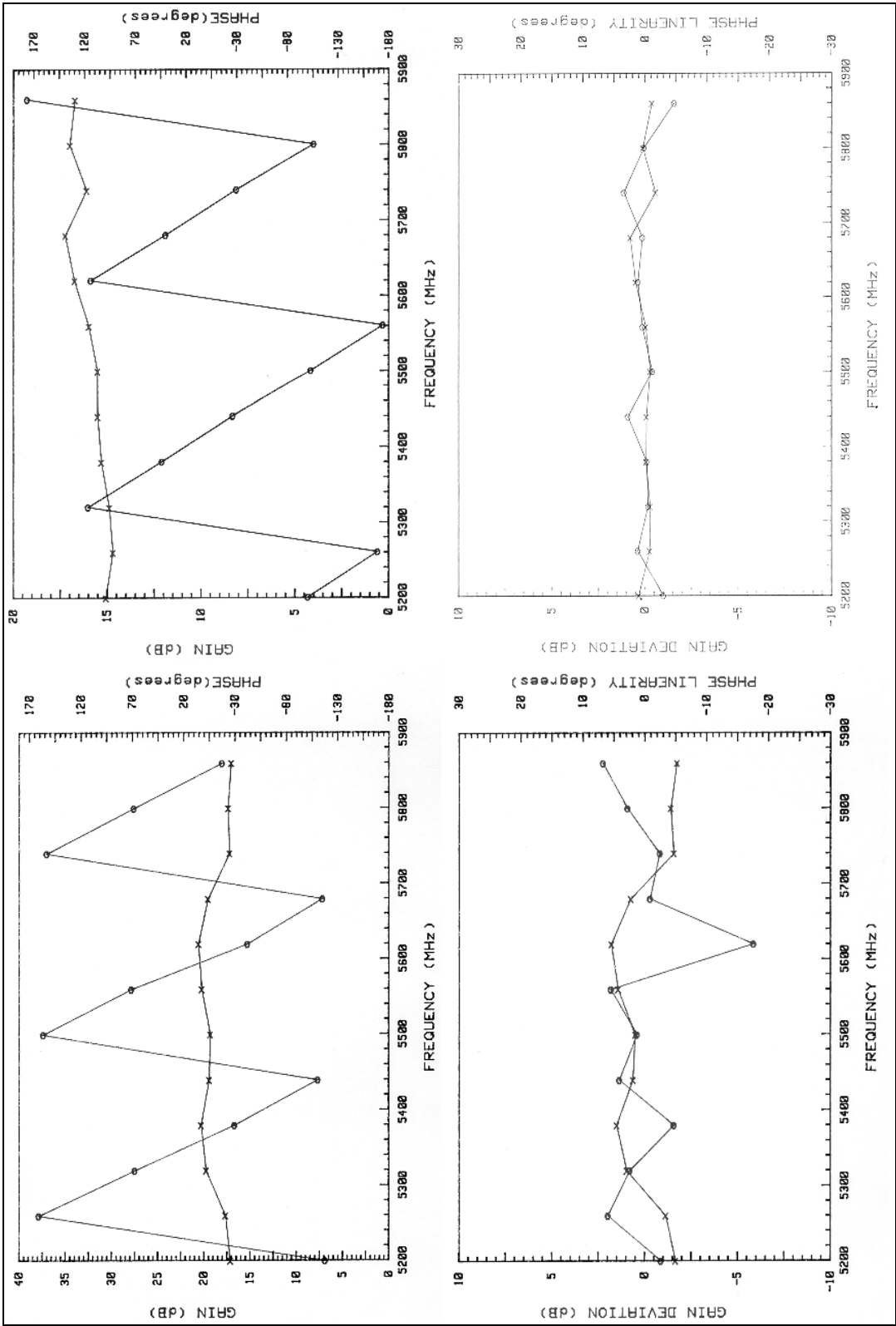


FIGURE A.9 - PHASE 1 TESTING C-BAND MODULE SN042 (LEFT) TRANSMIT & (RIGHT) RECEIVE

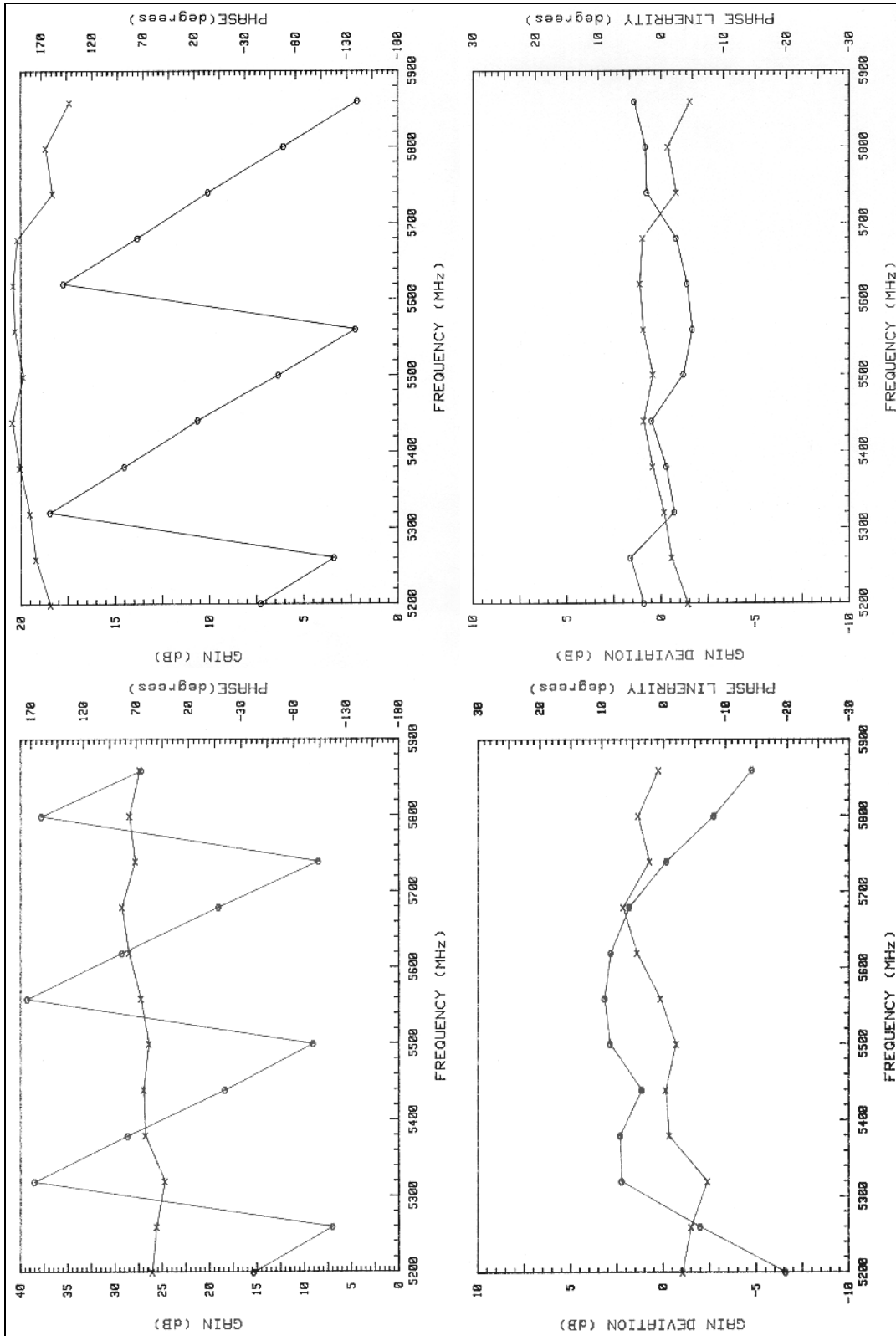


FIGURE A.10 - PHASE 1 TESTING C-BAND MODULE SN044 (LEFT) TRANSMIT & (RIGHT) RECEIVE

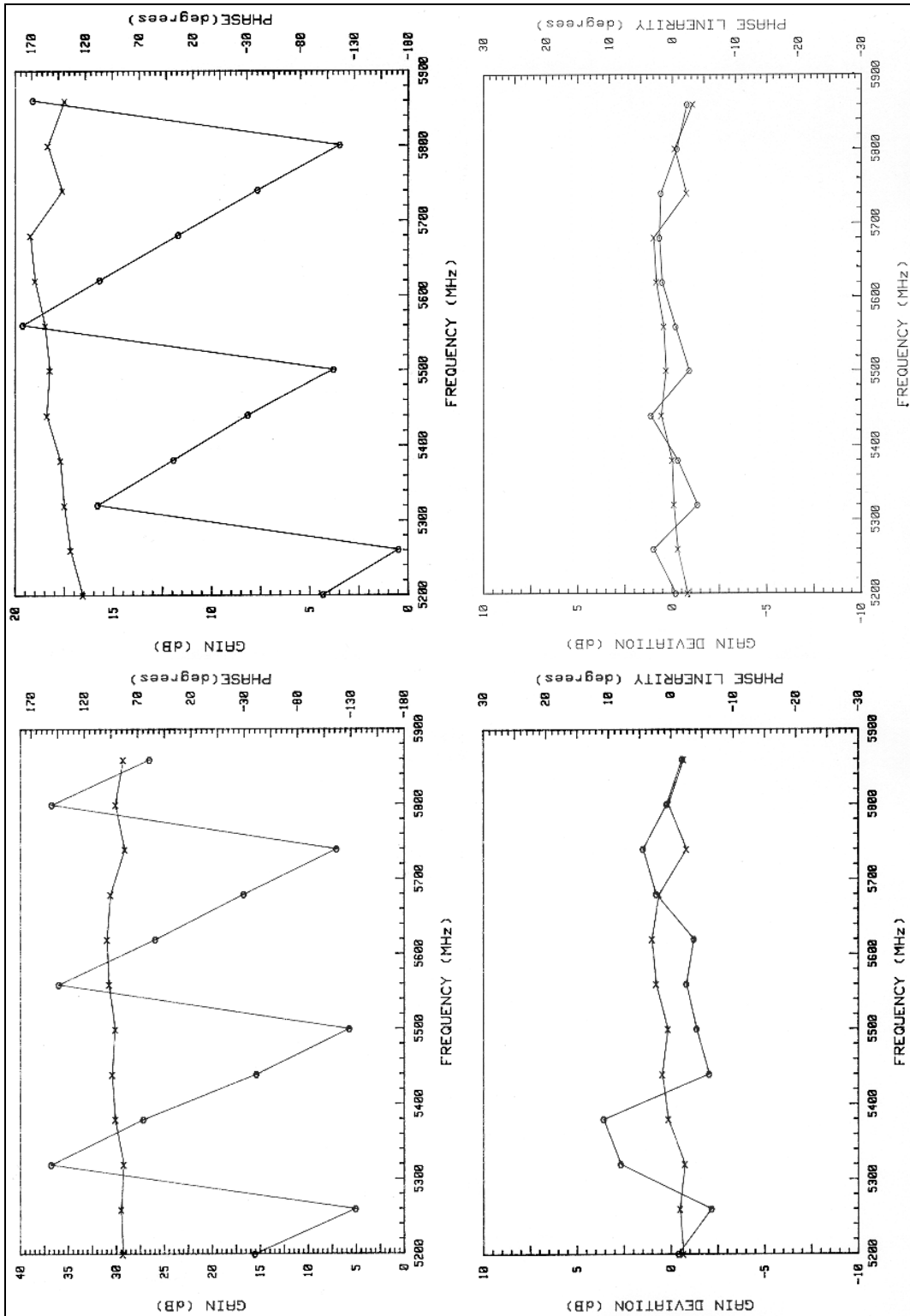


FIGURE A.11 - PHASE I TESTING C-BAND MODULE SN056 (LEFT) TRANSMIT & (RIGHT) RECEIVE

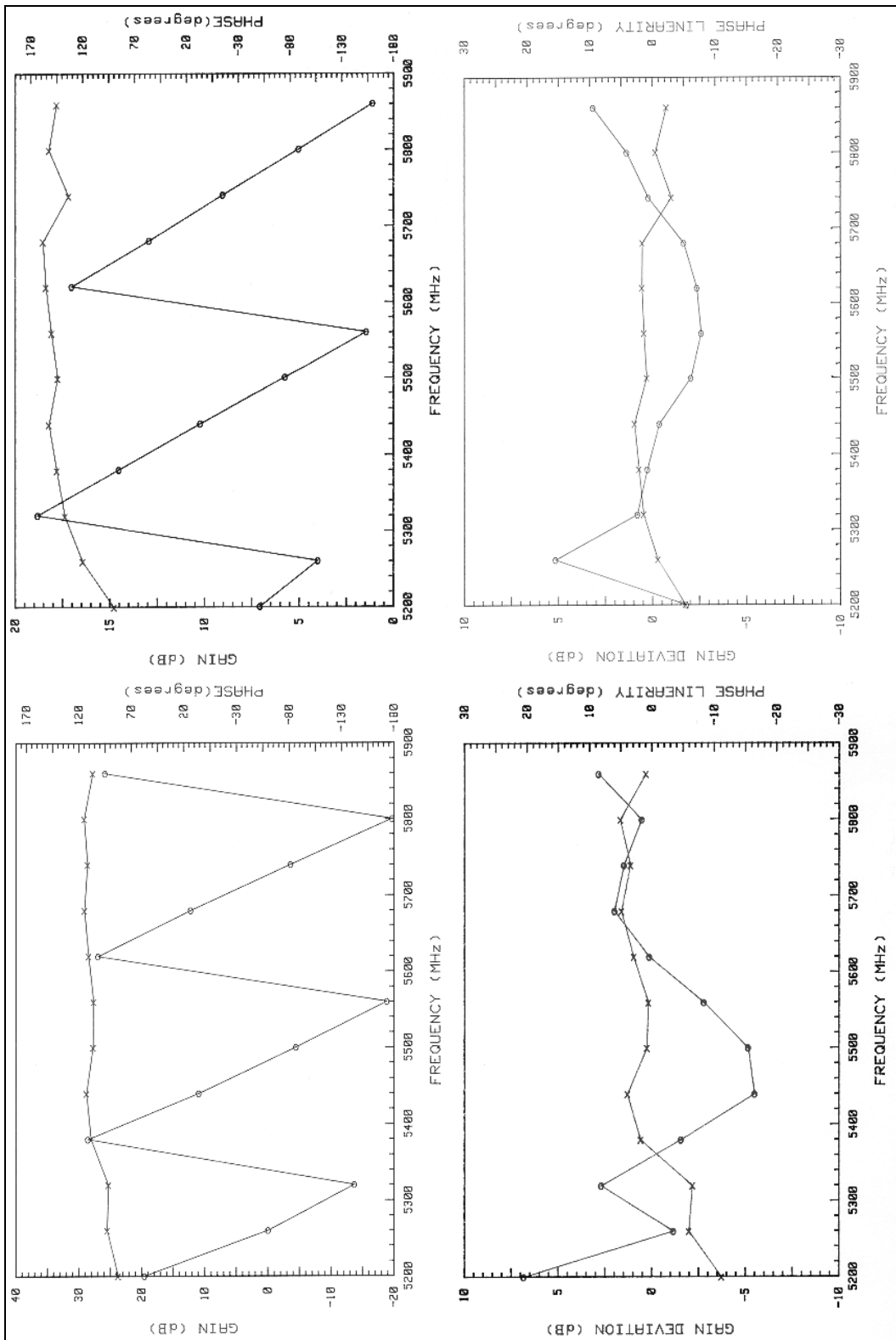


FIGURE A.12 - PHASE 1 TESTING C-BAND MODULE SN057 (LEFT) TRANSMIT & (RIGHT) RECEIVE

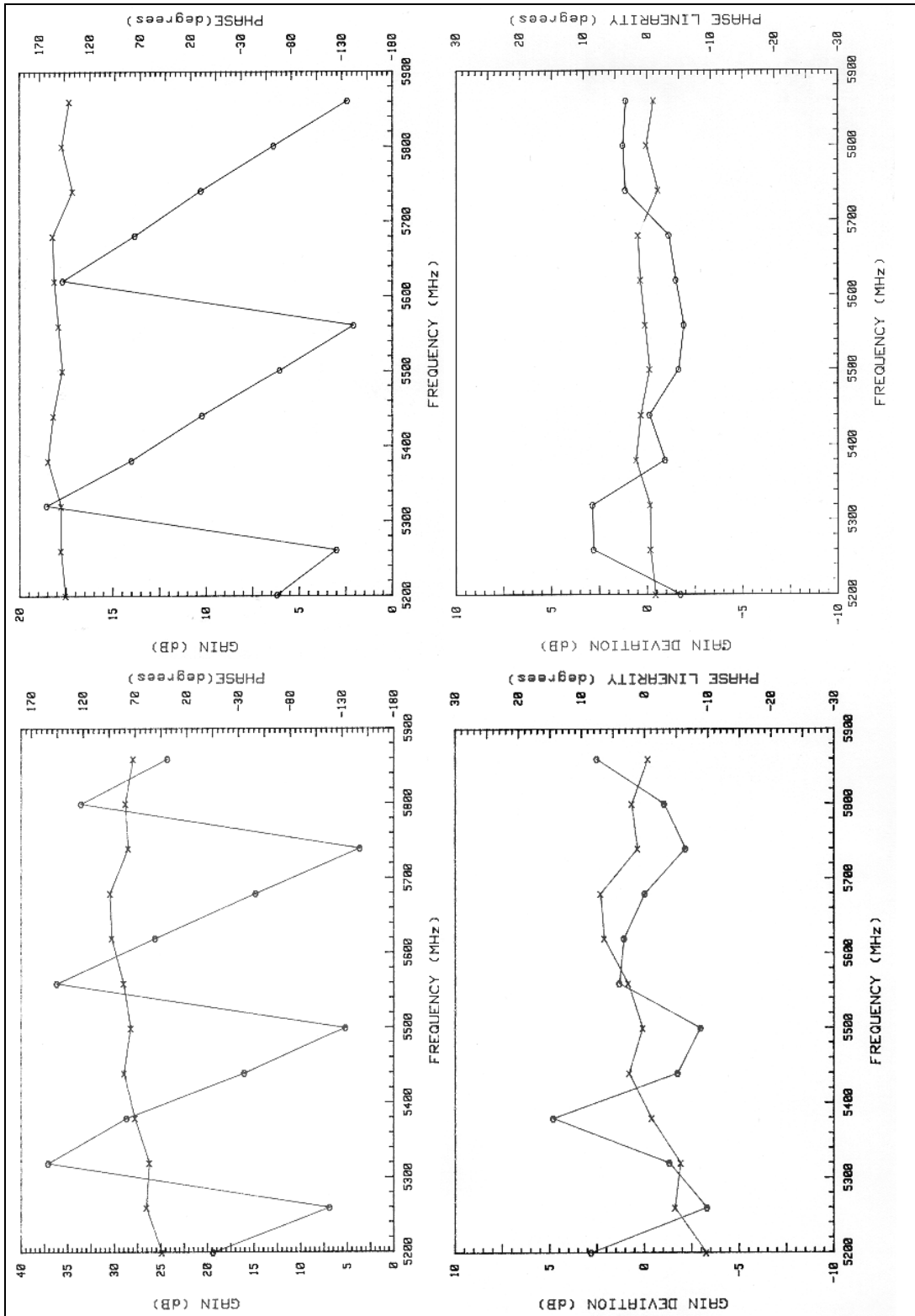


FIGURE A.13 - PHASE 1 TESTING C-BAND MODULE SN058 (LEFT) TRANSMIT & (RIGHT) RECEIVE

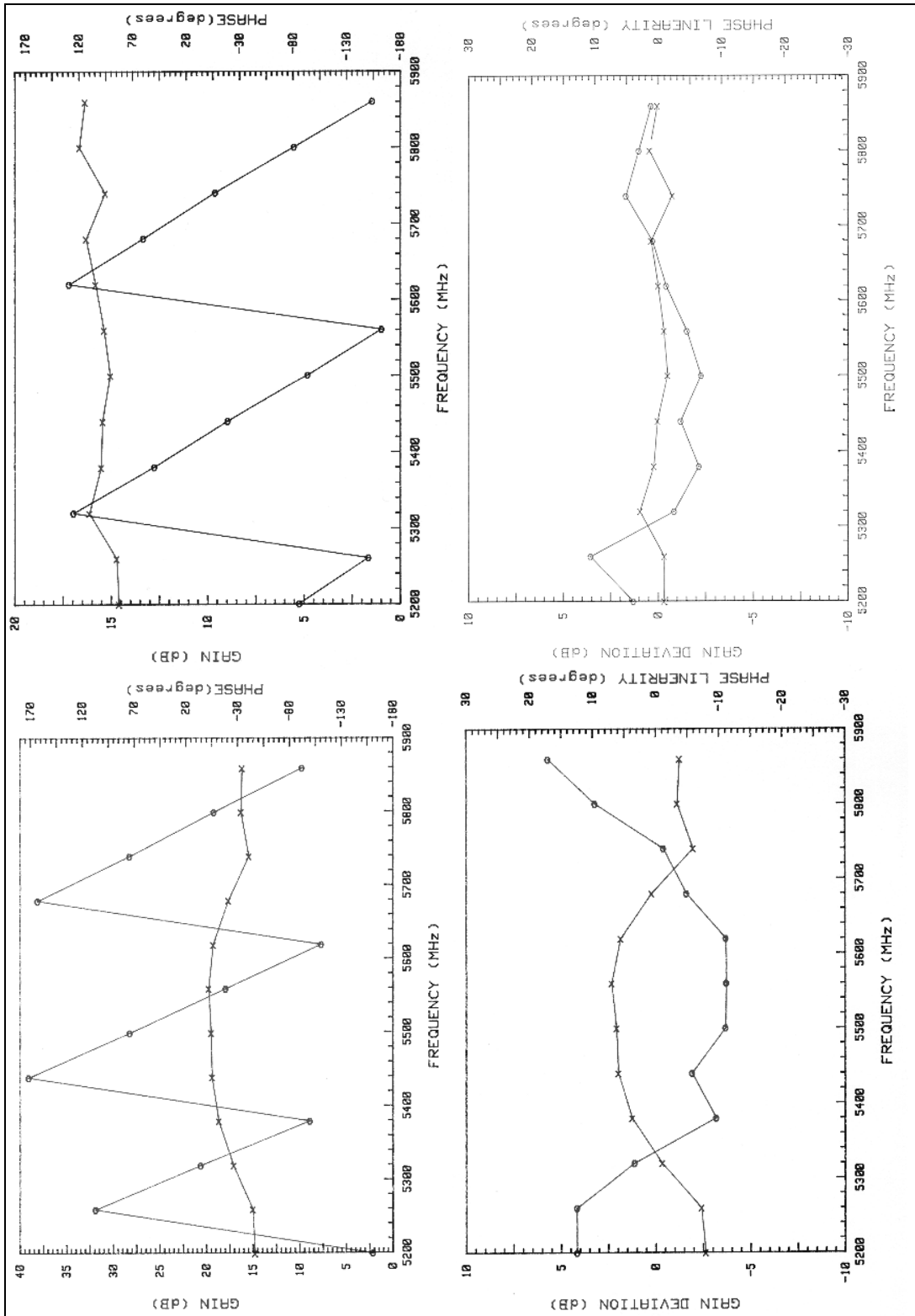


FIGURE A.14 - PHASE I TESTING C-BAND MODULE SN063 (LEFT) TRANSMIT & (RIGHT) RECEIVE

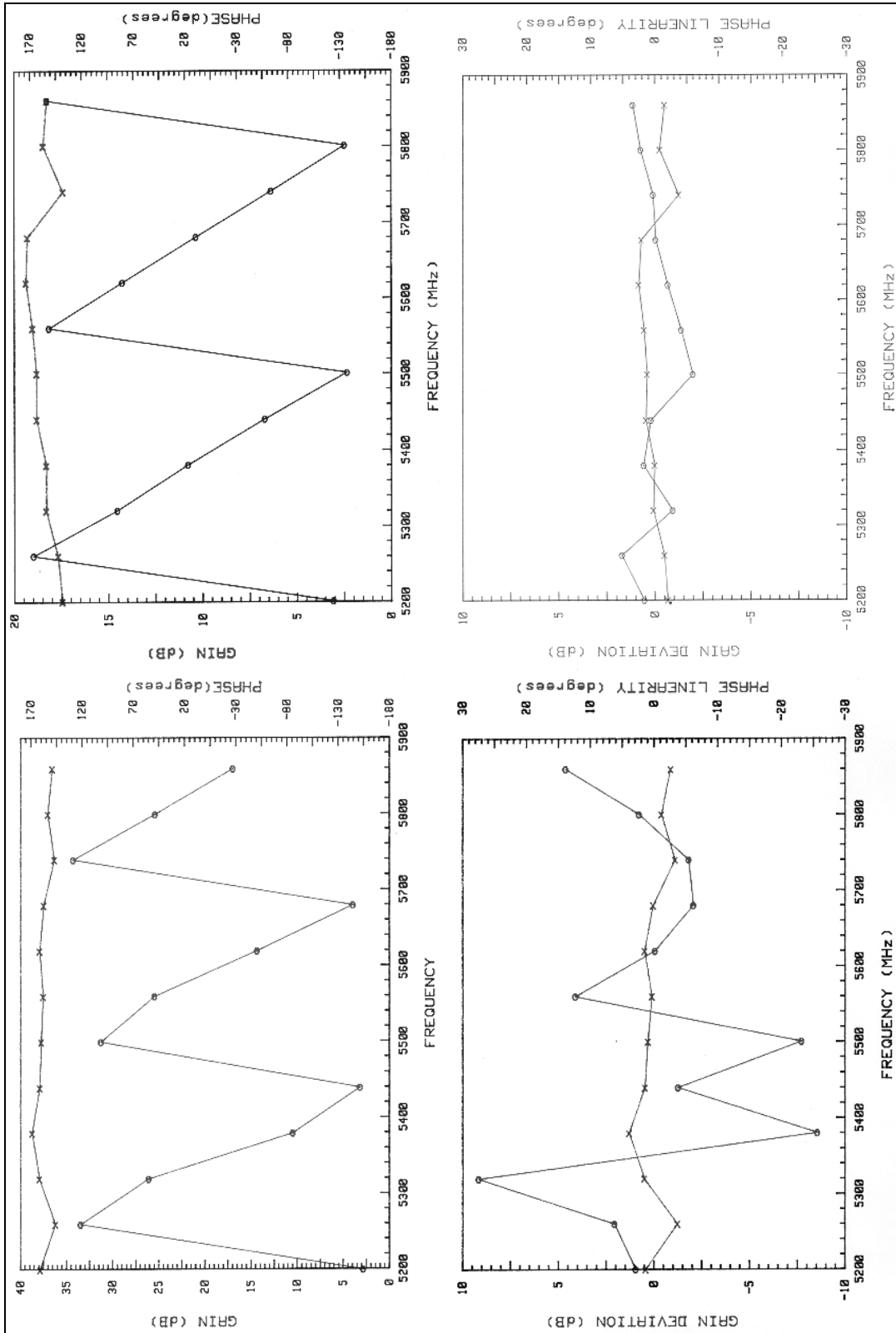


FIGURE A.15 - PHASE 1 TESTING C-BAND MODULE SN065 (LEFT) TRANSMIT & (RIGHT) RECEIVE

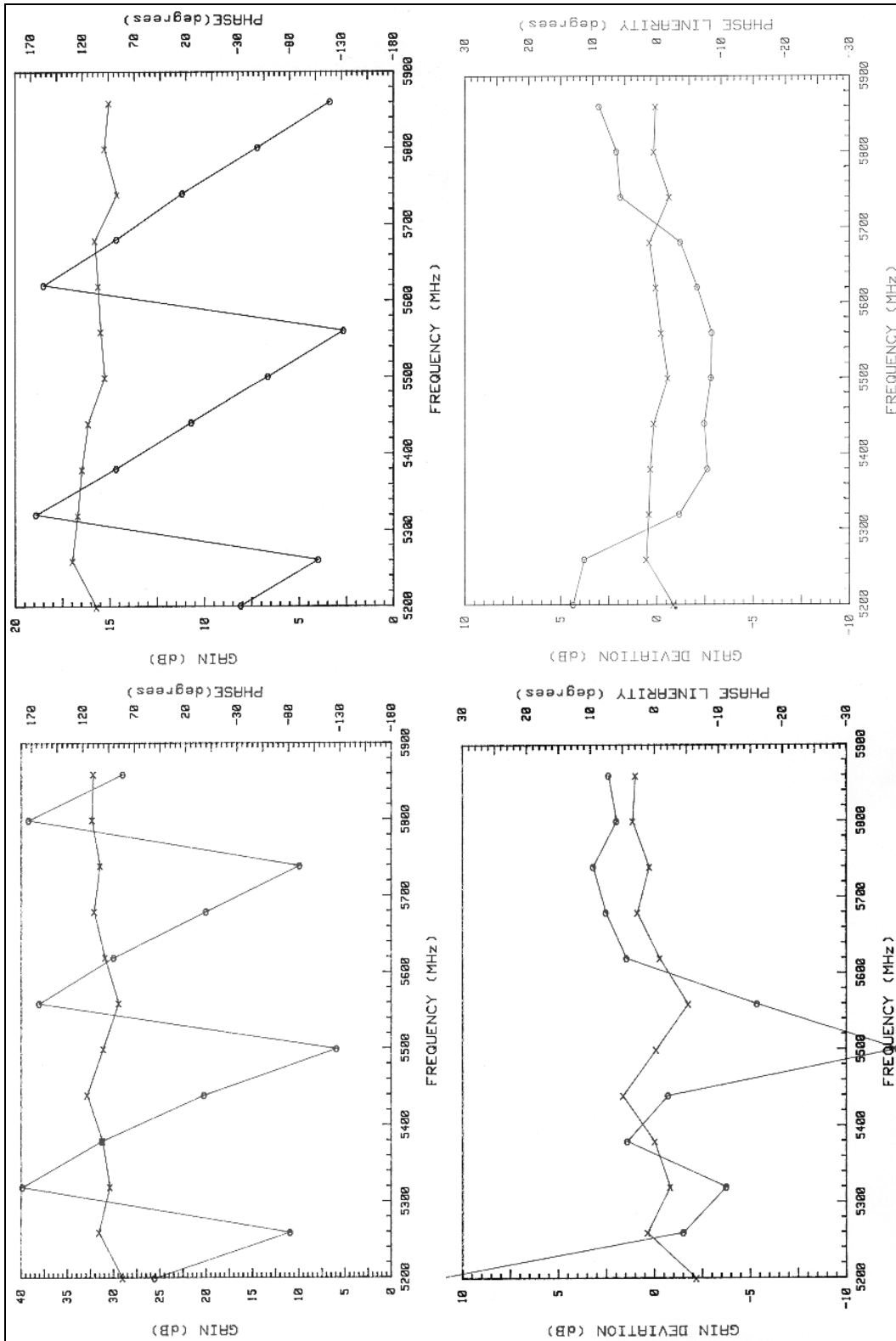


FIGURE A.16 - PHASE 1 TESTING C-BAND MODULE SN070 (LEFT) TRANSMIT & (RIGHT) RECEIVE

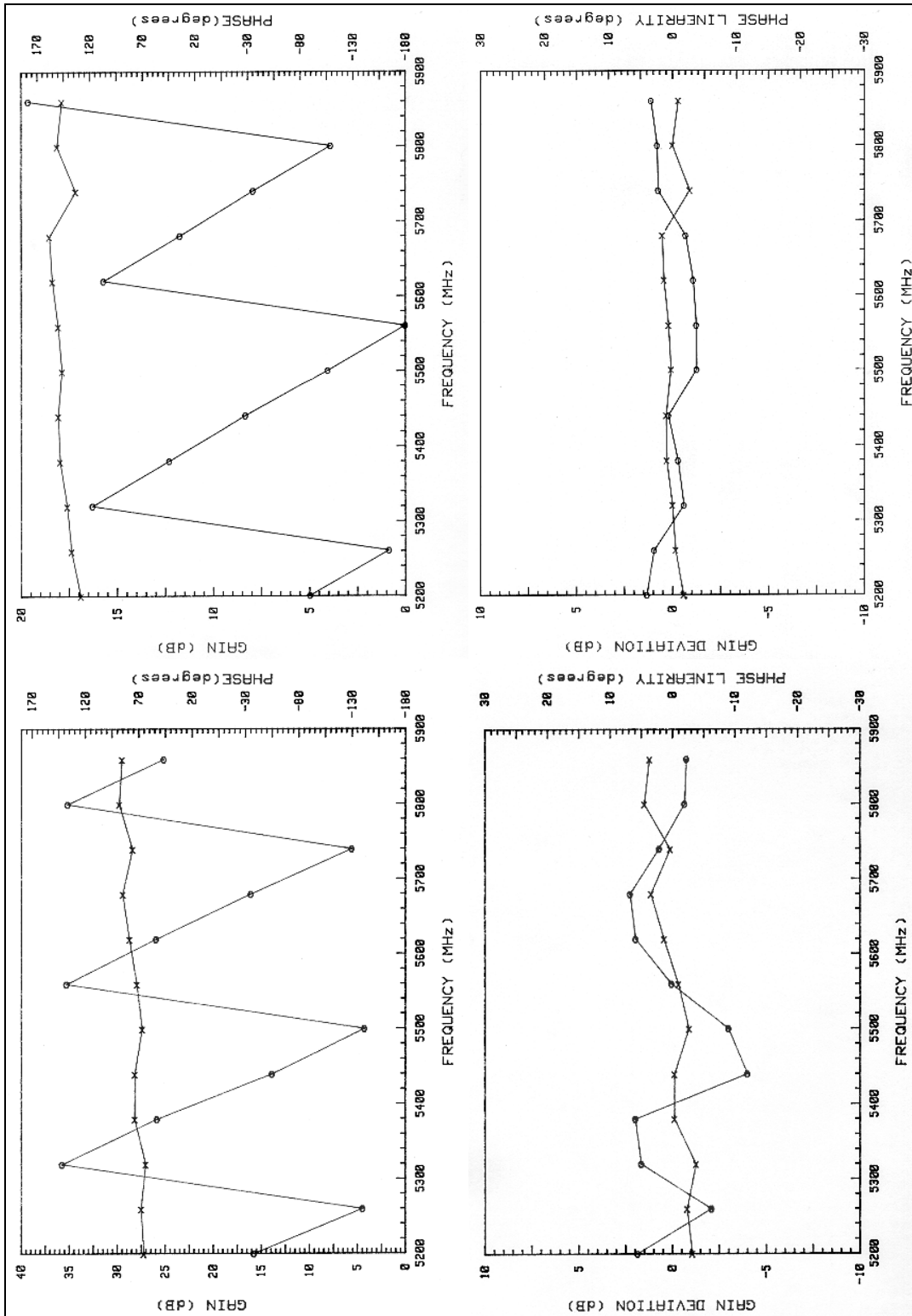


FIGURE A.17 - PHASE 1 TESTING C-BAND MODULE SN073 (LEFT) TRANSMIT & (RIGHT) RECEIVE

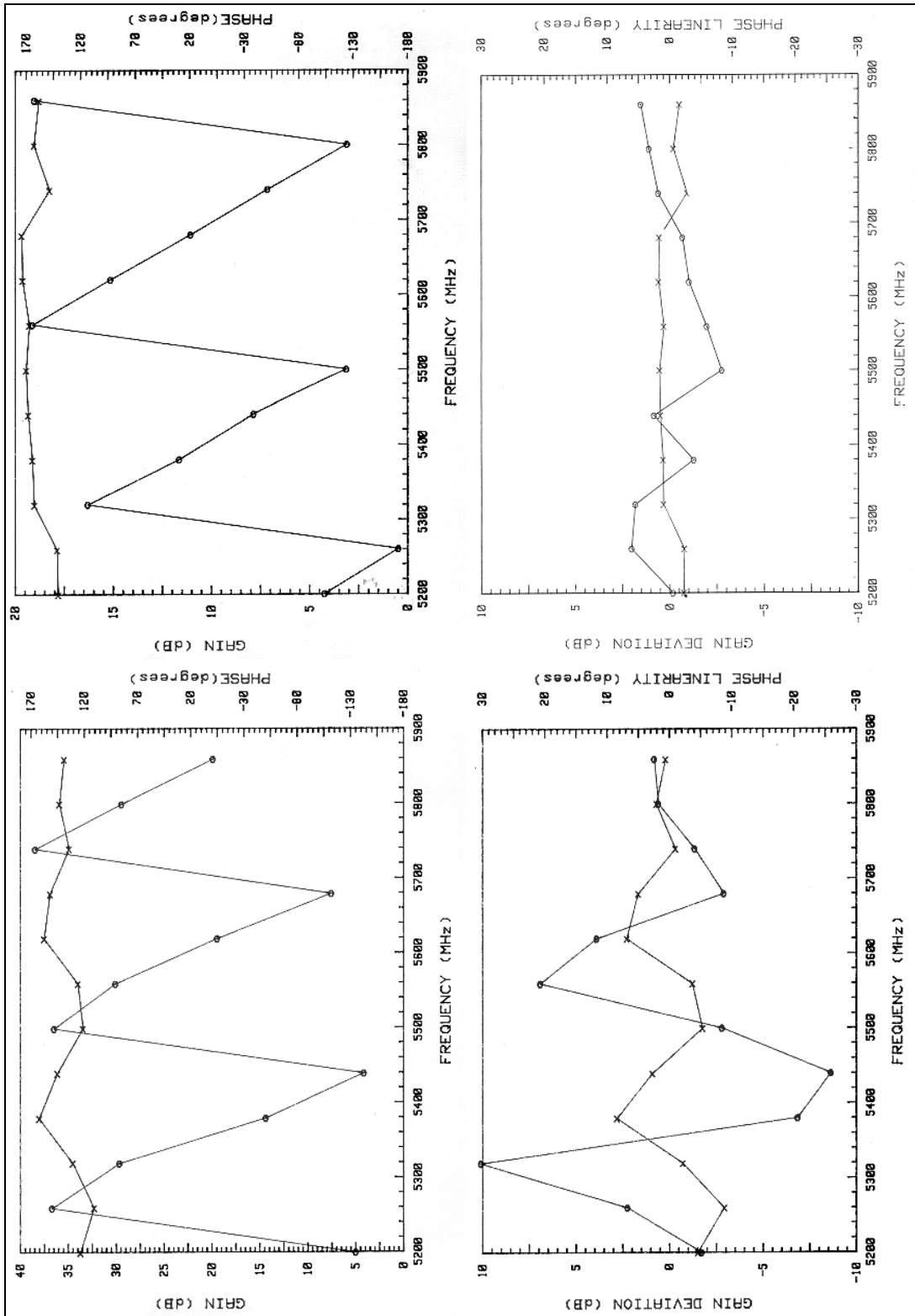


FIGURE A.18 - PHASE 1 TESTING C-BAND MODULE SN084 (LEFT) TRANSMIT & (RIGHT) RECEIVE

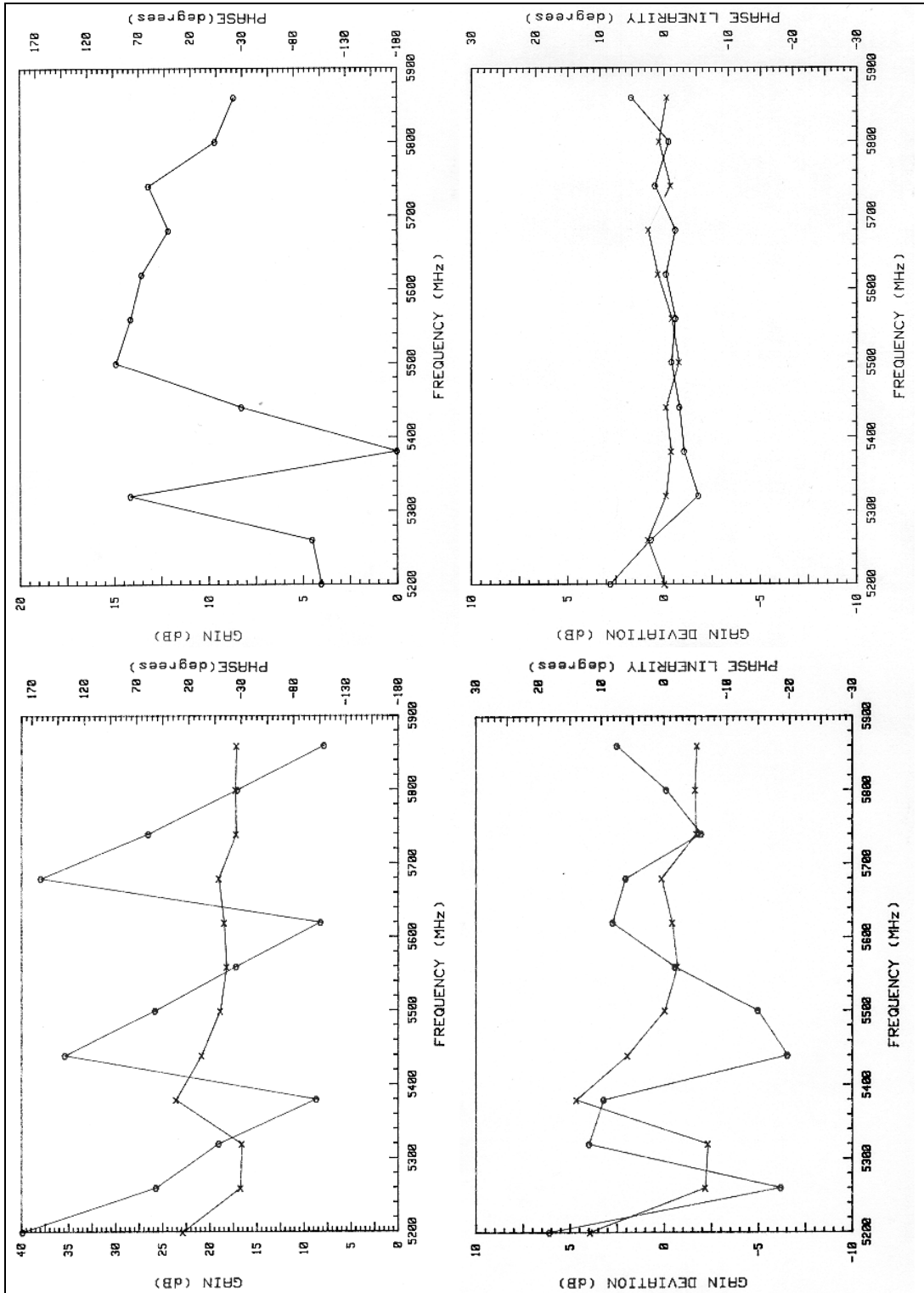


FIGURE A.19 - PHASE 1 TESTING C-BAND MODULE SN085 (LEFT) TRANSMIT & (RIGHT) RECEIVE

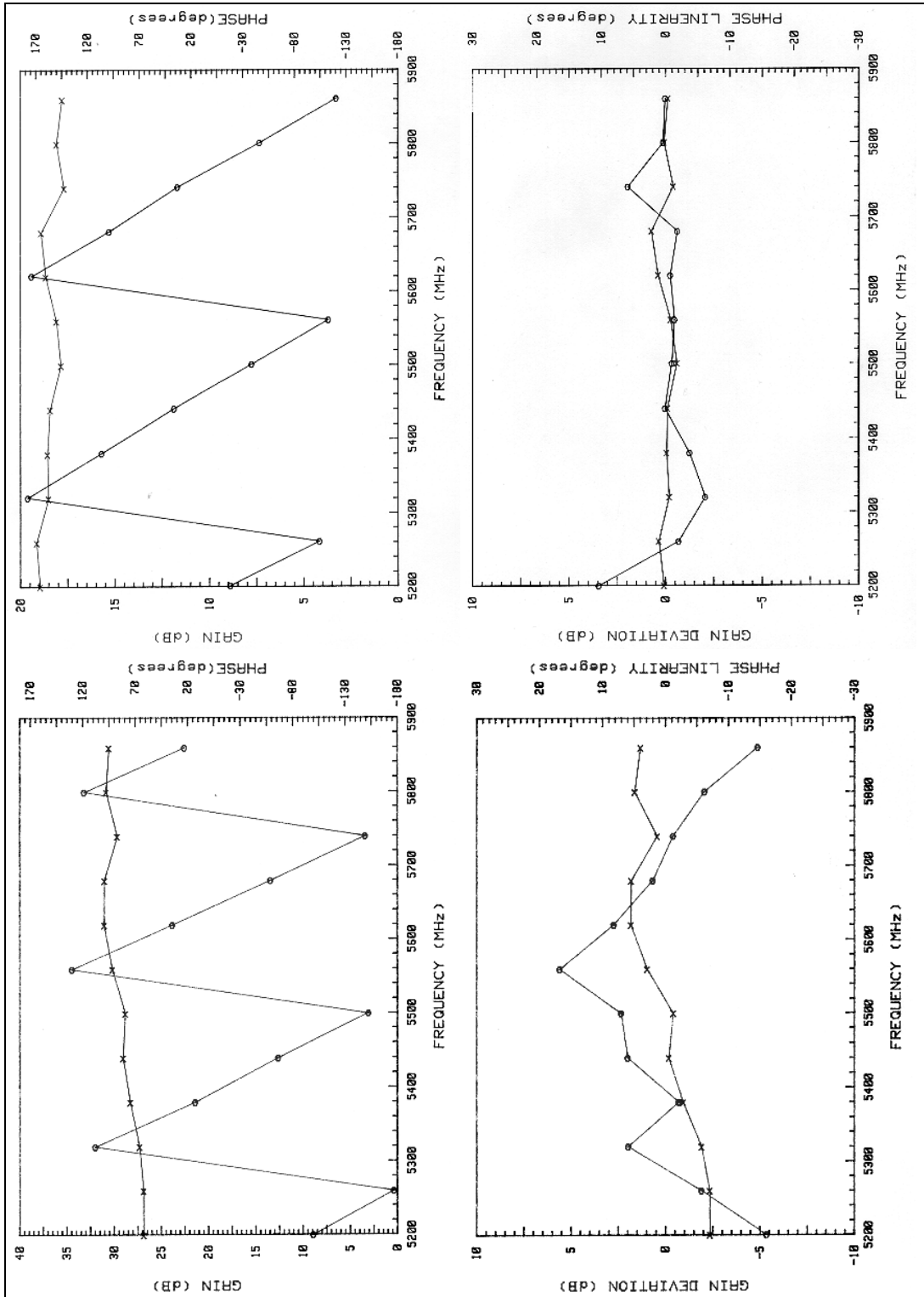


FIGURE A.20 - PHASE 1 TESTING C-BAND MODULE SN089 (LEFT) TRANSMIT & (RIGHT) RECEIVE

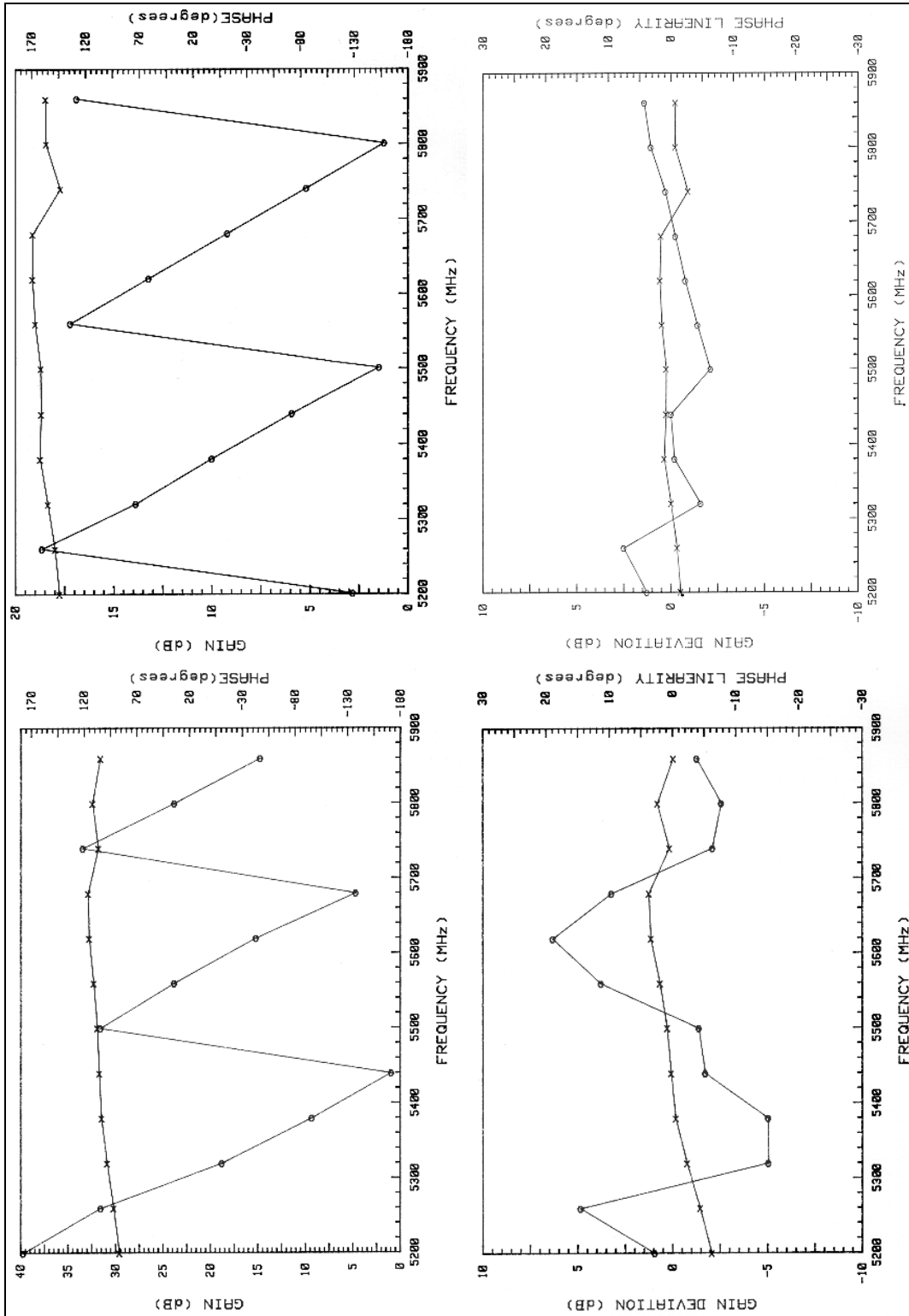


FIGURE A.21 - PHASE I TESTING C-BAND MODULE SN118 (LEFT) TRANSMIT & (RIGHT) RECEIVE

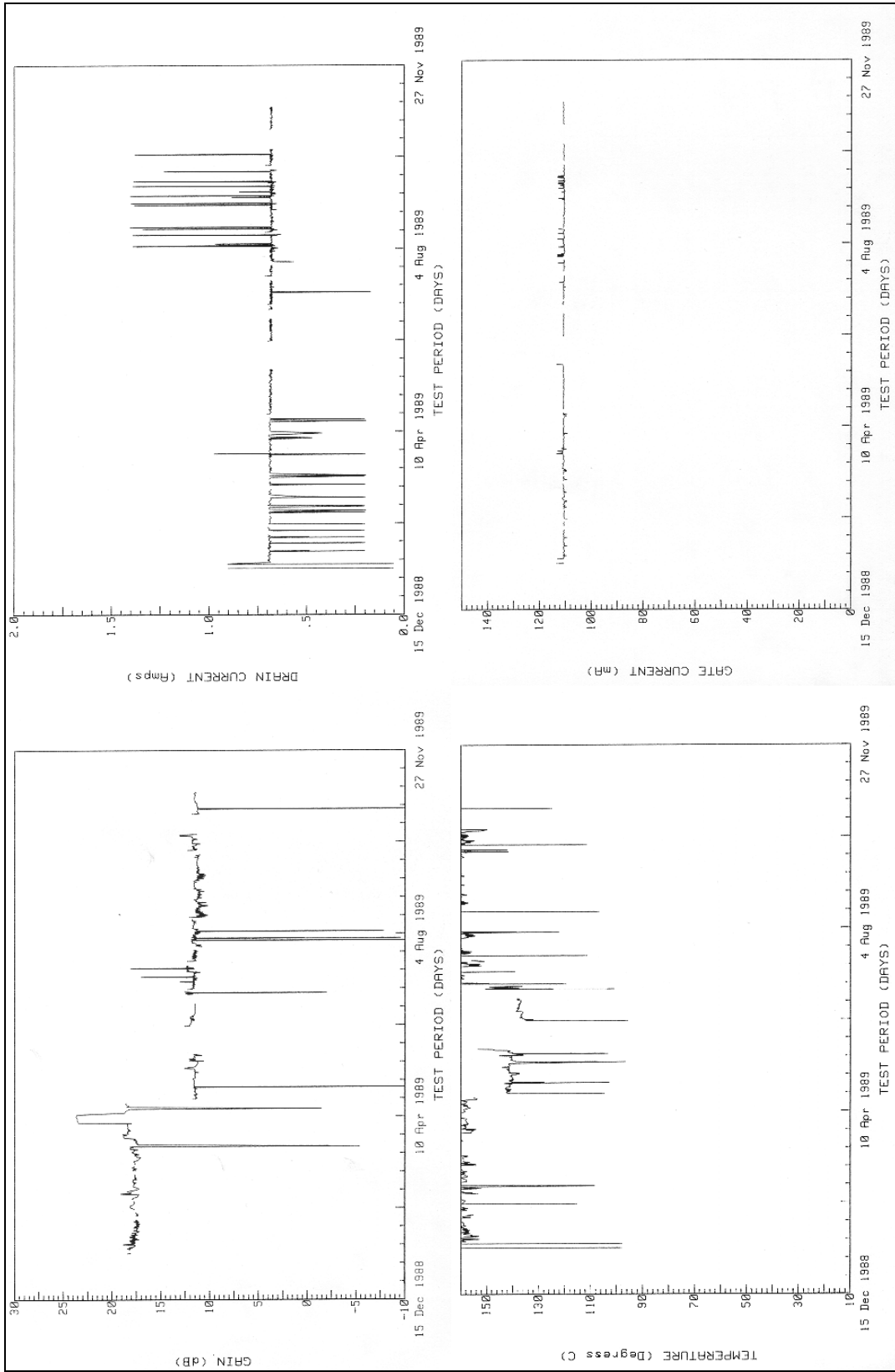


FIGURE A.21 - PHASE 2 TESTING DEVICE CA2

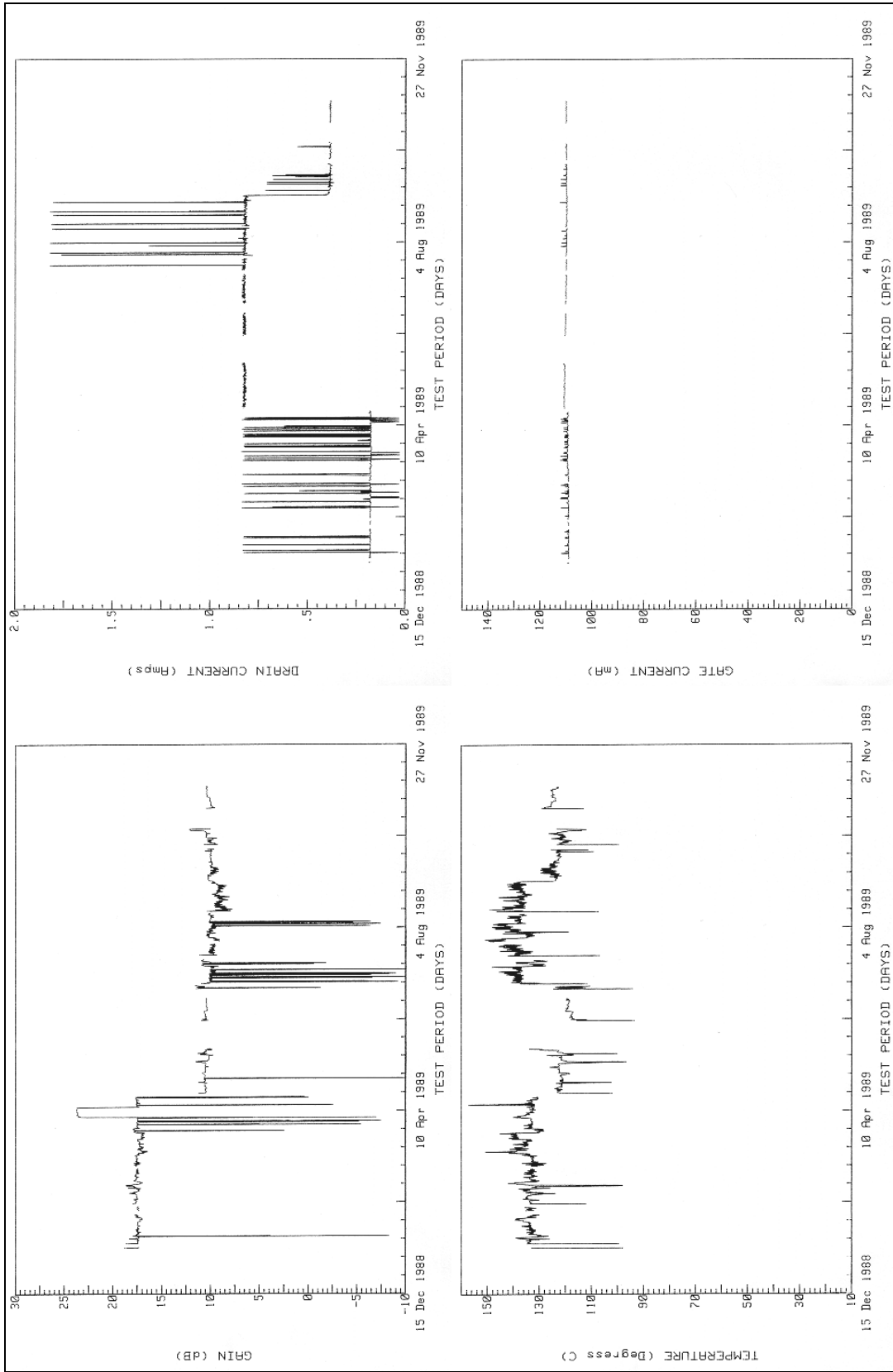


FIGURE A.22 - PHASE 2 TESTING DEVICE CA4

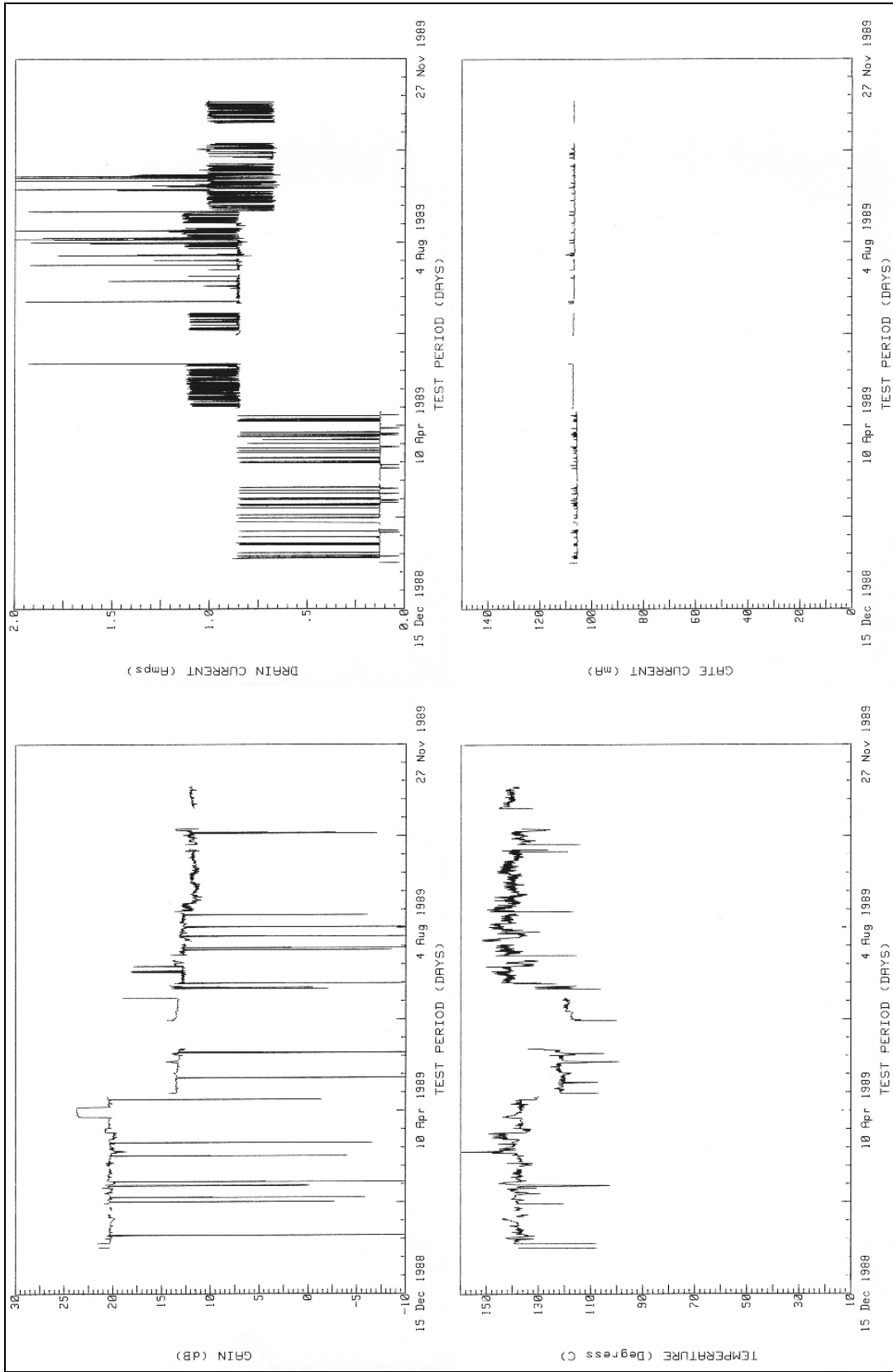


FIGURE A.23 - PHASE 2 TESTING DEVICE CB2

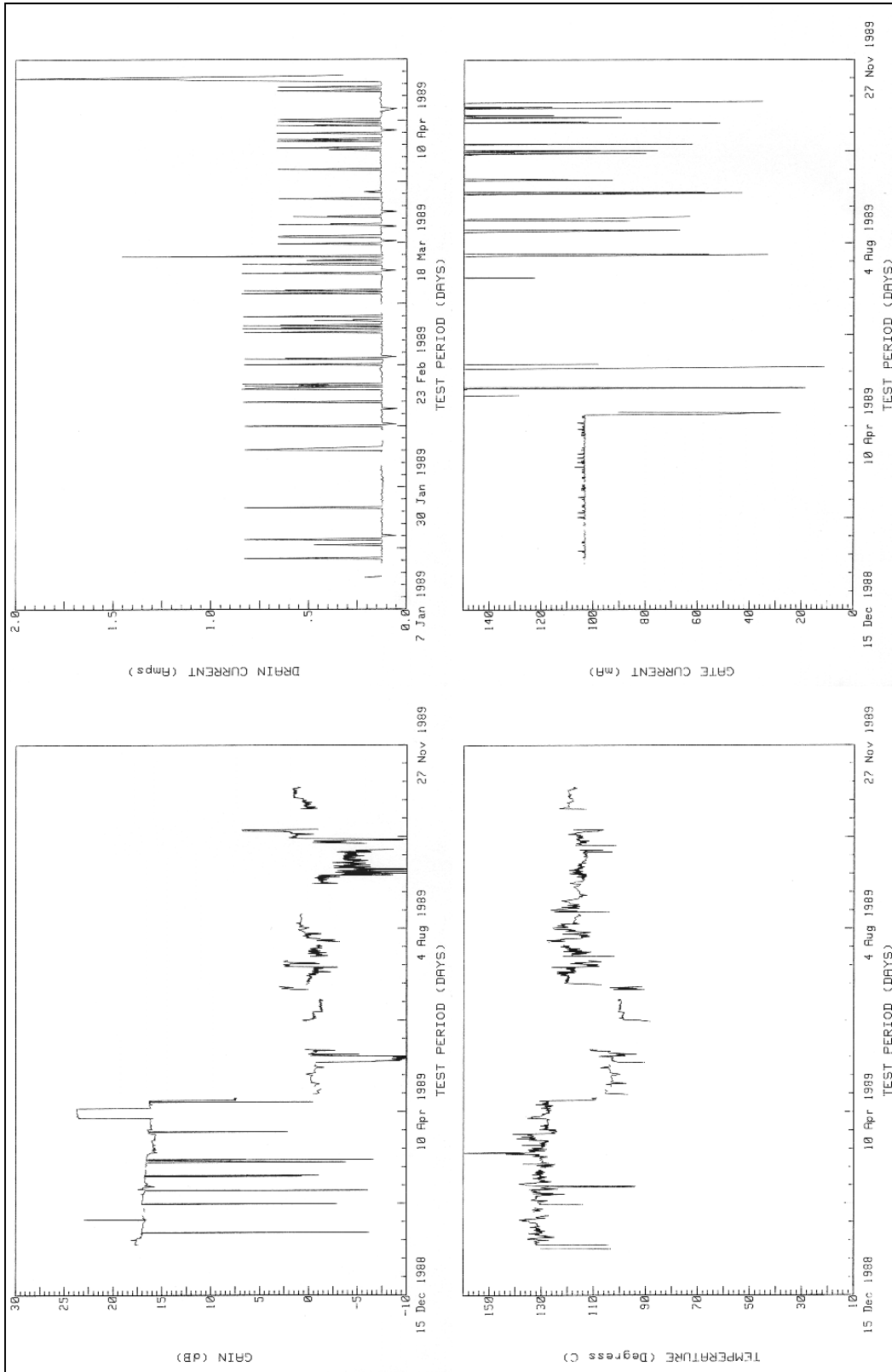


FIGURE A.24 - PHASE 2 TESTING DEVICE CB4

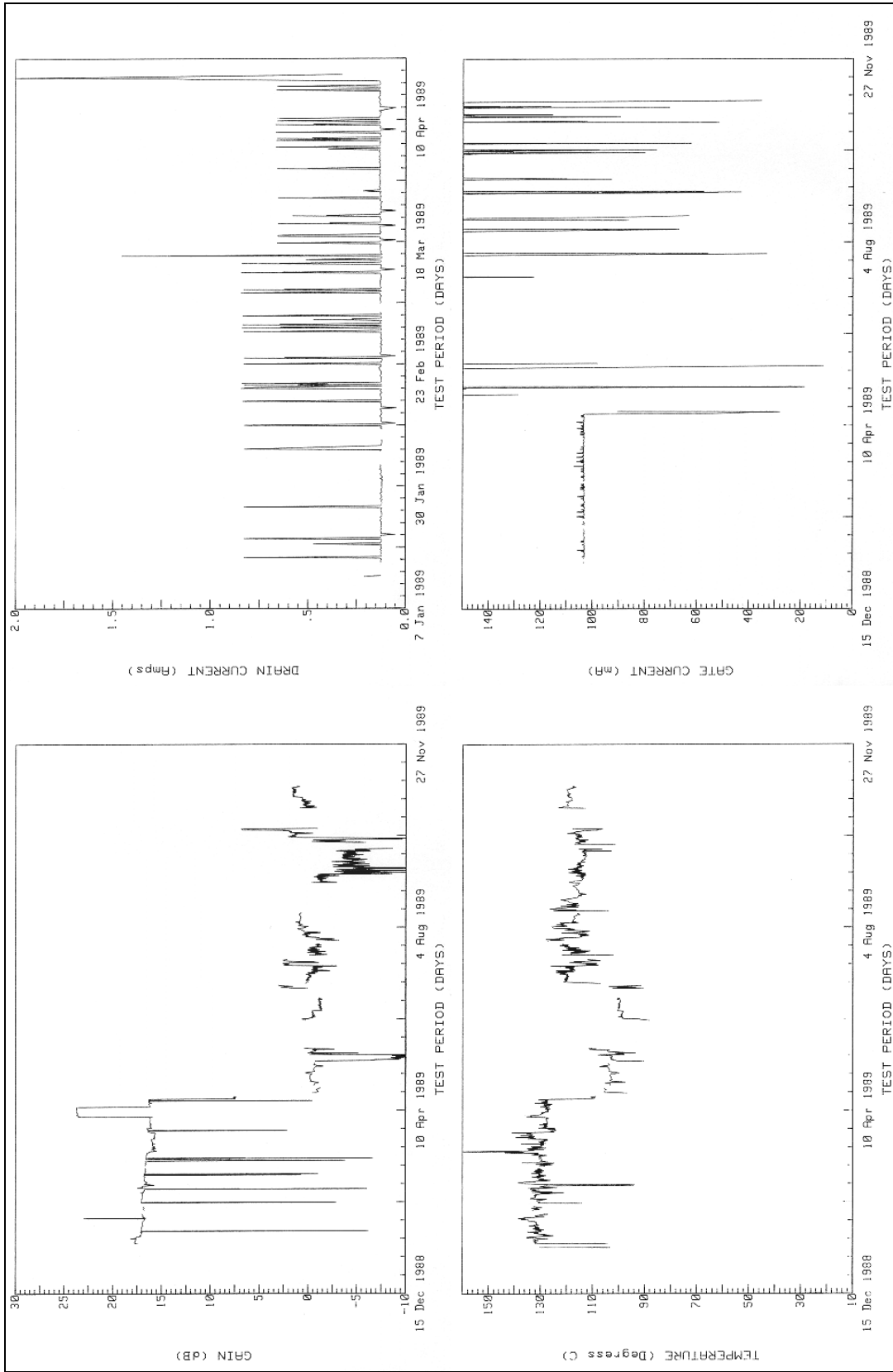


FIGURE A.24 – PHASE 2 TESTING DEVICE CB4

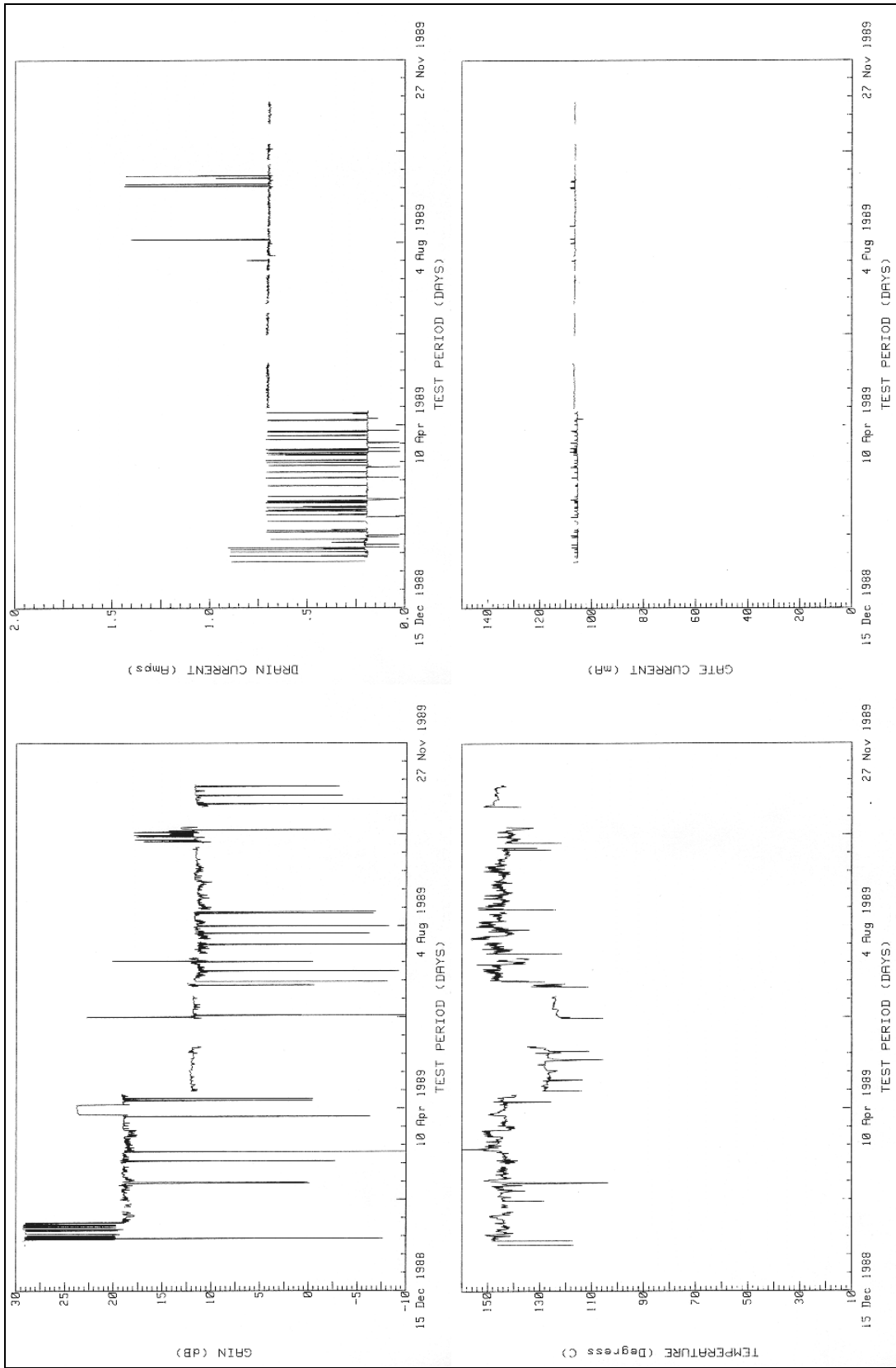


FIGURE A.25 - PHASE 2 TESTING DEVICE CC2

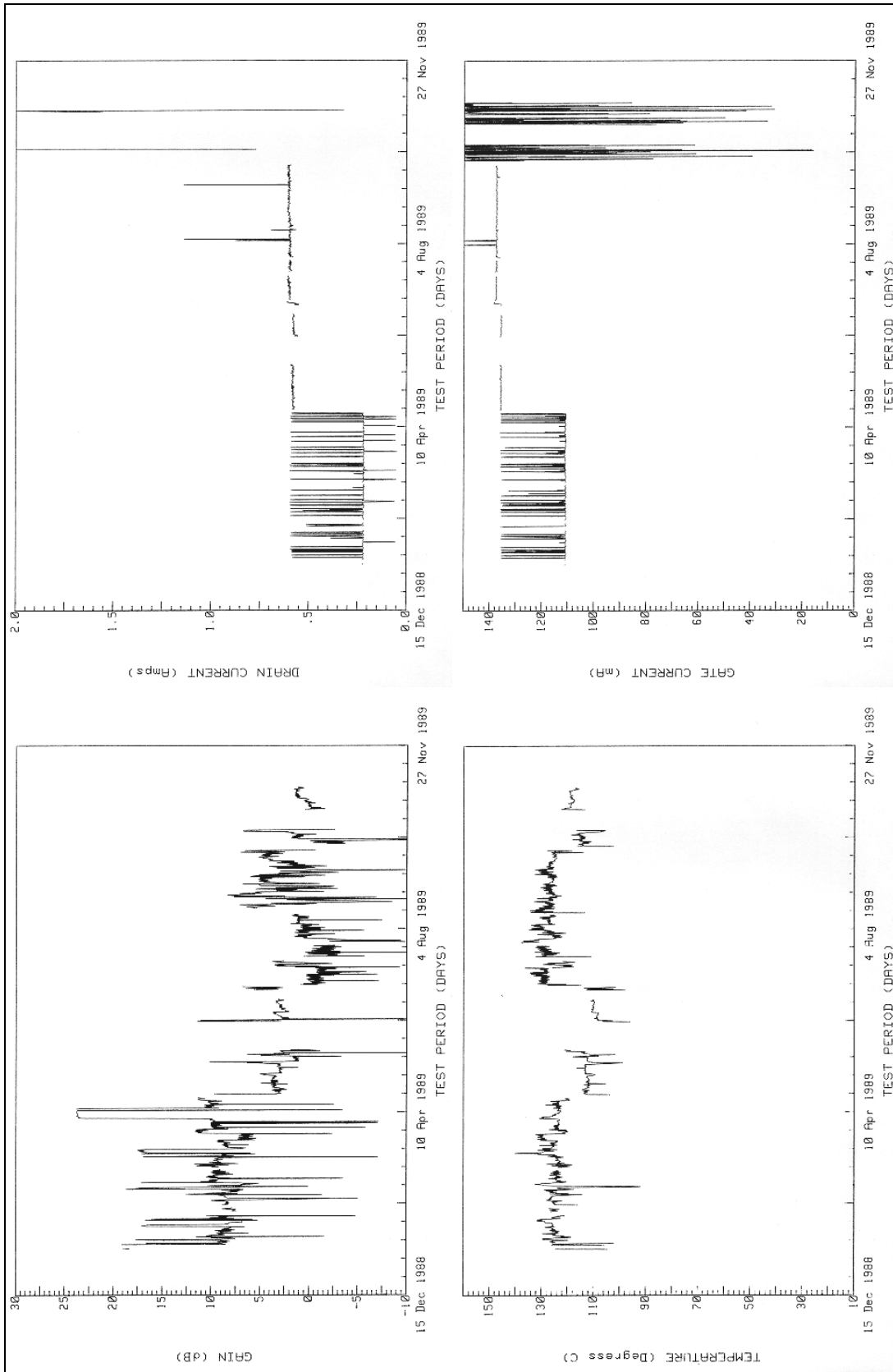


FIGURE A.26 - PHASE 2 TESTING DEVICE CC4

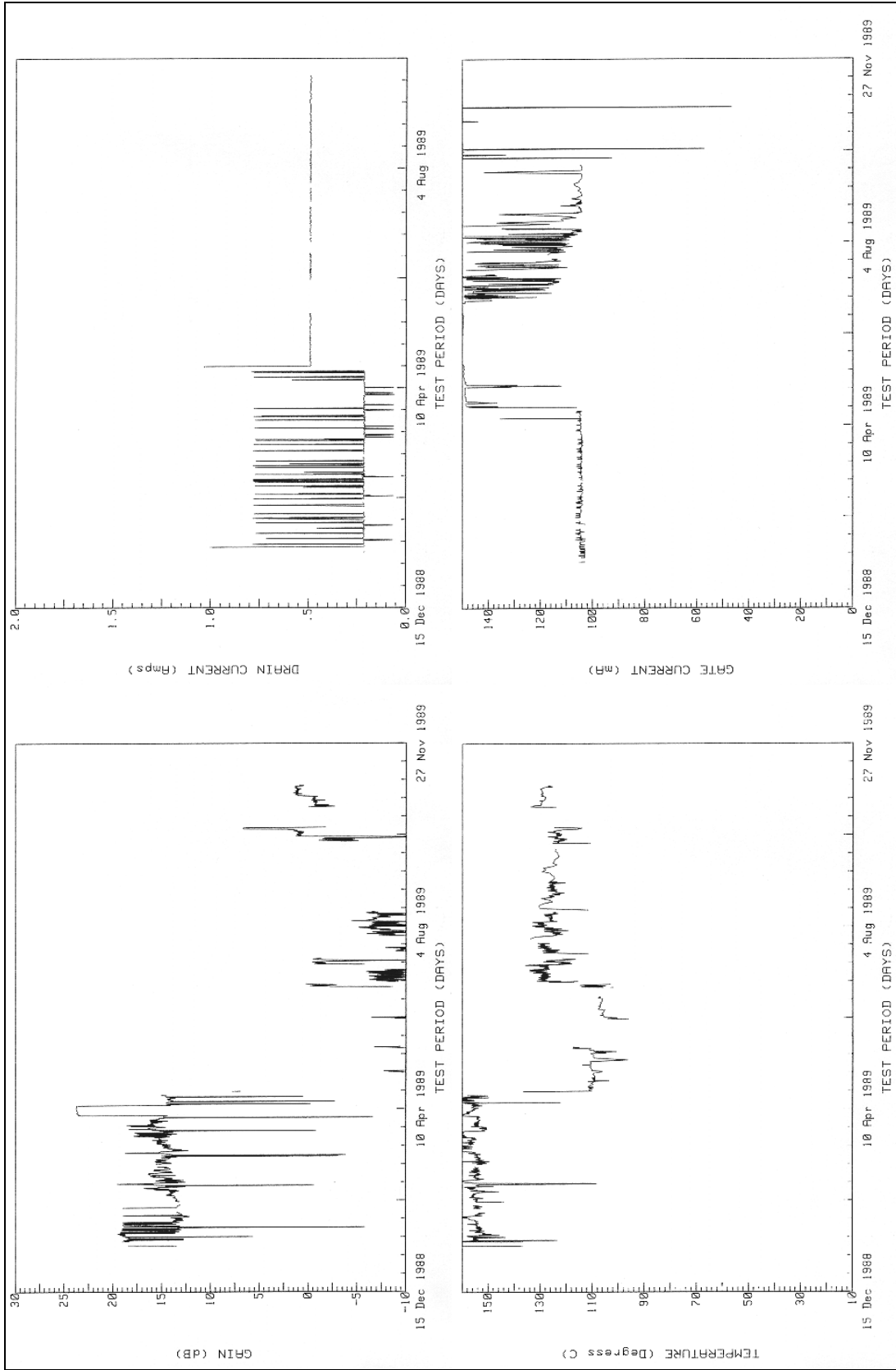


FIGURE A.27 - PHASE 2 TESTING DEVICE CD2

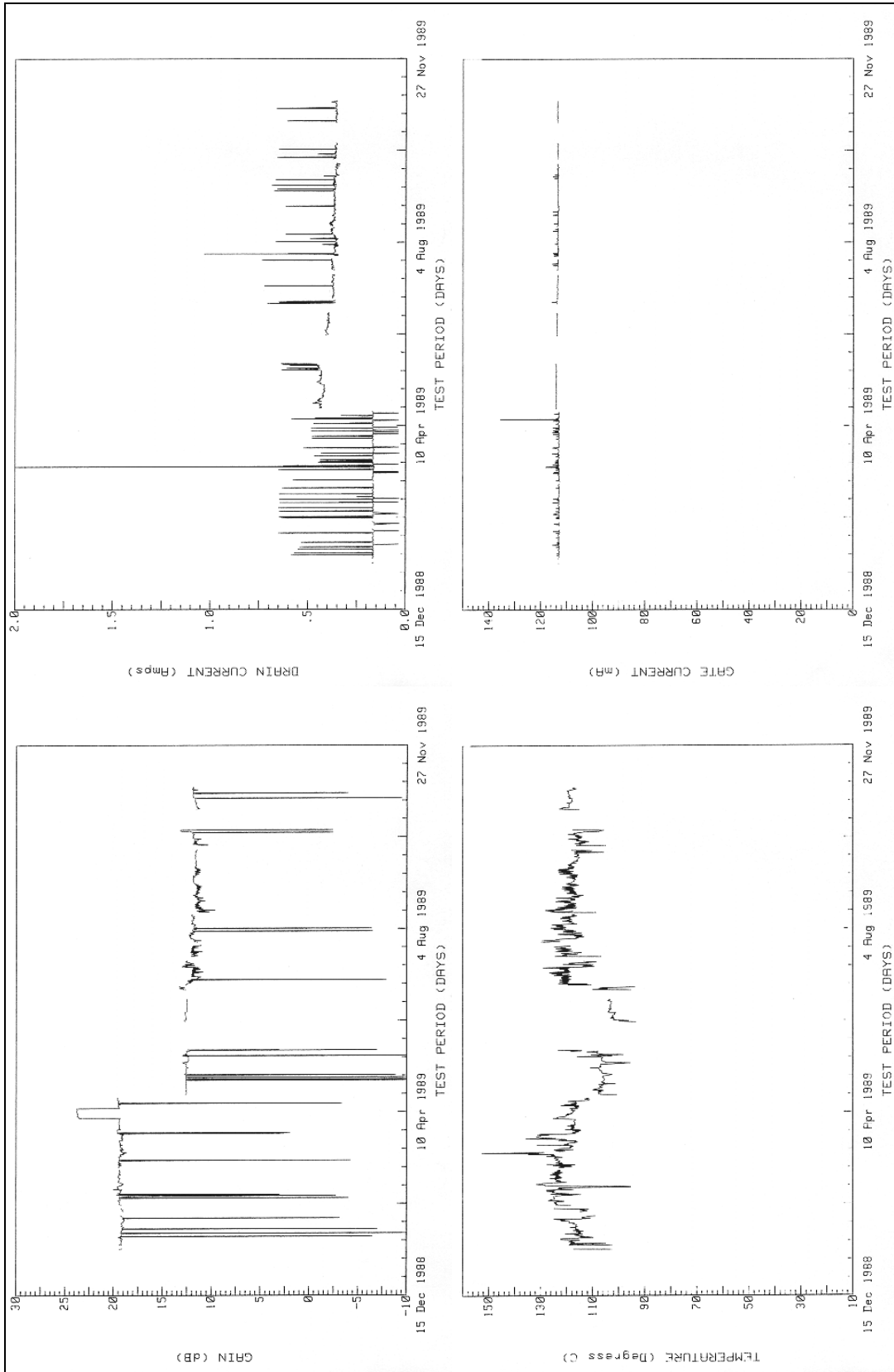


FIGURE A.28 - PHASE 2 TESTING DEVICE CD4

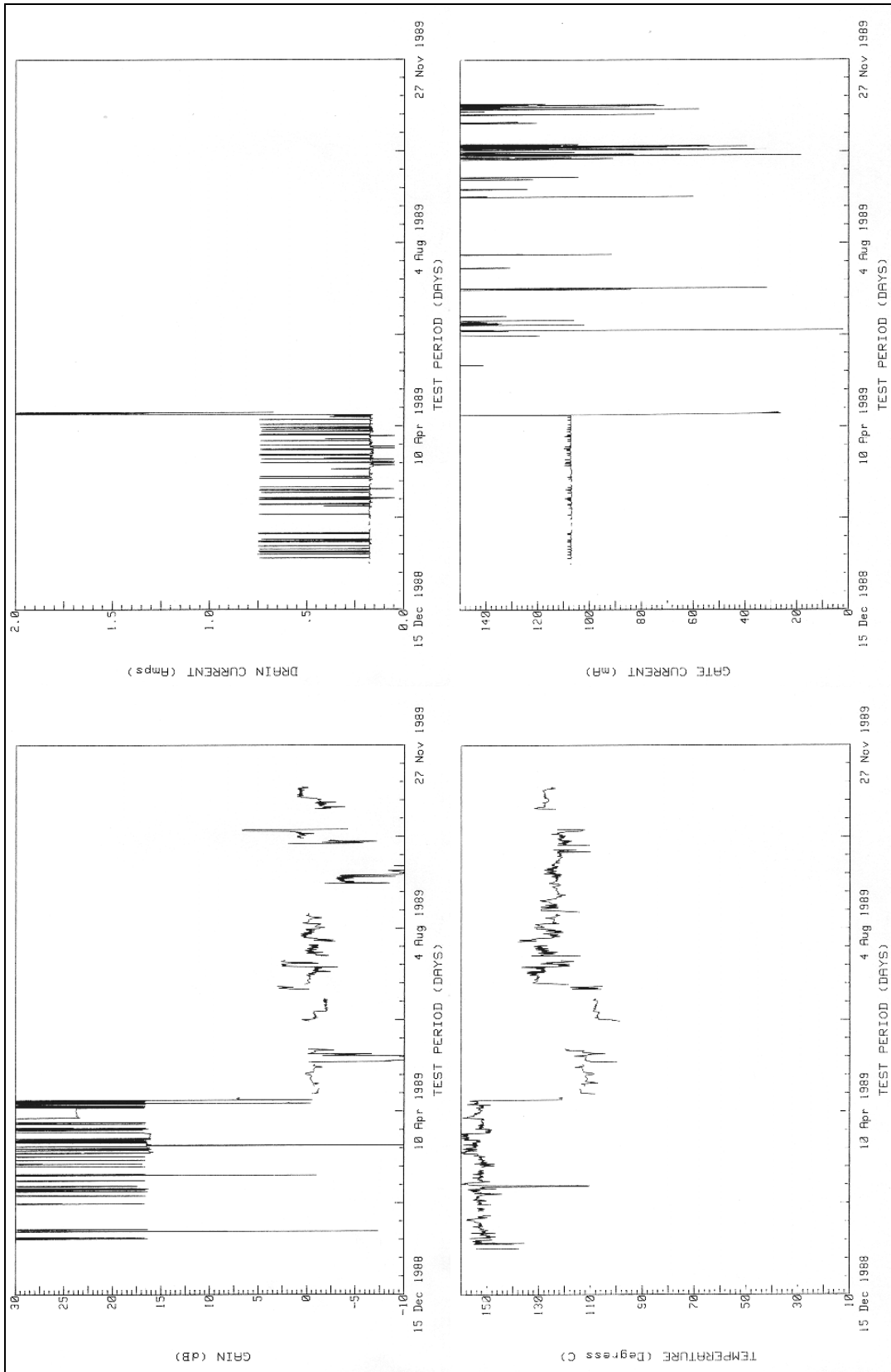


FIGURE A.29 - PHASE 2 TESTING DEVICE CE2

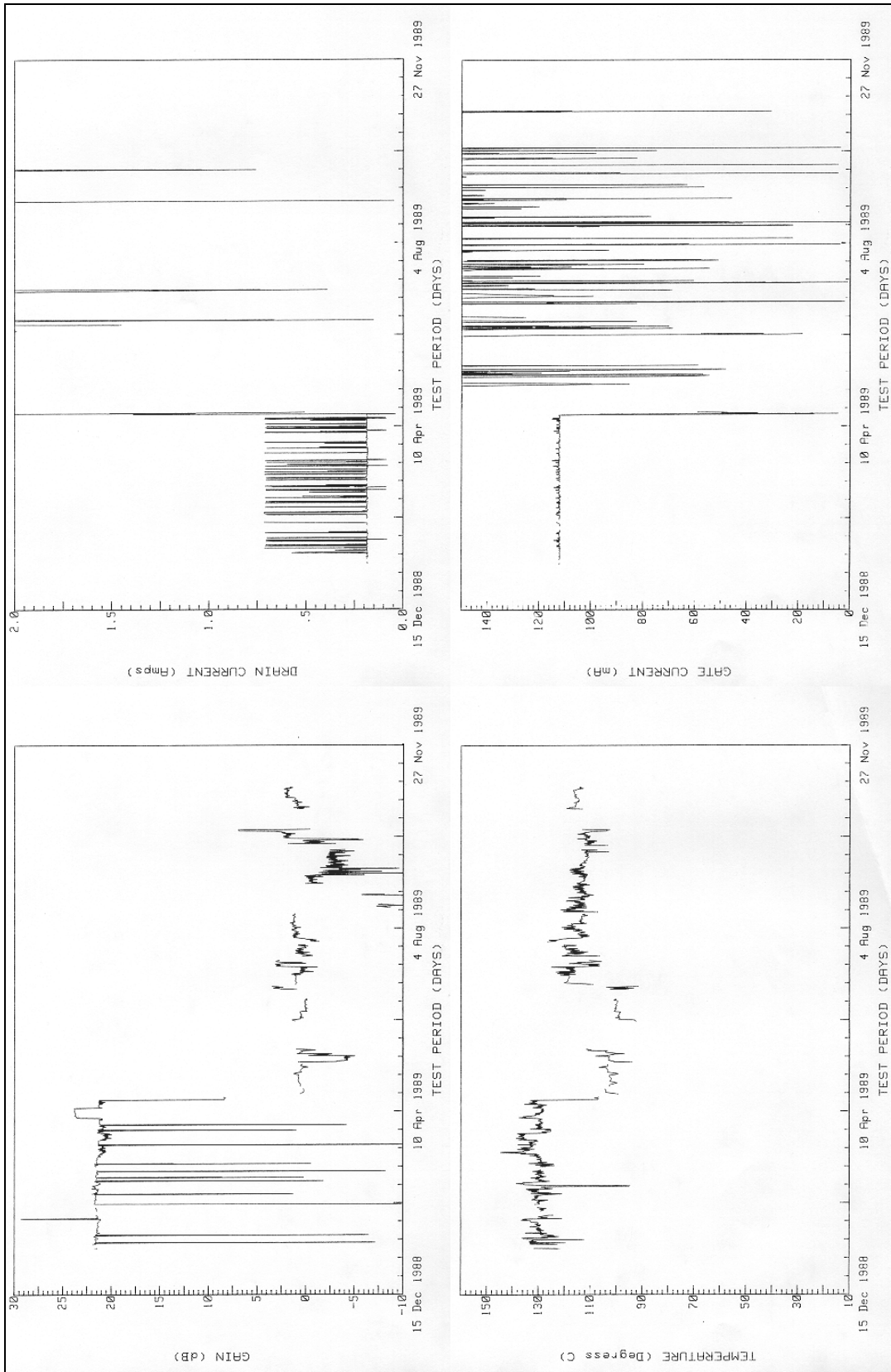


FIGURE A.30 - PHASE 2 TESTING DEVICE CE4

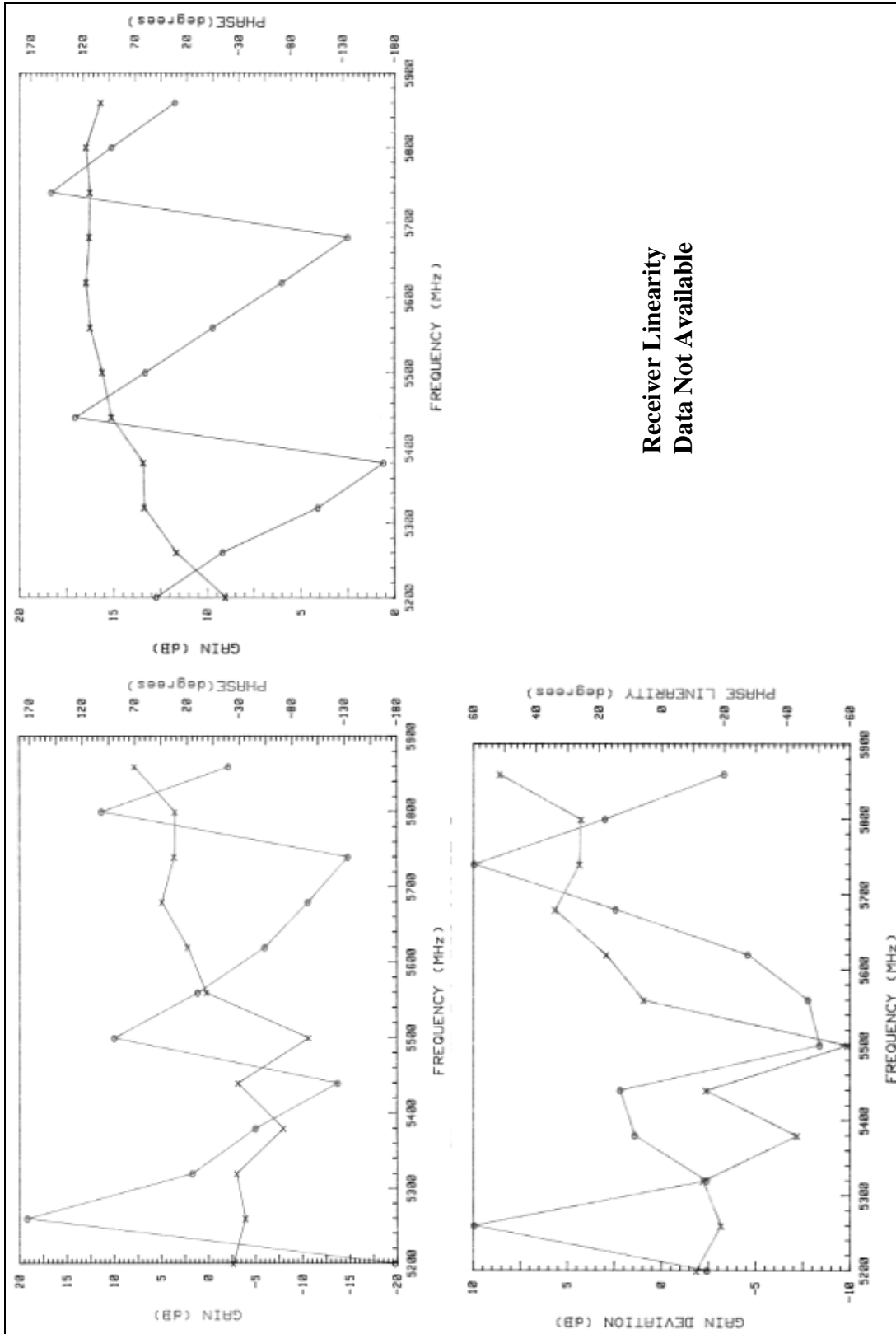


FIGURE A.31 - PHASE 3 TESTING C-BAND MODULE SN006 (LEFT) TRANSMIT & (RIGHT) RECEIVE

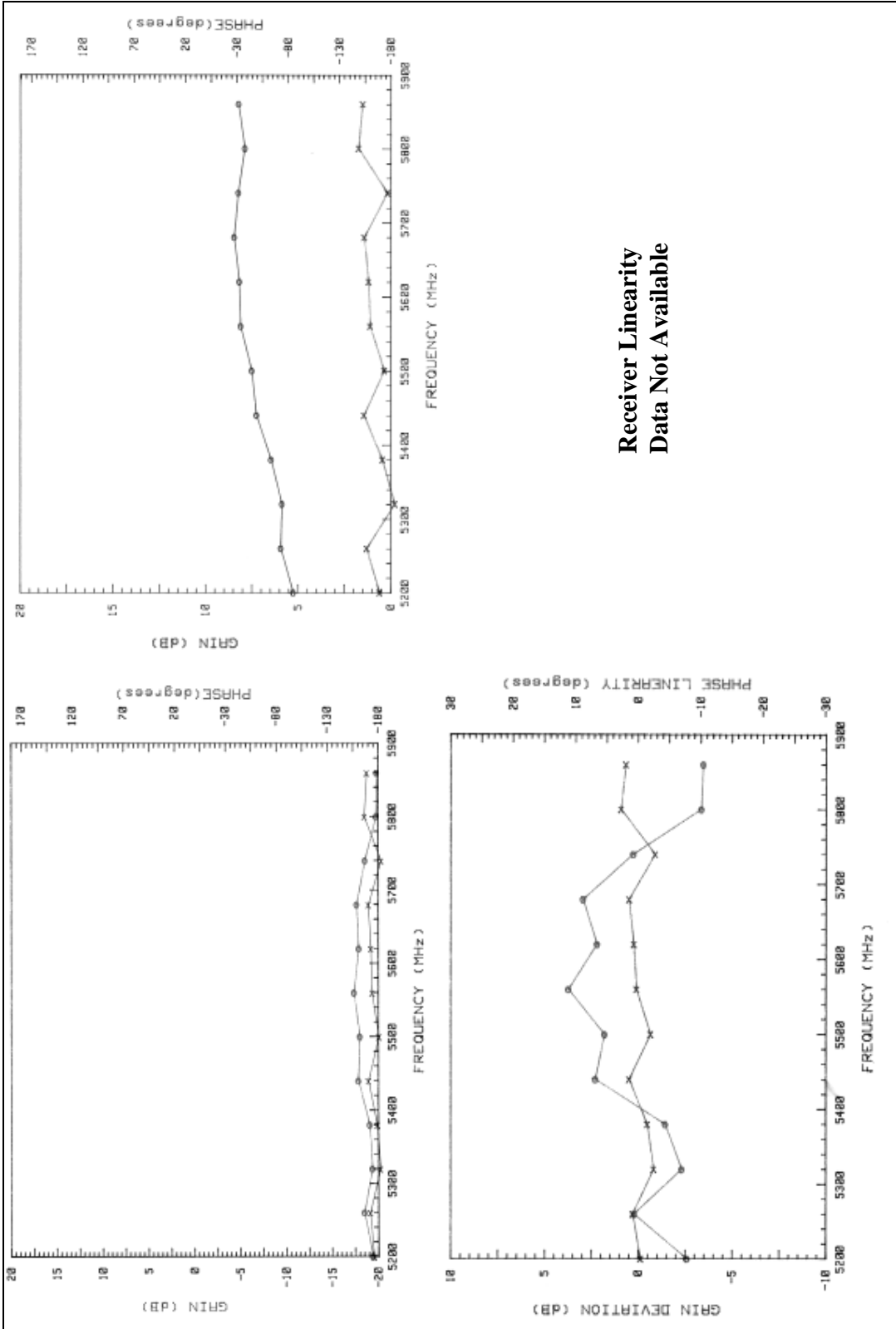


FIGURE A.32 - PHASE 3 TESTING C-BAND MODULE SN017 (LEFT) TRANSMIT & (RIGHT) RECEIVE

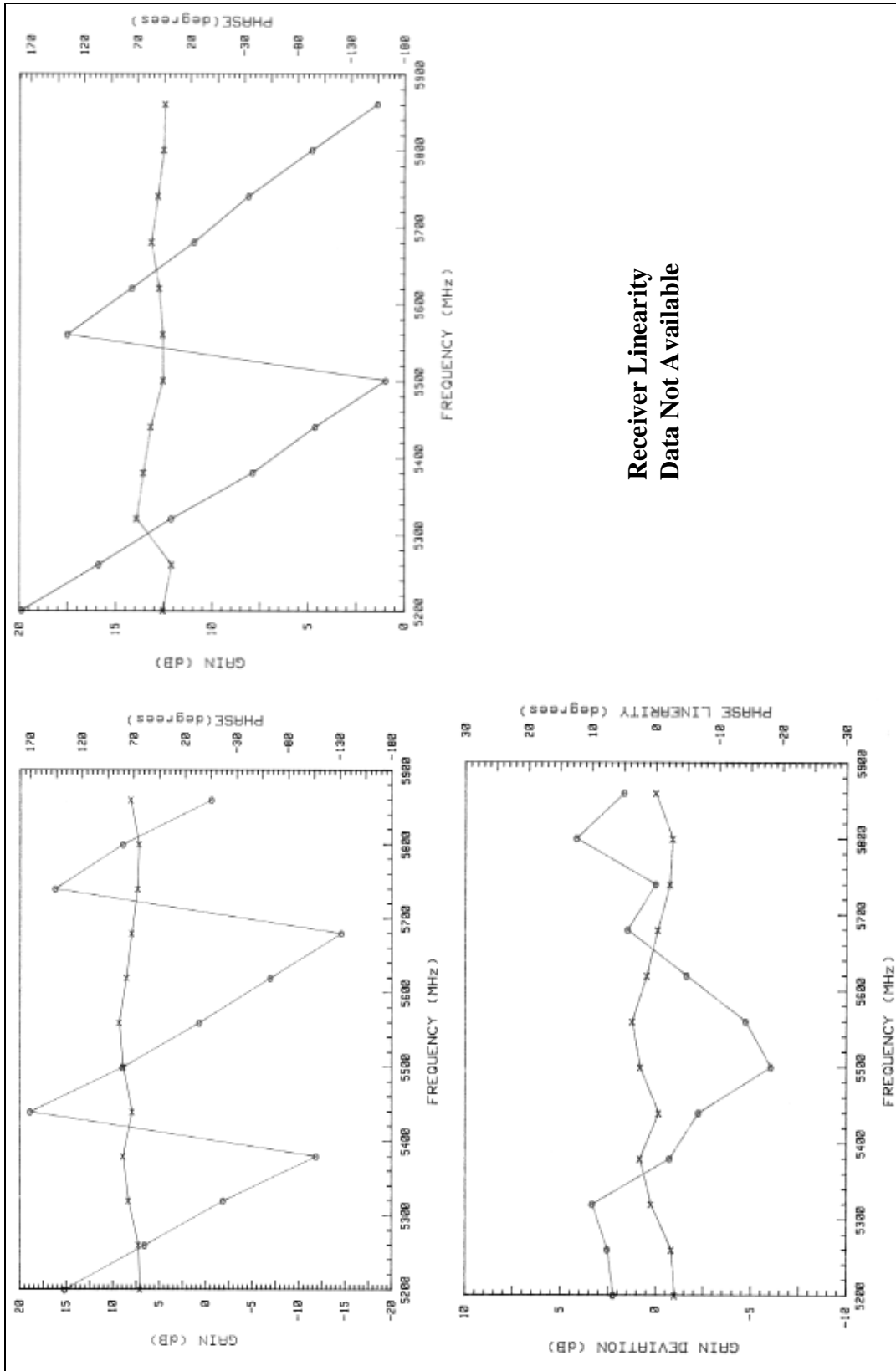


FIGURE A. 33 - PHASE 3 TESTING C-BAND MODULE SN022 (LEFT) TRANSMIT & (RIGHT) RECEIVE

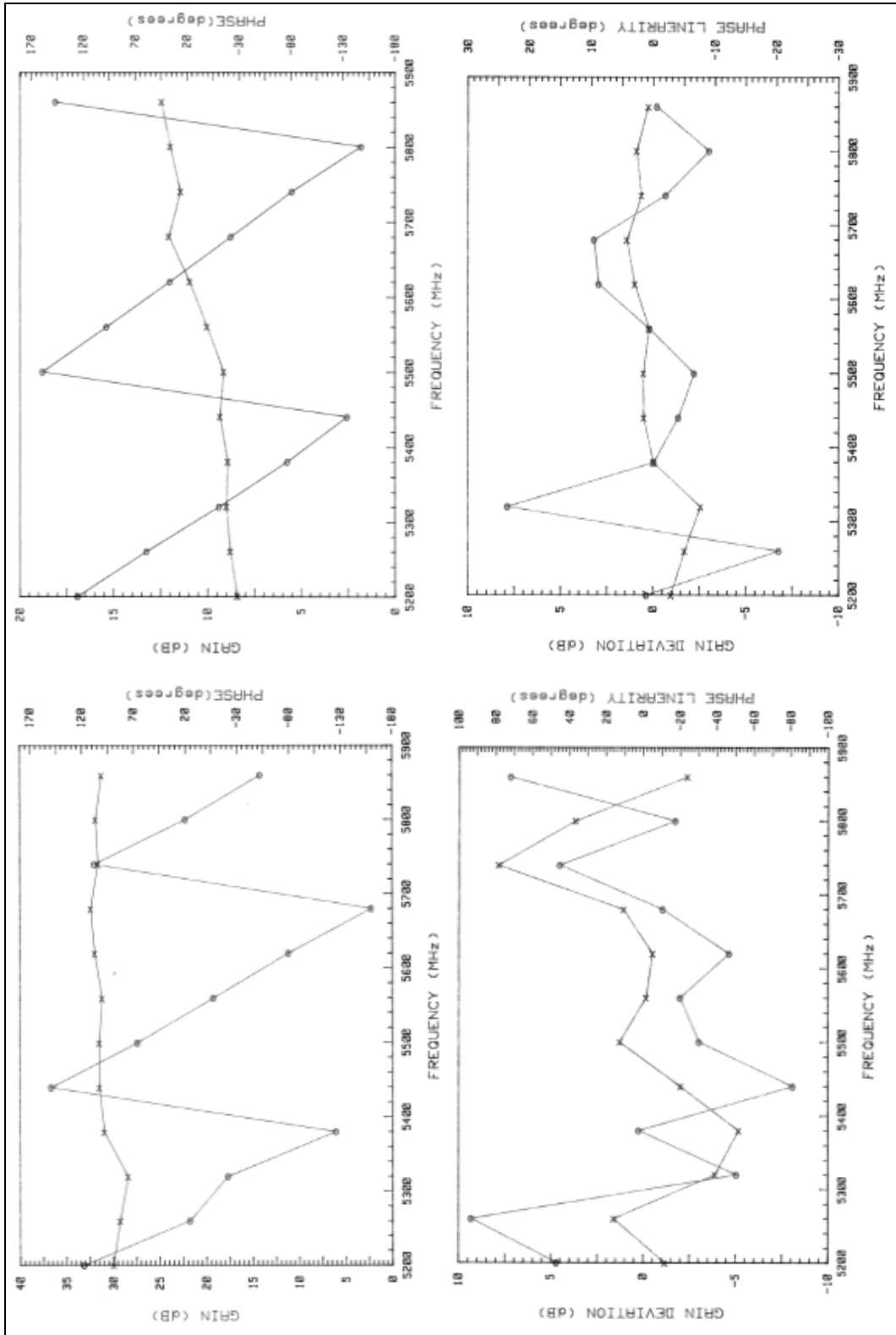


FIGURE A.34 - PHASE 3 TESTING C-BAND MODULE SN032 (LEFT) TRANSMIT & (RIGHT) RECEIVE

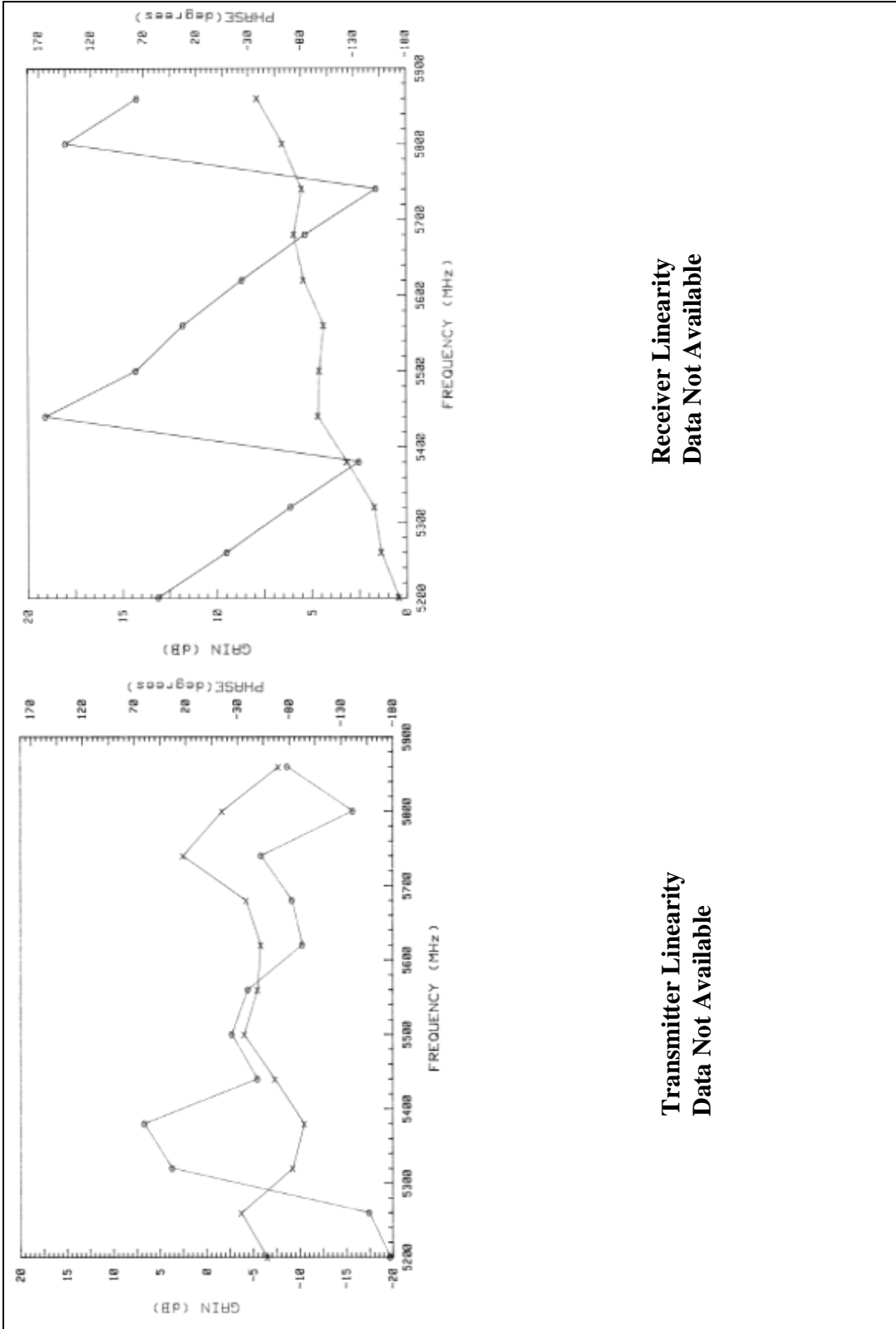


FIGURE A.35 - PHASE 3 TESTING C-BAND MODULE SN033 (LEFT) TRANSMIT & (RIGHT) RECEIVE

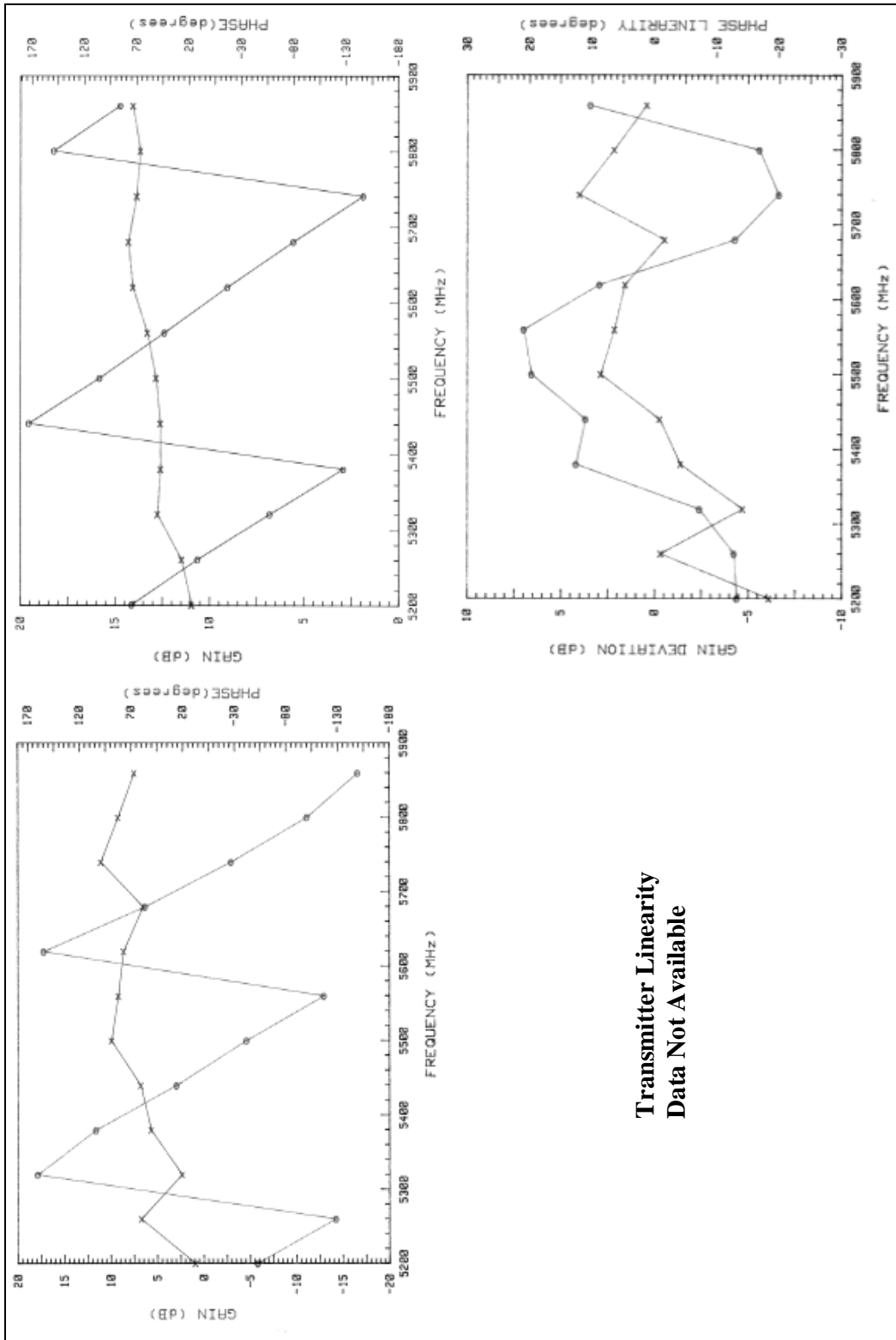


FIGURE A.36 - PHASE 3 TESTING C-BAND MODULE SN039 (LEFT) TRANSMIT & (RIGHT) RECEIVE

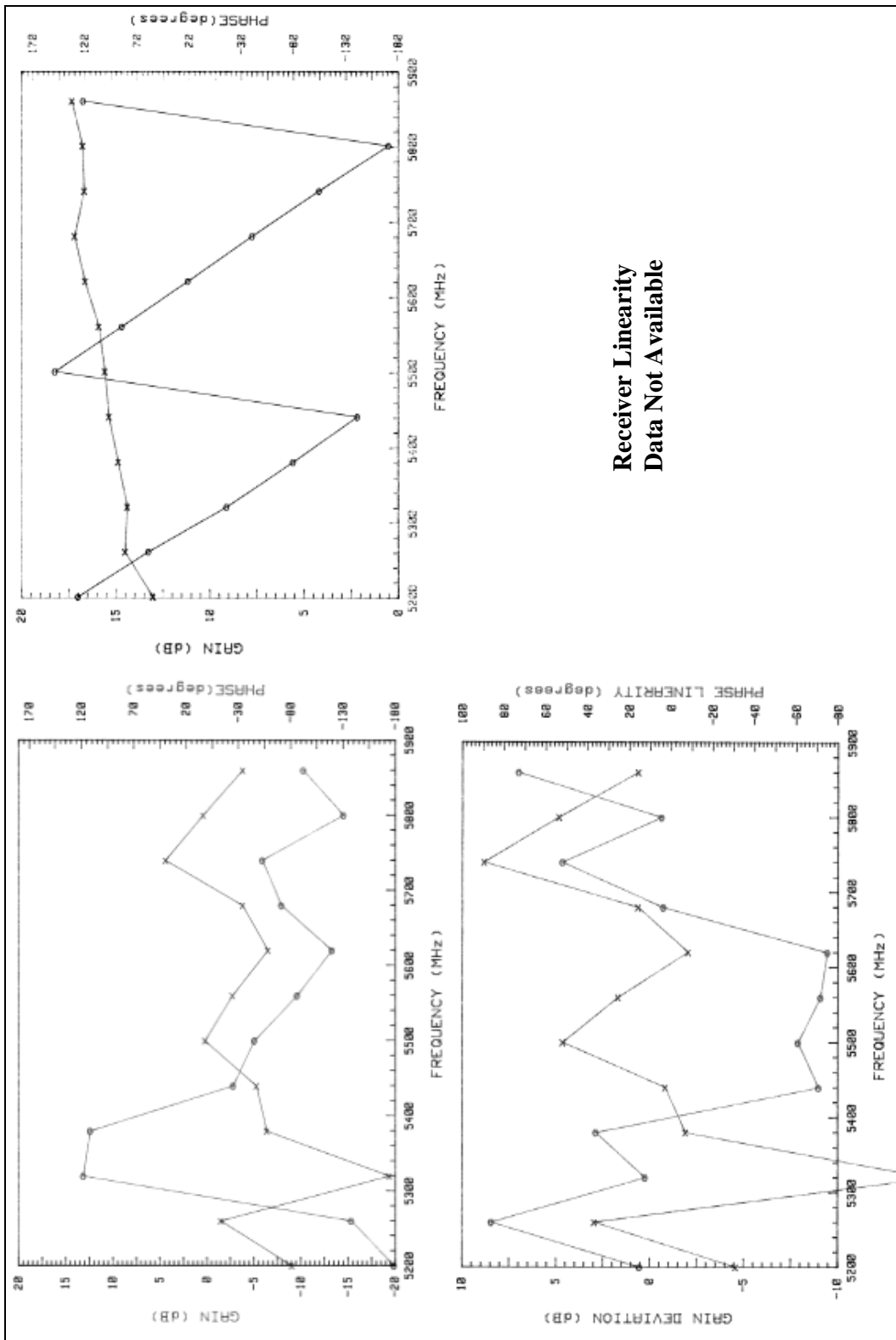


FIGURE A.37 - PHASE 3 TESTING C-BAND MODULE SN040 (LEFT) TRANSMIT & (RIGHT) RECEIVE

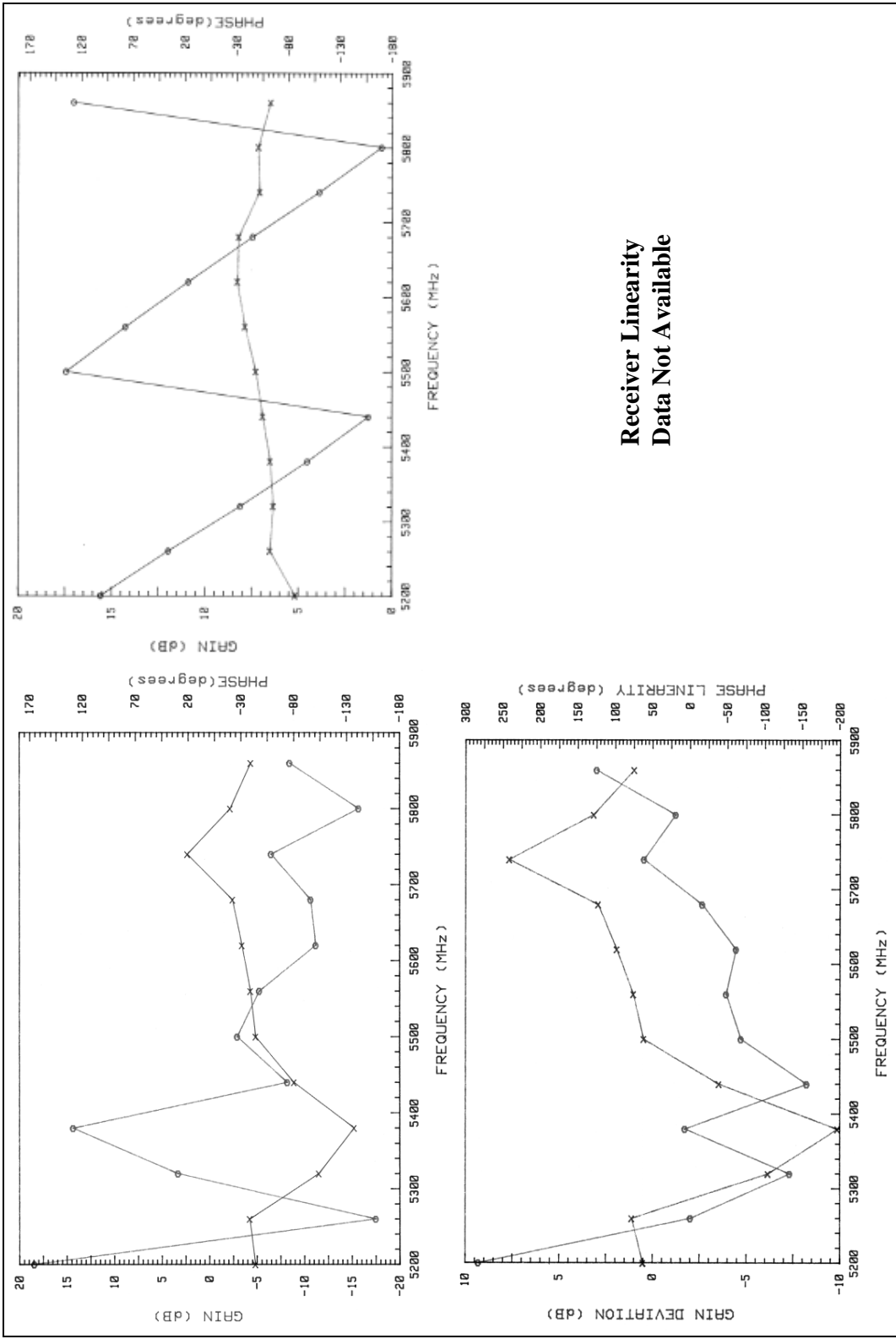


FIGURE A.38 - PHASE 3 TESTING C-BAND MODULE SN056 (LEFT) TRANSMIT & (RIGHT) RECEIVE

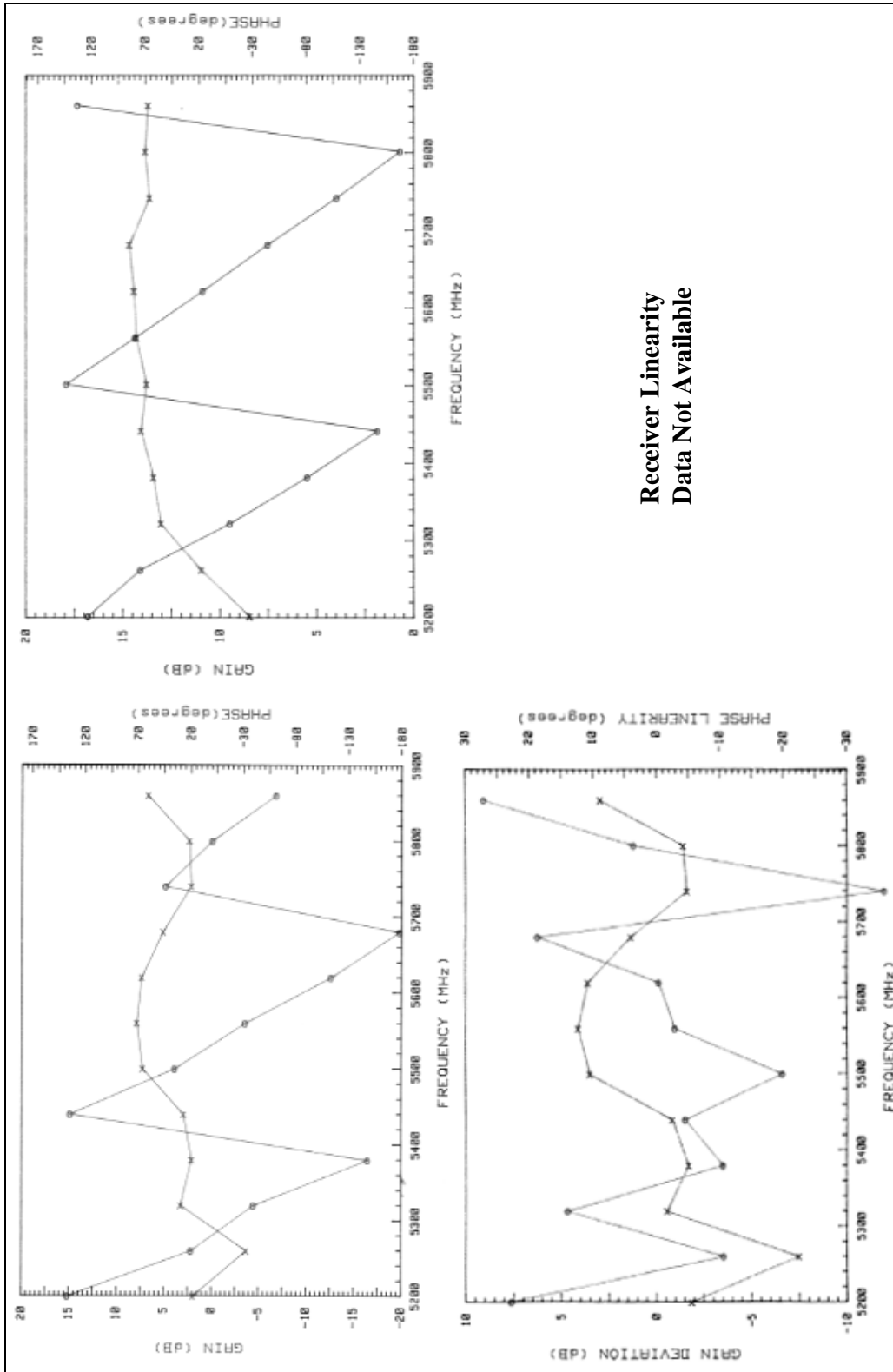


FIGURE A.39 - PHASE 3 TESTING C-BAND MODULE SN057 (LEFT) TRANSMIT & (RIGHT) RECEIVE

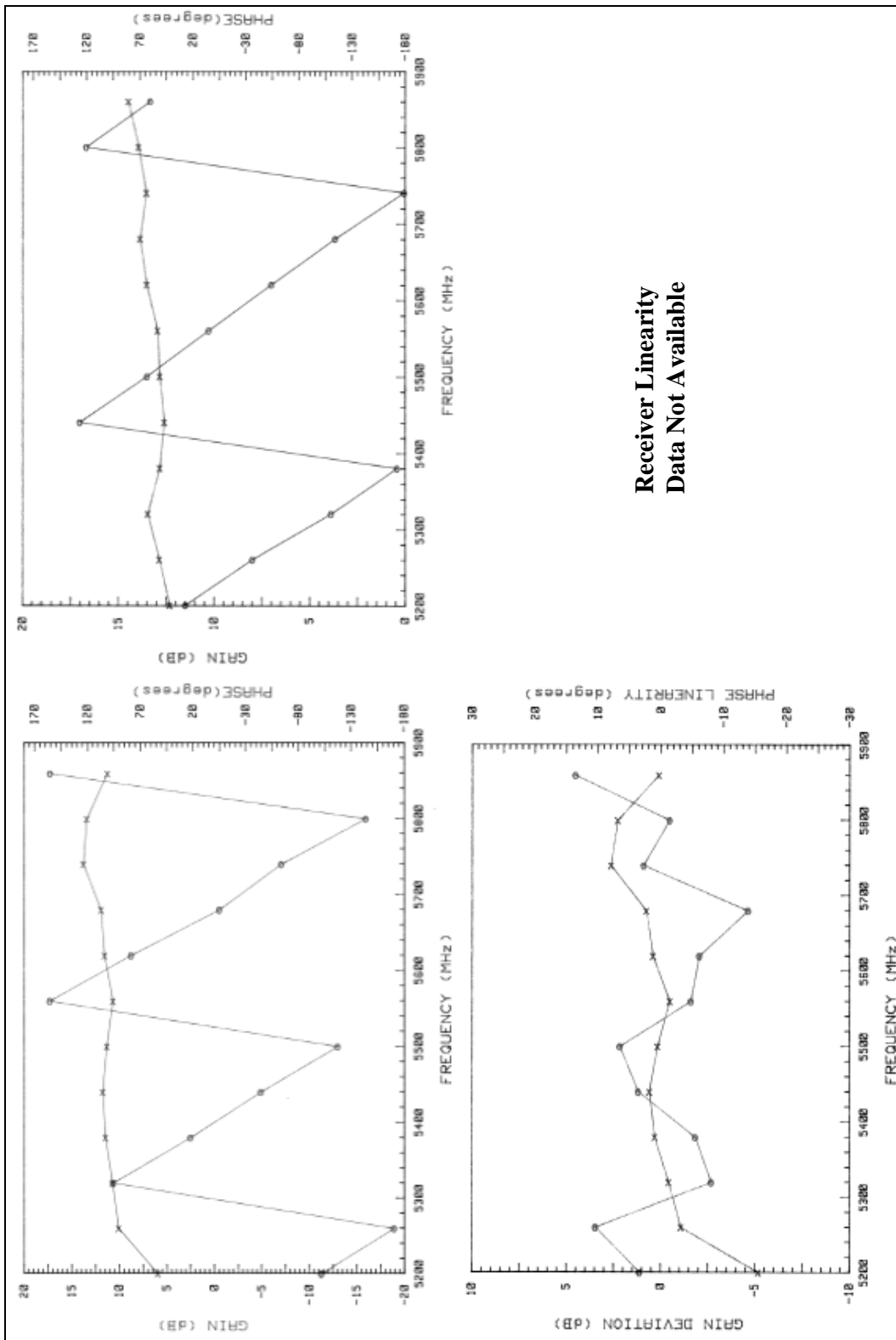


FIGURE A.40 - PHASE 3 TESTING C-BAND MODULE SN065 (LEFT) TRANSMIT & (RIGHT) RECEIVE

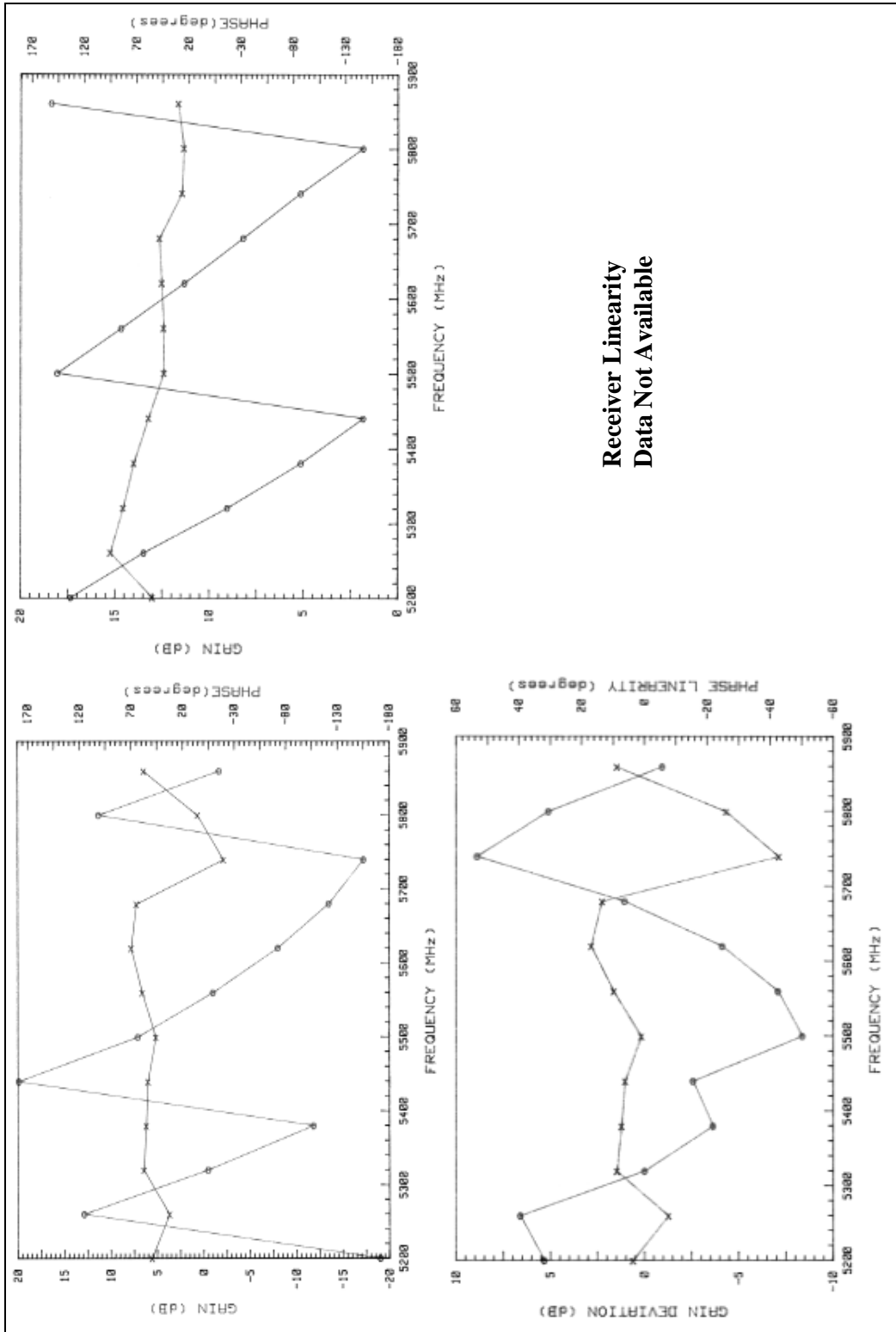


FIGURE A.41 - PHASE 3 TESTING C-BAND MODULE SN070 (LEFT) TRANSMIT & (RIGHT) RECEIVE

**Transmitter Gain & Phase
Data Not Available**

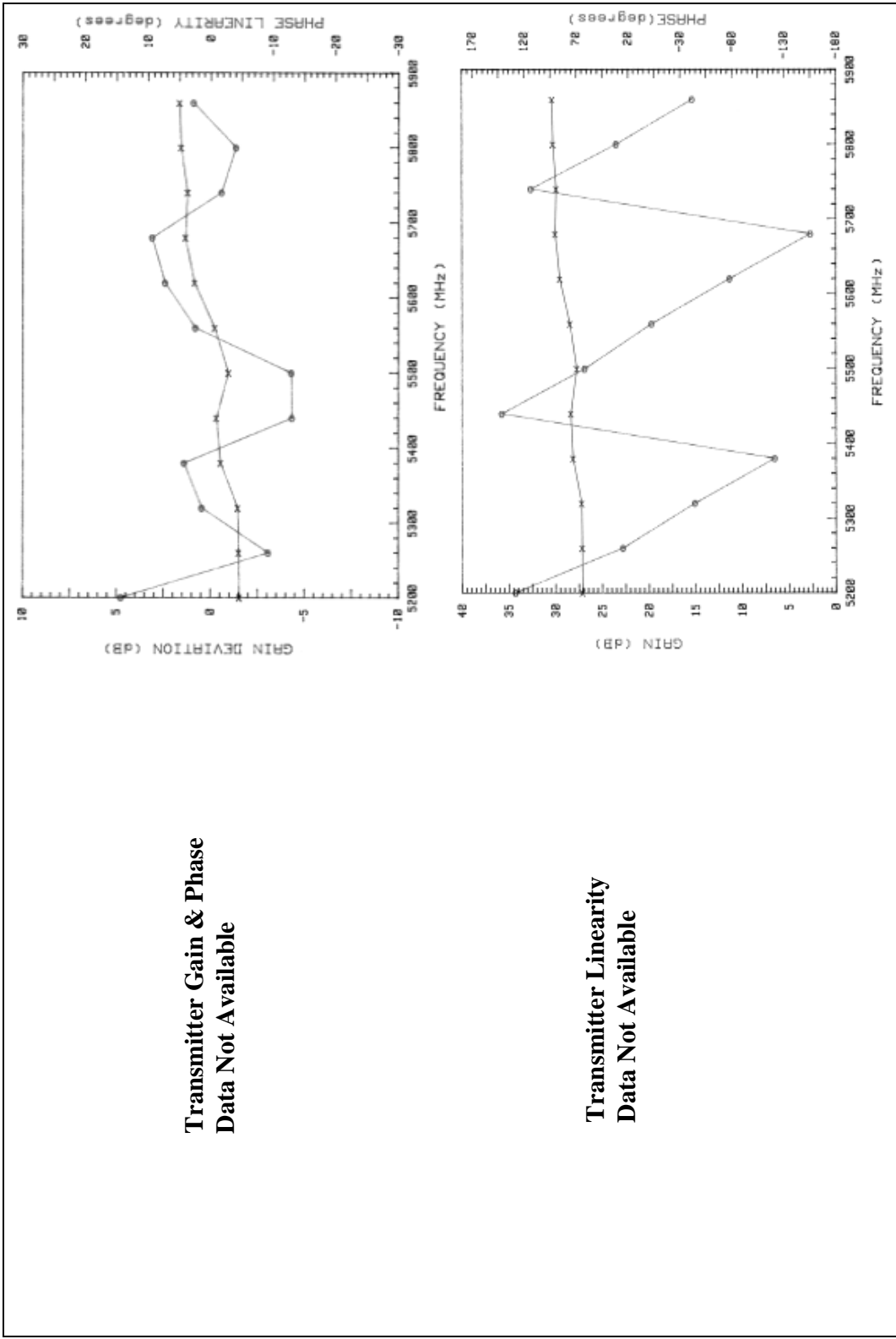


FIGURE A.42 - PHASE 3 TESTING C-BAND MODULE SN073 (LEFT) TRANSMIT & (RIGHT) RECEIVE

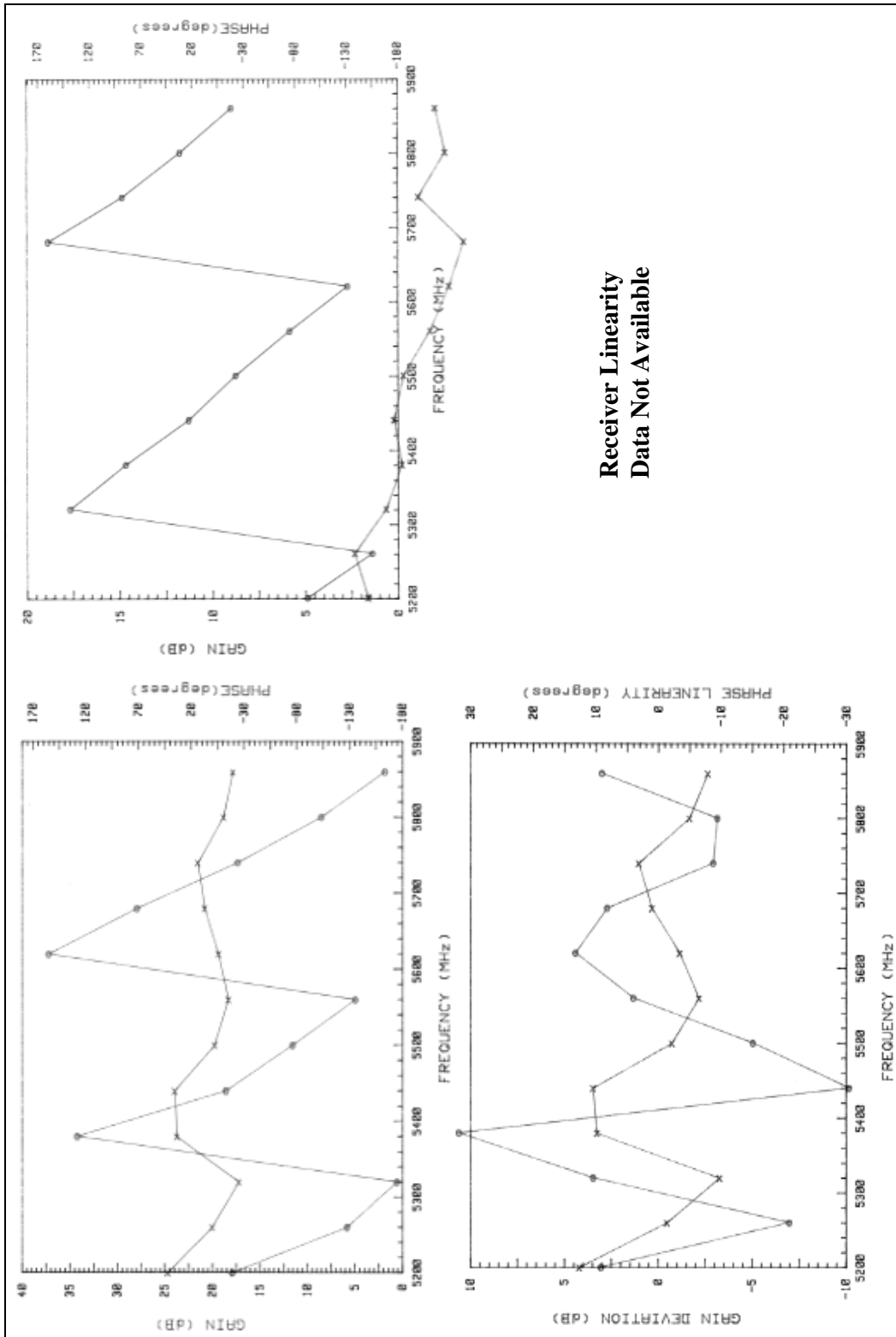


FIGURE A.43 - PHASE 3 TESTING C-BAND MODULE SN085 (LEFT) TRANSMIT & (RIGHT) RECEIVE

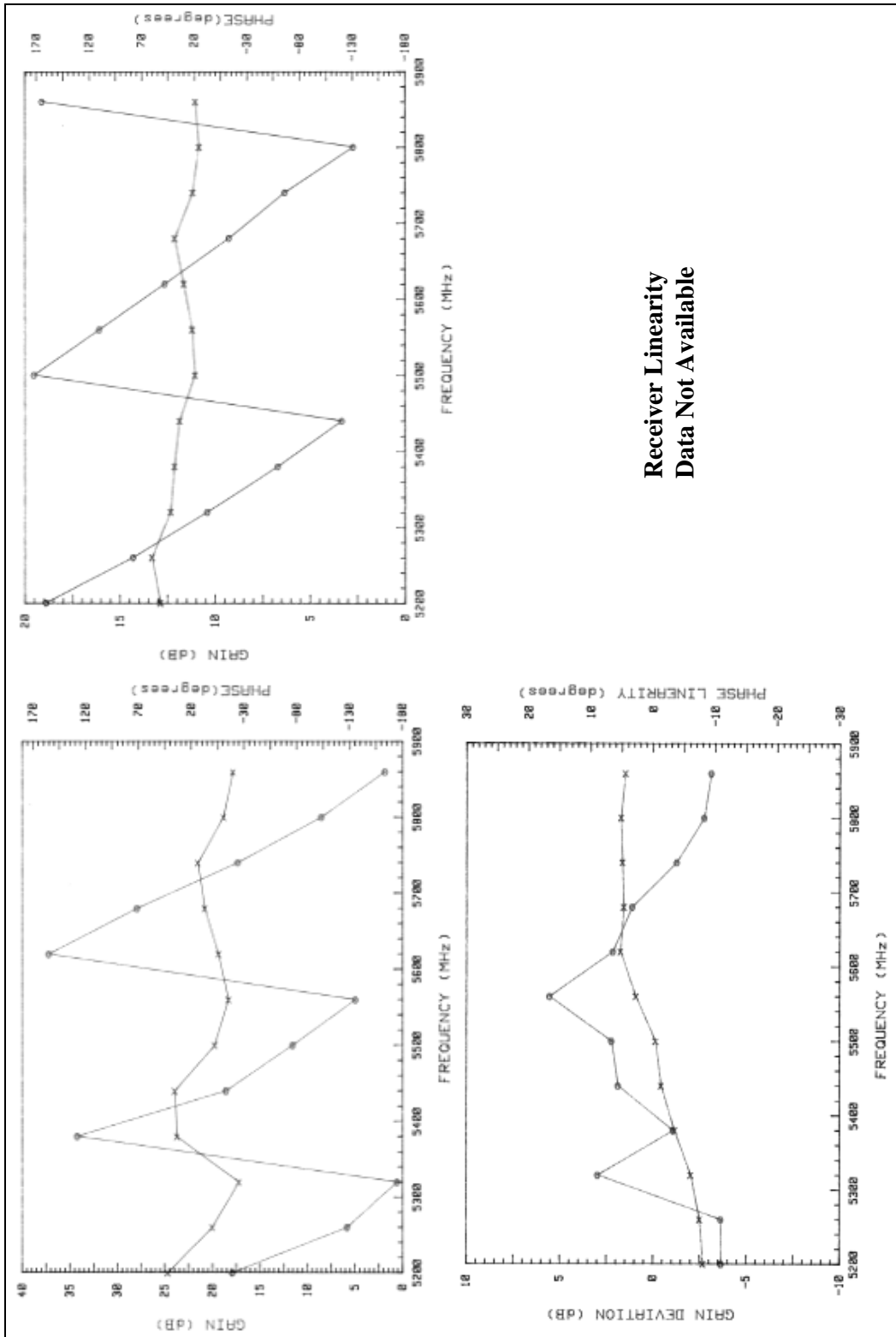


FIGURE A.44 - PHASE 3 TESTING C-BAND MODULE SN089 (LEFT) TRANSMIT & (RIGHT) RECEIVE

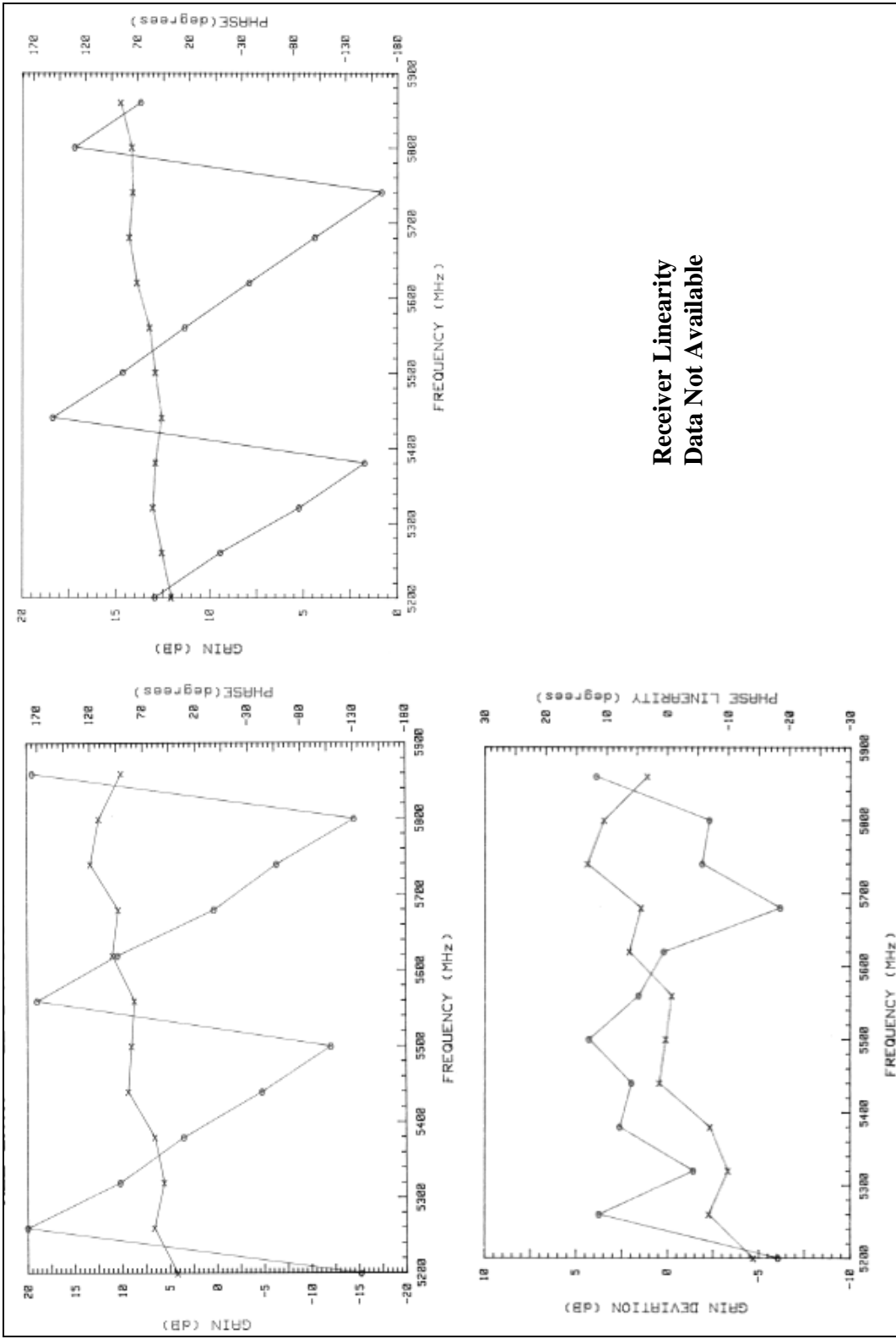


FIGURE A.45 - Phase 3 TESTING C-BAND MODULE SN118 (left) Transmit & (RIGHT) Receive